

Simulations for estimation of heterogeneity variance τ^2 in constant and inverse variance weights meta-analysis of log-odds-ratios

Elena Kulinskaya and David C. Hoaglin

August 2, 2022

Abstract

A number of popular estimators of the between-study variance, τ^2 , are based on the Cochran's Q statistic for testing heterogeneity in meta analysis. We introduce new point and interval estimators of τ^2 for log-odds-ratio. These include new DerSimonian-Kacker-type moment estimators based on the first moment of Q_F , the Q statistic with effective-sample-size weights, and novel median-unbiased estimators. We study, by simulation, bias and coverage of these new estimators of τ^2 and, for comparative purposes, bias and coverage of a number of well-known estimators based on the Q statistic with inverse-variance weights, Q_{IV} , such as the Mandel-Paule, DerSimonian-Laird, and restricted-maximum-likelihood estimators, and an estimator based on the Kulinskaya-Dollinger (2015) improved approximation to Q_{IV} .

Keywords inverse-variance weights, effective-sample-size weights, random effects, heterogeneity

1 Introduction

When the individual studies in a meta-analysis report binary outcomes in the treatment and control arms, the most common measure of effect is the odds ratio (OR) or its log (LOR).

In studying estimation of the overall effect in random-effects meta-analyses of the mean difference (MD), the standardized mean difference (SMD), and LOR, we found that SSW,

a weighted mean whose weights involve only the studies' arm-level sample sizes, performed well, avoiding shortcomings associated with estimators that use inverse-variance weights based on estimated variances (Bakbergenuly et al. [2020a,b]).

We also previously studied Q_F , a version of Cochran's Q statistic [Cochran, 1954] for assessment of heterogeneity that uses those constant weights. That work draws on favorable results for Q with effective-sample-size-based weights when the measure of effect is the mean difference (MD) (Kulinskaya et al. [2021b]) or the standardized mean difference (SMD) (Kulinskaya et al. [2021b]). Here we introduce and investigate several new estimators of τ^2 for LOR, based on Q_F . These include new DerSimonian-Kacker-type moment estimators based on the first moment of Q_F , the Q statistic with effective-sample-size weights, and novel median-unbiased estimators.

We study, by simulation, the bias of point estimators of τ^2 and the coverage of confidence intervals for τ^2 . For comparison we include the usual version of Q (Q_{IV}), which uses inverse-variance weights, and familiar point and interval estimators of τ^2 .

2 Study-level estimation of log-odds-ratio

Consider K studies that used a particular individual-level binary outcome. Study i ($i = 1, \dots, K$) reports X_{iT} and X_{iC} , the numbers of events in the n_{iT} subjects in the Treatment arm and the n_{iC} subjects in the Control arm. It is customary to treat X_{iT} and X_{iC} as independent binomial variables:

$$X_{iT} \sim \text{Bin}(n_{iT}, p_{iT}) \quad \text{and} \quad X_{iC} \sim \text{Bin}(n_{iC}, p_{iC}). \quad (2.1)$$

The log-odds-ratio for Study i is

$$\theta_i = \log_e \left(\frac{p_{iT}(1 - p_{iC})}{p_{iC}(1 - p_{iT})} \right) \quad \text{estimated by} \quad \hat{\theta}_i = \log_e \left(\frac{\hat{p}_{iT}(1 - \hat{p}_{iC})}{\hat{p}_{iC}(1 - \hat{p}_{iT})} \right). \quad (2.2)$$

As inputs, a two-stage meta-analysis uses estimates of the θ_i ($\hat{\theta}_i$) and estimates of their variances (\hat{v}_i^2). The maximum likelihood estimator of p is $\tilde{p} = X/n$. It is helpful to have an unbiased estimator of θ . The use of $\hat{p} = (X + 0.5)/(n + 1)$ eliminates $O(1/n)$ bias and provides the least biased estimator of log-odds (Gart et al. [1985]). We use \hat{p} when estimating LOR in the Q_F .

The (conditional, given p_{ij} and n_{ij}) asymptotic variance of $\hat{\theta}_i$, derived by the delta

method, is

$$v_i^2 = \text{Var}(\hat{\theta}_i) = \frac{1}{n_{iT}p_{iT}(1-p_{iT})} + \frac{1}{n_{iC}p_{iC}(1-p_{iC})}, \quad (2.3)$$

estimated by substituting \hat{p}_{ij} for p_{ij} . This estimator of the variance is unbiased in large samples, but Gart et al. [1985] note that it overestimates the variance for small sample sizes.

Our simulations yield an exact calculation of conditional central moments of LOR, following the implementation of Kulinskaya and Dollinger [2015].

3 Random-effects model and the Q statistic

We consider a generic random-effects model (REM): For Study i ($i = 1, \dots, K$) the estimate of the effect is $\hat{\theta}_i \sim G(\theta_i, v_i^2)$, where the effect-measure-specific distribution G has mean θ_i and variance v_i^2 , and $\theta_i \sim N(\theta, \tau^2)$. Thus, the $\hat{\theta}_i$ are unbiased estimates of the true conditional effects θ_i , and the $v_i^2 = \text{Var}(\hat{\theta}_i|\theta_i)$ are the true conditional variances.

Cochran's Q statistic is a weighted sum of the squared deviations of the estimated effects $\hat{\theta}_i$ from their weighted mean $\bar{\theta}_w = \sum w_i \hat{\theta}_i / \sum w_i$:

$$Q = \sum w_i (\hat{\theta}_i - \bar{\theta}_w)^2. \quad (3.1)$$

In Cochran [1954] w_i is the reciprocal of the *estimated* variance of $\hat{\theta}_i$, hence the notation Q_{IV} . In meta-analysis those w_i come from the fixed-effect model. In what follows, we derive estimators of τ^2 based on Q_F , discussed by DerSimonian and Kacker [2007] and further studied by Kulinskaya et al. [2021b], in which the w_i are arbitrary positive constants. A particular choice of the fixed weights which we usually specify in Q_F is $w_i = \tilde{n}_i$, where $\tilde{n}_i = n_{iC}n_{iT}/n_i$, the effective sample size in Study i ($n_i = n_{iC} + n_{iT}$).

Define $W = \sum w_i$, $q_i = w_i/W$, and $\Theta_i = \hat{\theta}_i - \theta$. In this notation, and expanding $\bar{\theta}_w$, Equation (3.1) can be written as

$$Q = W \left[\sum q_i (1 - q_i) \Theta_i^2 - \sum_{i \neq j} q_i q_j \Theta_i \Theta_j \right]. \quad (3.2)$$

We distinguish between the conditional distribution of Q (given the θ_i) and the unconditional distribution, and the respective moments of Θ_i . For instance, the conditional second moment of Θ_i is $M_{2i}^c = v_i^2$, and the unconditional second moment is $M_{2i} = \text{E}(\Theta_i^2) = \text{Var}(\hat{\theta}_i) = \text{E}(v_i^2)$, given in Equation (3.4).

Under the above REM, it is straightforward to obtain the first moment of Q_F as

$$E(Q_F) = W \left[\sum q_i(1 - q_i)\text{Var}(\Theta_i) \right] = W \left[\sum q_i(1 - q_i)(E(v_i^2)) \right]. \quad (3.3)$$

This expression is similar to Equation (4) in DerSimonian and Kacker [2007]; they use the conditional variance $v_i^2 + \tau^2$ instead of the unconditional mean $E(v_i^2)$.

The full (unconditional) variance of $\hat{\theta}_i$ depends on the generation mechanism and was derived in Kulinskaya et al. [2021a] under a bivariate normal model for $(\text{logit}(p_{iC}), \text{logit}(p_{iT}))$.

In the conventionally assumed fixed-intercept model (i.e., when the p_{iC} are fixed),

$$E(v_i^2) = \frac{1}{n_{iT}\check{p}_{iT}(1 - \check{p}_{iT})} + \frac{1}{n_{iC}p_{iC}(1 - p_{iC})} + \tau^2 \left(1 + \frac{1}{2n_{iT}} ([\check{p}_{iT}(1 - \check{p}_{iT})]^{-1} - 2) \right) \quad (3.4)$$

for $\check{p}_{iT} = \text{expit}(\alpha_i + \theta)$. This unconditional variance can be estimated by substituting \hat{p}_{iC} for p_{iC} and $\text{expit}(\hat{\alpha}_i + \hat{\theta})$ for \check{p}_{iT} , where $\hat{\alpha}_i = \text{logit}(\hat{p}_{iC})$ and $\hat{\theta}$ is the estimated LOR. We refer to this estimate of p_{iT} as **model-based**. Alternatively, a **naïve** estimate would use \hat{p}_{iT} . An advantage of such a naïve estimate is that it maintains the variance inflation of $E(v_i^2)$ in comparison with $v_i^2 + \tau^2$.

4 Approximations to the distributions of Q_F and Q_{IV}

Standard approximation to the distribution of Q_{IV} is the chi-square distribution with $K - 1$ degrees of freedom. A few estimators of τ^2 , such as DerSimonian-Laird and Mandel-Paule, are based on the chi-square moments. However, it is well known that this approximation is not satisfactory for small to moderate sample sizes. Kulinskaya and Dollinger [2015] provided an improved approximation to the null distribution of Q_{IV} based on a two-moment gamma approximation; we study point and interval estimators of τ^2 based on this approximation, denoted by KD.

For LOR, Q_F is a quadratic form in asymptotically normal variables. The Farebrother algorithm [Farebrother, 1984], applicable for quadratic forms in normal variables, may provide a satisfactory approximation for larger sample sizes, though it may not behave well for small n . To apply it, we plug in estimated variances. We study point and interval estimators of τ^2 based on this approximation to the distribution of Q_F .

5 Point and interval estimators of τ^2 for LOR

5.1 Point estimators

The unconditional variance of $\hat{\theta}$ in Equation (3.4) can be written as a sum of two terms,

$$E(v_i^2) = v_i^2 + \tau^2 \left(1 + \frac{1}{2n_{iT}} ([p_{iT}(1 - p_{iT})]^{-1} - 2)\right). \quad (5.1)$$

Rearranging the terms in Equation (3.2) gives the moment-based estimator of τ^2 :

$$\hat{\tau}_U^2 = \frac{Q/W - \sum q_i(1 - q_i)\hat{v}_i^2}{\sum q_i(1 - q_i)C_i}, \quad (5.2)$$

for $C_i = 1 + \frac{1}{2n_{iT}} ([\hat{p}_{iT}(1 - \hat{p}_{iT})]^{-1} - 2)$.

DerSimonian and Kacker [2007] obtain a similar result; they use the conditional estimate, $\hat{v}_i^2 + \hat{\tau}^2$, instead of the unconditional estimate, $\hat{E}(v_i^2)$, obtaining

$$\hat{\tau}_M^2 = \frac{Q/W - \sum q_i(1 - q_i)\hat{v}_i^2}{\sum q_i(1 - q_i)}. \quad (5.3)$$

We study both estimators with effective-sample-size weights. With the conditional estimated variances in Equation (5.3), we denote the estimator by SSC for ‘‘Sample Sizes Conditional’’; with the unconditional estimated variances, as in Equation (5.2), it is SSU for ‘‘Sample Sizes Unconditional’’. These estimators differ by a term of order $O(1/n_i)$ and will be very similar for large sample sizes.

The estimators $\hat{\tau}_U^2$ and $\hat{\tau}_M^2$ arose from setting the observed value of Q equal to its expected value and solving for τ^2 . Instead of the expected value, one could use the median of the distribution of Q given τ^2 (Bakbergenuly et al. [2021], Brown [1947], Viechtbauer [2021]). If the true (or approximate) cumulative distribution function is $F(\cdot|\tau^2)$, a point estimator of τ^2 can be found as

$$\hat{\tau}_{med}^2 = \max(0, \{\tau^2 : F(Q|\tau^2) = 0.5\}).$$

In the Farebrother approximation to the distribution of Q (Section 4), one can use either the conditional estimated variances or the unconditional estimated variances. We denote the resulting estimators by SMC and SMU (‘‘Sample sizes Median (Un)Conditional’’), respectively. Depending on the chosen estimate of p_{iT} in $E(v_i^2)$ (3.4), we have ‘‘model-based’’ or ‘‘naïve’’ versions of SSU and SMU: SSU model or SSU naïve and SMU model or SMU naïve. The SSC and the SMC estimators can be obtained from the procedure *rma* in

metafor by choosing the method as GENQ or GENQM, respectively, and specifying *nbar* weights (Viechtbauer [2010]).

For comparison, our simulations (Section 6) include four estimators that use inverse-variance weights: DerSimonian and Laird [1986] (DL), REML, Mandel and Paule [1970] (MP), and an estimator (KD) based on the work of Kulinskaya and Dollinger [2015] and discussed by Bakbergenuly et al. [2020b]. KD uses an improved non-null first moment of Q and has better performance than most other estimators.

A perennial question involves whether analysts should add 1/2 to each of X_{iT} , X_{iC} , $n_{iT} - X_{iT}$, $n_{iC} - X_{iC}$ only when one of them is zero, or in all studies. To obtain evidence on this issue, we included the corresponding two versions, “only” and “always”, of DL, REML, MP, SSC, and SMC. (We follow the prevalent practice of omitting “double-zero” studies, in which two of those cell counts are zero.)

5.2 Interval estimators

Straightforward use of the cumulative distribution function $F(\cdot|\tau^2)$ also yields a $100(1-\alpha)\%$ confidence interval for τ^2 :

$$\{\tau^2 \geq 0 : F(Q|\tau^2) \in [\alpha/2, 1 - \alpha/2]\}.$$

We use both the conditional estimated variances and the unconditional estimated variances in the Farebrother approximation to F ; we refer to the resulting profile estimators as FPC and FPU (“Farebrother Profile (Un)Conditional” intervals). Jackson [2013] introduced a similar approach using conditional variances. The FPC interval can be obtained from *confint* procedure in *metafor* for GENQ or GENQM objects which used *nbar* weights (Viechtbauer [2010]). For FPU intervals, we further distinguish between “model-based” or “naïve” versions, FPU model or FMU naïve, respectively, depending on the chosen estimate of p_{iT} in M_{2i} (3.4).

Our simulations (Section 6) also include the Q-profile (QP) interval (Viechtbauer [2007]), the profile-likelihood (PL) interval (Hardy and Thompson [1996]), and the KD interval, which is based on the chi-square distribution with the corrected first moment developed by Kulinskaya and Dollinger [2015].

For evidence on whether to add 1/2 to all four observed numbers X_{iT} , X_{iC} , $n_{iT} - X_{iT}$, $n_{iC} - X_{iC}$ only when one of these is zero, or always, we included two versions of the

PL, QP, and FPC methods.

6 Simulation design and results

6.1 Simulation design

Our simulation design follows that described in Bakbergenuly et al. [2020b]. Briefly, we varied five parameters: the overall true effect (θ), the between-studies variance (τ^2), the number of studies (K), the studies' total sample size (n or \bar{n}), and the probability in the control arm (p_{iC}). We kept the proportion of observations in the control arm (f) at $1/2$.

The values of LOR θ (0, 0.1, 0.5, 1, 1.5, and 2) aim to represent the range containing most values encountered in practice. LOR is a symmetric effect measure, so the sign of θ is not relevant.

The choices of sample sizes corresponding to \bar{n} follow a suggestion of Sánchez-Meca and Marín-Martínez [2000], who constructed the studies' sample sizes to have skewness 1.464, which they regarded as typical in behavioral and health sciences. For $K = 5$, Table 1 lists the sets of five sample sizes. The simulations for $K = 10$ and $K = 30$ used each set of unequal sample sizes twice and six times, respectively.

We generated the true effect sizes θ_i from a normal distribution: $\theta_i \sim N(\theta, \tau^2)$. The values of p_{iC} and θ_i defined the probabilities p_{iT} , and the counts X_{iC} and X_{iT} were generated from the respective binomial distributions. We used a total of 10,000 repetitions for each combination of parameters. We discarded 'double-zero' or 'double- n ' studies and reduced the observed value of K accordingly. We discarded repetitions with $K < 3$ and used the observed number of repetitions for analysis.

We used R statistical software [R Core Team, 2016] for the simulations. We used *metafor* for all methods of interest that it implemented. The user-friendly R programs implementing our methods are available in Kulinskaya and Hoaglin [2022].

6.2 Summary of simulation results

6.2.1 Bias of point estimators of τ^2 for LOR (Appendix A)

For small sample sizes, all estimators of τ^2 are considerably biased, positively at $\tau^2 = 0$ and linearly decreasing to negative values for larger τ^2 . The lines for different estimators

Table 1: *Values of parameters in the simulations*

Parameter	Equal study sizes	Unequal study sizes
K (number of studies)	5, 10, 30	5, 10, 30
n or \bar{n} (average (individual) study size — total of the two arms) For $K = 10$ and $K = 30$, the same set of unequal study sizes is used twice or six times, respectively.	20, 40, 100, 250	30 (12,16,18,20,84), 60 (24,32,36,40,168), 100 (64,72,76,80,208), 160 (124,132,136,140,268)
f (proportion of observations in the control arm)	1/2	1/2
p_{iC} (probability in the control arm)	.1, .2, .5	.1, .2, .5
θ (true value of LOR)	0, 0.5, 1, 1.5, 2	0, 0.5, 1, 1.5, 2
τ^2 (variance of random effects)	0(0.1)1	0(0.1)1

are parallel. When $p_{iC} = .1$ and $n = 100$, the bias of all estimators is almost constant in τ^2 ; for $p_{iC} = .5$ this happens by $n = 40$. For larger sample sizes, different estimators acquire positive or negative trends in bias.

The best estimators, almost unbiased by $n = 250$ when $p_{iC} = .1$, are MP “only”, KD, SSU model and SSC “always”. The same estimators are recommended for larger P_{iC} values, where they are, in general, less biased earlier.

6.2.2 Median bias of point estimators of τ^2 for LOR (Appendix B)

We define median bias as $P(\hat{\tau}^2 \geq \tau^2) - P(\hat{\tau}^2 \leq \tau^2)$. For a median, the median bias is zero.

For $0.1 \leq \tau^2 \leq 1$, all estimators of τ^2 are negatively biased for small to medium sample sizes $n \leq 40$. Interestingly, the median bias is almost constant across the range of τ^2 values. The negative bias is also present for the majority of the standard estimators of τ^2 for larger values of n . This means that the standard estimators of τ^2 usually provide values of $\hat{\tau}^2$ that are too low. The KD estimator is the least median-biased for $n = 20$. For larger values of n , from $n = 40$ at $p_{iC} \geq .2$ and $n \geq 100$ for $P_{iC} = .1$, the new median-unbiased estimators perform well. We recommend the SMC estimator with added 1/2 and the SMU model estimator. Both consistently result in almost median-unbiased estimation across the range of p_{iC} values.

6.2.3 Coverage of interval estimators of τ^2 for LOR (Appendix C)

When $P_{iC} = .1$, all confidence intervals but PL provide good coverage when $K = 5$ and $K = 10$. PL is too conservative, with constant coverage of 1. When $K = 30$, PL and, to a lesser degree, QP have much too low coverage for n up to 40, or even 100. This is exacerbated when 1/2 is added. Then the coverage of PL deteriorates dramatically. For $K = 30$, only KD provides good coverage for $n = 20$. The coverage of FPC “only” is satisfactory from $n = 40$, and from $n = 20$ for $p_{iC} \geq .2$. FPC “only” has somewhat higher coverage than FPC “always” for $n \leq 40$, but this is reversed from $n = 100$. QP works well from $n = 100$, and from $n = 20$ for $p_{iC} = .5$. We do not recommend FPU.

To summarize, KD and FPC intervals are recommended for use in practice.

6.2.4 Left coverage error (Appendix D)

A left coverage error (or “miss left”) occurs when the value of the parameter is to the left of the lower confidence limit of the confidence interval. For central confidence intervals the probability of this should be near the nominal 2.5% level.

When $p_{iC} = .1$, the observed miss-left probability is very close to zero for all estimators, for sample sizes up to 40, unless $\theta \geq 1.5$. KD is the only interval with non-zero, though also rather low, probability. For larger p_{iC} values, this probability is somewhat higher but still very low for $n \leq 40$. KD, FPU model and FPC “always” levels are closer to 2.5% from $n = 100$, and QP levels are typically lower than nominal when $p_{iC} = .1$ but improve for larger p_{iC} values. PL levels are especially low for all sample sizes.

6.2.5 Right coverage error (Appendix E)

A right coverage error (or “miss right”) occurs when the value of the parameter is to the right of the upper confidence limit of the confidence interval. For central confidence intervals, the miss-right probability should be near 2.5%.

For $p_{iC} = .1$, KD, QP “always”, and FPC “always” are the closest when $n = 20$ and $K = 5$, but they acquire some positive bias for larger n . FPC “only” and QP “only” are reasonably close to 2.5% from $n = 40$ when $K = 5$ or $K = 10$. KD is consistently close to 2.5% for $K = 10$. For $K = 30$, the results are more varied. KD, QP “only” and FPC “always” are close to 2.5% from $n = 100$. Miss-right probabilities for all other estimators are typically higher. PL has erratic levels, from 0 to above .1. For larger values of p_{iC} ,

the behavior of all estimators, with the exception of PL, improves earlier, so that KD, QP “only” and FPC “always” are all close to 2.5% when $n = 40$ and $p_{iC} = .5$, even when $K = 30$.

Acknowledgements

The work by E. Kulinskaya was supported by the Economic and Social Research Council [grant number ES/L011859/1].

References

- Ilyas Bakbergenuly, David C. Hoaglin, and Elena Kulinskaya. Estimation in meta-analyses of mean difference and standardized mean difference. *Statistics in Medicine*, 39(2):171–191, 2020a.
- Ilyas Bakbergenuly, David C. Hoaglin, and Elena Kulinskaya. Methods for estimating between-study variance and overall effect in meta-analysis of odds ratios. *Research Synthesis Methods*, 11(3):426–442, 2020b. doi: <https://doi.org/10.1002/jrsm.1404>. URL <https://onlinelibrary.wiley.com/doi/abs/10.1002/jrsm.1404>.
- Ilyas Bakbergenuly, David C. Hoaglin, and Elena Kulinskaya. On the Q statistic with constant weights for standardized mean difference. *British Journal of Mathematical and Statistical Psychology*, 2021. doi: <https://doi.org/10.1111/bmsp.12263>.
- George W. Brown. On small-sample estimation. *Annals of Mathematical Statistics*, 18: 582–585, 1947.
- William G. Cochran. The combination of estimates from different experiments. *Biometrics*, 10(1):101–129, 1954.
- Rebecca DerSimonian and Raghu Kacker. Random-effects model for meta-analysis of clinical trials: an update. *Contemporary Clinical Trials*, 28(2):105–114, 2007.
- Rebecca DerSimonian and Nan Laird. Meta-analysis in clinical trials. *Controlled Clinical Trials*, 7(3):177–188, 1986.
- R. W. Farebrother. Algorithm AS 204: The distribution of a positive linear combination of χ^2 random variables. *Journal of the Royal Statistical Society, Series C*, 33(3):332–339, 1984.
- John J. Gart, Hugh M. Pettigrew, and Donald G. Thomas. The effect of bias, variance estimation, skewness and kurtosis of the empirical logit on weighted least squares analyses. *Biometrika*, 72(1):179–190, 1985.
- Rebecca J. Hardy and Simon G. Thompson. A likelihood approach to meta-analysis with random effects. *Statistics in Medicine*, 15:619–629, 1996.

- Dan Jackson. Confidence intervals for the between-study variance in random effects meta-analysis using generalised Cochran heterogeneity statistics. *Research Synthesis Methods*, 4(3):220–229, 2013. doi: <https://doi.org/10.1002/jrsm.1081>.
- Elena Kulinskaya and Michael B. Dollinger. An accurate test for homogeneity of odds ratios based on Cochran’s Q -statistic. *BMC Medical Research Methodology*, 15(1):49, 2015.
- Elena Kulinskaya and David C. Hoaglin. R programs for estimation of heterogeneity variance τ^2 for log-odds-ratio using the generalised Q statistic with constant and inverse variance weights. OSF, <https://osf.io/5n3vd>, July 27 2022. URL osf.io/yqgsk.
- Elena Kulinskaya, David C. Hoaglin, and Ilyas Bakbergenuly. Exploring consequences of simulation design for apparent performance of methods of meta-analysis. *Statistical Methods in Medical Research*, 30(7):1667–1690, 2021a. doi: [10.1177/09622802211013065](https://doi.org/10.1177/09622802211013065). URL <https://doi.org/10.1177/09622802211013065>. PMID: 34110941.
- Elena Kulinskaya, David C. Hoaglin, Ilyas Bakbergenuly, and Joseph Newman. A Q statistic with constant weights for assessing heterogeneity in meta-analysis. *Research Synthesis Methods*, 12:711–730, 2021b. doi: <https://doi.org/10.1002/jrsm.1491>.
- John Mandel and Robert C. Paule. Interlaboratory evaluation of a material with unequal numbers of replicates. *Analytical Chemistry*, 42(11):1194–1197, 1970.
- R Core Team. *R: A Language and Environment for Statistical Computing*. R Foundation for Statistical Computing, Vienna, Austria, 2016. URL <https://www.R-project.org/>.
- Julio Sánchez-Meca and Fulgencio Marín-Martínez. Testing the significance of a common risk difference in meta-analysis. *Computational Statistics & Data Analysis*, 33(3):299–313, 2000.
- Wolfgang Viechtbauer. Confidence intervals for the amount of heterogeneity in meta-analysis. *Statistics in Medicine*, 26(1):37–52, 2007.
- Wolfgang Viechtbauer. Conducting meta-analyses in R with the metafor package. *Journal of Statistical Software*, 36:3, 2010. URL <https://doi.org/10.18637/jss.v036.i03>. Website: <https://www.metafor-project.org>.

Wolfgang Viechtbauer. Median-unbiased estimators for the amount of heterogeneity in meta-analysis. 9th European Congress of Methodology. European Association of Methodology, 2021. URL https://www.wvbauer.com/lib/exe/fetch.php/talks:2021_viechtbauer_eam_median_tau2.pdf.

Appendices

- Appendix A: Bias in point estimators of between-study variance
- Appendix B: Median bias in point estimators of between-study variance
- Appendix C: Coverage of 95% confidence intervals for between-study variance
- Appendix D: Sample miss-left probability for 95% confidence intervals for between-study variance
- Appendix E: Sample miss-right probability for 95% confidence intervals for between-study variance

Appendix A: Bias in point estimators of between-study variance

Each figure corresponds to a value of the probability of an event in the Control arm p_{iC} ($= .1, .2, .5$).

The fraction of each study's sample size in the Control arm (f) is held constant at 0.5. For each combination of a value of n ($= 20, 40, 100, 250$) or \bar{n} ($= 30, 60, 100, 160$) and a value of K ($= 5, 10, 30$), a panel plots bias versus τ^2 ($= 0.0(0.1)1$).

The point estimators of τ^2 are

- DL (DerSimonian-Laird method, inverse-variance weights)
- REML method, inverse-variance weights)
- MP (Mandel-Paule method, inverse-variance weights)
- KD (Kulinskaya-Dollinger (2015) approximation, inverse-variance weights)
- SSC method, effective-sample-size weights, conditional variance of LOR
- SMC method, median-unbiased, effective-sample-size weights, conditional variance of LOR
- SSU method, effective-sample-size weights, unconditional variance of LOR
- SMU method, median-unbiased, effective-sample-size weights, unconditional variance of LOR

The plots include two versions of DL, REML, MP, SSC, and SMC: adding 1/2 to all four of X_{iT} , X_{iC} , $n_{iT} - X_{iT}$, $n_{iC} - X_{iC}$ only when one of these is zero (solid lines) or always (dashed lines).

Plots also include two versions of SSU and SMU: model-based estimation of p_{iT} (solid lines) or naïve estimation (dashed lines).

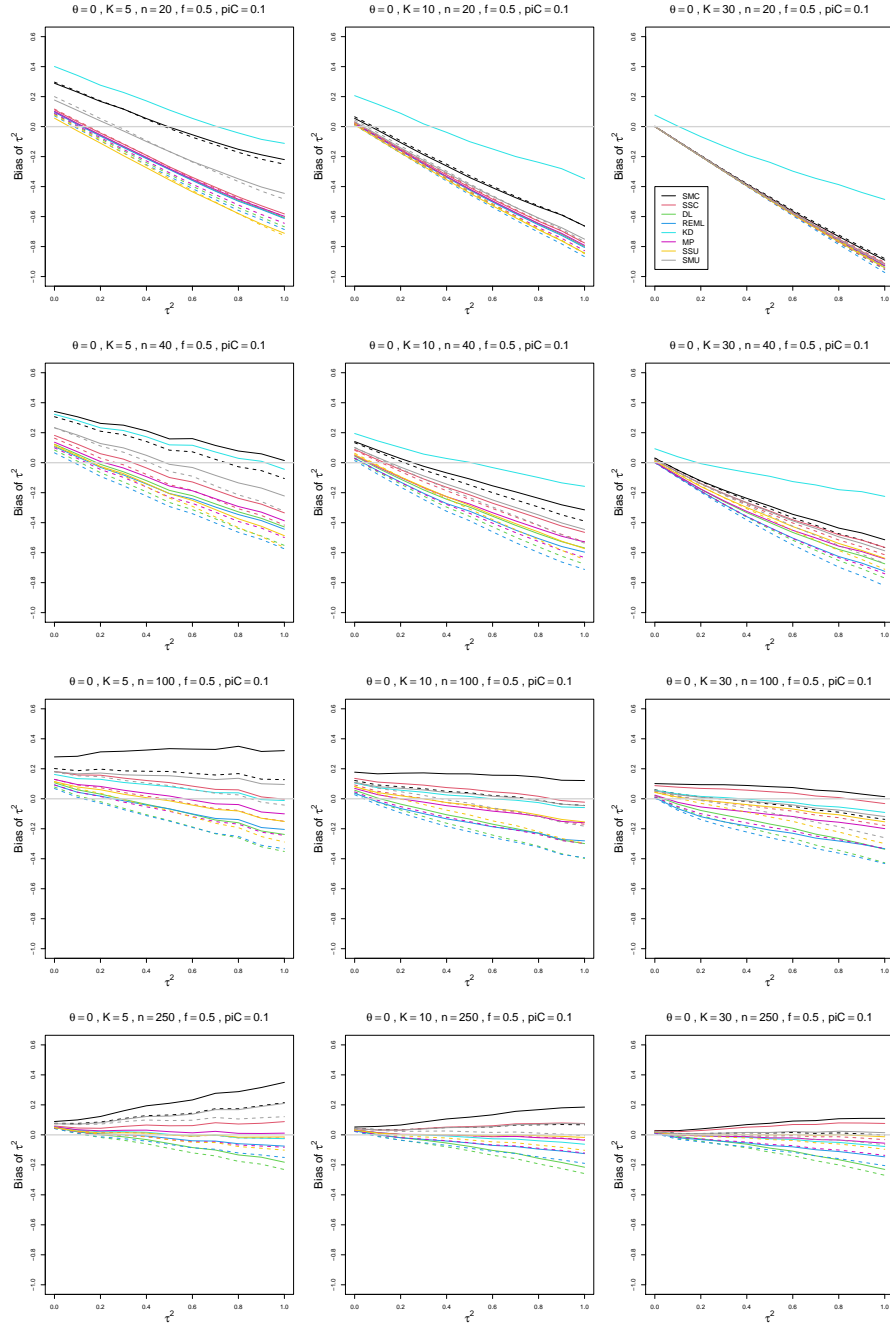


Figure A.1: Bias of estimators of between-study variance of LOR (DL, REML, KD, MP, SMC, SSC, SMU, and SSU) vs τ^2 , for equal sample sizes $n = 20, 40, 100$ and 250 , $p_{iC} = .1$, $\theta = 0$ and $f = 0.5$. Solid lines: DL, REML, MP, SSC, SMC “only”; KD; SSU and SMU model-based. Dashed lines: DL, REML, MP, SSC, SMC “always”; SSU and SMU naïve.

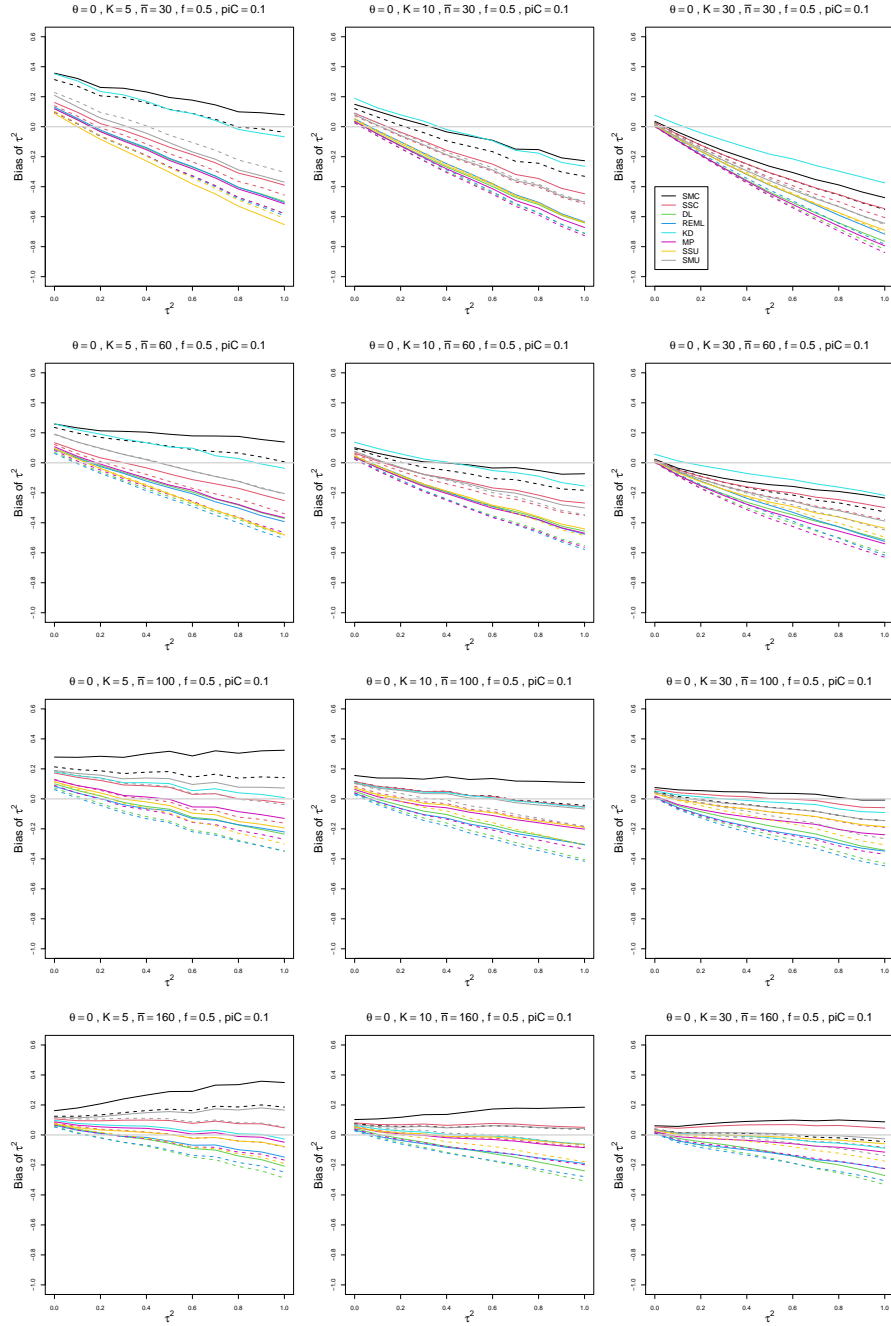


Figure A.2: Bias of estimators of between-study variance of LOR (DL, REML, KD, MP, SMC, SSC, SMU, and SSU) vs τ^2 , for unequal sample sizes $\bar{n} = 30, 60, 100$ and 160 , $p_{iC} = .1$, $\theta = 0$ and $f = 0.5$. Solid lines: DL, REML, MP, SSC, SMC “only”; KD; SSU and SMU model-based. Dashed lines: DL, REML, MP, SSC, SMC “always”; SSU and SMU naïve.

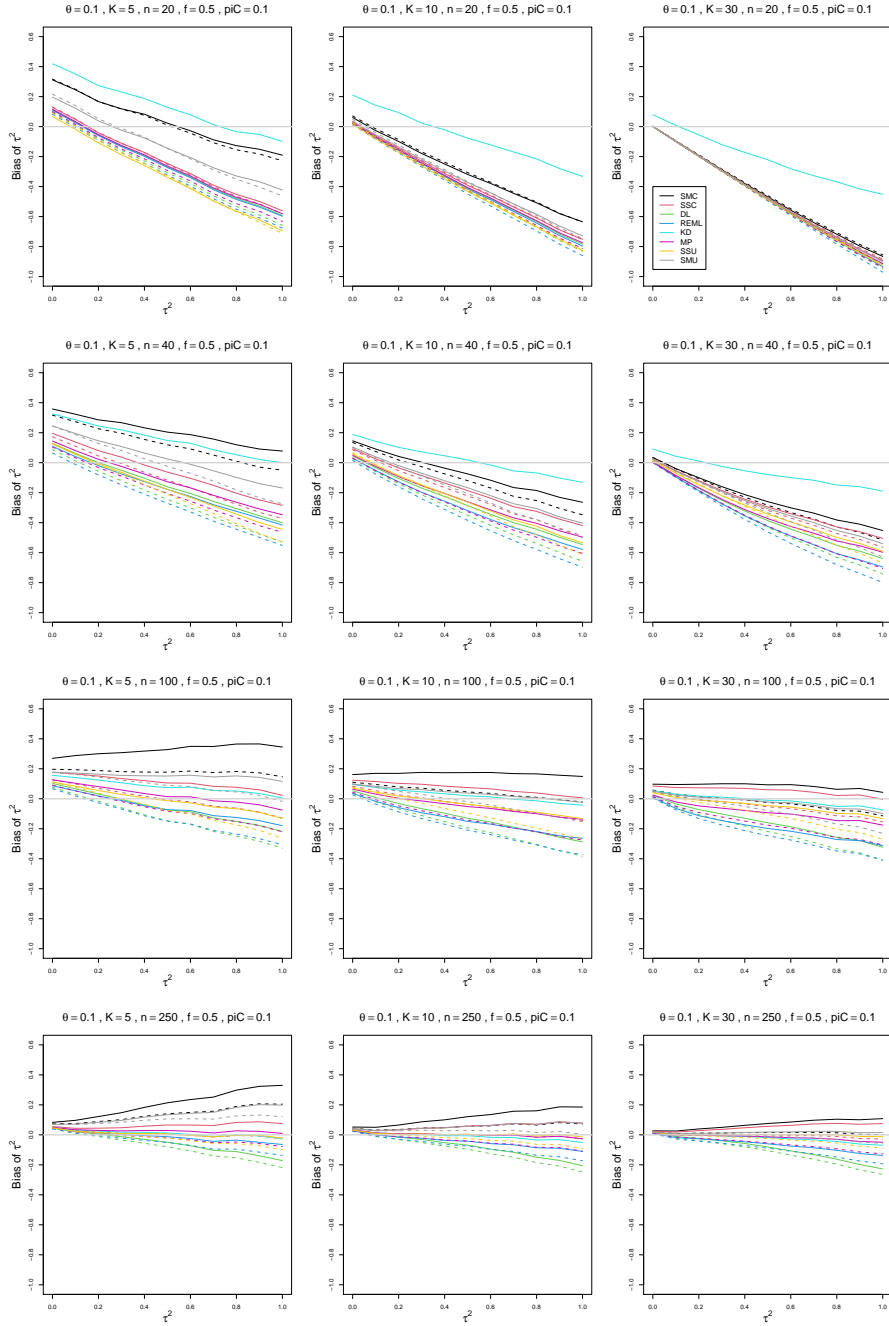


Figure A.3: Bias of estimators of between-study variance of LOR (DL, REML, KD, MP, SMC, SSC, SMU, and SSU) vs τ^2 , for equal sample sizes $n = 20, 40, 100$ and 250 , $p_{iC} = .1$, $\theta = 0.1$ and $f = 0.5$. Solid lines: DL, REML, MP, SSC, SMC “only”; KD; SSU and SMU model-based. Dashed lines: DL, REML, MP, SSC, SMC “always”; SSU and SMU naïve.

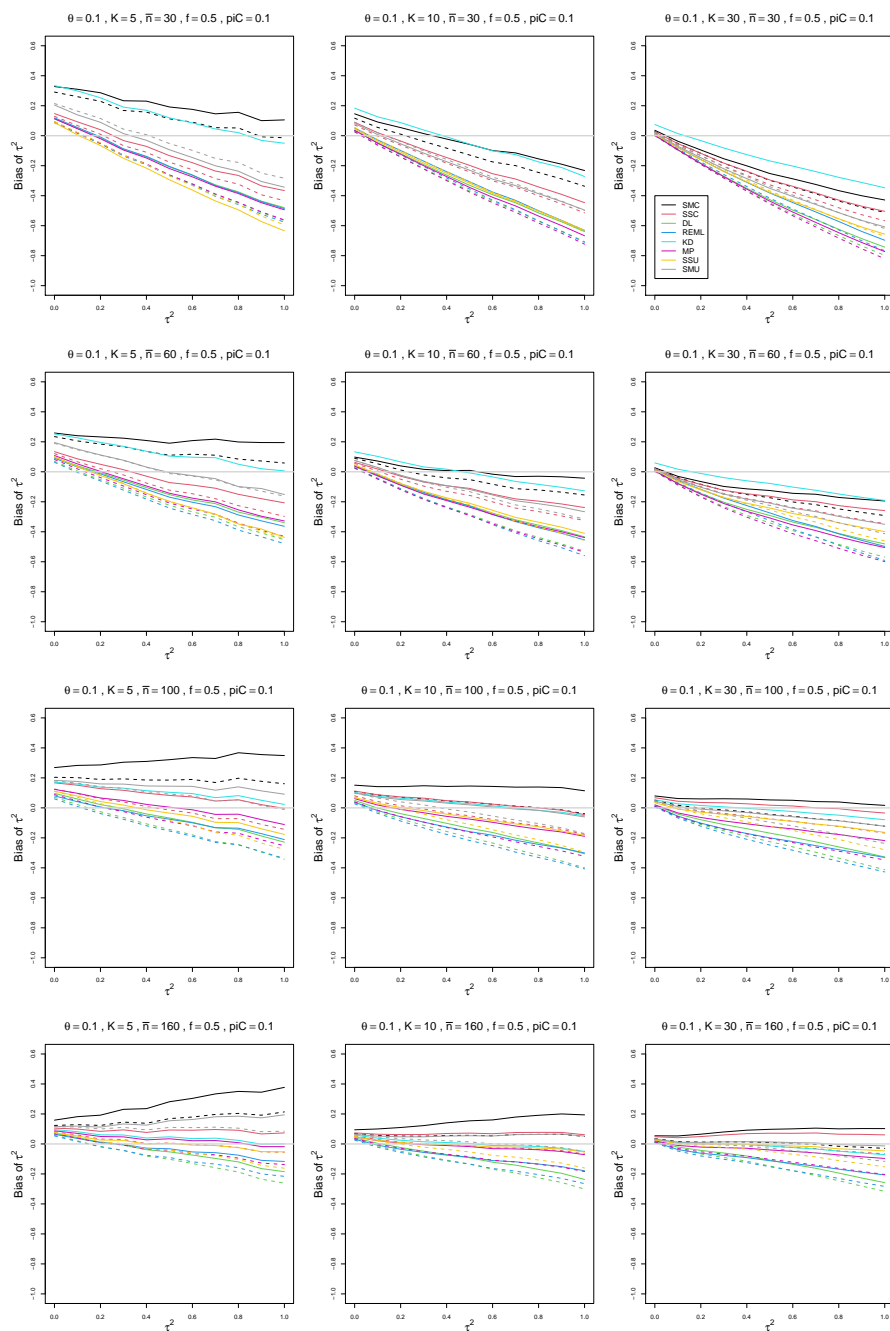


Figure A.4: Bias of estimators of between-study variance of LOR (DL, REML, KD, MP, SMC, SSC, SMU, and SSU) vs τ^2 , for unequal sample sizes $\bar{n} = 30, 60, 100$ and 160 , $p_{iC} = .1$, $\theta = 0.1$ and $f = 0.5$. Solid lines: DL, REML, MP, SSC, SMC “only”; KD; SSU and SMU model-based. Dashed lines: DL, REML, MP, SSC, SMC “always”; SSU and SMU naïve.

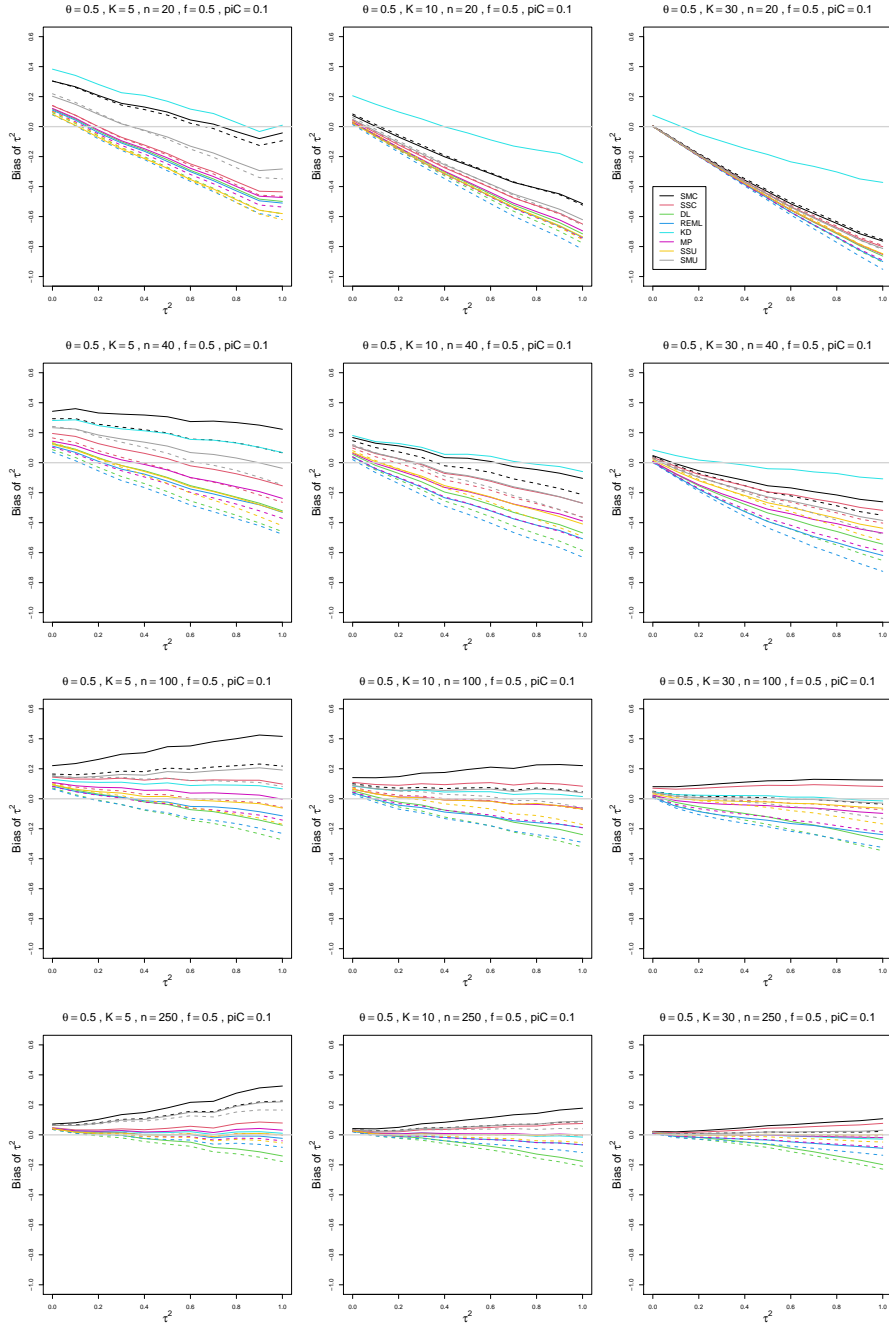


Figure A.5: Bias of estimators of between-study variance of LOR (DL, REML, KD, MP, SMC, SSC, SMU, and SSU) vs τ^2 , for equal sample sizes $n = 20, 40, 100$ and 250 , $p_{iC} = .1$, $\theta = 0.5$ and $f = 0.5$. Solid lines: DL, REML, MP, SSC, SMC “only”; KD; SSU and SMU model-based. Dashed lines: DL, REML, MP, SSC, SMC “always”; SSU and SMU naïve.

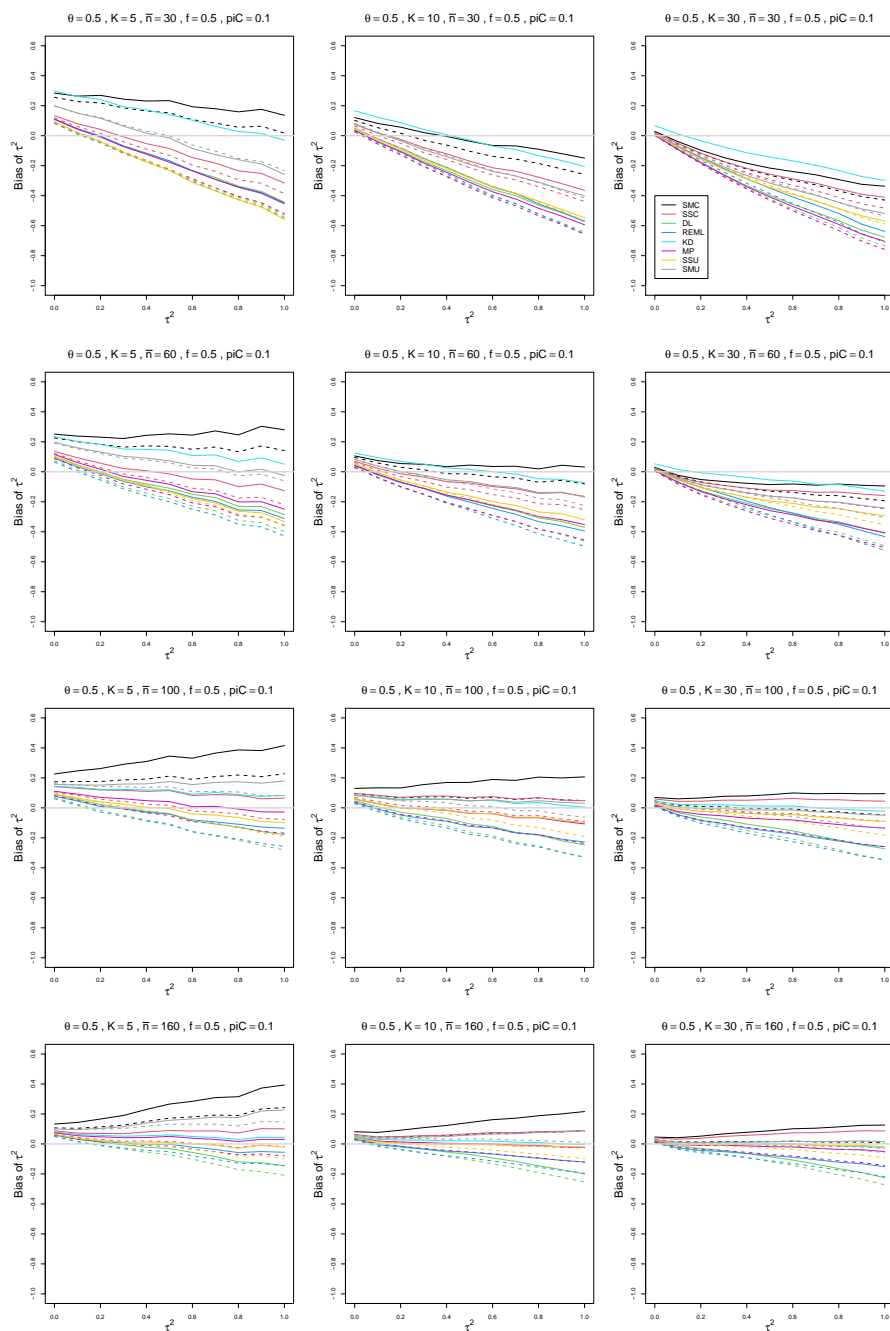


Figure A.6: Bias of estimators of between-study variance of LOR (DL, REML, KD, MP, SMC, SSC, SMU, and SSU) vs τ^2 , for unequal sample sizes $\bar{n} = 30, 60, 100$ and 160 , $p_{iC} = .1$, $\theta = 0.5$ and $f = 0.5$. Solid lines: DL, REML, MP, SSC, SMC “only”; KD; SSU and SMU model-based. Dashed lines: DL, REML, MP, SSC, SMC “always”; SSU and SMU naïve.

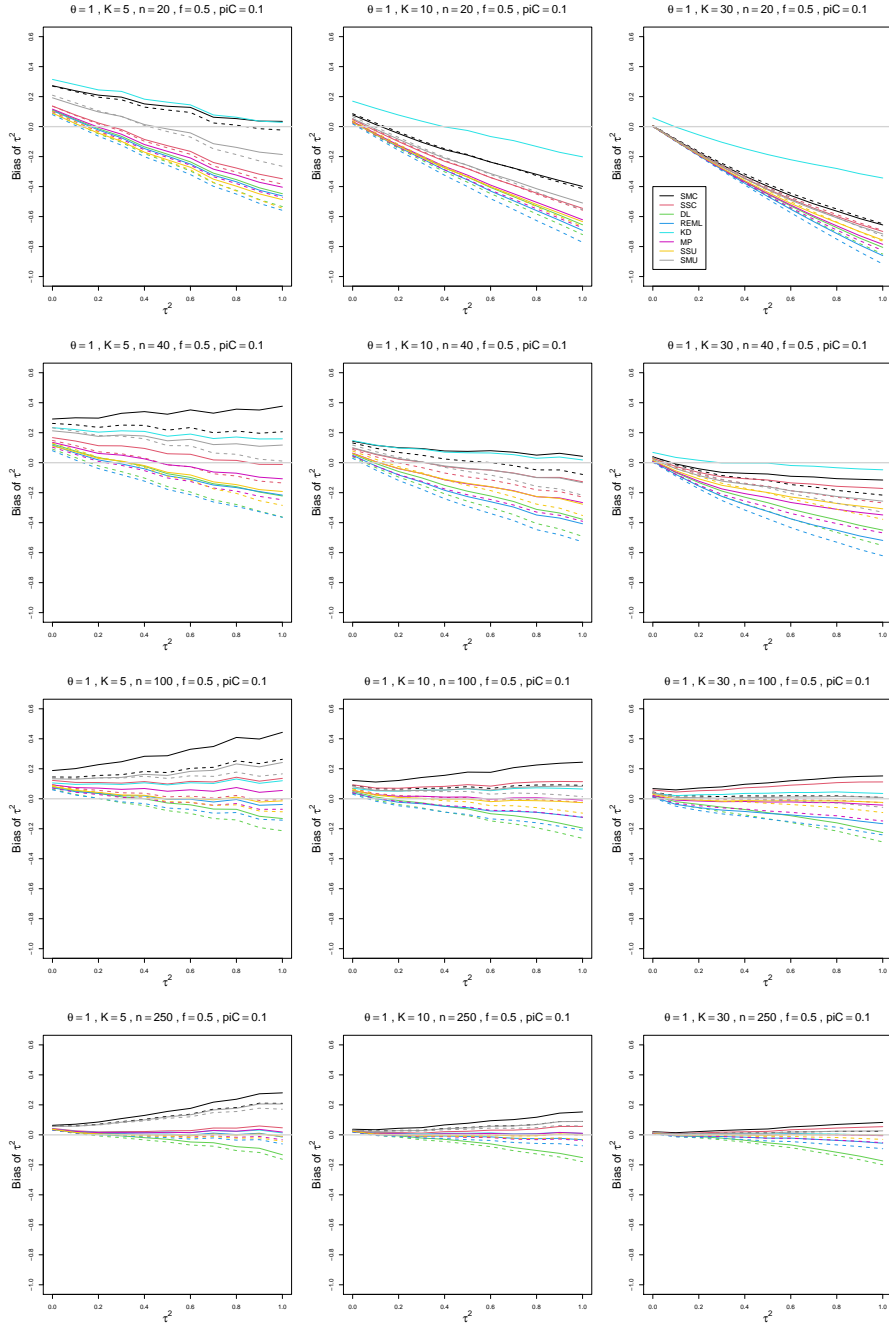


Figure A.7: Bias of estimators of between-study variance of LOR (DL, REML, KD, MP, SMC, SSC, SMU, and SSU) vs τ^2 , for equal sample sizes $n = 20, 40, 100$ and 250 , $p_{iC} = .1$, $\theta = 1$ and $f = 0.5$. Solid lines: DL, REML, MP, SSC, SMC “only”; KD; SSU and SMU model-based. Dashed lines: DL, REML, MP, SSC, SMC “always”; SSU and SMU naïve.

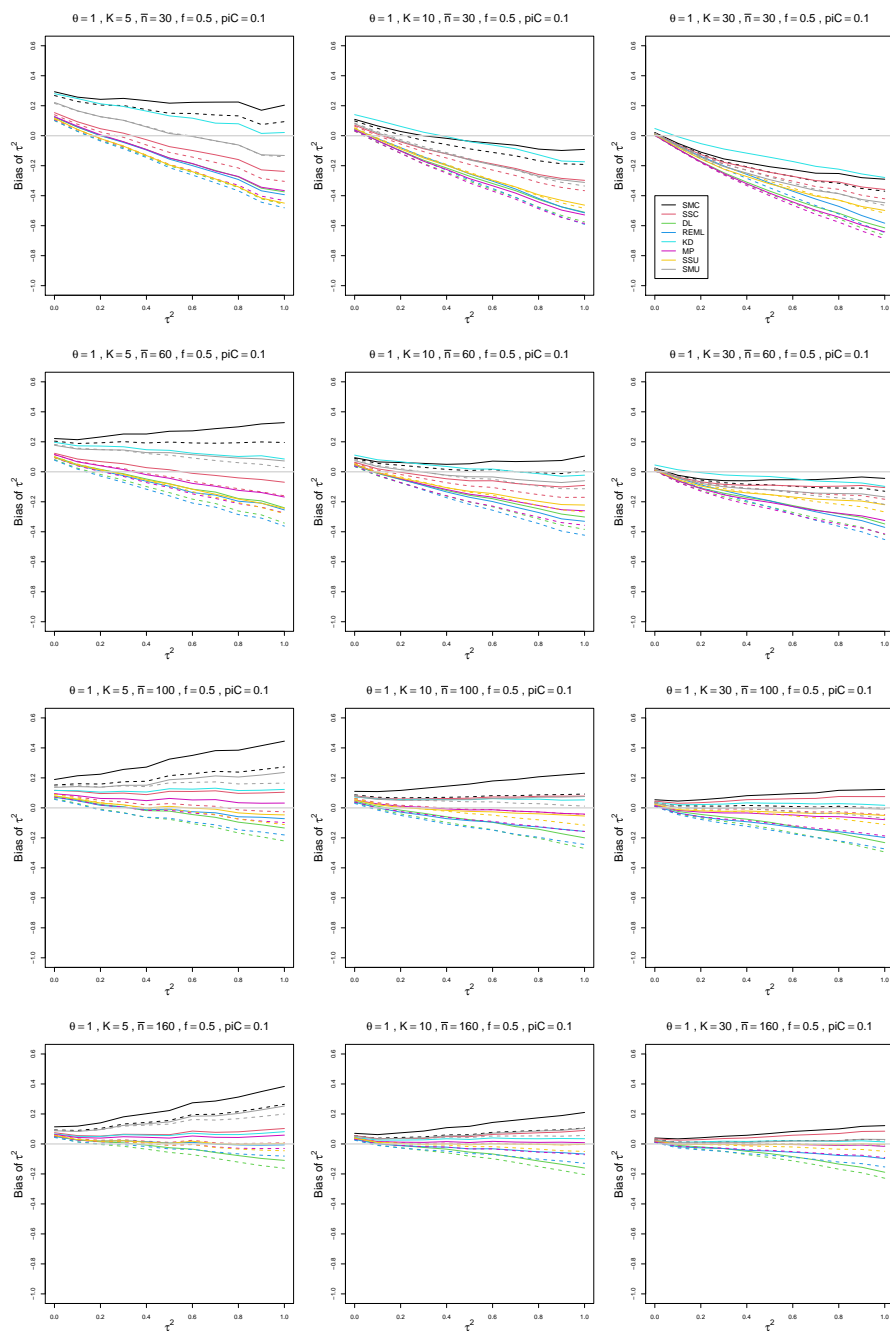


Figure A.8: Bias of estimators of between-study variance of LOR (DL, REML, KD, MP, SMC, SSC, SMU, and SSU) vs τ^2 , for unequal sample sizes $\bar{n} = 30, 60, 100$ and 160 , $p_{iC} = .1$, $\theta = 1$ and $f = 0.5$. Solid lines: DL, REML, MP, SSC, SMC “only”; KD; SSU and SMU model-based. Dashed lines: DL, REML, MP, SSC, SMC “always”; SSU and SMU naïve.

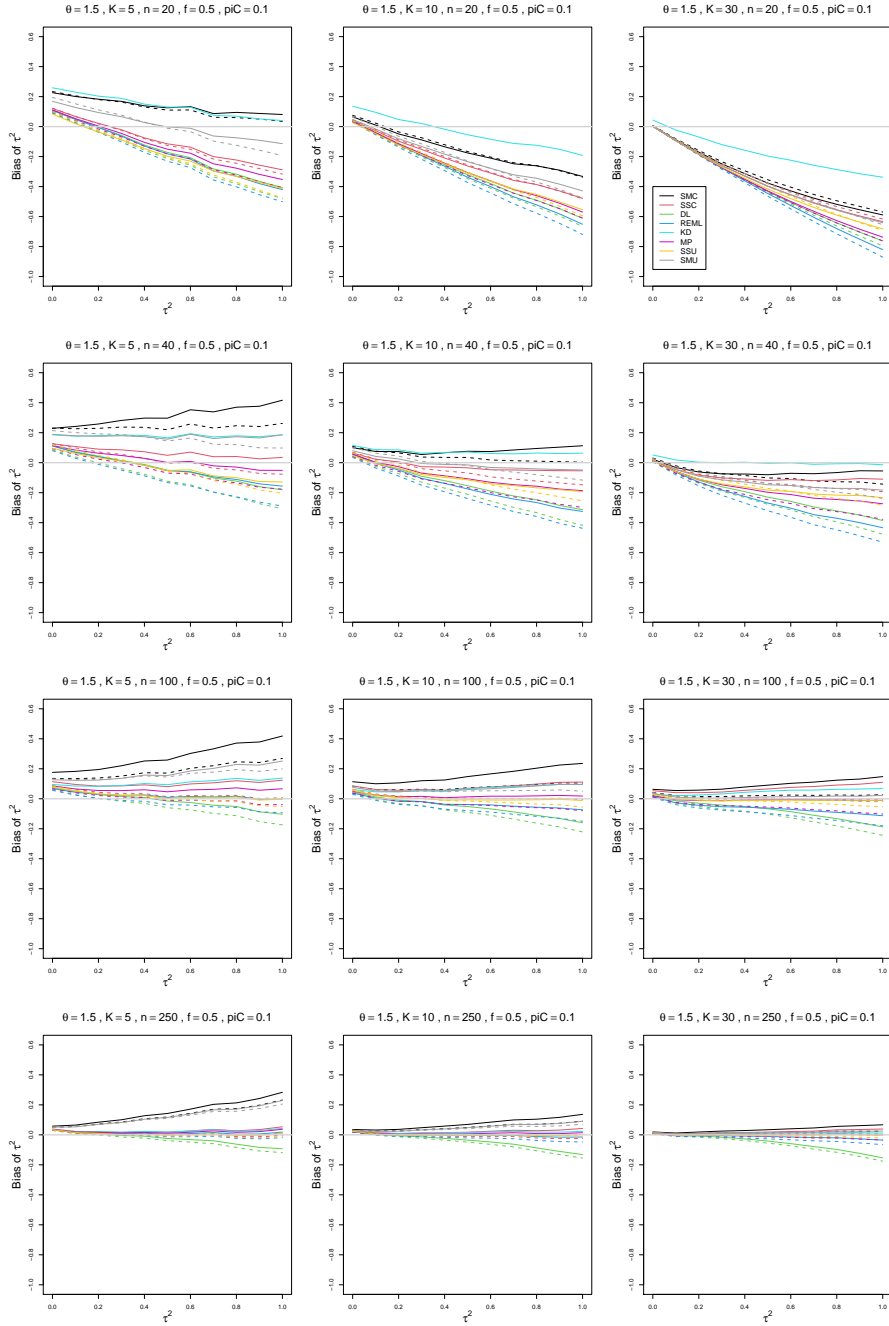


Figure A.9: Bias of estimators of between-study variance of LOR (DL, REML, KD, MP, SMC, SSC, SMU, and SSU) vs τ^2 , for equal sample sizes $n = 20, 40, 100$ and 250 , $p_{iC} = .1$, $\theta = 1.5$ and $f = 0.5$. Solid lines: DL, REML, MP, SSC, SMC “only”; KD; SSU and SMU model-based. Dashed lines: DL, REML, MP, SSC, SMC “always”; SSU and SMU naïve.

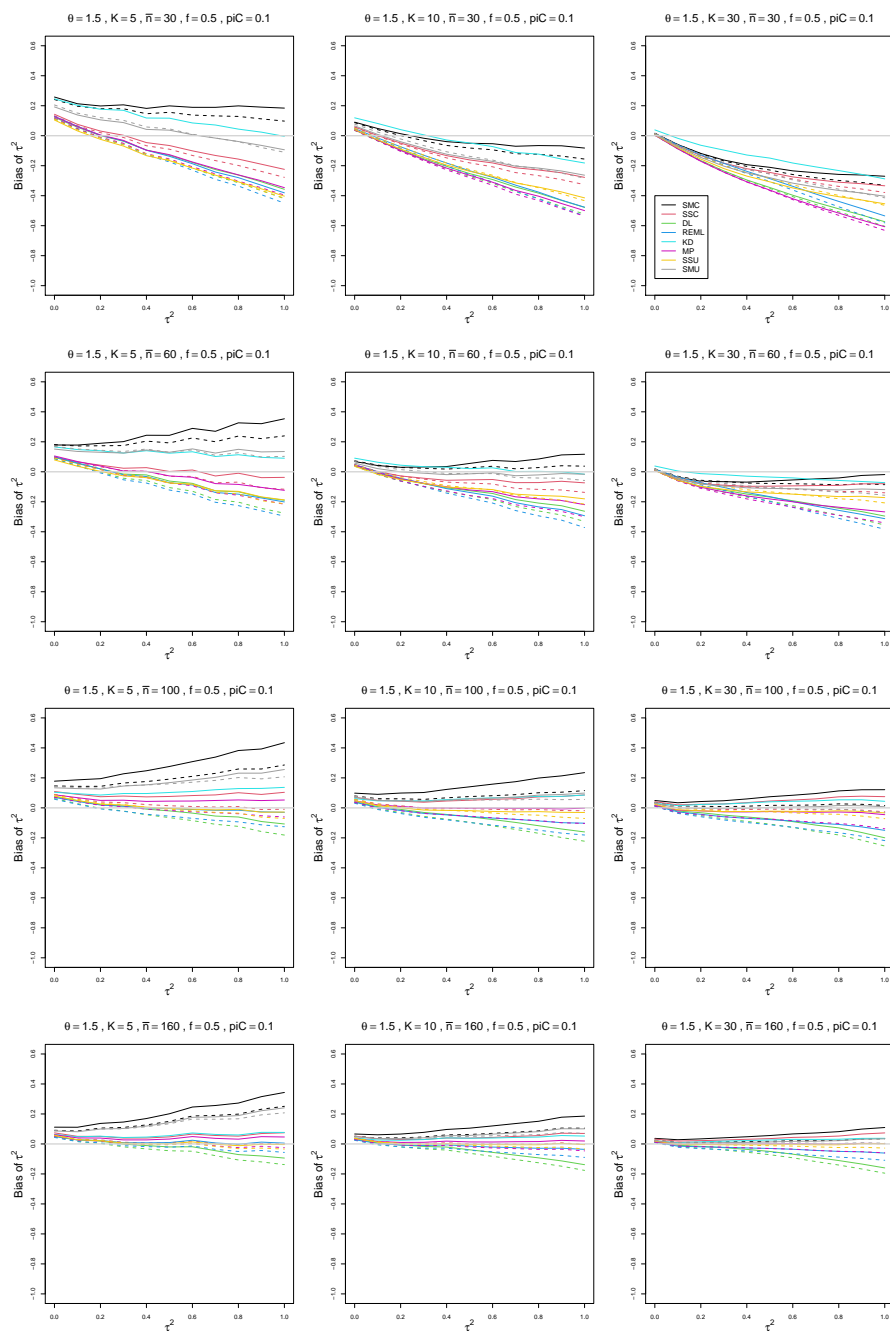


Figure A.10: Bias of estimators of between-study variance of LOR (DL, REML, KD, MP, SMC, SSC, SMU, and SSU) vs τ^2 , for unequal sample sizes $\bar{n} = 30, 60, 100$ and 160 , $p_{iC} = .1$, $\theta = 1.5$ and $f = 0.5$. Solid lines: DL, REML, MP, SSC, SMC “only”; KD; SSU and SMU model-based. Dashed lines: DL, REML, MP, SSC, SMC “always”; SSU and SMU naïve.

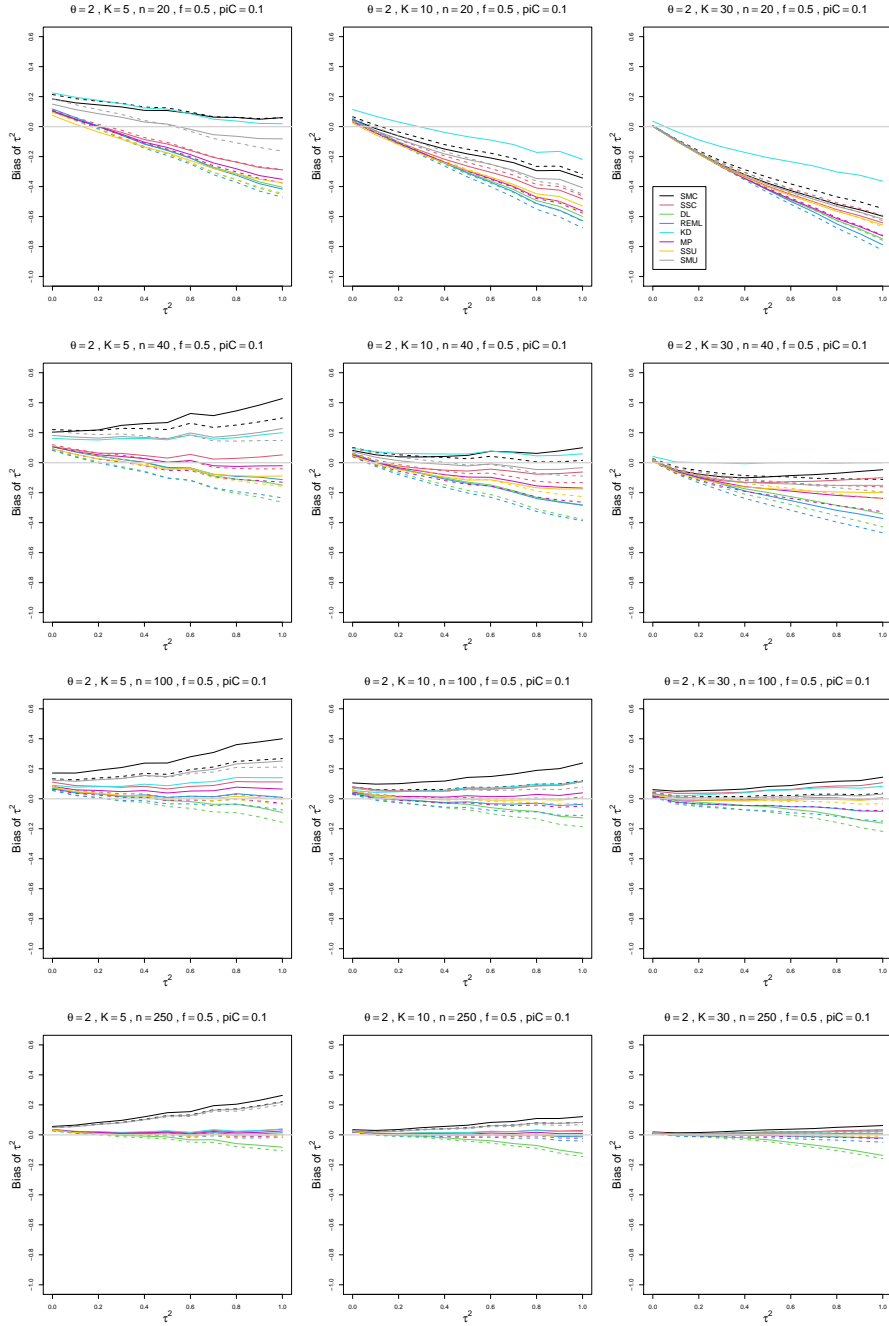


Figure A.11: Bias of estimators of between-study variance of LOR (DL, REML, KD, MP, SMC, SSC, SMU, and SSU) vs τ^2 , for equal sample sizes $n = 20, 40, 100$ and 250 , $p_{iC} = .1$, $\theta = 2$ and $f = 0.5$. Solid lines: DL, REML, MP, SSC, SMC “only”; KD; SSU and SMU model-based. Dashed lines: DL, REML, MP, SSC, SMC “always”; SSU and SMU naïve.

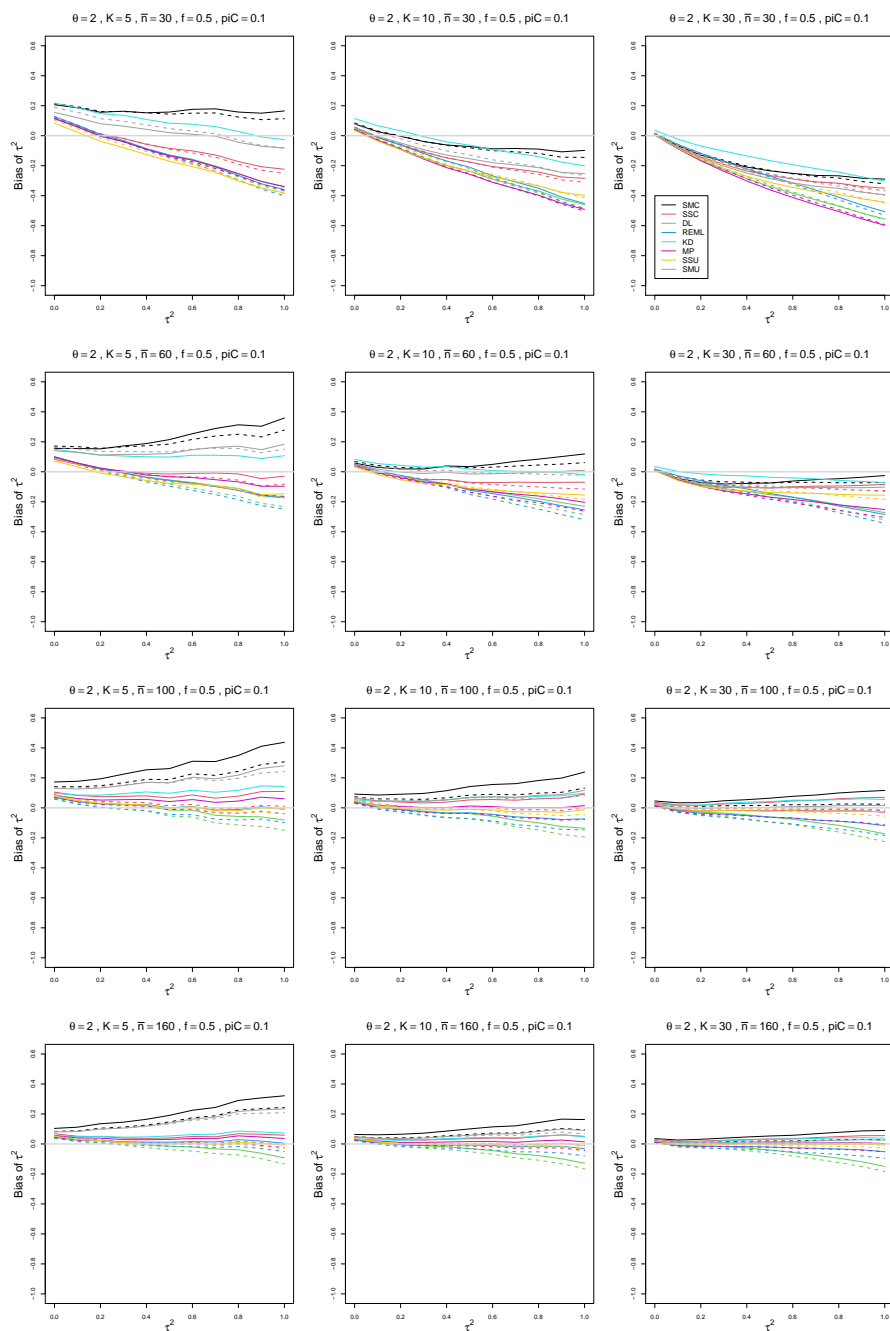


Figure A.12: Bias of estimators of between-study variance of LOR (DL, REML, KD, MP, SMC, SSC, SMU, and SSU) vs τ^2 , for unequal sample sizes $\bar{n} = 30, 60, 100$ and 160 , $p_{iC} = .1$, $\theta = 2$ and $f = 0.5$. Solid lines: DL, REML, MP, SSC, SMC “only”; KD; SSU and SMU model-based. Dashed lines: DL, REML, MP, SSC, SMC “always”; SSU and SMU naïve.

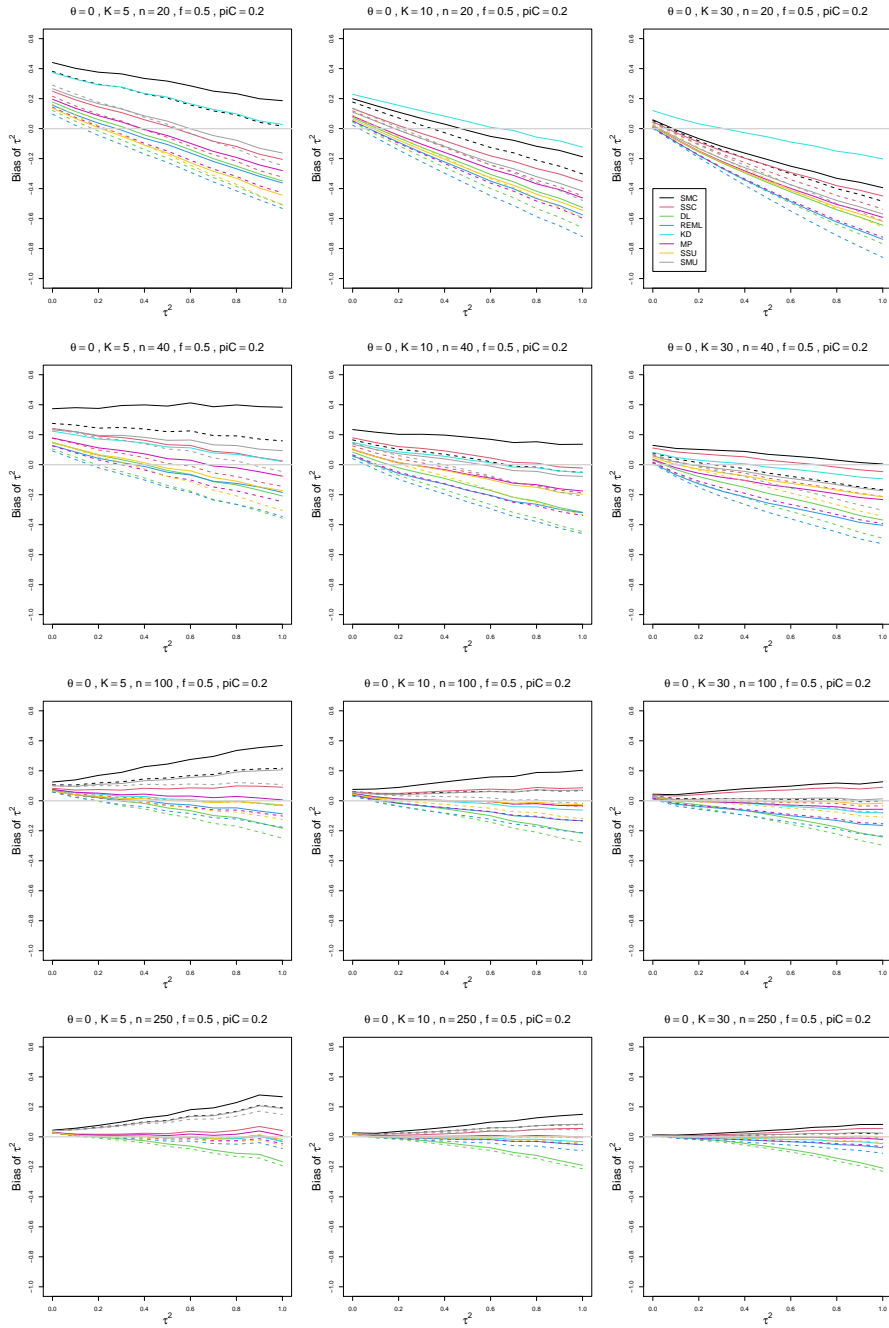


Figure A.13: Bias of estimators of between-study variance of LOR (DL, REML, KD, MP, SMC, SSC, SMU, and SSU) vs τ^2 , for equal sample sizes $n = 20, 40, 100$ and 250 , $p_{iC} = .2$, $\theta = 0$ and $f = 0.5$. Solid lines: DL, REML, MP, SSC, SMC “only”; KD; SSU and SMU model-based. Dashed lines: DL, REML, MP, SSC, SMC “always”; SSU and SMU naïve.

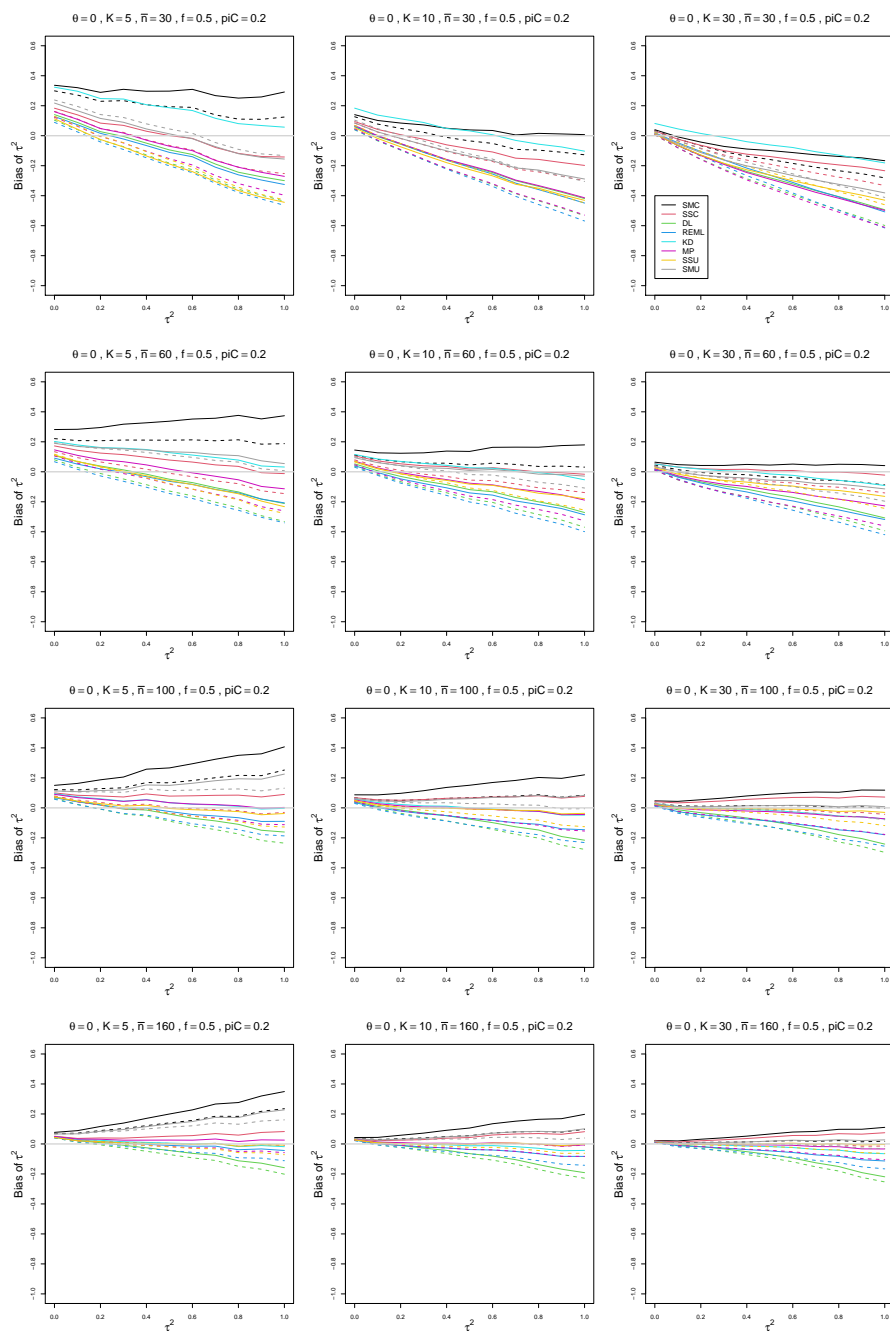


Figure A.14: Bias of estimators of between-study variance of LOR (DL, REML, KD, MP, SMC, SSC, SMU, and SSU) vs τ^2 , for unequal sample sizes $\bar{n} = 30, 60, 100$ and 160 , $p_{iC} = .2$, $\theta = 0$ and $f = 0.5$. Solid lines: DL, REML, MP, SSC, SMC “only”; KD; SSU and SMU model-based. Dashed lines: DL, REML, MP, SSC, SMC “always”; SSU and SMU naïve.

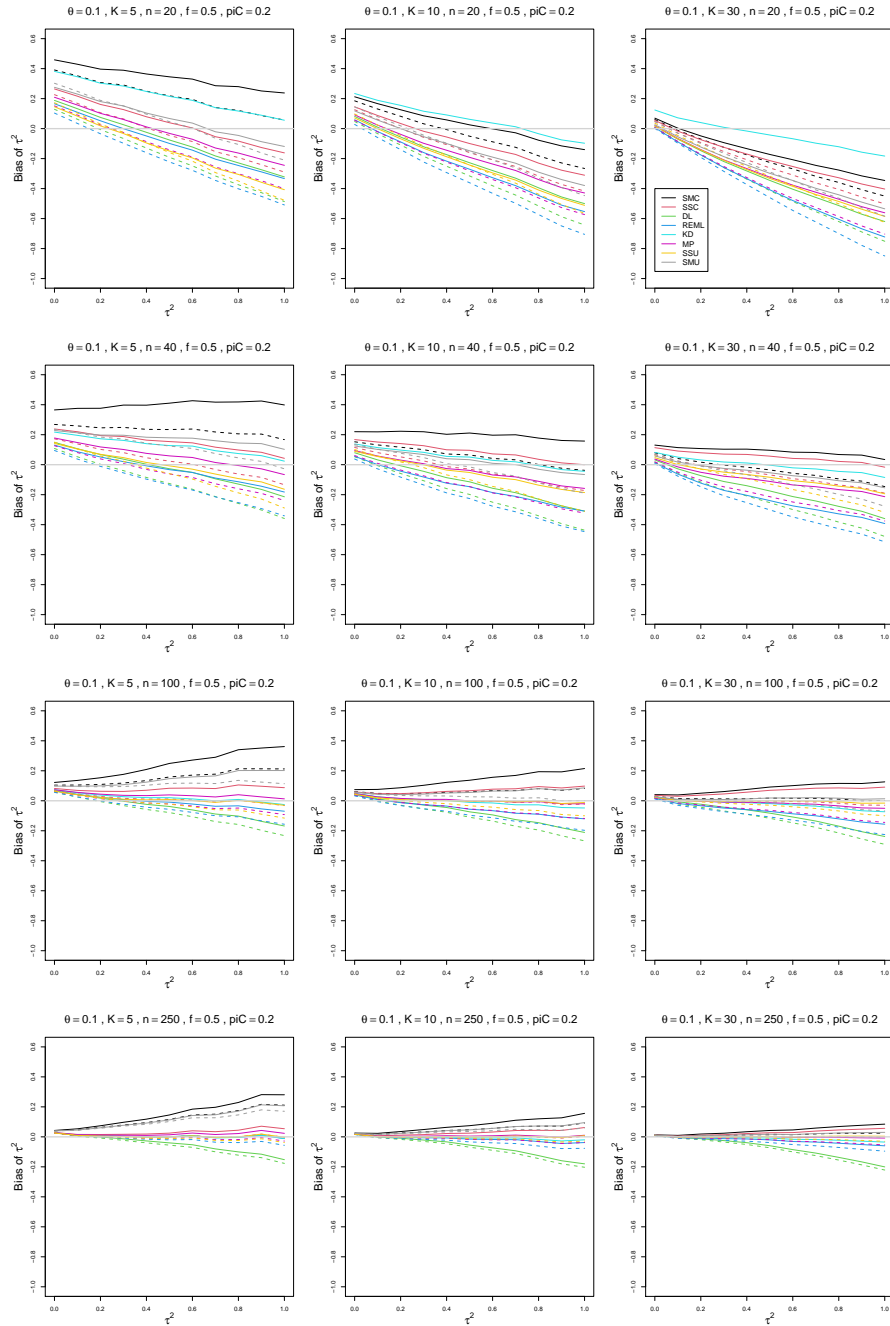


Figure A.15: Bias of estimators of between-study variance of LOR (DL, REML, KD, MP, SMC, SSC, SMU, and SSU) vs τ^2 , for equal sample sizes $n = 20, 40, 100$ and 250 , $p_{iC} = .2$, $\theta = 0.1$ and $f = 0.5$. Solid lines: DL, REML, MP, SSC, SMC “only”; KD; SSU and SMU model-based. Dashed lines: DL, REML, MP, SSC, SMC “always”; SSU and SMU naïve.

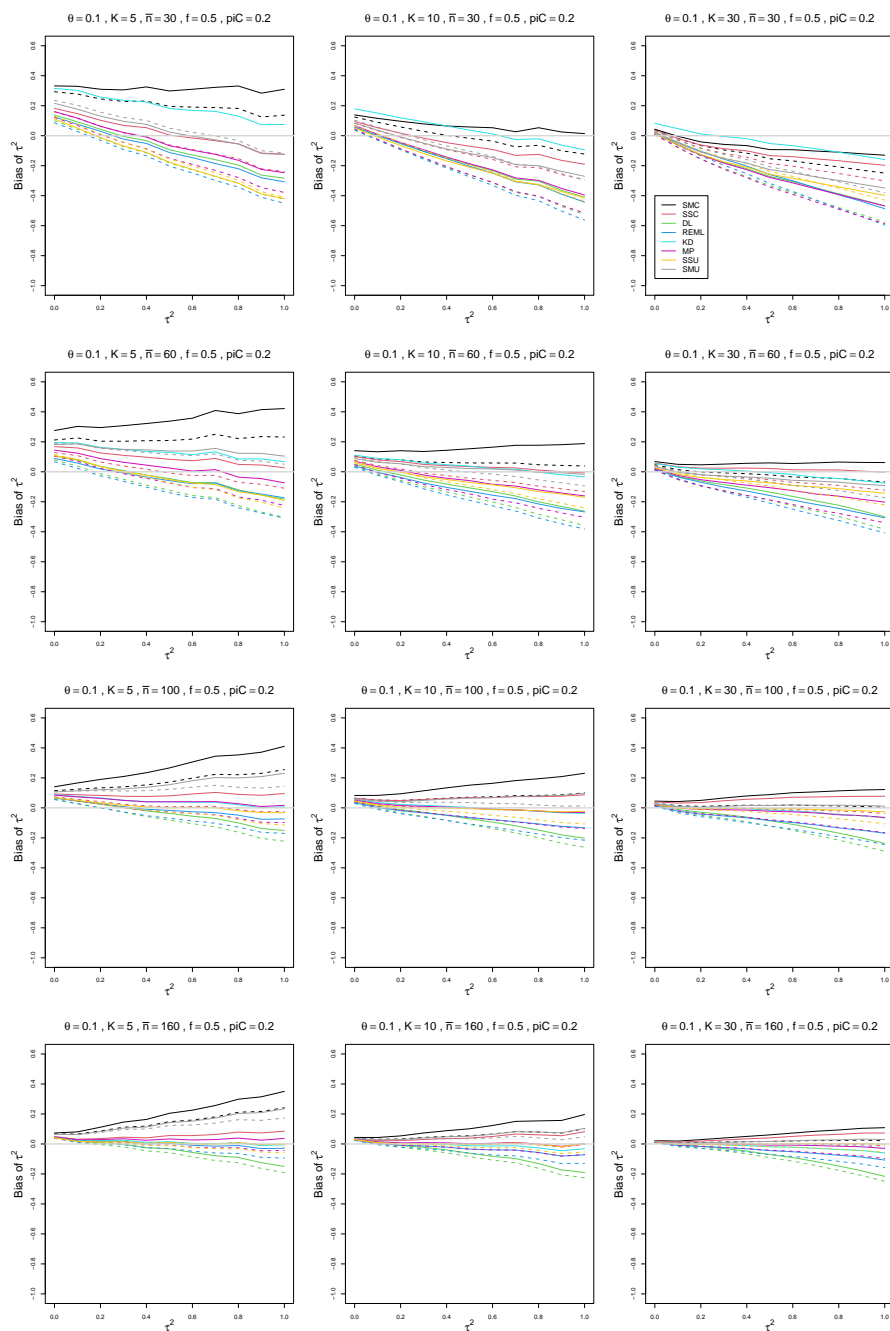


Figure A.16: Bias of estimators of between-study variance of LOR (DL, REML, KD, MP, SMC, SSC, SMU, and SSU) vs τ^2 , for unequal sample sizes $\bar{n} = 30, 60, 100$ and 160 , $p_{iC} = .2$, $\theta = 0.1$ and $f = 0.5$. Solid lines: DL, REML, MP, SSC, SMC “only”; KD; SSU and SMU model-based. Dashed lines: DL, REML, MP, SSC, SMC “always”; SSU and SMU naïve.

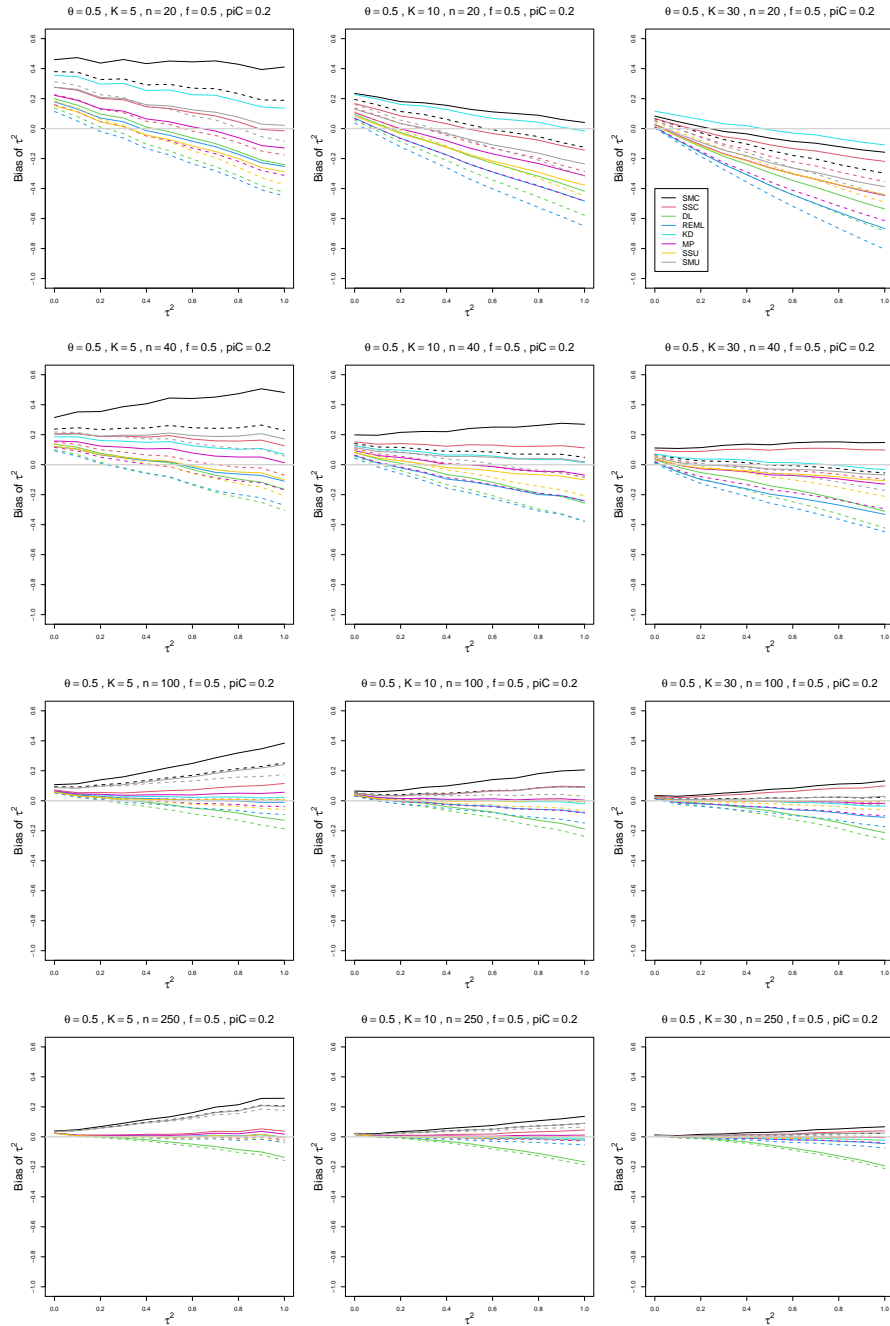


Figure A.17: Bias of estimators of between-study variance of LOR (DL, REML, KD, MP, SMC, SSC, SMU, and SSU) vs τ^2 , for equal sample sizes $n = 20, 40, 100$ and 250 , $p_{iC} = .2$, $\theta = 0.5$ and $f = 0.5$. Solid lines: DL, REML, MP, SSC, SMC “only”; KD; SSU and SMU model-based. Dashed lines: DL, REML, MP, SSC, SMC “always”; SSU and SMU naïve.

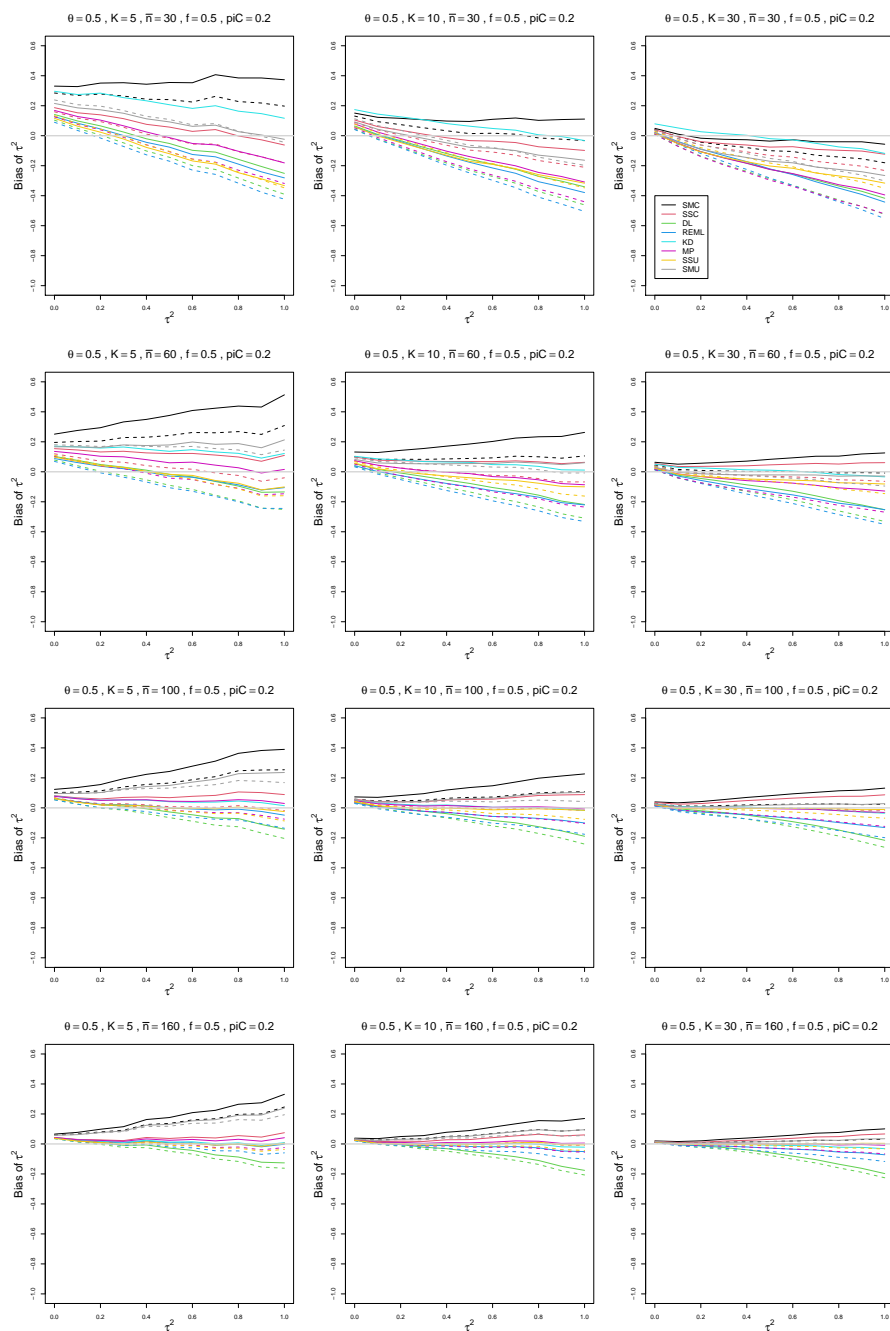


Figure A.18: Bias of estimators of between-study variance of LOR (DL, REML, KD, MP, SMC, SSC, SMU, and SSU) vs τ^2 , for unequal sample sizes $\bar{n} = 30, 60, 100$ and 160 , $p_{iC} = .2$, $\theta = 0.5$ and $f = 0.5$. Solid lines: DL, REML, MP, SSC, SMC “only”; KD; SSU and SMU model-based. Dashed lines: DL, REML, MP, SSC, SMC “always”; SSU and SMU naïve.

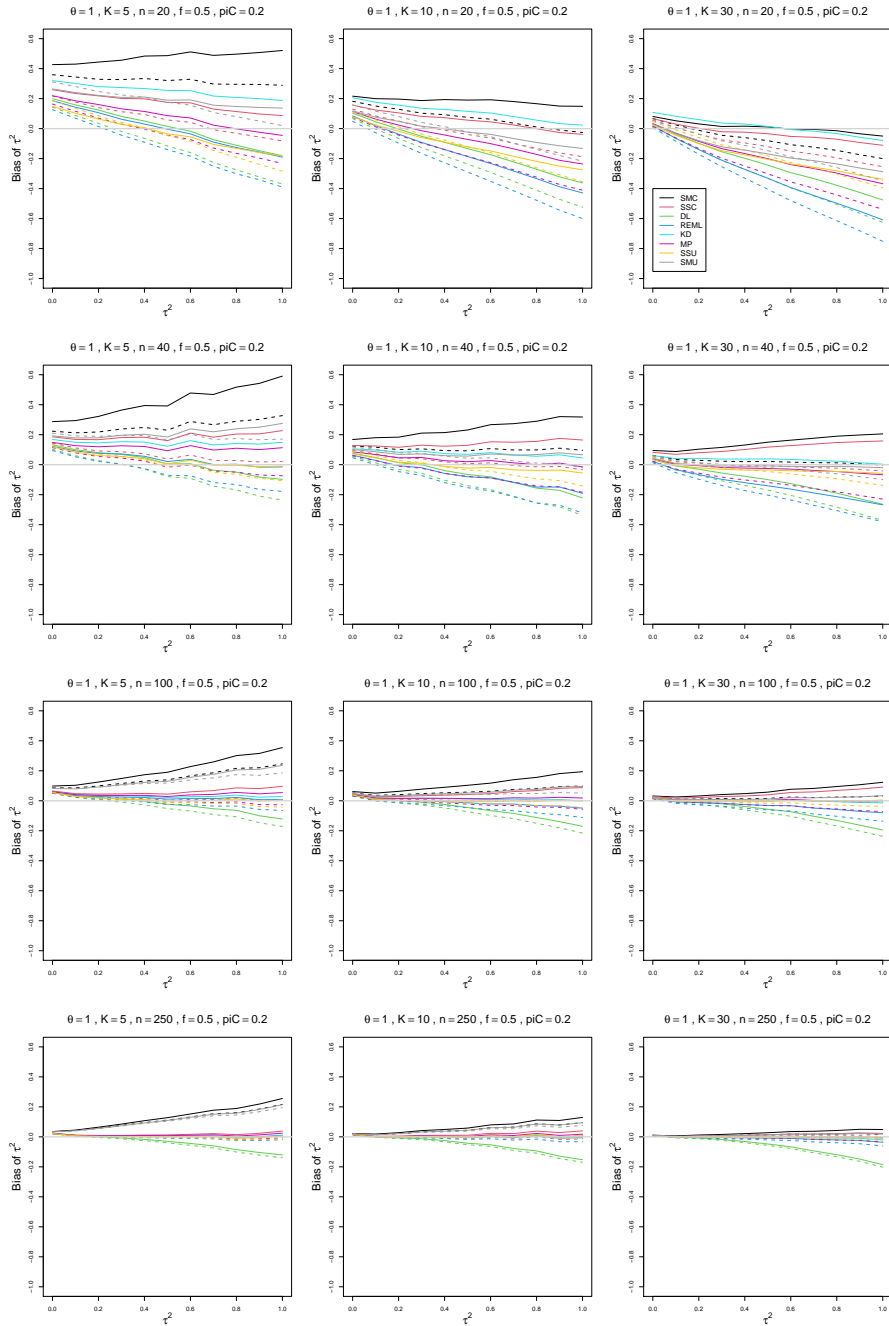


Figure A.19: Bias of estimators of between-study variance of LOR (DL, REML, KD, MP, SMC, SSC, SMU, and SSU) vs τ^2 , for equal sample sizes $n = 20, 40, 100$ and 250 , $p_{iC} = .2$, $\theta = 1$ and $f = 0.5$. Solid lines: DL, REML, MP, SSC, SMC “only”; KD; SSU and SMU model-based. Dashed lines: DL, REML, MP, SSC, SMC “always”; SSU and SMU naïve.

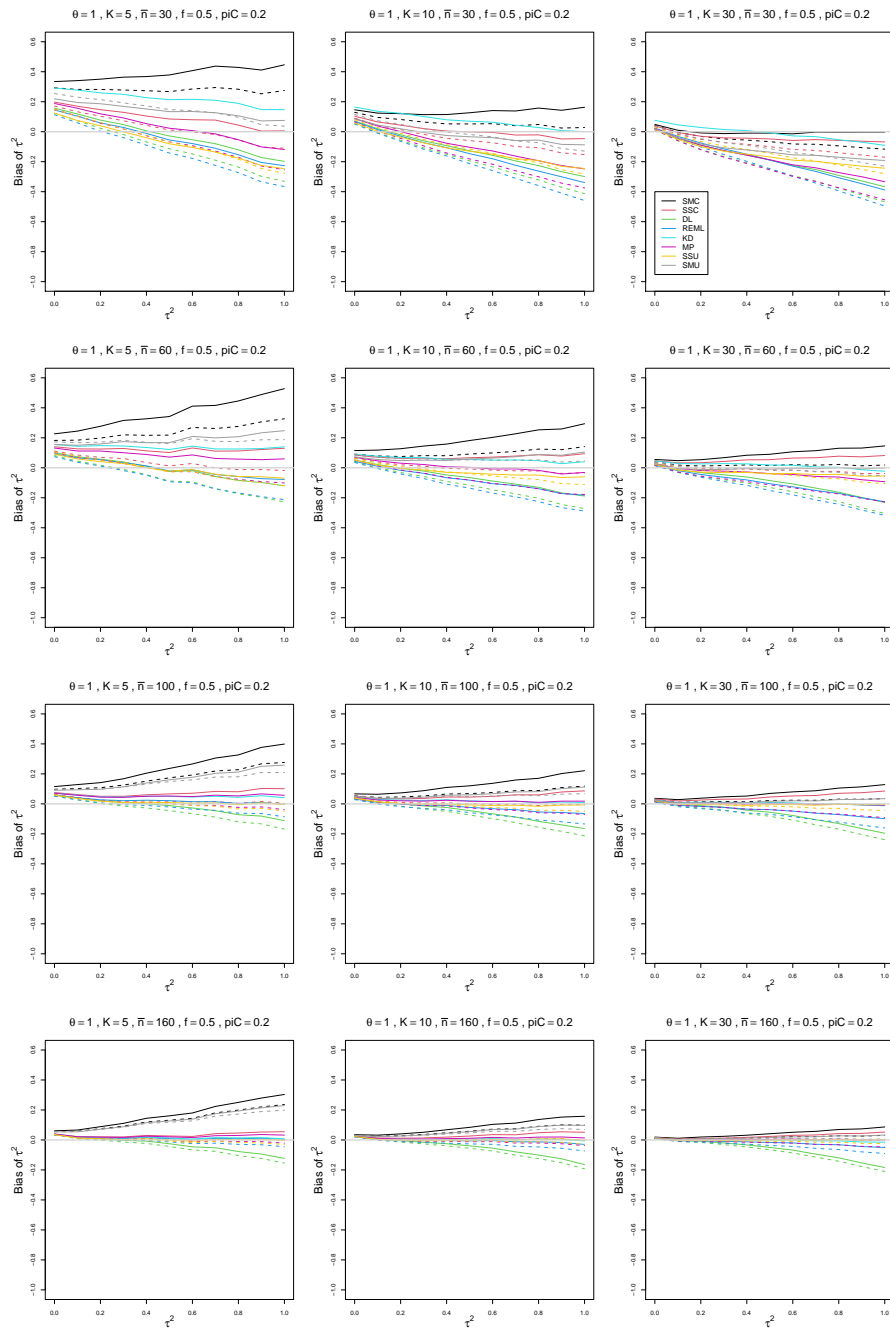


Figure A.20: Bias of estimators of between-study variance of LOR (DL, REML, KD, MP, SMC, SSC, SMU, and SSU) vs τ^2 , for unequal sample sizes $\bar{n} = 30, 60, 100$ and 160 , $p_{iC} = .2$, $\theta = 1$ and $f = 0.5$. Solid lines: DL, REML, MP, SSC, SMC “only”; KD; SSU and SMU model-based. Dashed lines: DL, REML, MP, SSC, SMC “always”; SSU and SMU naïve.

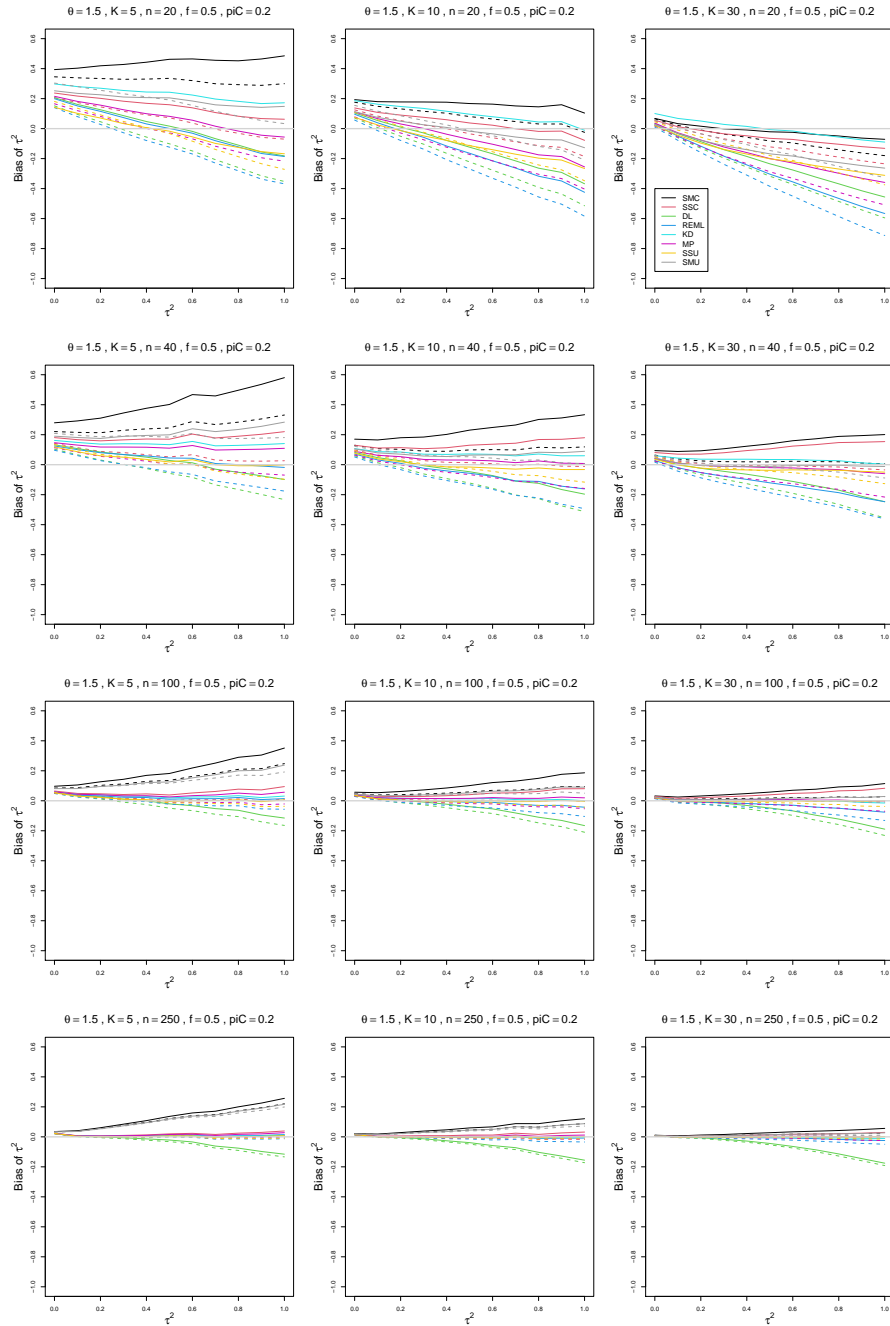


Figure A.21: Bias of estimators of between-study variance of LOR (DL, REML, KD, MP, SMC, SSC, SMU, and SSU) vs τ^2 , for equal sample sizes $n = 20, 40, 100$ and 250 , $p_{iC} = .2$, $\theta = 1.5$ and $f = 0.5$. Solid lines: DL, REML, MP, SSC, SMC “only”; KD; SSU and SMU model-based. Dashed lines: DL, REML, MP, SSC, SMC “always”; SSU and SMU naïve.

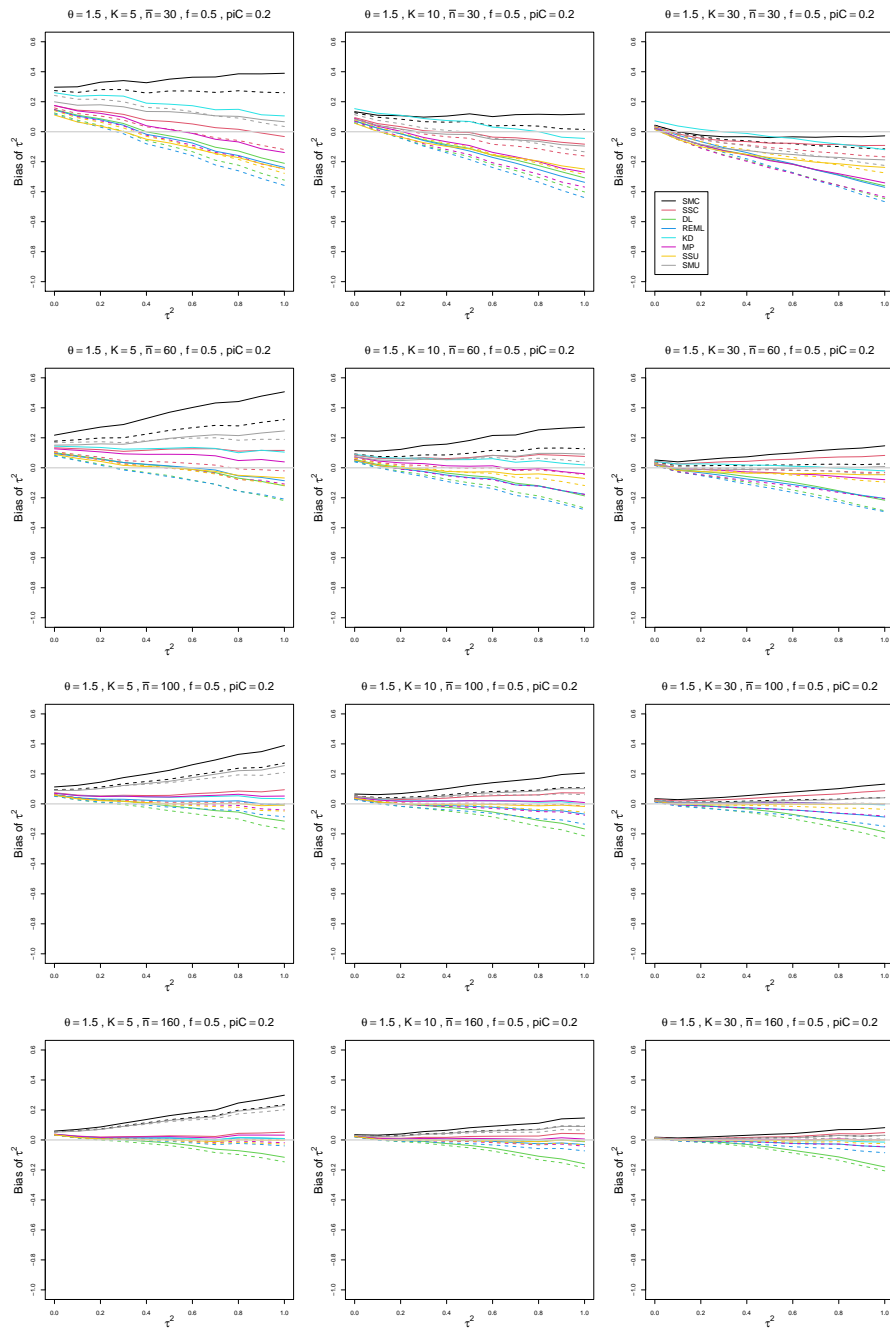


Figure A.22: Bias of estimators of between-study variance of LOR (DL, REML, KD, MP, SMC, SSC, SMU, and SSU) vs τ^2 , for unequal sample sizes $\bar{n} = 30, 60, 100$ and 160 , $p_{iC} = .2$, $\theta = 1.5$ and $f = 0.5$. Solid lines: DL, REML, MP, SSC, SMC “only”; KD; SSU and SMU model-based. Dashed lines: DL, REML, MP, SSC, SMC “always”; SSU and SMU naïve.

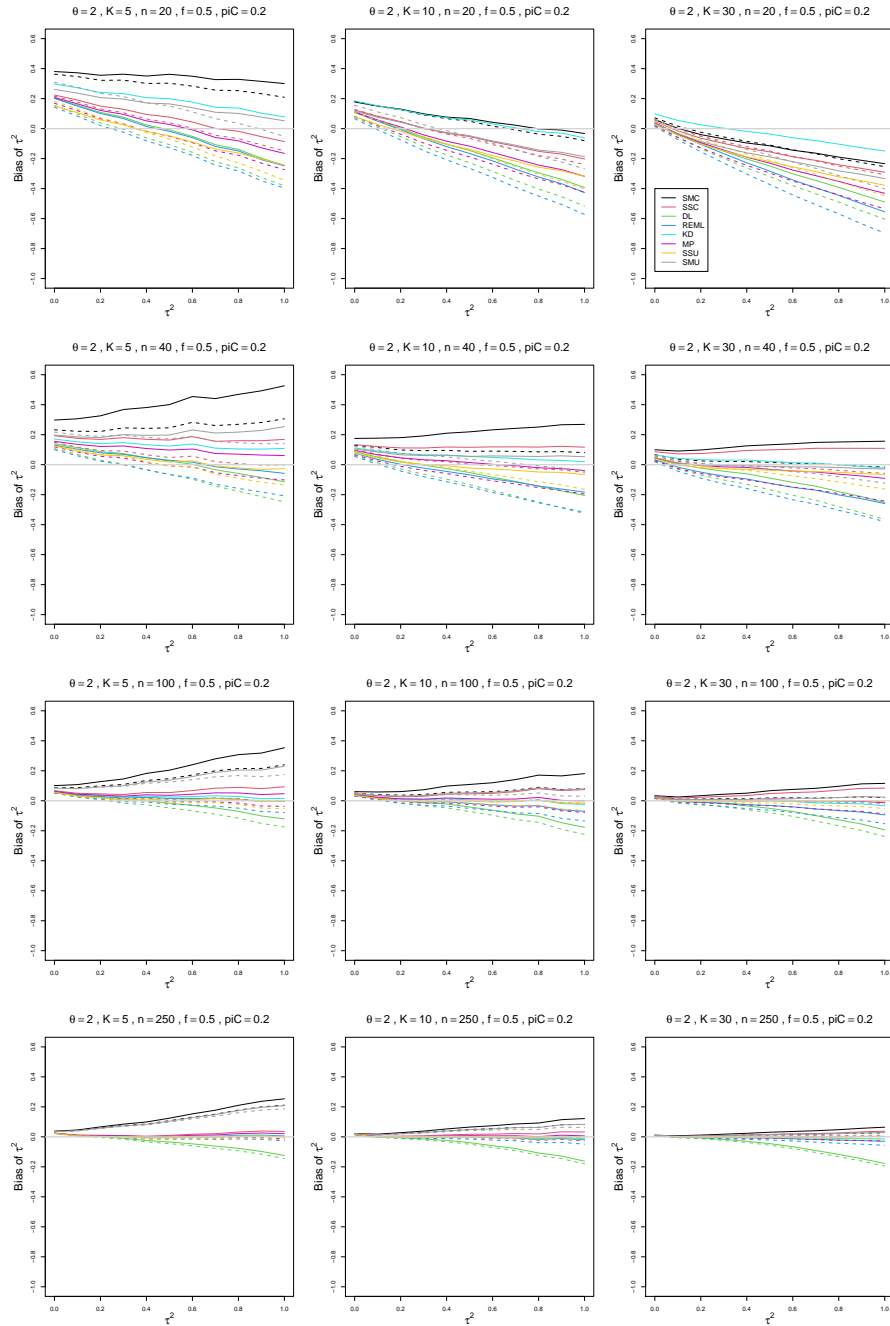


Figure A.23: Bias of estimators of between-study variance of LOR (DL, REML, KD, MP, SMC, SSC, SMU, and SSU) vs τ^2 , for equal sample sizes $n = 20, 40, 100$ and 250 , $p_{iC} = .2$, $\theta = 2$ and $f = 0.5$. Solid lines: DL, REML, MP, SSC, SMC “only”; KD; SSU and SMU model-based. Dashed lines: DL, REML, MP, SSC, SMC “always”; SSU and SMU naïve.

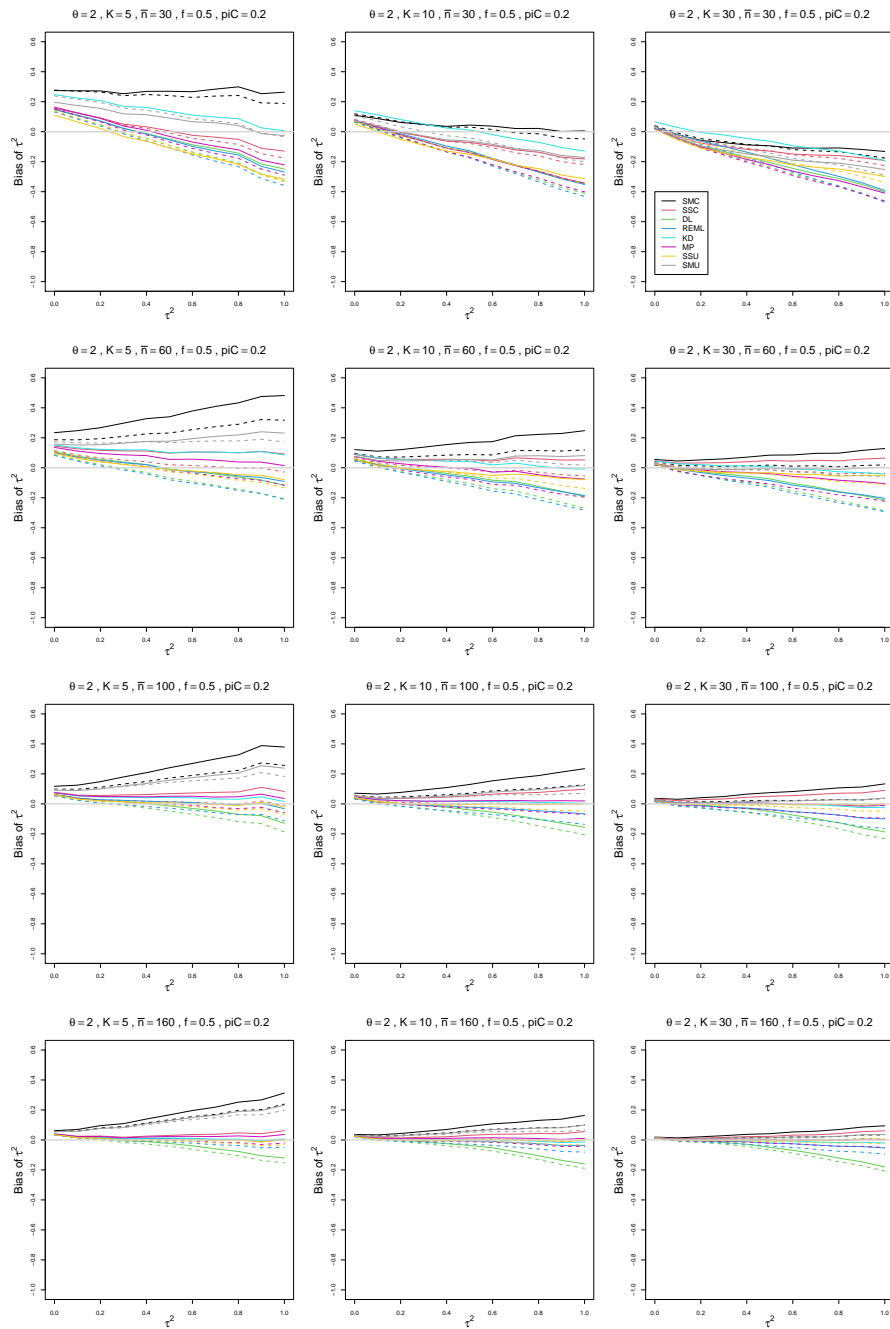


Figure A.24: Bias of estimators of between-study variance of LOR (DL, REML, KD, MP, SMC, SSC, SMU, and SSU) vs τ^2 , for unequal sample sizes $\bar{n} = 30, 60, 100$ and 160 , $p_{iC} = .2$, $\theta = 2$ and $f = 0.5$. Solid lines: DL, REML, MP, SSC, SMC “only”; KD; SSU and SMU model-based. Dashed lines: DL, REML, MP, SSC, SMC “always”; SSU and SMU naïve.

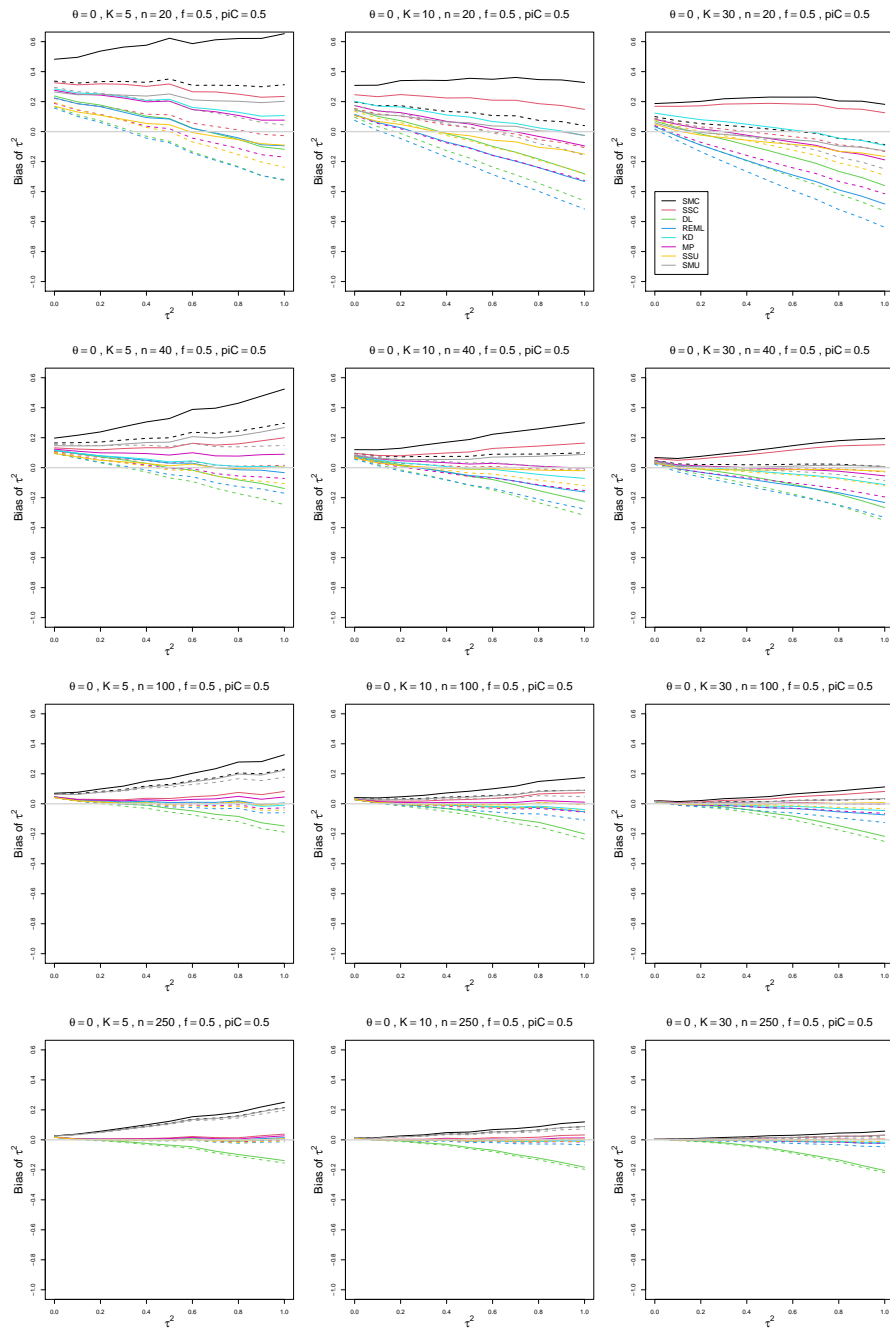


Figure A.25: Bias of estimators of between-study variance of LOR (DL, REML, KD, MP, SMC, SSC, SMU, and SSU) vs τ^2 , for equal sample sizes $n = 20, 40, 100$ and 250 , $p_{iC} = .5$, $\theta = 0$ and $f = 0.5$. Solid lines: DL, REML, MP, SSC, SMC “only”; KD; SSU and SMU model-based. Dashed lines: DL, REML, MP, SSC, SMC “always”; SSU and SMU naïve.

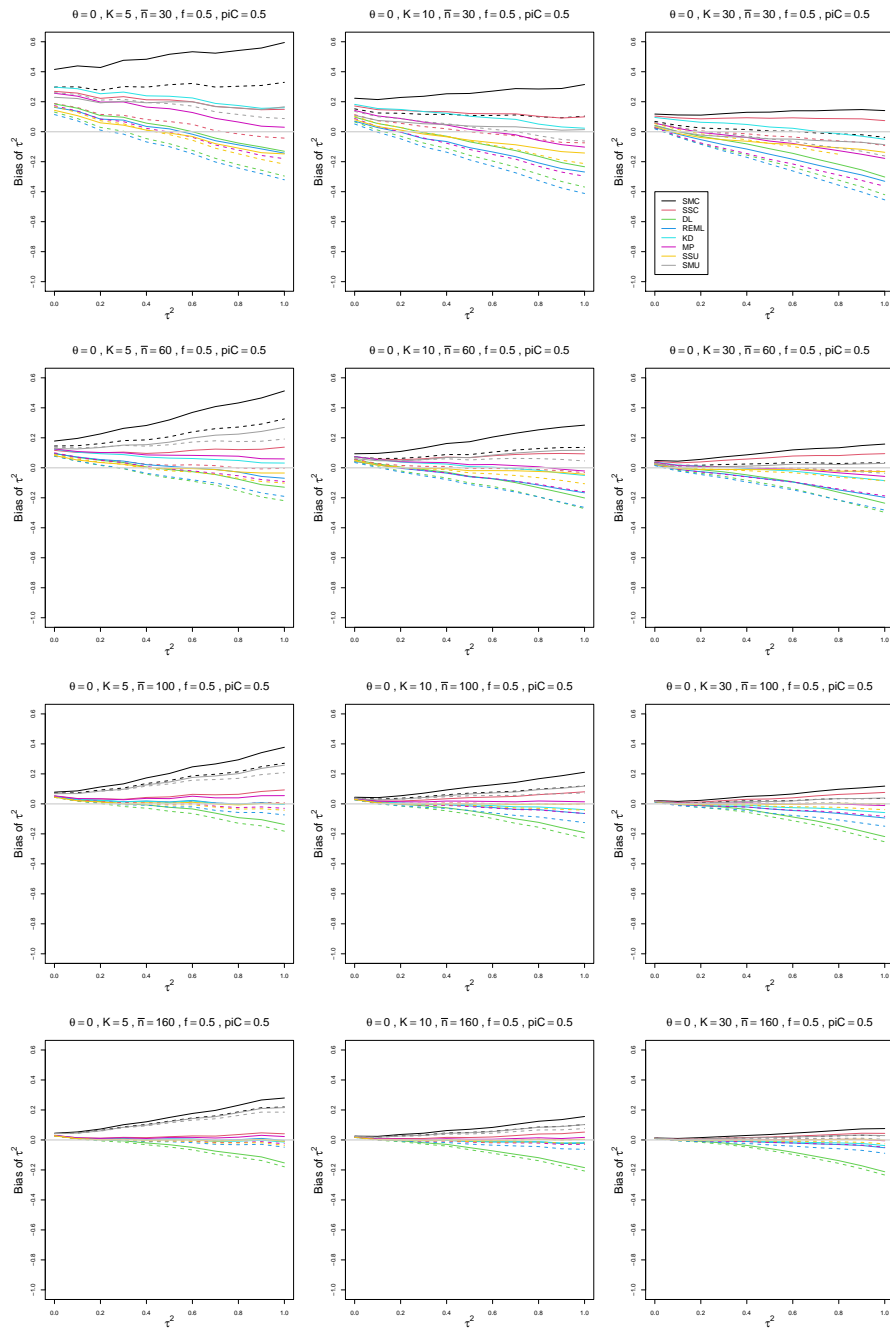


Figure A.26: Bias of estimators of between-study variance of LOR (DL, REML, KD, MP, SMC, SSC, SMU, and SSU) vs τ^2 , for unequal sample sizes $\bar{n} = 30, 60, 100$ and 160 , $p_{iC} = .5$, $\theta = 0$ and $f = 0.5$. Solid lines: DL, REML, MP, SSC, SMC “only”; KD; SSU and SMU model-based. Dashed lines: DL, REML, MP, SSC, SMC “always”; SSU and SMU naïve.

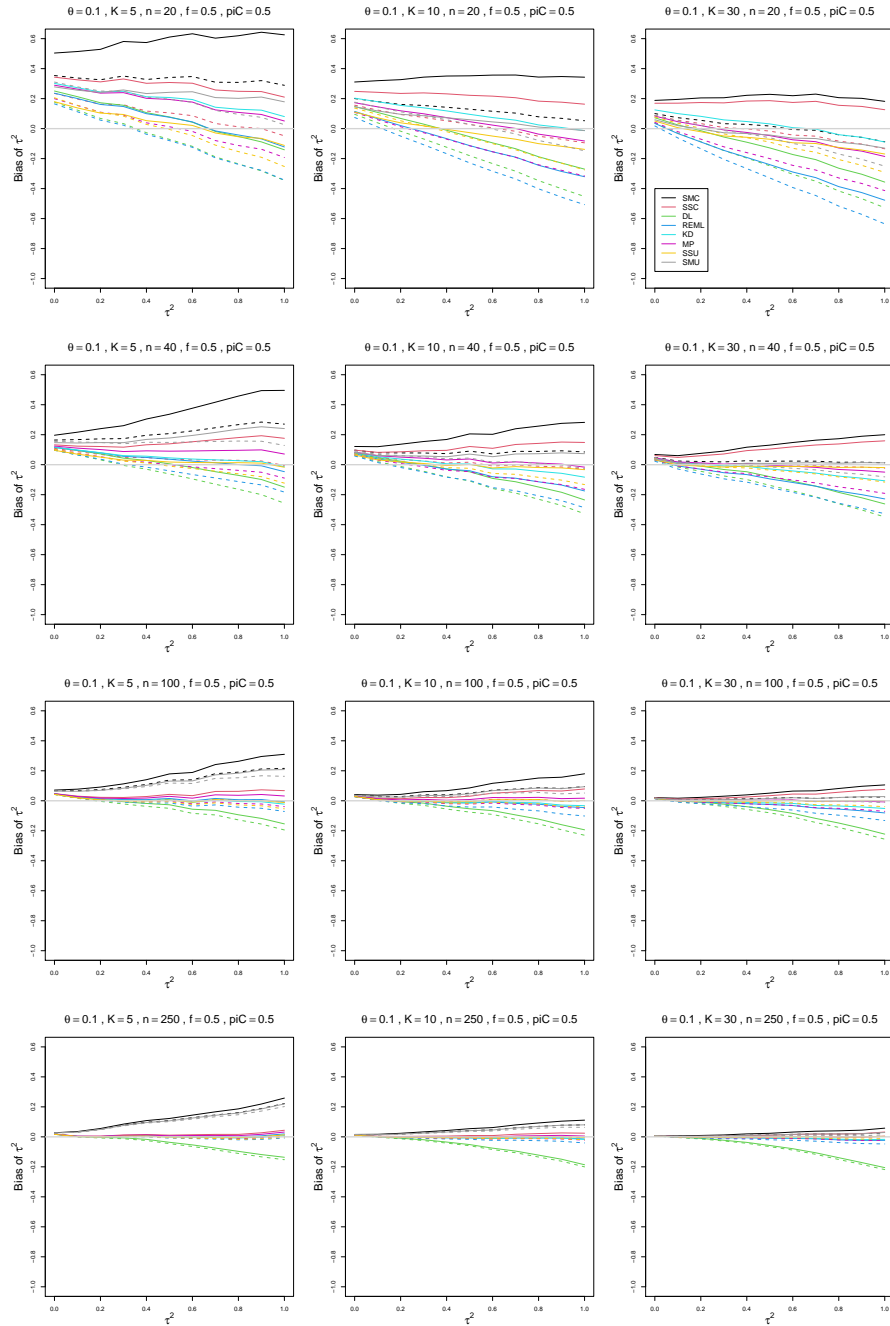


Figure A.27: Bias of estimators of between-study variance of LOR (DL, REML, KD, MP, SMC, SSC, SMU, and SSU) vs τ^2 , for equal sample sizes $n = 20, 40, 100$ and 250 , $p_{iC} = .5$, $\theta = 0.1$ and $f = 0.5$. Solid lines: DL, REML, MP, SSC, SMC “only”; KD; SSU and SMU model-based. Dashed lines: DL, REML, MP, SSC, SMC “always”; SSU and SMU naïve.

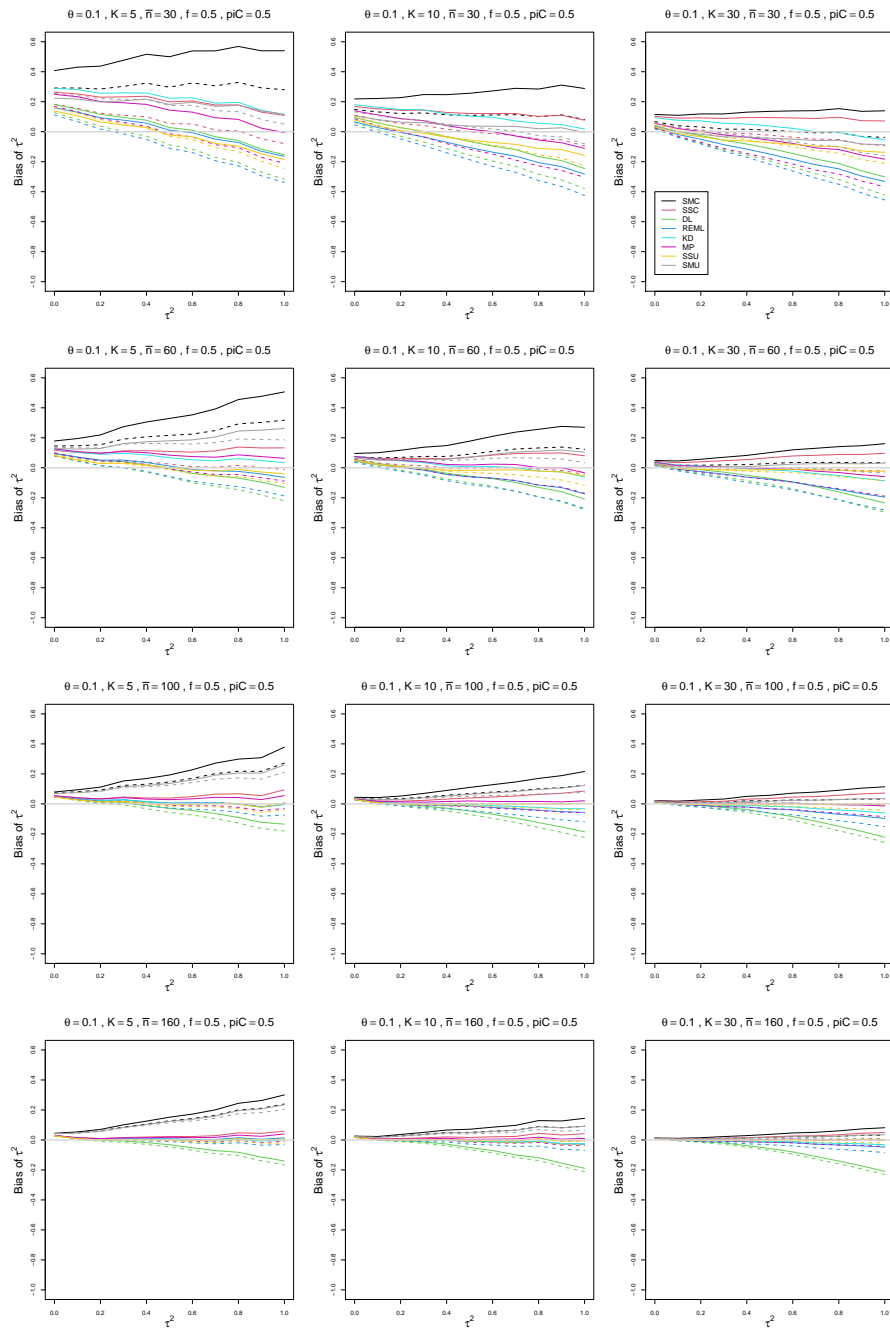


Figure A.28: Bias of estimators of between-study variance of LOR (DL, REML, KD, MP, SMC, SSC, SMU, and SSU) vs τ^2 , for unequal sample sizes $\bar{n} = 30, 60, 100$ and 160 , $p_{iC} = .5$, $\theta = 0.1$ and $f = 0.5$. Solid lines: DL, REML, MP, SSC, SMC “only”; KD; SSU and SMU model-based. Dashed lines: DL, REML, MP, SSC, SMC “always”; SSU and SMU naïve.

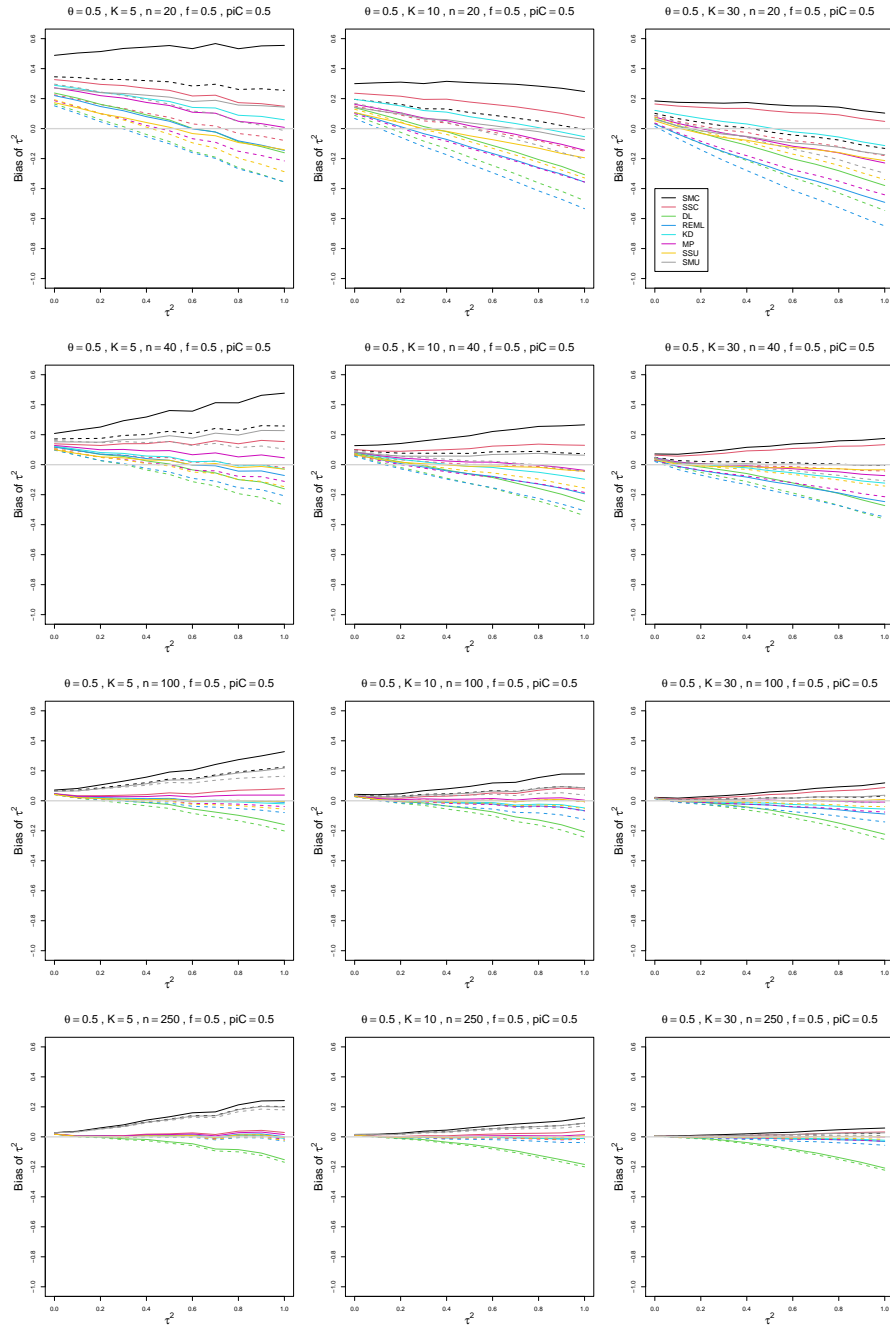


Figure A.29: Bias of estimators of between-study variance of LOR (DL, REML, KD, MP, SMC, SSC, SMU, and SSU) vs τ^2 , for equal sample sizes $n = 20, 40, 100$ and 250 , $p_{iC} = .5$, $\theta = 0.5$ and $f = 0.5$. Solid lines: DL, REML, MP, SSC, SMC “only”; KD; SSU and SMU model-based. Dashed lines: DL, REML, MP, SSC, SMC “always”; SSU and SMU naïve.

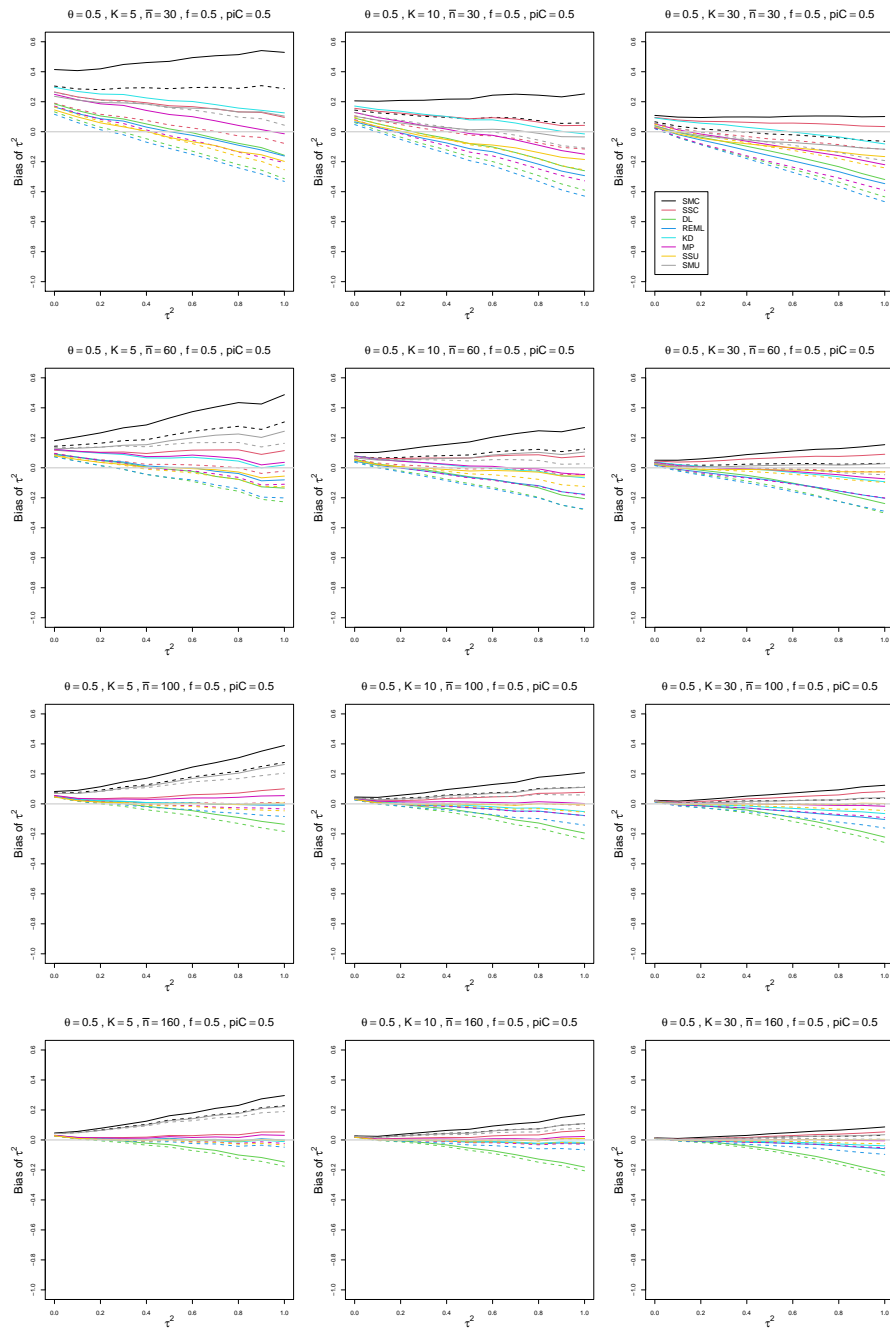


Figure A.30: Bias of estimators of between-study variance of LOR (DL, REML, KD, MP, SMC, SSC, SMU, and SSU) vs τ^2 , for unequal sample sizes $\bar{n} = 30, 60, 100$ and 160 , $p_{iC} = .5$, $\theta = 0.5$ and $f = 0.5$. Solid lines: DL, REML, MP, SSC, SMC “only”; KD; SSU and SMU model-based. Dashed lines: DL, REML, MP, SSC, SMC “always”; SSU and SMU naïve.

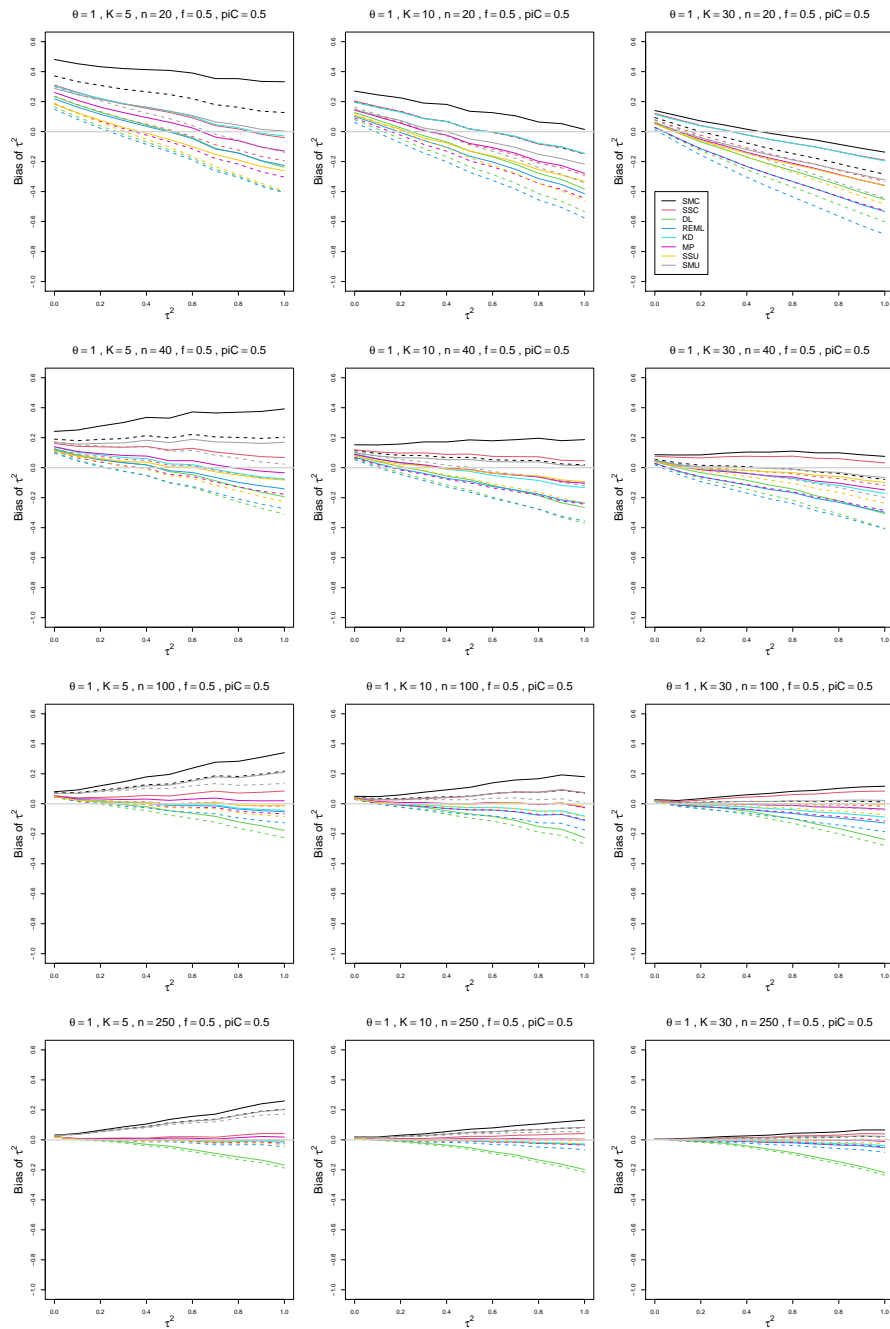


Figure A.31: Bias of estimators of between-study variance of LOR (DL, REML, KD, MP, SMC, SSC, SMU, and SSU) vs τ^2 , for equal sample sizes $n = 20, 40, 100$ and 250 , $p_{iC} = .5$, $\theta = 1$ and $f = 0.5$. Solid lines: DL, REML, MP, SSC, SMC “only”; KD; SSU and SMU model-based. Dashed lines: DL, REML, MP, SSC, SMC “always”; SSU and SMU naïve.

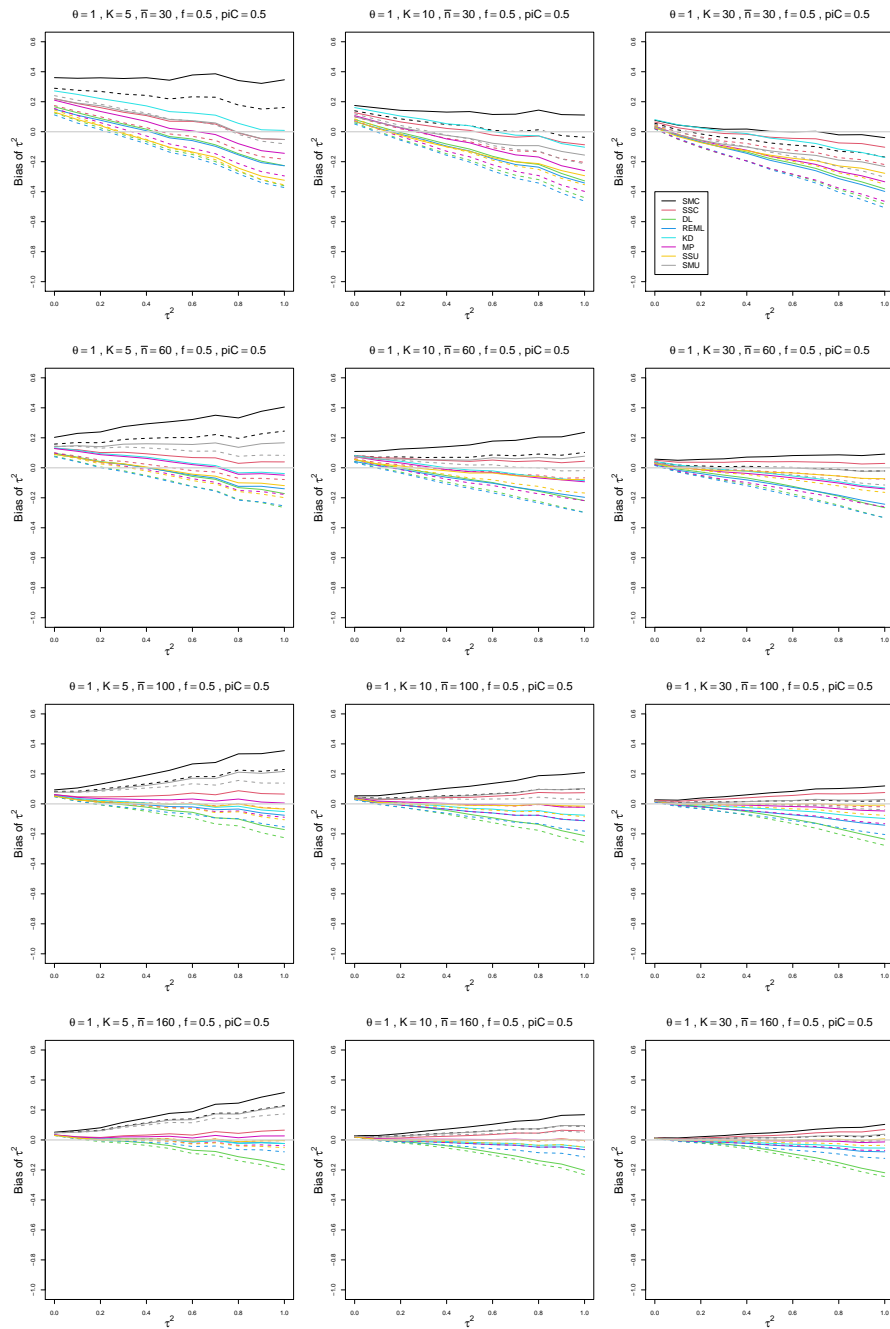


Figure A.32: Bias of estimators of between-study variance of LOR (DL, REML, KD, MP, SMC, SSC, SMU, and SSU) vs τ^2 , for unequal sample sizes $\bar{n} = 30, 60, 100$ and 160 , $p_{iC} = .5$, $\theta = 1$ and $f = 0.5$. Solid lines: DL, REML, MP, SSC, SMC “only”; KD; SSU and SMU model-based. Dashed lines: DL, REML, MP, SSC, SMC “always”; SSU and SMU naïve.

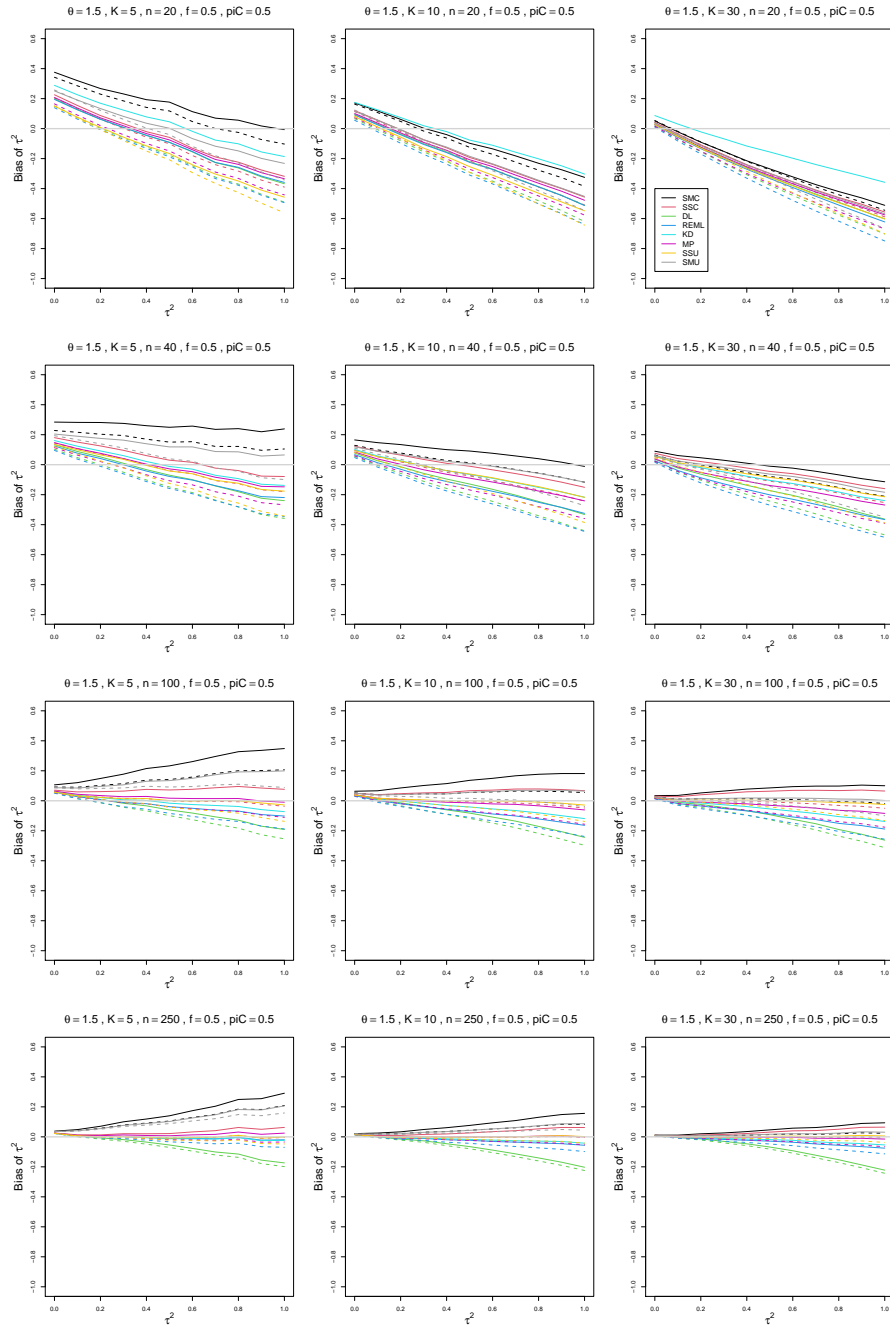


Figure A.33: Bias of estimators of between-study variance of LOR (DL, REML, KD, MP, SMC, SSC, SMU, and SSU) vs τ^2 , for equal sample sizes $n = 20, 40, 100$ and 250 , $p_{iC} = .5$, $\theta = 1.5$ and $f = 0.5$. Solid lines: DL, REML, MP, SSC, SMC “only”; KD; SSU and SMU model-based. Dashed lines: DL, REML, MP, SSC, SMC “always”; SSU and SMU naïve.

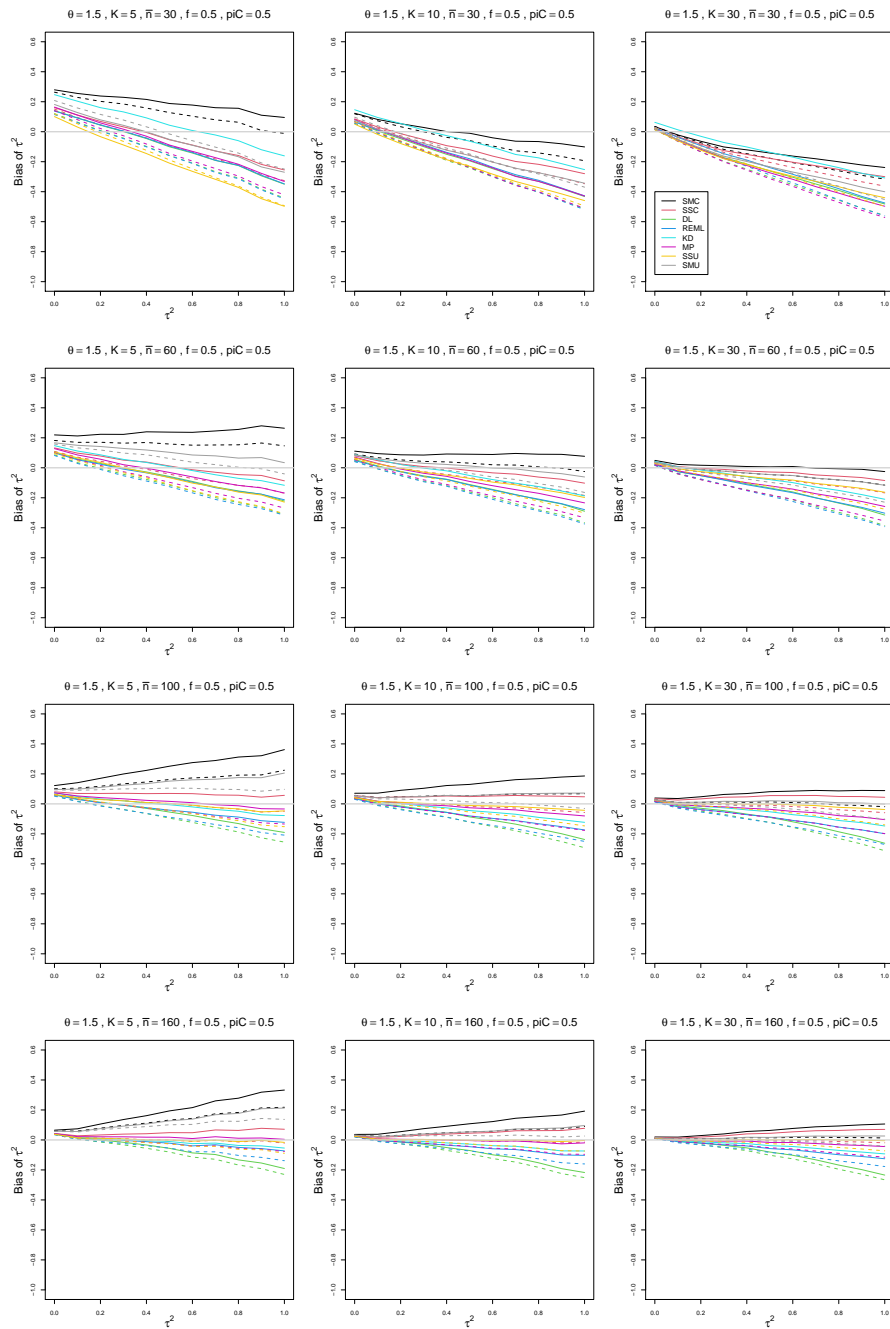


Figure A.34: Bias of estimators of between-study variance of LOR (DL, REML, KD, MP, SMC, SSC, SMU, and SSU) vs τ^2 , for unequal sample sizes $\bar{n} = 30, 60, 100$ and 160 , $p_{iC} = .5$, $\theta = 1.5$ and $f = 0.5$. Solid lines: DL, REML, MP, SSC, SMC “only”; KD; SSU and SMU model-based. Dashed lines: DL, REML, MP, SSC, SMC “always”; SSU and SMU naïve.

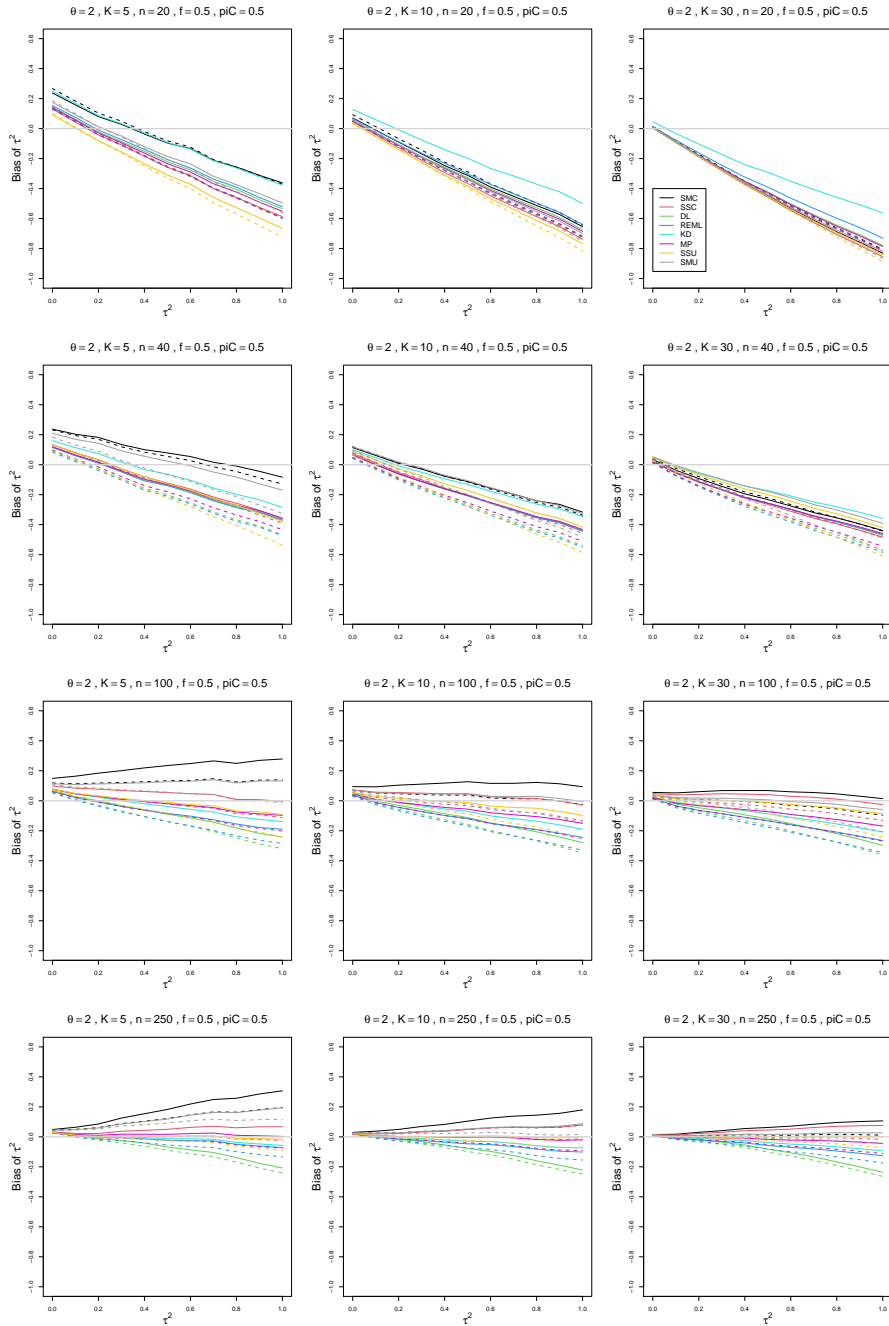


Figure A.35: Bias of estimators of between-study variance of LOR (DL, REML, KD, MP, SMC, SSC, SMU, and SSU) vs τ^2 , for equal sample sizes $n = 20, 40, 100$ and 250 , $p_{iC} = .5$, $\theta = 2$ and $f = 0.5$. Solid lines: DL, REML, MP, SSC, SMC “only”; KD; SSU and SMU model-based. Dashed lines: DL, REML, MP, SSC, SMC “always”; SSU and SMU naïve.

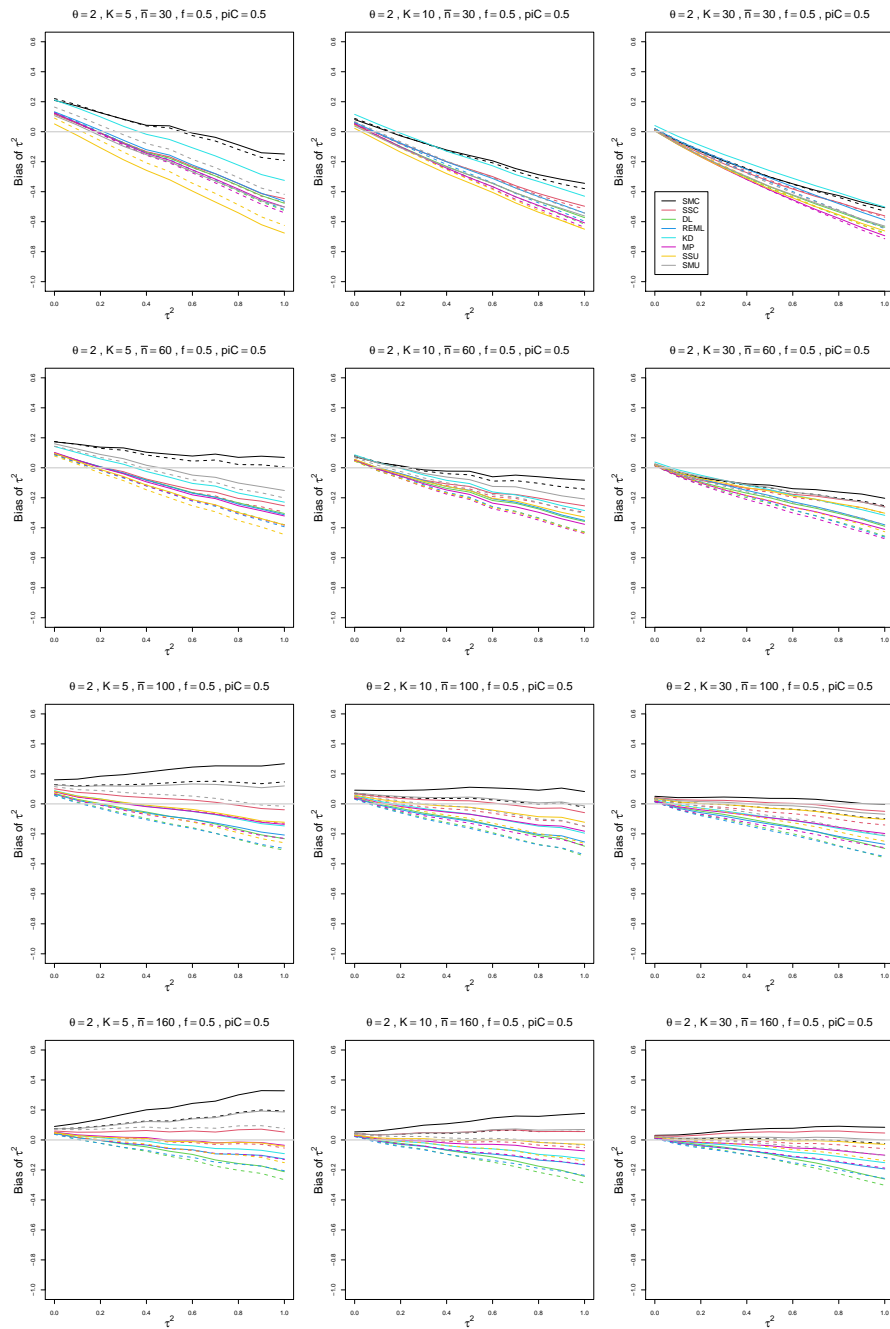


Figure A.36: Bias of estimators of between-study variance of LOR (DL, REML, KD, MP, SMC, SSC, SMU, and SSU) vs τ^2 , for unequal sample sizes $\bar{n} = 30, 60, 100$ and 160 , $p_{iC} = .5$, $\theta = 2$ and $f = 0.5$. Solid lines: DL, REML, MP, SSC, SMC “only”; KD; SSU and SMU model-based. Dashed lines: DL, REML, MP, SSC, SMC “always”; SSU and SMU naïve.

Appendix B: Median bias in point estimators of between-study variance

Each figure corresponds to a value of the probability of an event in the Control arm p_{iC} ($= .1, .2, .5$).

The fraction of each study's sample size in the Control arm (f) is held constant at 0.5. For each combination of a value of n ($= 20, 40, 100, 250$) or \bar{n} ($= 30, 60, 100, 160$) and a value of K ($= 5, 10, 30$), a panel plots median bias versus τ^2 ($= 0.0(0.1)1$).

The point estimators of τ^2 are

- DL (DerSimonian-Laird method, inverse-variance weights)
- REML method, inverse-variance weights)
- MP (Mandel-Paule method, inverse-variance weights)
- KD (Kulinskaya-Dollinger (2015) approximation, inverse-variance weights)
- SSC method, effective-sample-size weights, conditional variance of LOR
- SMC method, median-unbiased, effective-sample-size weights, conditional variance of LOR
- SSU method, effective-sample-size weights, unconditional variance of LOR
- SMU method, median-unbiased, effective-sample-size weights, unconditional variance of LOR

The plots include two versions of DL, REML, MP, SSC and SMC: adding 1/2 to all four of X_{iT} , X_{iC} , $n_{iT} - X_{iT}$, $n_{iC} - X_{iC}$ only when one of these is zero (solid lines) or always (dashed lines).

The plots also include two versions of SSU and SMU: model-based estimation of p_{iT} (solid lines) or naïve estimation (dashed lines).

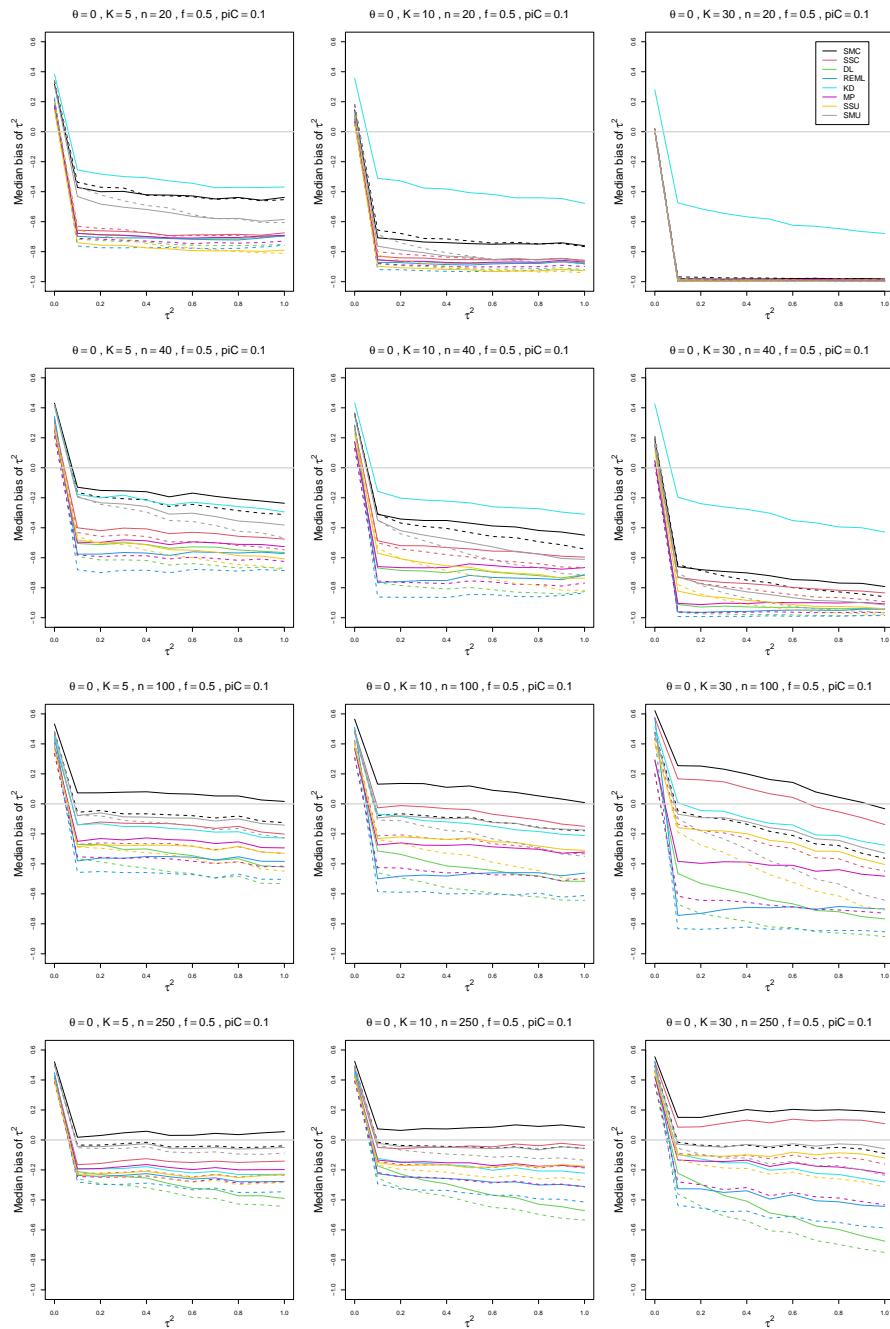


Figure B.1: Median bias of estimators of between-study variance of LOR (DL, REML, KD, MP, SMC, SSC, SMU, and SSU) vs τ^2 , for equal sample sizes $n = 20, 40, 100$ and 250 , $p_{iC} = .1$, $\theta = 0$ and $f = 0.5$. Solid lines: DL, REML, MP, SSC, SMC “only”; KD; SSU and SMU model-based. Dashed lines: DL, REML, MP, SSC, SMC “always”; SSU and SMU naïve.

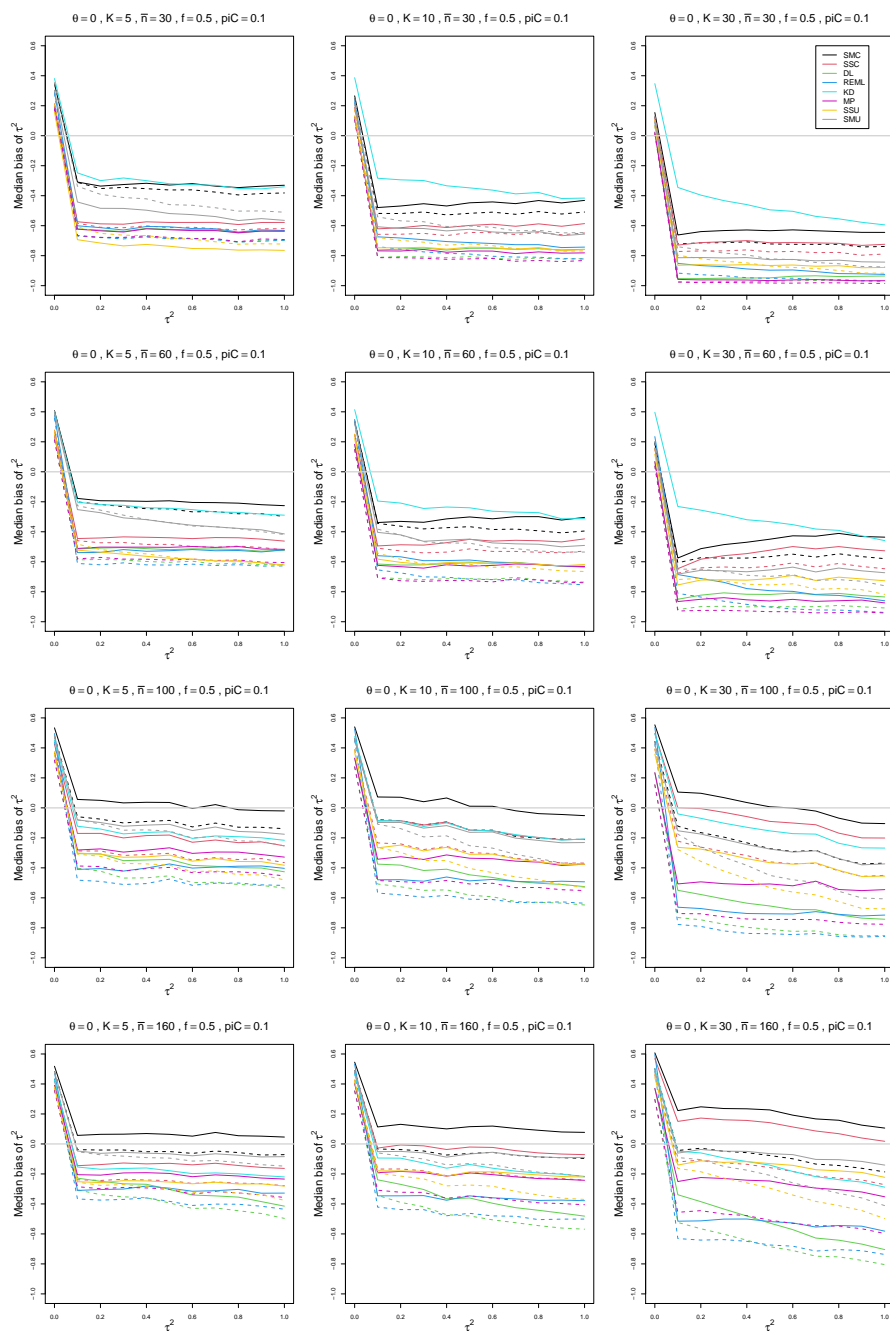


Figure B.2: Median bias of estimators of between-study variance of LOR (DL, REML, KD, MP, SMC, SSC, SMU, and SSU) vs τ^2 , for unequal sample sizes $\bar{n} = 30, 60, 100$ and 160 , $p_{iC} = .1$, $\theta = 0$ and $f = 0.5$. Solid lines: DL, REML, MP, SSC, SMC “only”; KD; SSU and SMU model-based. Dashed lines: DL, REML, MP, SSC, SMC “always”; SSU and SMU naïve.

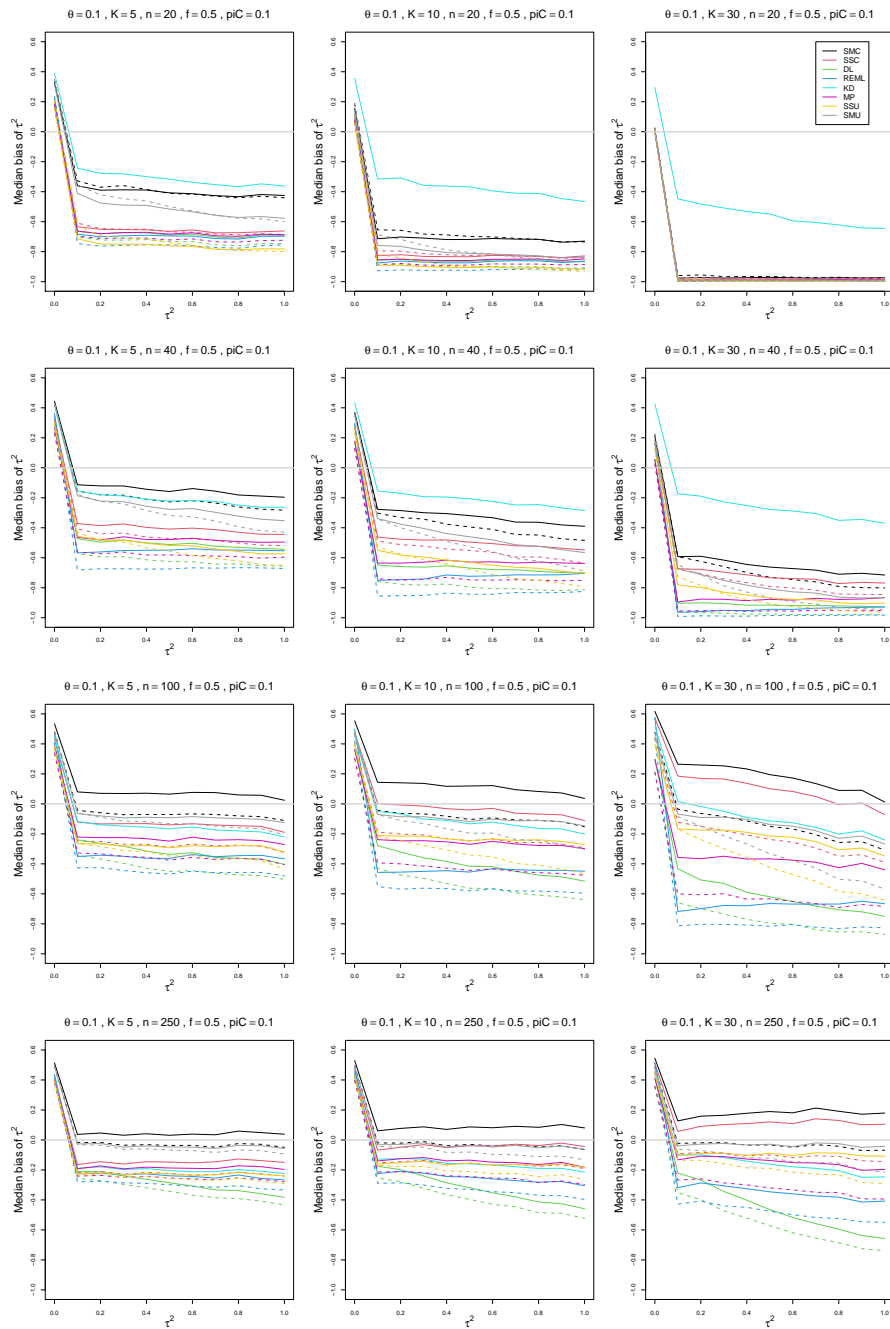


Figure B.3: Median bias of estimators of between-study variance of LOR (DL, REML, KD, MP, SMC, SSC, SMU, and SSU) vs τ^2 , for equal sample sizes $n = 20, 40, 100$ and 250 , $p_{iC} = .1$, $\theta = 0.1$ and $f = 0.5$. Solid lines: DL, REML, MP, SSC, SMC “only”; KD; SSU and SMU model-based. Dashed lines: DL, REML, MP, SSC, SMC “always”; SSU and SMU naïve.

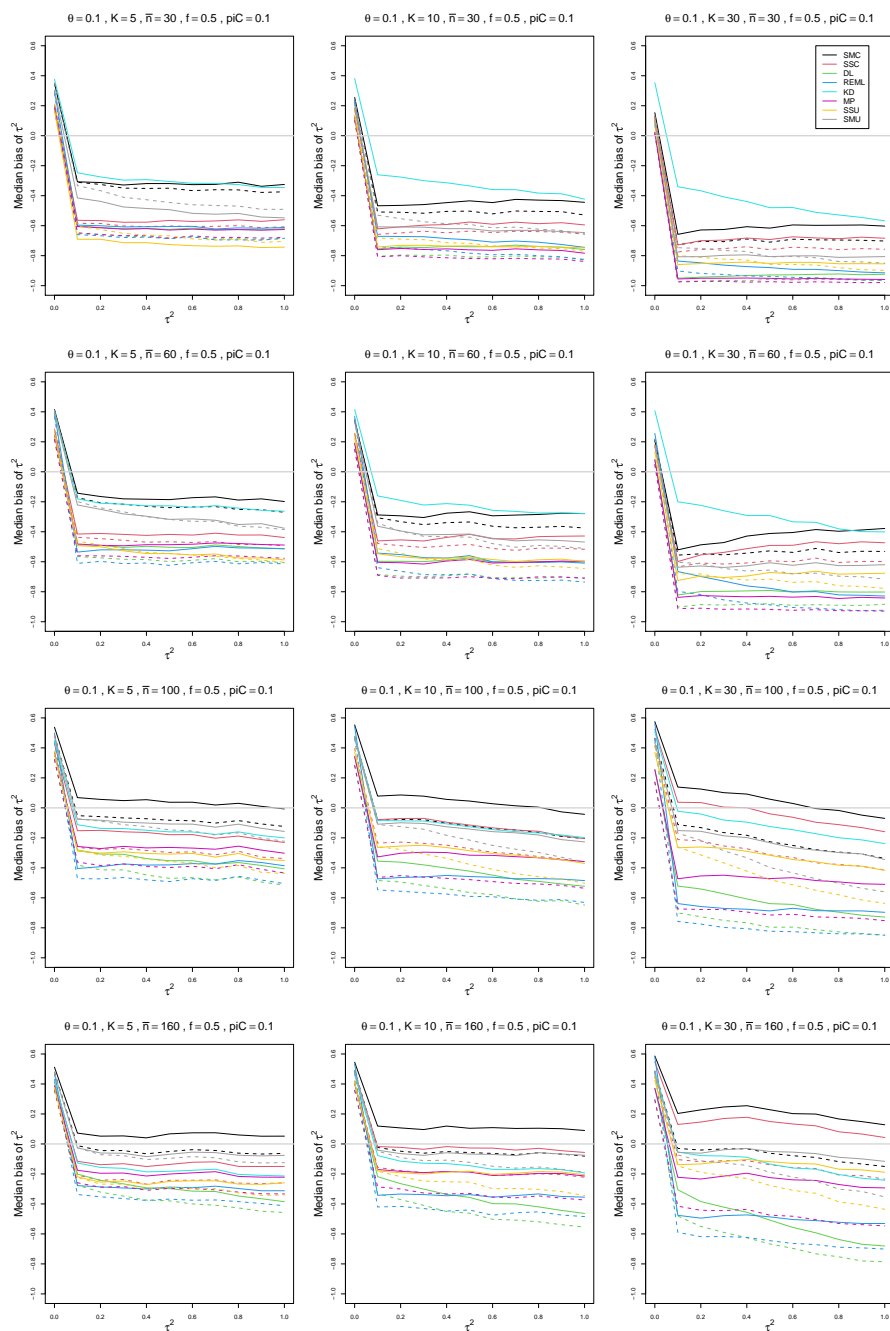


Figure B.4: Median bias of estimators of between-study variance of LOR (DL, REML, KD, MP, SMC, SSC, SMU, and SSU) vs τ^2 , for unequal sample sizes $\bar{n} = 30, 60, 100$ and 160 , $p_{iC} = .1$, $\theta = 0.1$ and $f = 0.5$. Solid lines: DL, REML, MP, SSC, SMC “only”; KD; SSU and SMU model-based. Dashed lines: DL, REML, MP, SSC, SMC “always”; SSU and SMU naïve.

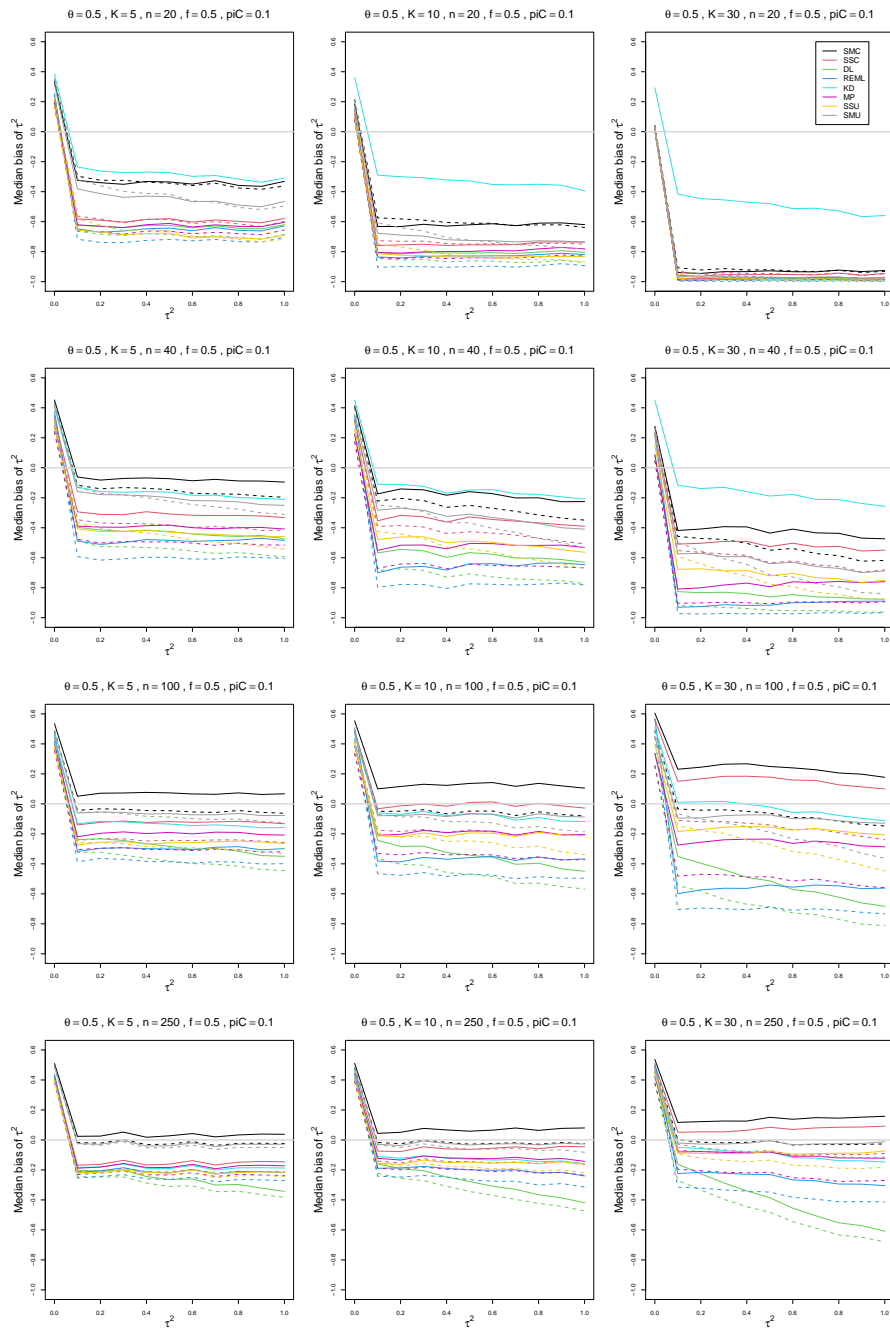


Figure B.5: Median bias of estimators of between-study variance of LOR (DL, REML, KD, MP, SMC, SSC, SMU, and SSU) vs τ^2 , for equal sample sizes $n = 20, 40, 100$ and 250 , $p_{iC} = .1$, $\theta = 0.5$ and $f = 0.5$. Solid lines: DL, REML, MP, SSC, SMC “only”; KD; SSU and SMU model-based. Dashed lines: DL, REML, MP, SSC, SMC “always”; SSU and SMU naïve.

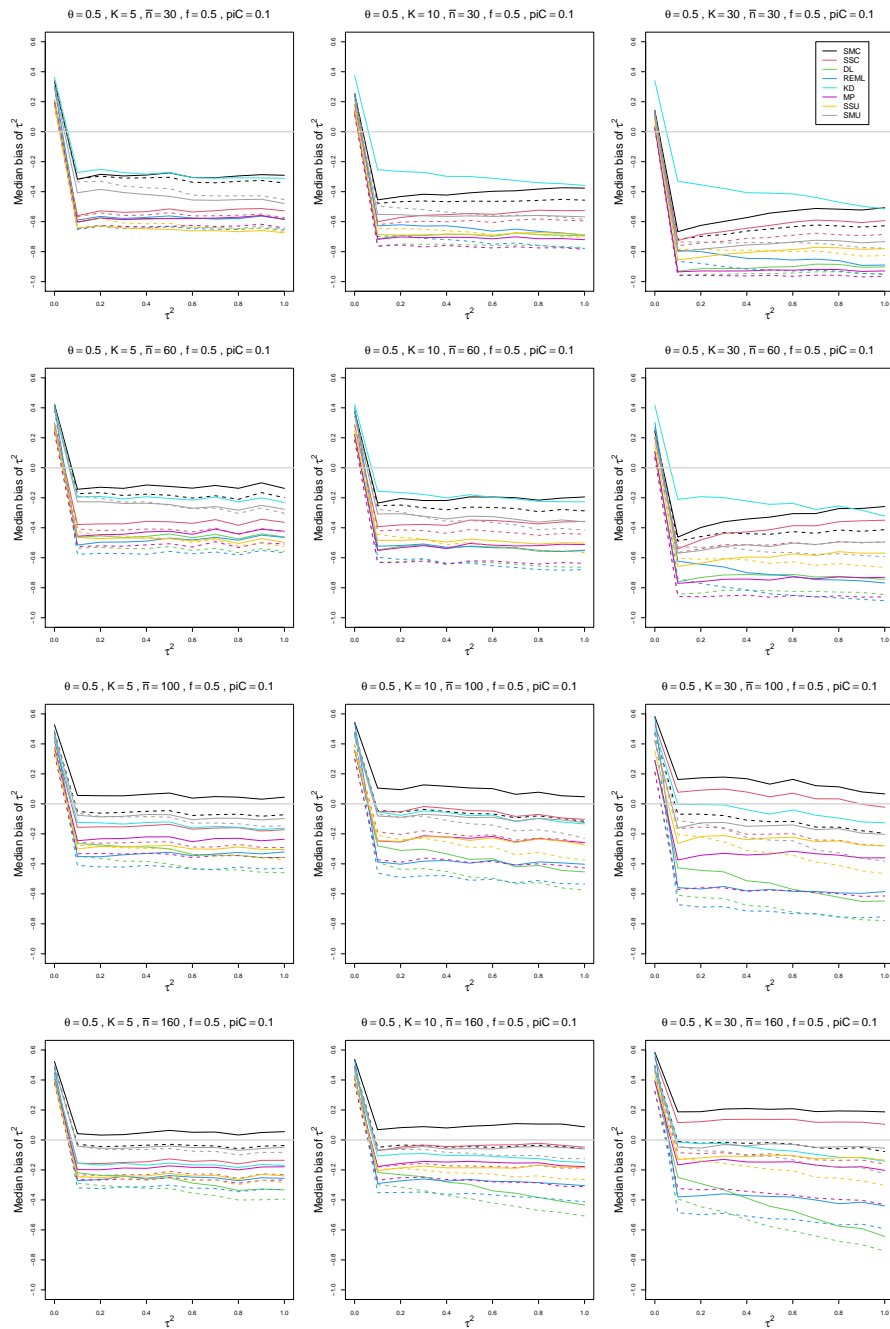


Figure B.6: Median bias of estimators of between-study variance of LOR (DL, REML, KD, MP, SMC, SSC, SMU, and SSU) vs τ^2 , for unequal sample sizes $\bar{n} = 30, 60, 100$ and 160 , $p_{iC} = .1$, $\theta = 0.5$ and $f = 0.5$. Solid lines: DL, REML, MP, SSC, SMC “only”; KD; SSU and SMU model-based. Dashed lines: DL, REML, MP, SSC, SMC “always”; SSU and SMU naïve.

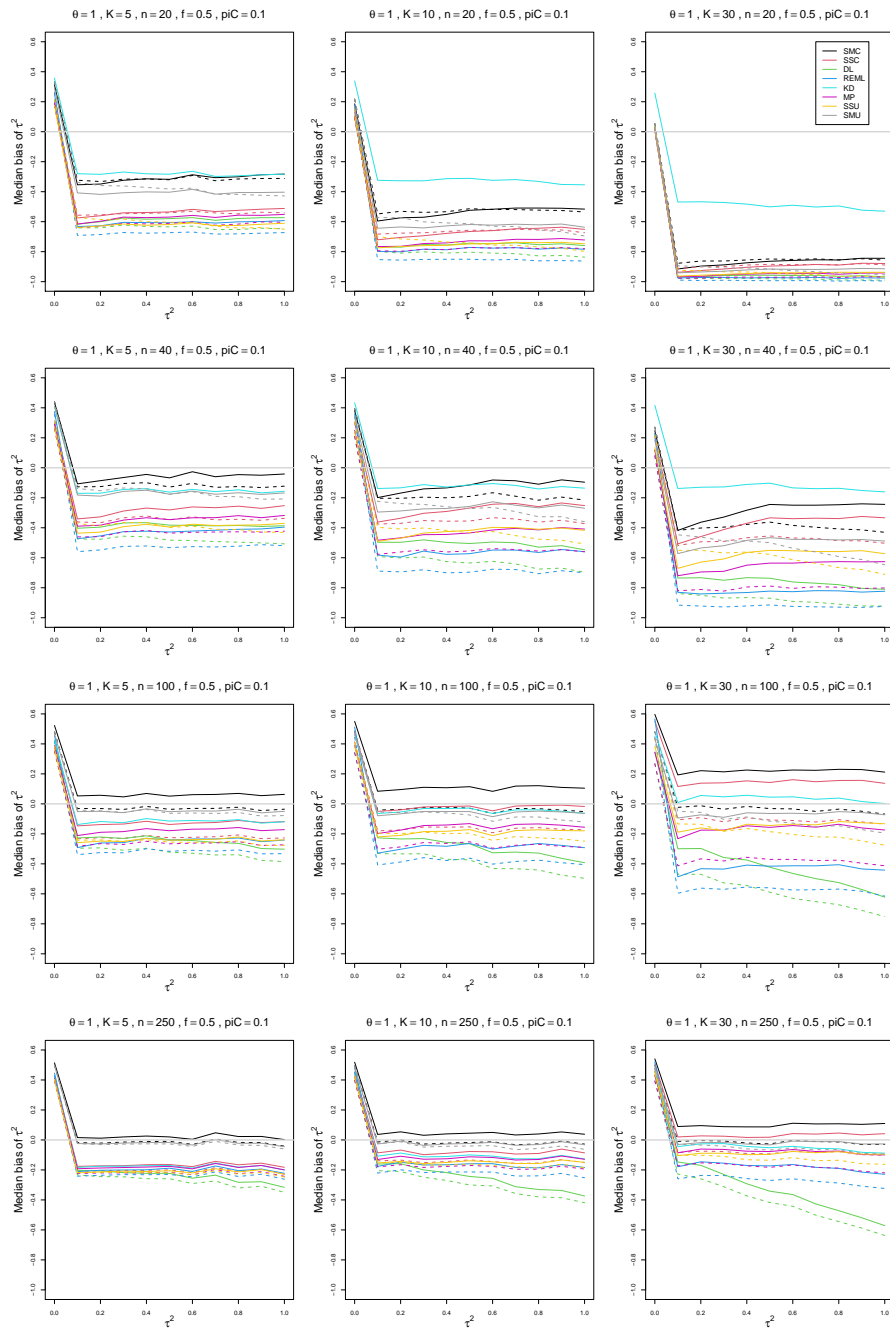


Figure B.7: Median bias of estimators of between-study variance of LOR (DL, REML, KD, MP, SMC, SSC, SMU, and SSU) vs τ^2 , for equal sample sizes $n = 20, 40, 100$ and 250 , $p_{iC} = .1$, $\theta = 1$ and $f = 0.5$. Solid lines: DL, REML, MP, SSC, SMC “only”; KD; SSU and SMU model-based. Dashed lines: DL, REML, MP, SSC, SMC “always”; SSU and SMU naïve.

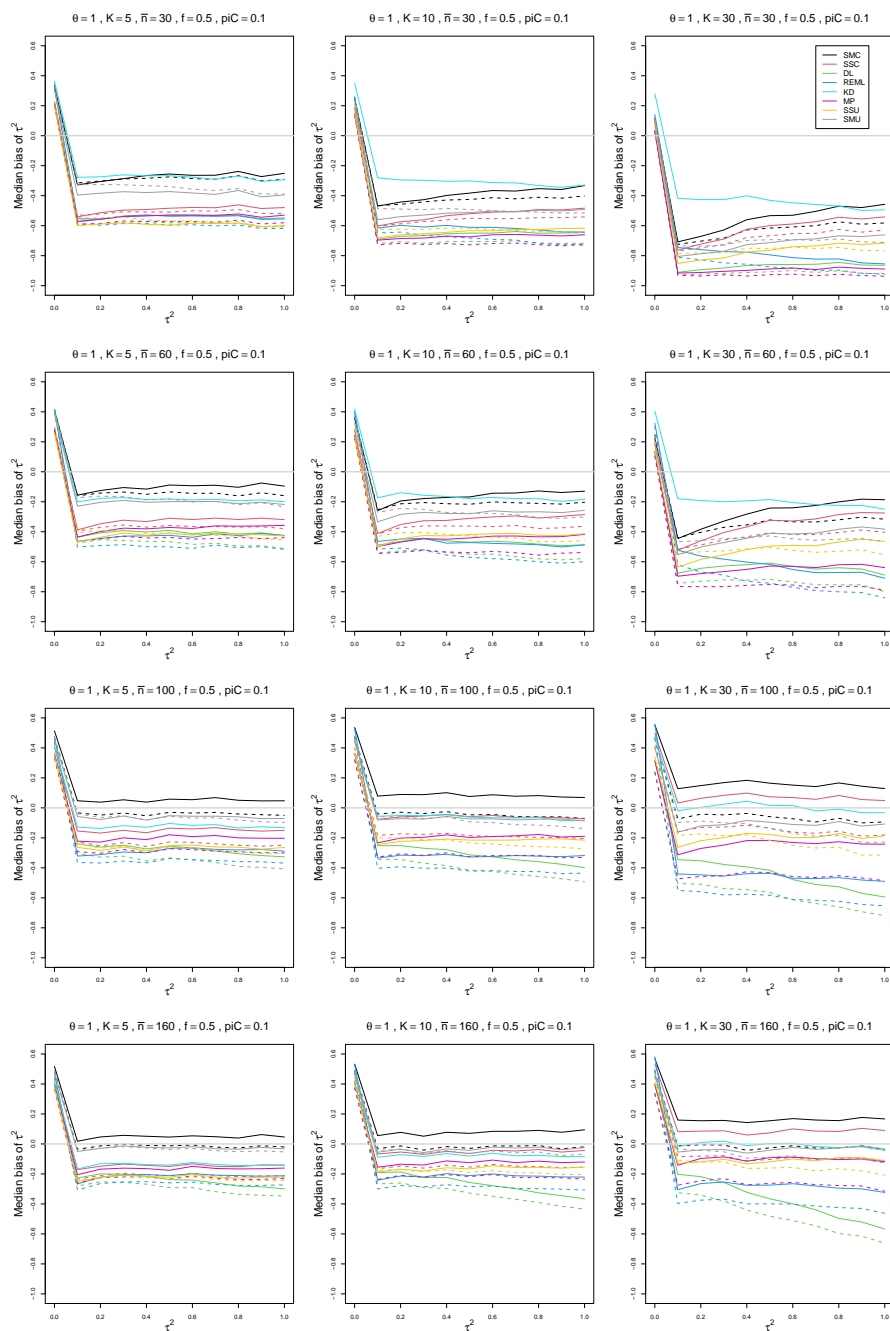


Figure B.8: Median bias of estimators of between-study variance of LOR (DL, REML, KD, MP, SMC, SSC, SMU, and SSU) vs τ^2 , for unequal sample sizes $\bar{n} = 30, 60, 100$ and 160 , $p_{iC} = .1$, $\theta = 1$ and $f = 0.5$. Solid lines: DL, REML, MP, SSC, SMC “only”; KD; SSU and SMU model-based. Dashed lines: DL, REML, MP, SSC, SMC “always”; SSU and SMU naïve.

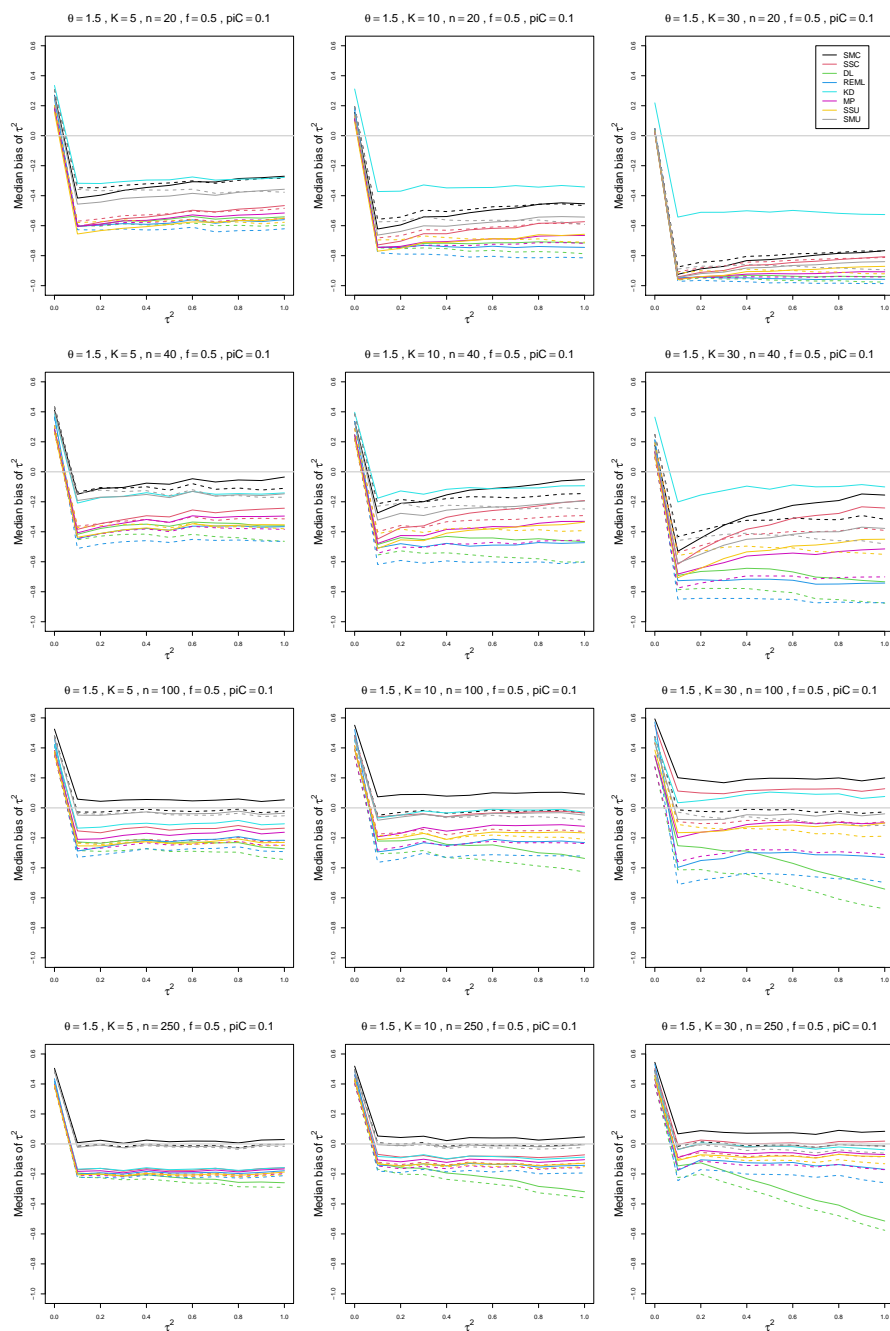


Figure B.9: Median bias of estimators of between-study variance of LOR (DL, REML, KD, MP, SMC, SSC, SMU, and SSU) vs τ^2 , for equal sample sizes $n = 20, 40, 100$ and 250 , $p_{iC} = .1$, $\theta = 1.5$ and $f = 0.5$. Solid lines: DL, REML, MP, SSC, SMC “only”; KD; SSU and SMU model-based. Dashed lines: DL, REML, MP, SSC, SMC “always”; SSU and SMU naïve.

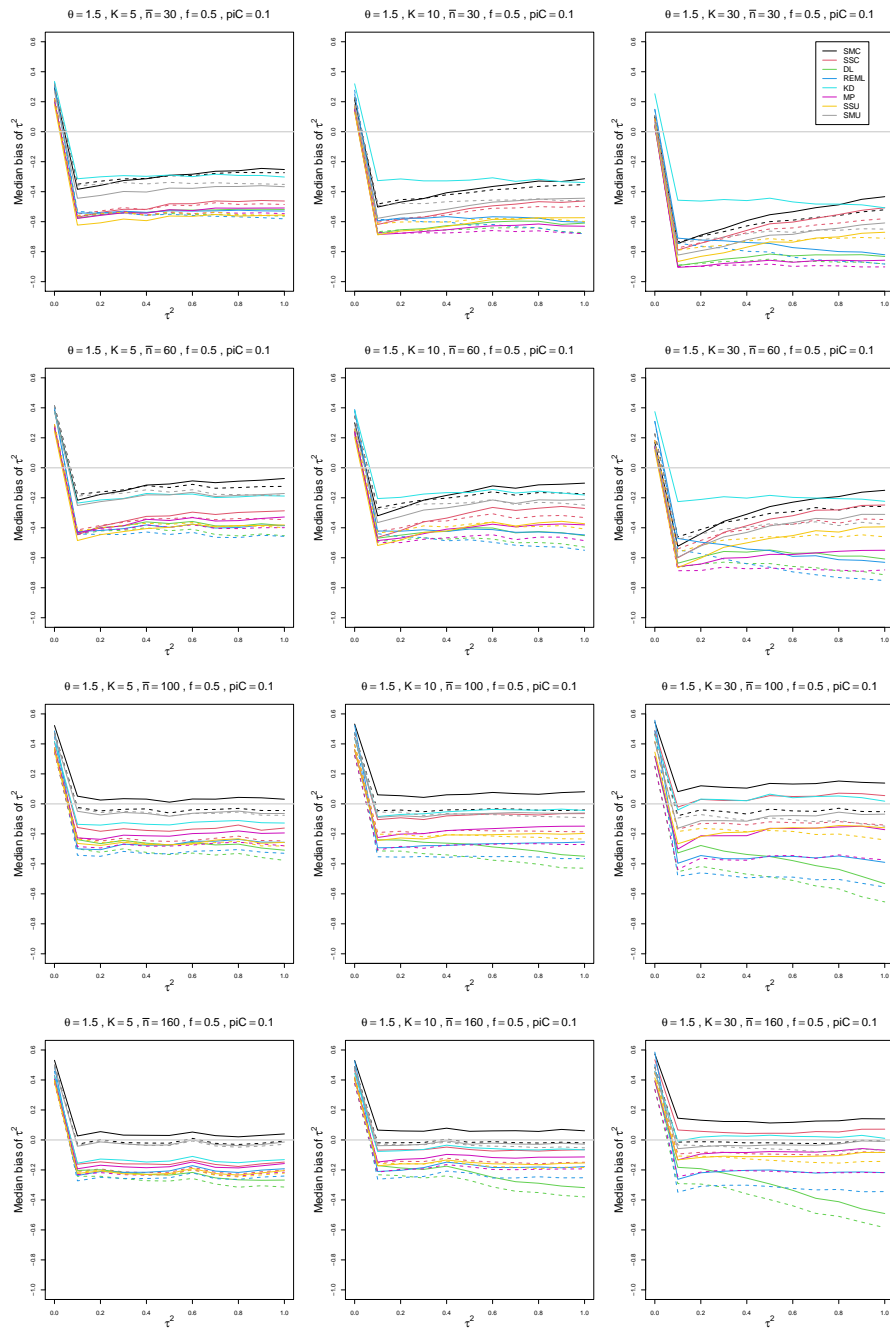


Figure B.10: Median bias of estimators of between-study variance of LOR (DL, REML, KD, MP, SMC, SSC, SMU, and SSU) vs τ^2 , for unequal sample sizes $\bar{n} = 30, 60, 100$ and 160 , $p_{iC} = .1$, $\theta = 1.5$ and $f = 0.5$. Solid lines: DL, REML, MP, SSC, SMC “only”; KD; SSU and SMU model-based. Dashed lines: DL, REML, MP, SSC, SMC “always”; SSU and SMU naïve.

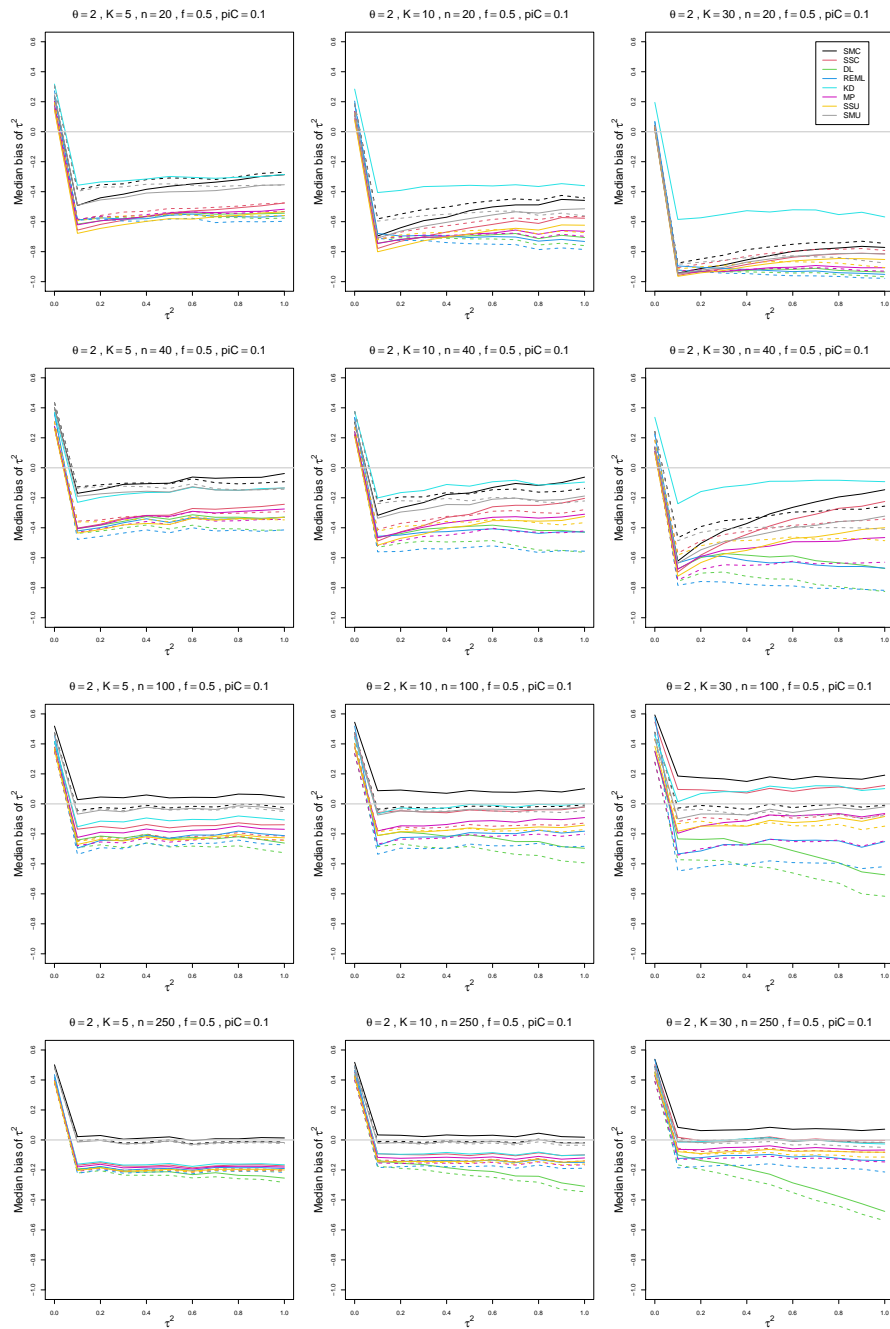


Figure B.11: Median bias of estimators of between-study variance of LOR (DL, REML, KD, MP, SMC, SSC, SMU, and SSU) vs τ^2 , for equal sample sizes $n = 20, 40, 100$ and 250 , $p_{iC} = .1$, $\theta = 2$ and $f = 0.5$. Solid lines: DL, REML, MP, SSC, SMC “only”; KD; SSU and SMU model-based. Dashed lines: DL, REML, MP, SSC, SMC “always”; SSU and SMU naïve.

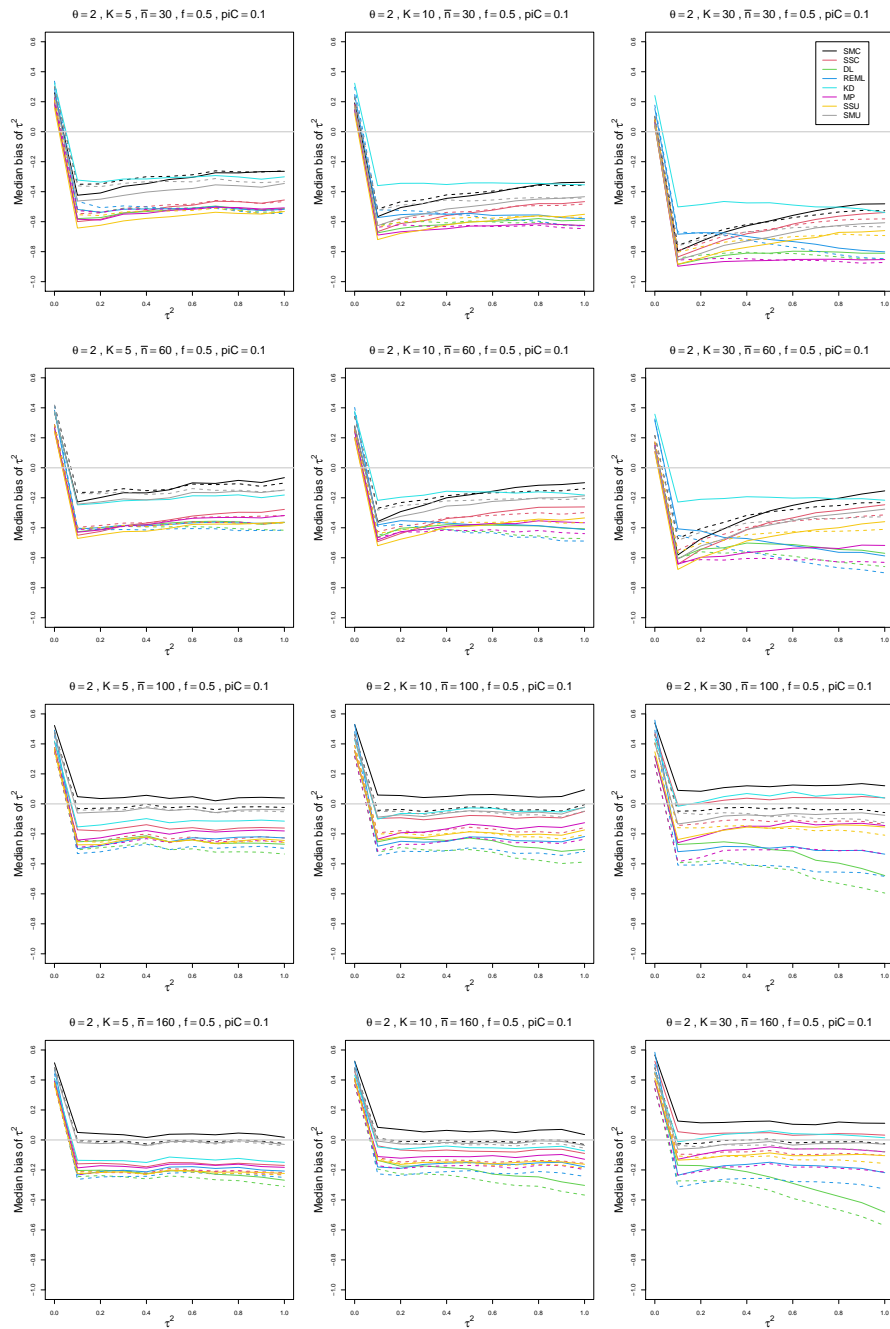


Figure B.12: Median bias of estimators of between-study variance of LOR (DL, REML, KD, MP, SMC, SSC, SMU, and SSU) vs τ^2 , for unequal sample sizes $\bar{n} = 30, 60, 100$ and 160 , $p_{iC} = .1$, $\theta = 2$ and $f = 0.5$. Solid lines: DL, REML, MP, SSC, SMC “only”; KD; SSU and SMU model-based. Dashed lines: DL, REML, MP, SSC, SMC “always”; SSU and SMU naïve.

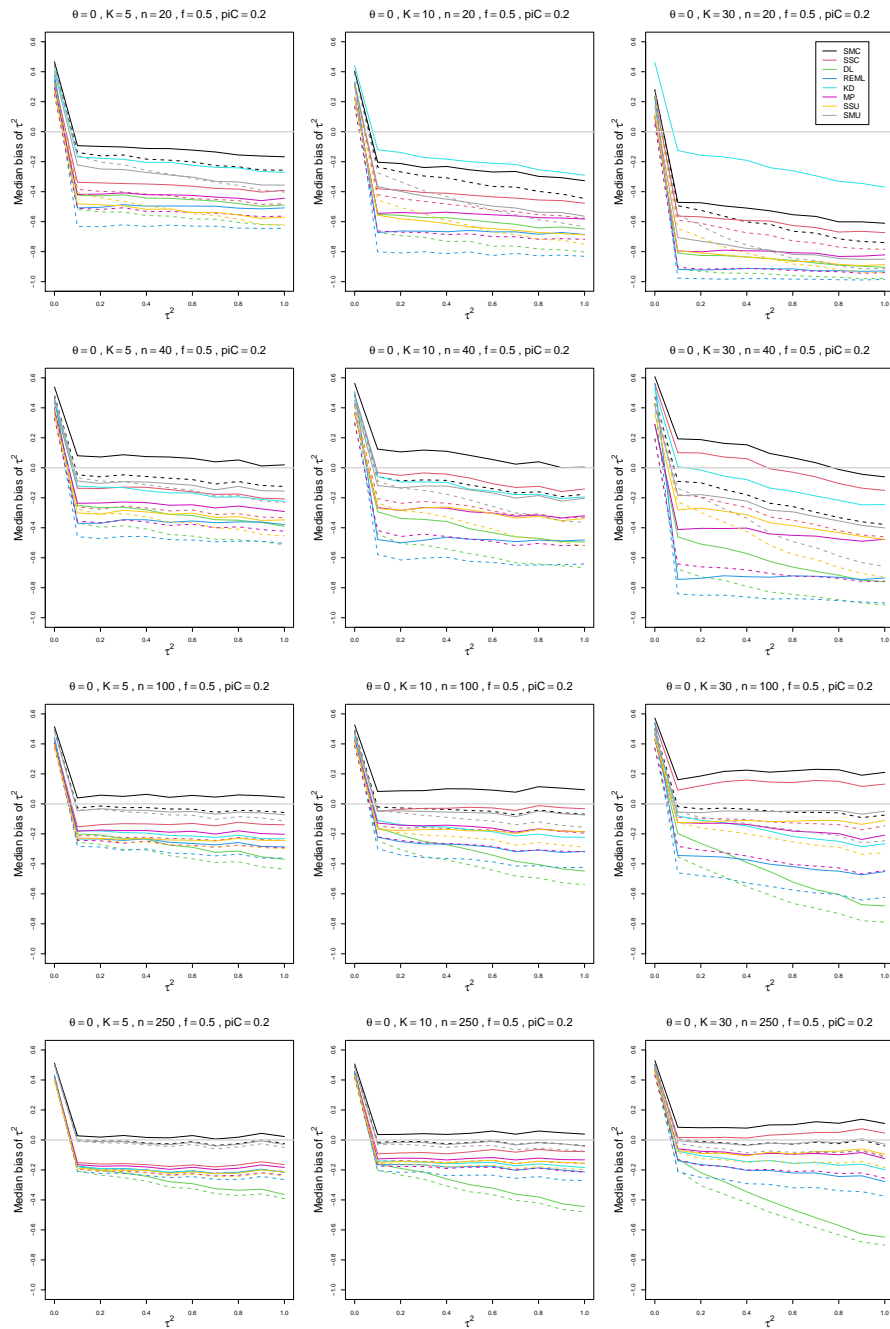


Figure B.13: Median bias of estimators of between-study variance of LOR (DL, REML, KD, MP, SMC, SSC, SMU, and SSU) vs τ^2 , for equal sample sizes $n = 20, 40, 100$ and 250 , $p_{iC} = .2$, $\theta = 0$ and $f = 0.5$. Solid lines: DL, REML, MP, SSC, SMC “only”; KD; SSU and SMU model-based. Dashed lines: DL, REML, MP, SSC, SMC “always”; SSU and SMU naïve.

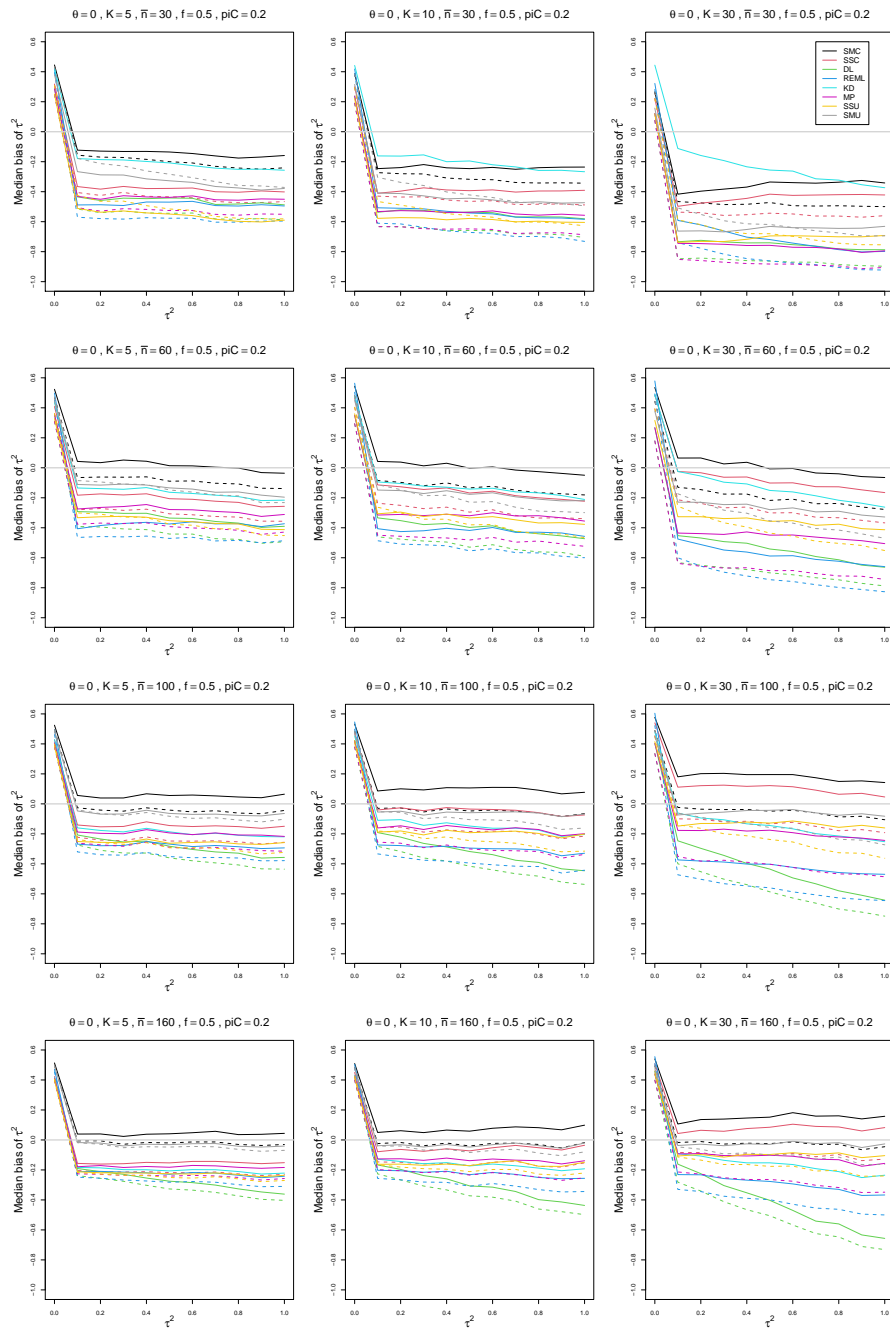


Figure B.14: Median bias of estimators of between-study variance of LOR (DL, REML, KD, MP, SMC, SSC, SMU, and SSU) vs τ^2 , for unequal sample sizes $\bar{n} = 30, 60, 100$ and 160 , $p_{iC} = .2$, $\theta = 0$ and $f = 0.5$. Solid lines: DL, REML, MP, SSC, SMC “only”; KD; SSU and SMU model-based. Dashed lines: DL, REML, MP, SSC, SMC “always”; SSU and SMU naïve.

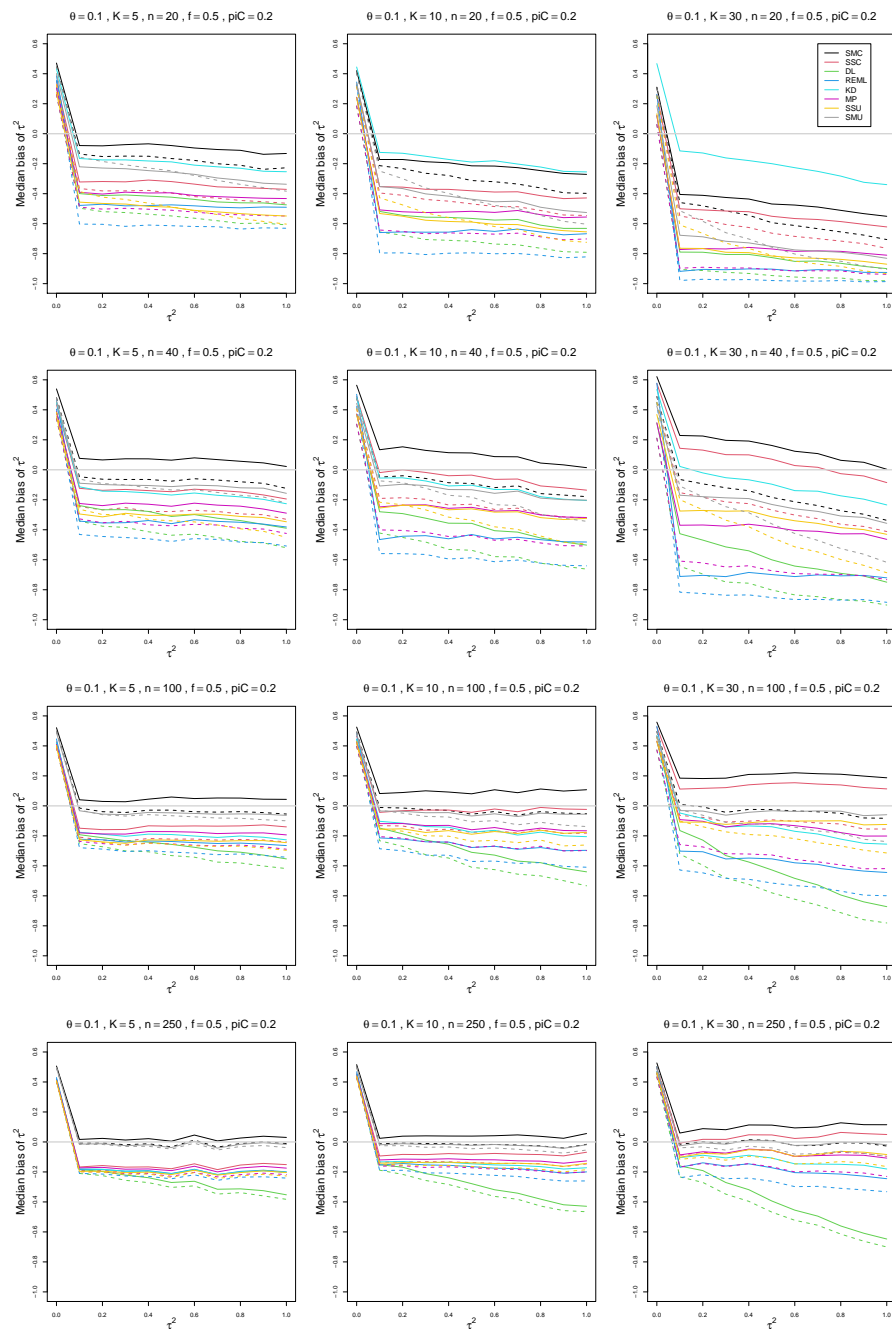


Figure B.15: Median bias of estimators of between-study variance of LOR (DL, REML, KD, MP, SMC, SSC, SMU, and SSU) vs τ^2 , for equal sample sizes $n = 20, 40, 100$ and 250 , $p_{iC} = .2$, $\theta = 0.1$ and $f = 0.5$. Solid lines: DL, REML, MP, SSC, SMC “only”; KD; SSU and SMU model-based. Dashed lines: DL, REML, MP, SSC, SMC “always”; SSU and SMU naïve.

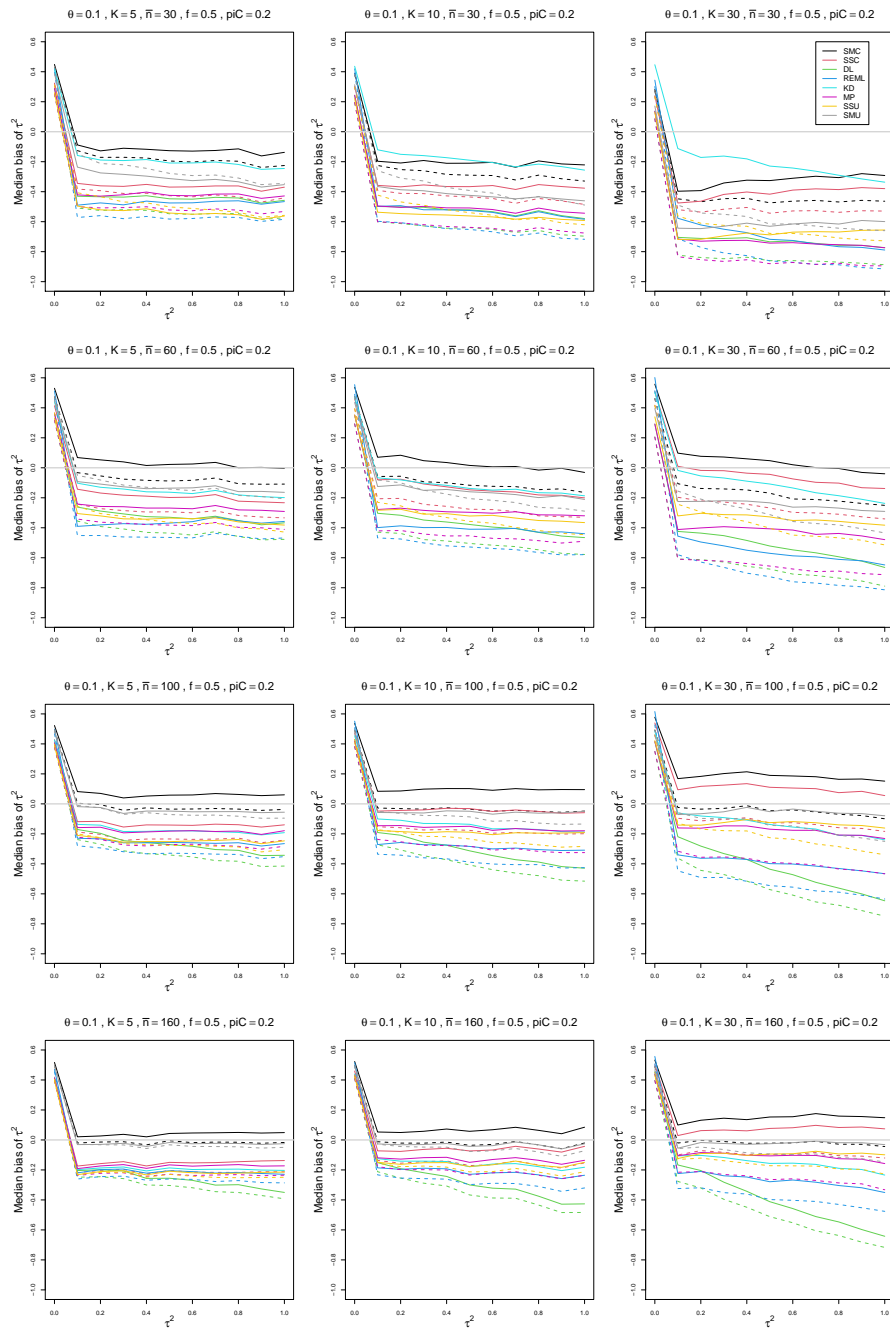


Figure B.16: Median bias of estimators of between-study variance of LOR (DL, REML, KD, MP, SMC, SSC, SMU, and SSU) vs τ^2 , for unequal sample sizes $\bar{n} = 30, 60, 100$ and 160 , $p_{iC} = .2$, $\theta = 0.1$ and $f = 0.5$. Solid lines: DL, REML, MP, SSC, SMC “only”; KD; SSU and SMU model-based. Dashed lines: DL, REML, MP, SSC, SMC “always”; SSU and SMU naïve.

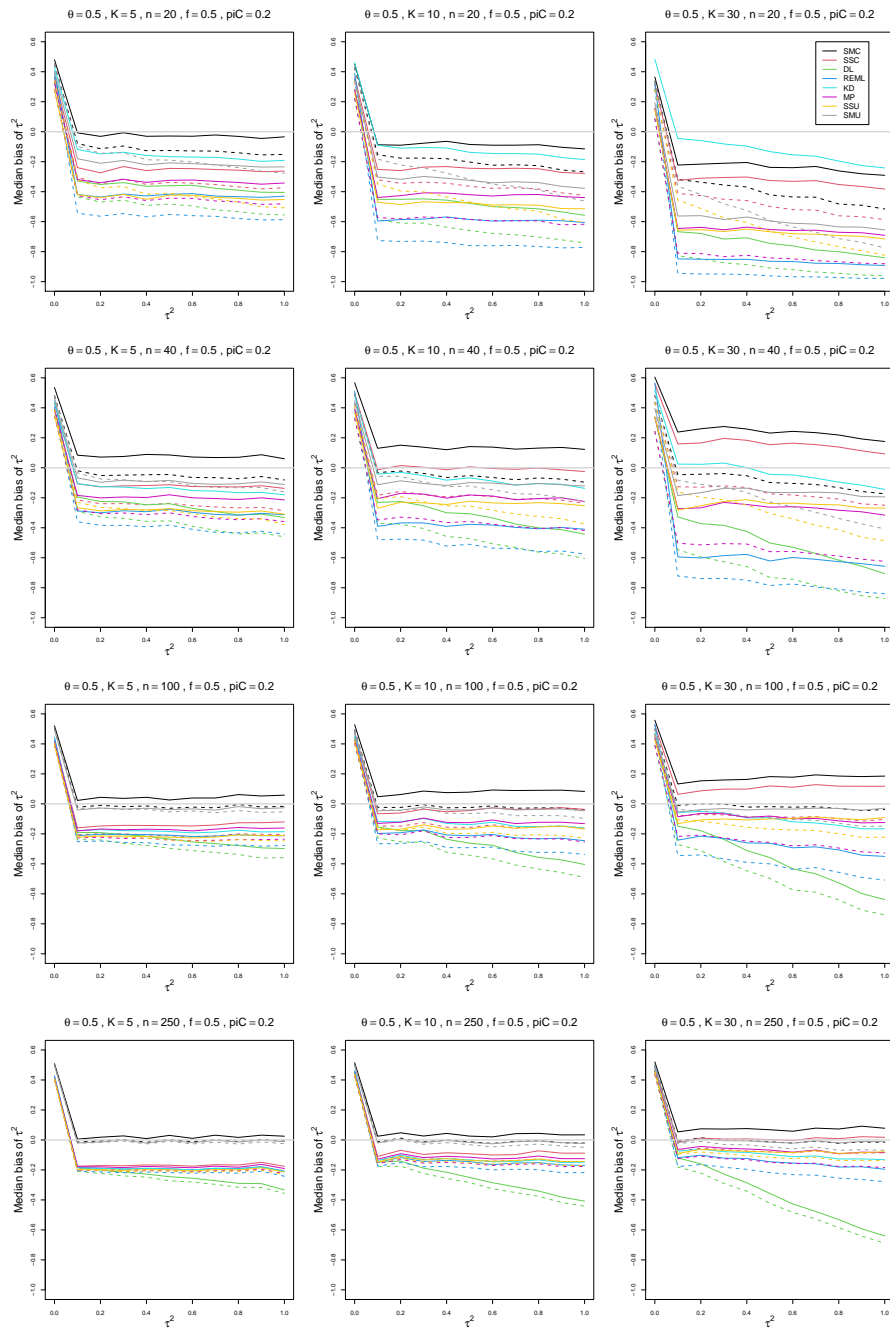


Figure B.17: Median bias of estimators of between-study variance of LOR (DL, REML, KD, MP, SMC, SSC, SMU, and SSU) vs τ^2 , for equal sample sizes $n = 20, 40, 100$ and 250 , $p_{iC} = .2$, $\theta = 0.5$ and $f = 0.5$. Solid lines: DL, REML, MP, SSC, SMC “only”; KD; SSU and SMU model-based. Dashed lines: DL, REML, MP, SSC, SMC “always”; SSU and SMU naïve.

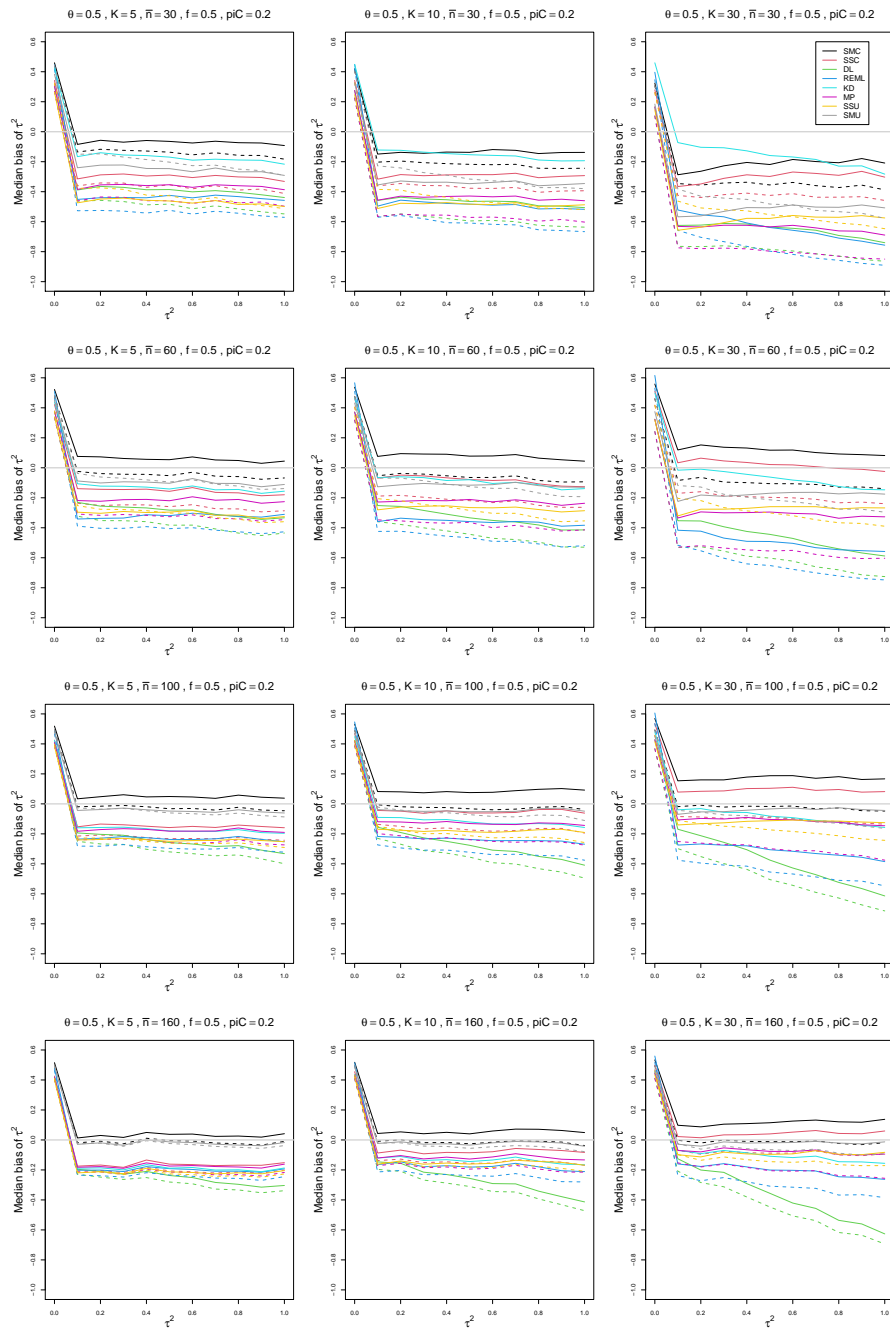


Figure B.18: Median bias of estimators of between-study variance of LOR (DL, REML, KD, MP, SMC, SSC, SMU, and SSU) vs τ^2 , for unequal sample sizes $\bar{n} = 30, 60, 100$ and 160 , $p_{iC} = .2$, $\theta = 0.5$ and $f = 0.5$. Solid lines: DL, REML, MP, SSC, SMC “only”; KD; SSU and SMU model-based. Dashed lines: DL, REML, MP, SSC, SMC “always”; SSU and SMU naïve.

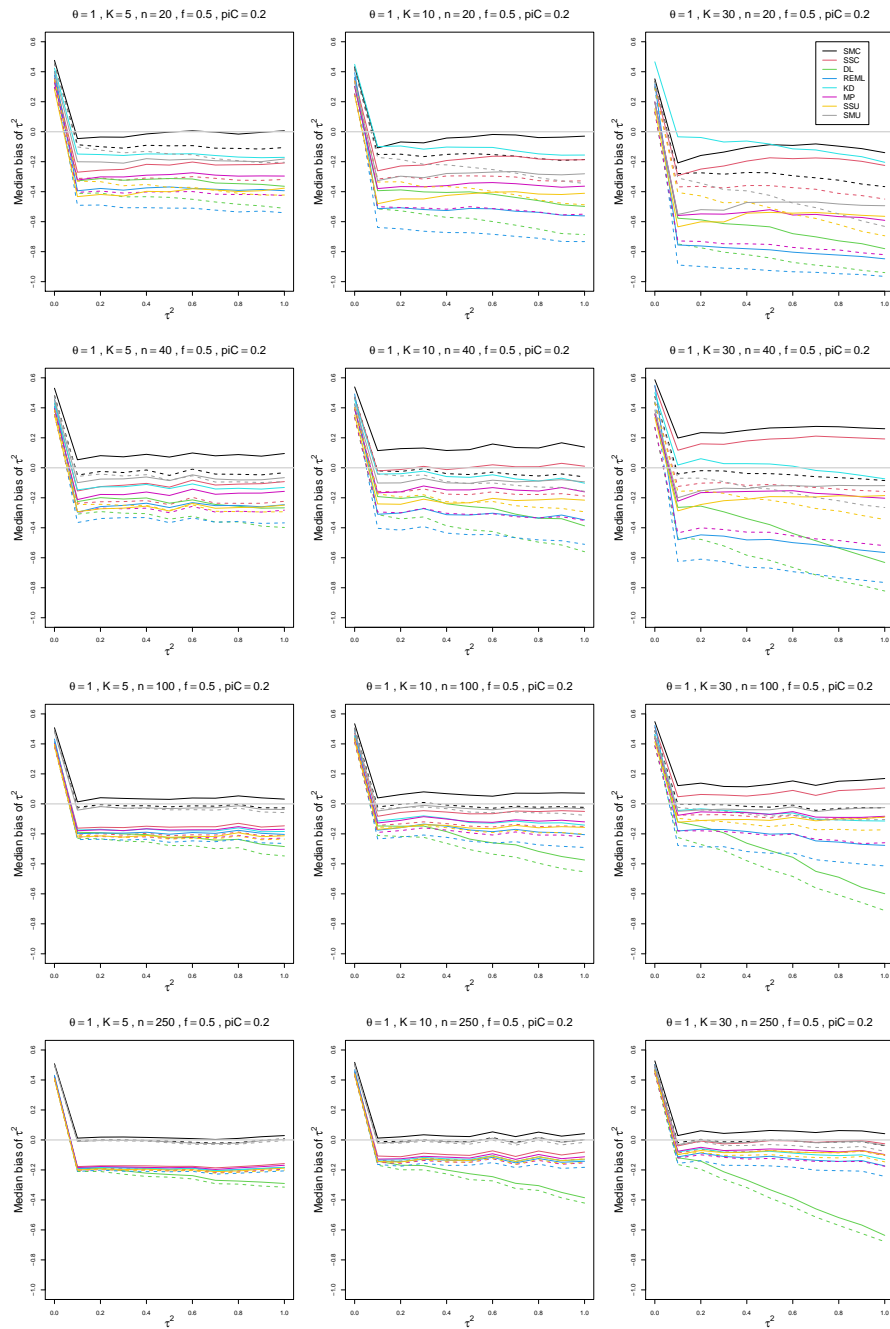


Figure B.19: Median bias of estimators of between-study variance of LOR (DL, REML, KD, MP, SMC, SSC, SMU, and SSU) vs τ^2 , for equal sample sizes $n = 20, 40, 100$ and 250 , $p_{iC} = .2$, $\theta = 1$ and $f = 0.5$. Solid lines: DL, REML, MP, SSC, SMC “only”; KD; SSU and SMU model-based. Dashed lines: DL, REML, MP, SSC, SMC “always”; SSU and SMU naïve.

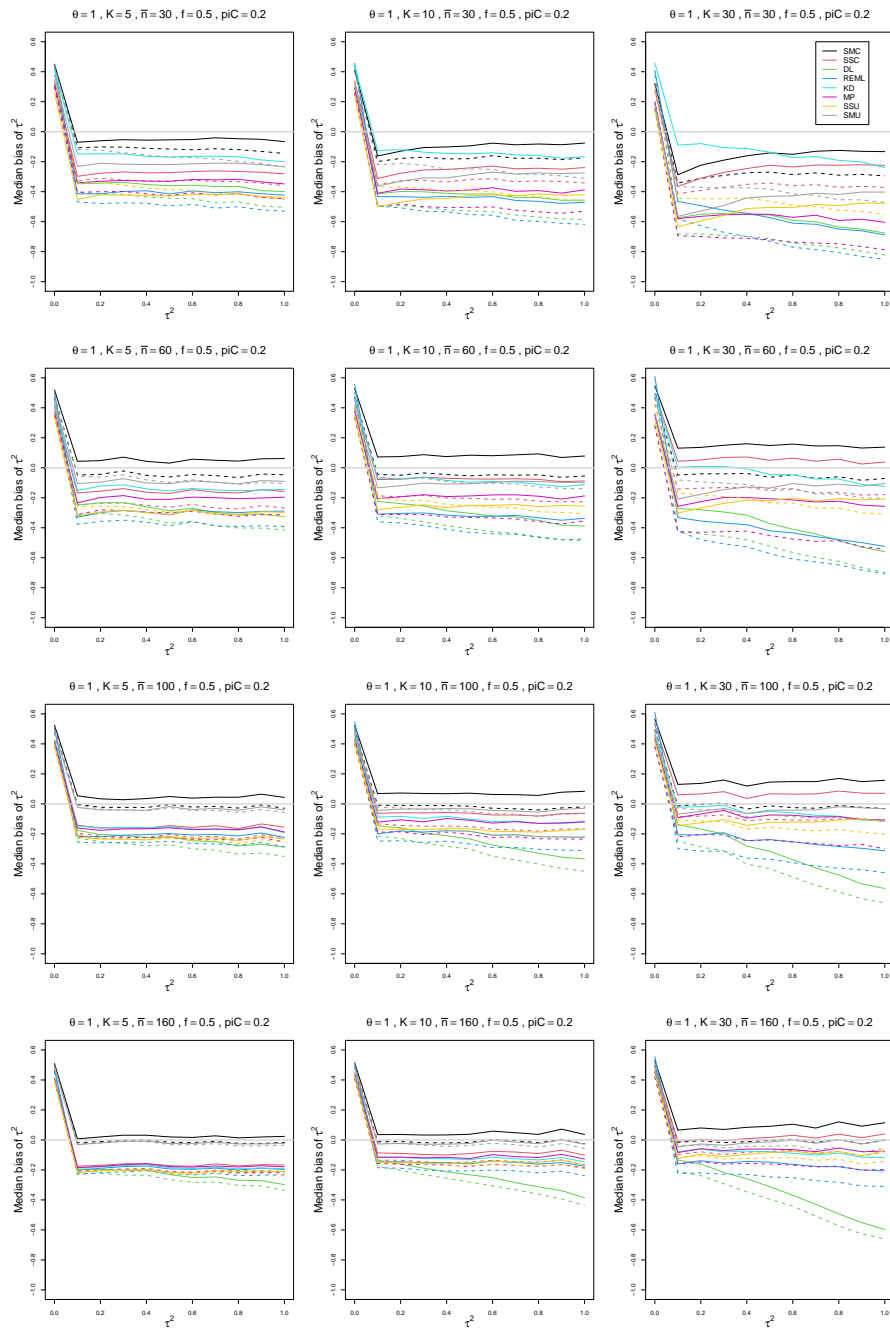


Figure B.20: Median bias of estimators of between-study variance of LOR (DL, REML, KD, MP, SMC, SSC, SMU, and SSU) vs τ^2 , for unequal sample sizes $\bar{n} = 30, 60, 100$ and 160 , $p_{iC} = .2$, $\theta = 1$ and $f = 0.5$. Solid lines: DL, REML, MP, SSC, SMC “only”; KD; SSU and SMU model-based. Dashed lines: DL, REML, MP, SSC, SMC “always”; SSU and SMU naïve.

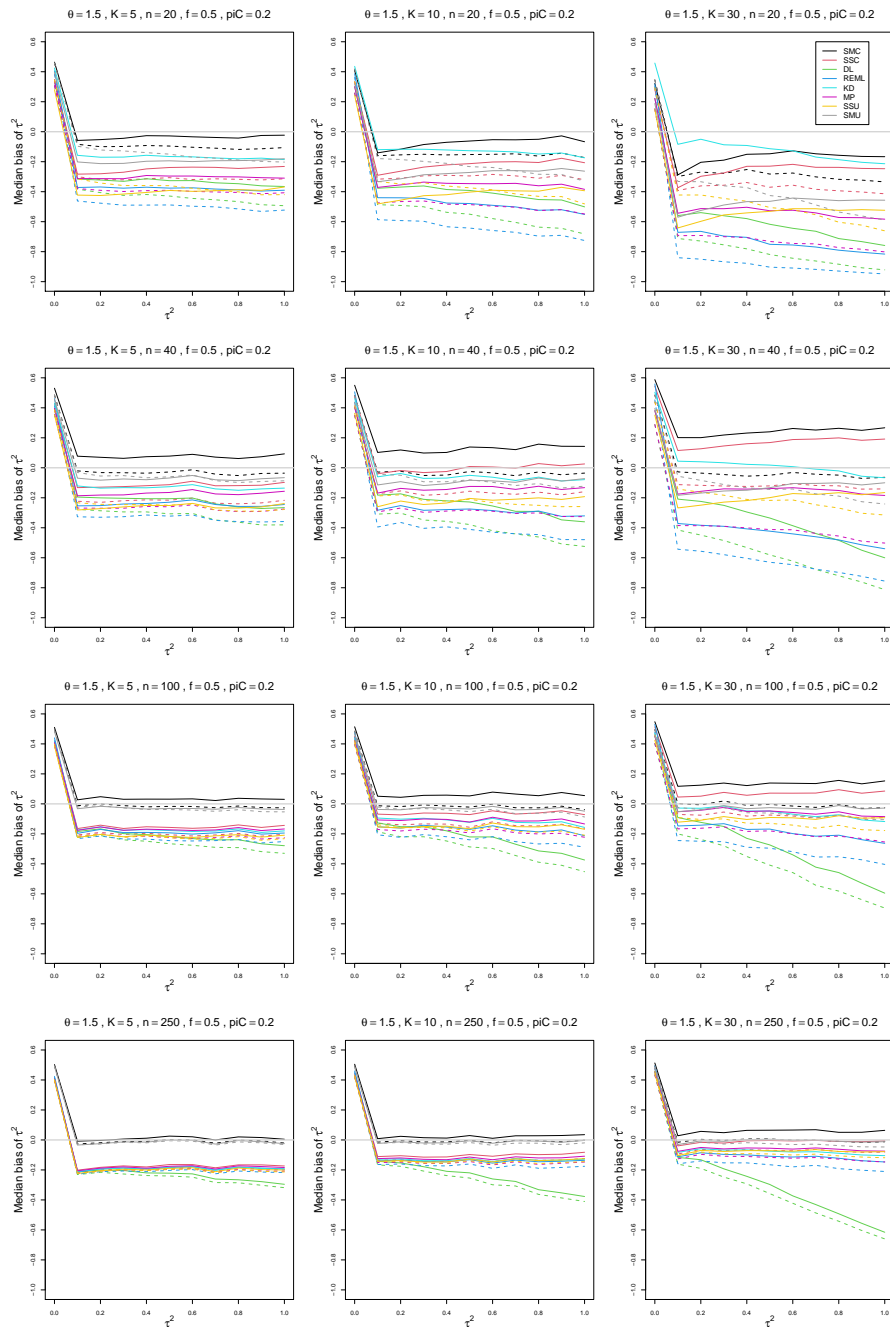


Figure B.21: Median bias of estimators of between-study variance of LOR (DL, REML, KD, MP, SMC, SSC, SMU, and SSU) vs τ^2 , for equal sample sizes $n = 20, 40, 100$ and 250 , $p_{iC} = .2$, $\theta = 1.5$ and $f = 0.5$. Solid lines: DL, REML, MP, SSC, SMC “only”; KD; SSU and SMU model-based. Dashed lines: DL, REML, MP, SSC, SMC “always”; SSU and SMU naïve.

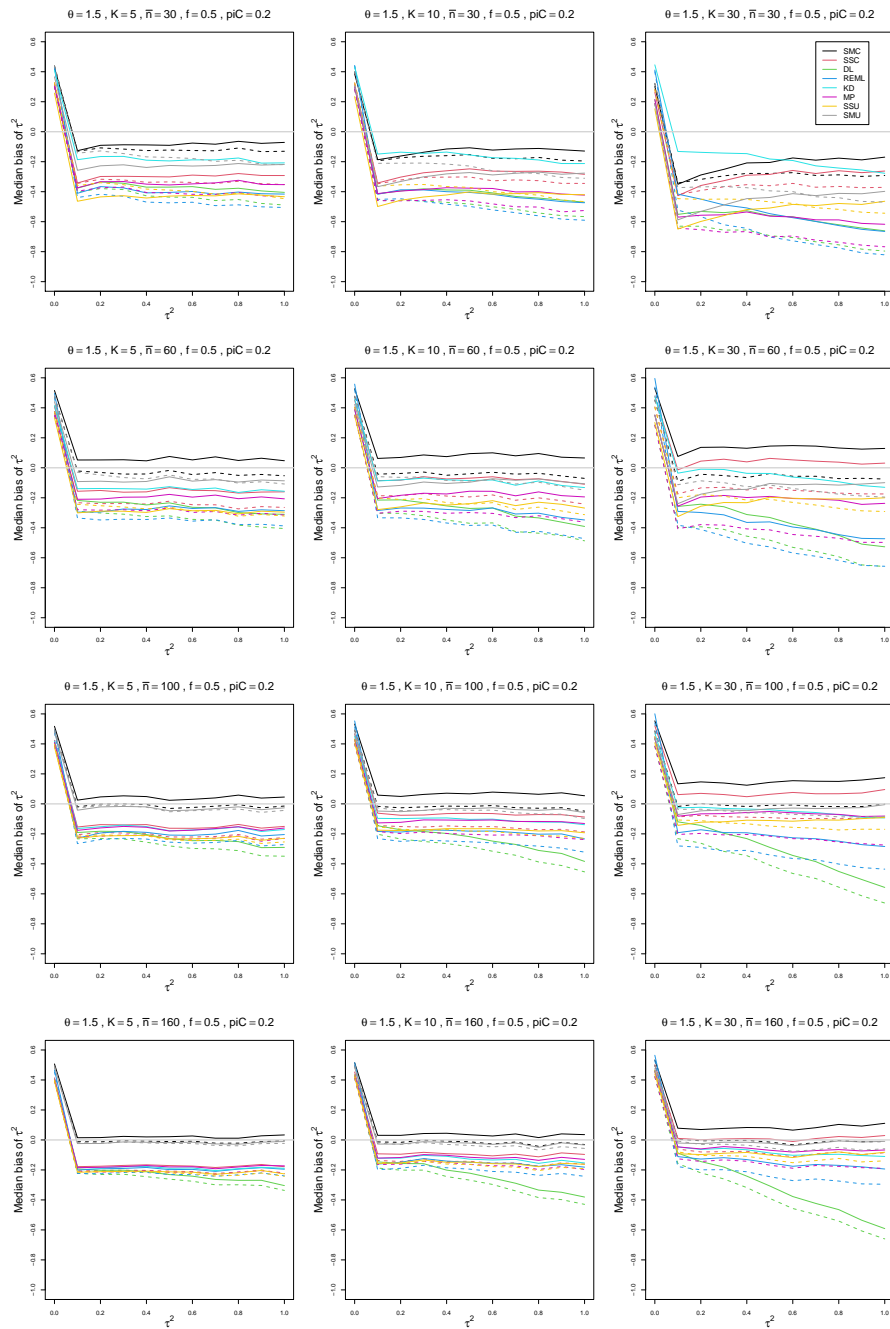


Figure B.22: Median bias of estimators of between-study variance of LOR (DL, REML, KD, MP, SMC, SSC, SMU, and SSU) vs τ^2 , for unequal sample sizes $\bar{n} = 30, 60, 100$ and 160 , $p_{iC} = .2$, $\theta = 1.5$ and $f = 0.5$. Solid lines: DL, REML, MP, SSC, SMC “only”; KD; SSU and SMU model-based. Dashed lines: DL, REML, MP, SSC, SMC “always”; SSU and SMU naïve.

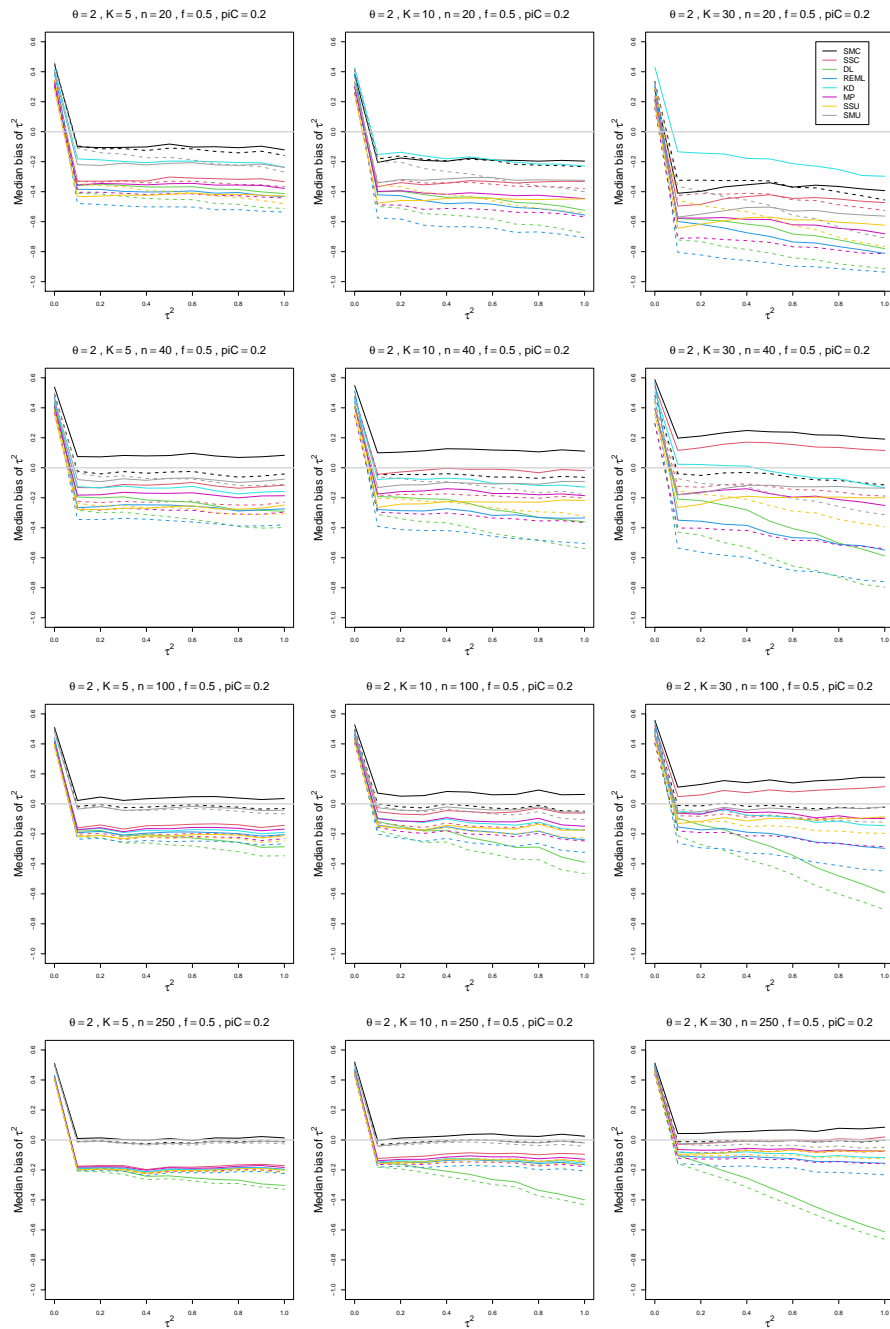


Figure B.23: Median bias of estimators of between-study variance of LOR (DL, REML, KD, MP, SMC, SSC, SMU, and SSU) vs τ^2 , for equal sample sizes $n = 20, 40, 100$ and 250 , $p_{iC} = .2$, $\theta = 2$ and $f = 0.5$. Solid lines: DL, REML, MP, SSC, SMC “only”; KD; SSU and SMU model-based. Dashed lines: DL, REML, MP, SSC, SMC “always”; SSU and SMU naïve.

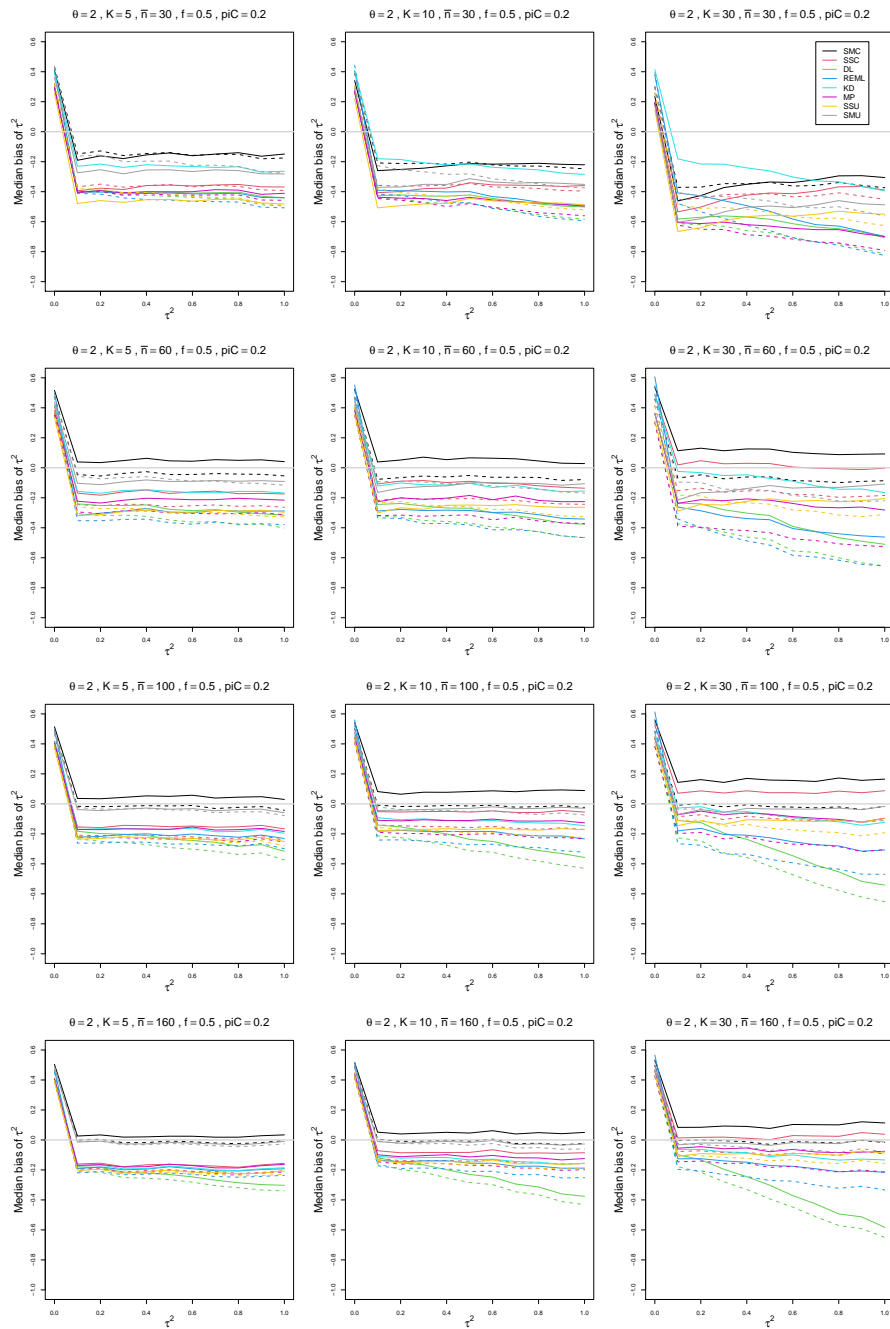


Figure B.24: Median bias of estimators of between-study variance of LOR (DL, REML, KD, MP, SMC, SSC, SMU, and SSU) vs τ^2 , for unequal sample sizes $\bar{n} = 30, 60, 100$ and 160 , $p_{iC} = .2$, $\theta = 2$ and $f = 0.5$. Solid lines: DL, REML, MP, SSC, SMC “only”; KD; SSU and SMU model-based. Dashed lines: DL, REML, MP, SSC, SMC “always”; SSU and SMU naïve.

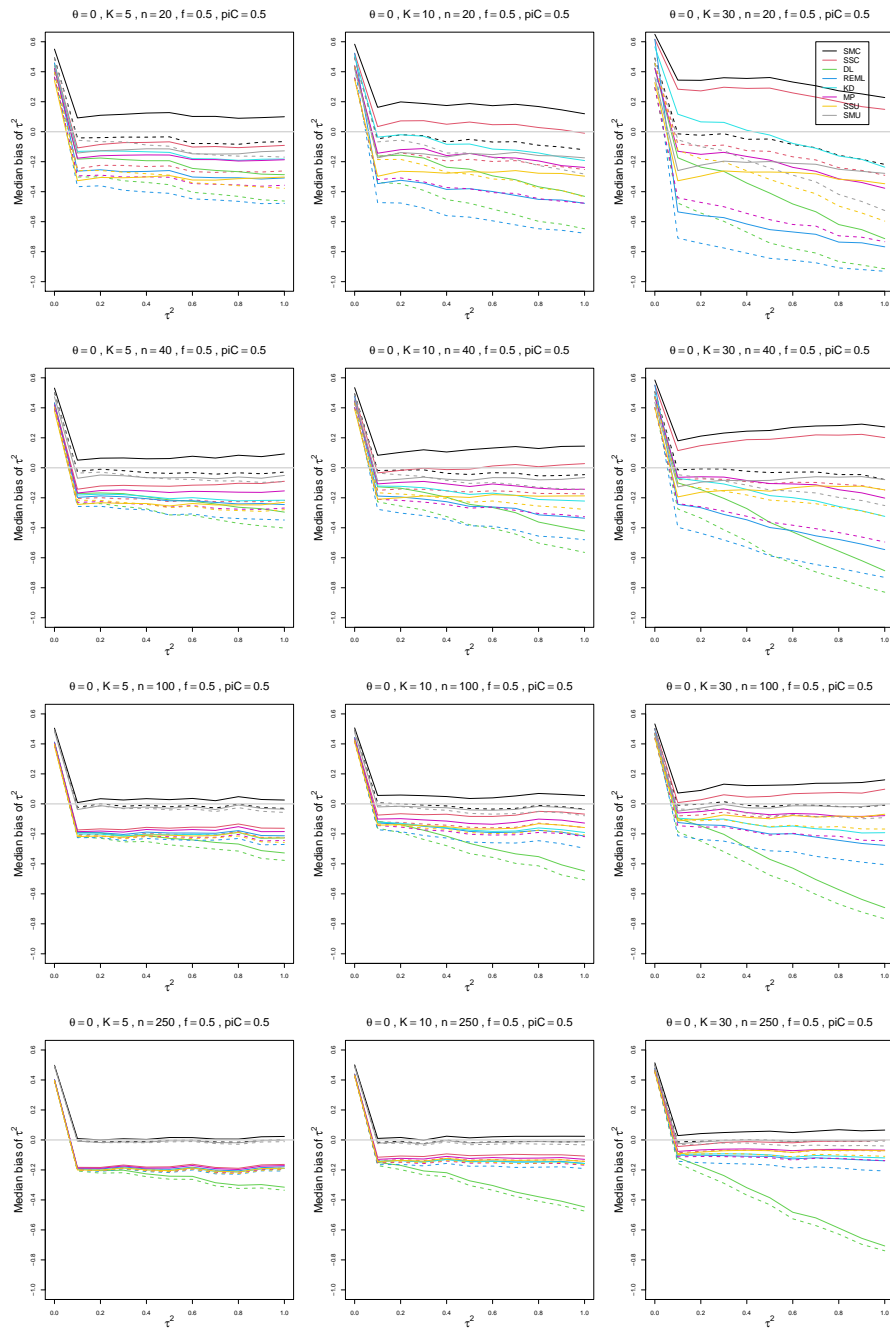


Figure B.25: Median bias of estimators of between-study variance of LOR (DL, REML, KD, MP, SMC, SSC, SMU, and SSU) vs τ^2 , for equal sample sizes $n = 20, 40, 100$ and 250 , $p_{iC} = .5$, $\theta = 0$ and $f = 0.5$. Solid lines: DL, REML, MP, SSC, SMC “only”; KD; SSU and SMU model-based. Dashed lines: DL, REML, MP, SSC, SMC “always”; SSU and SMU naïve.

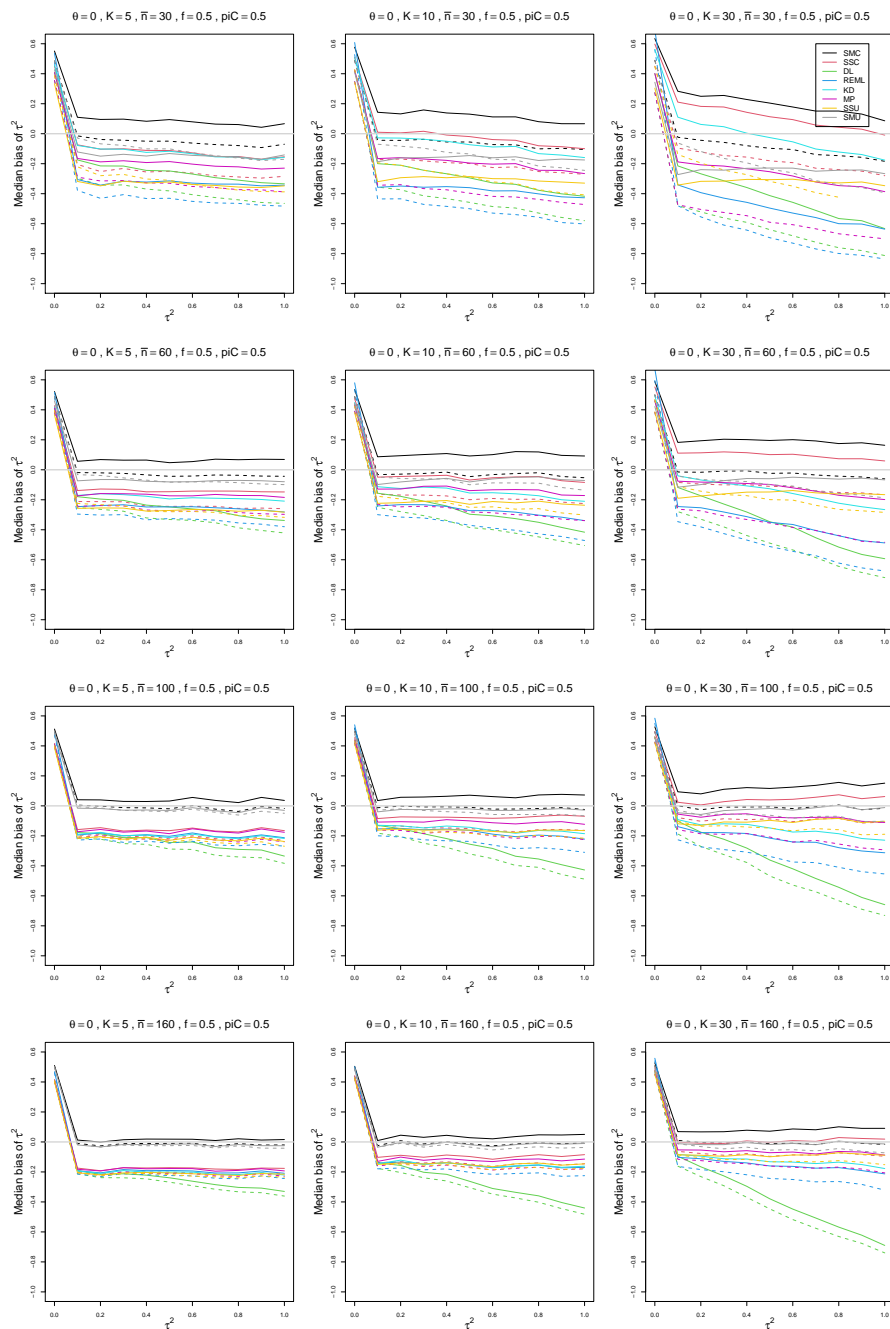


Figure B.26: Median bias of estimators of between-study variance of LOR (DL, REML, KD, MP, SMC, SSC, SMU, and SSU) vs τ^2 , for unequal sample sizes $\bar{n} = 30, 60, 100$ and 160 , $p_{iC} = .5$, $\theta = 0$ and $f = 0.5$. Solid lines: DL, REML, MP, SSC, SMC “only”; KD; SSU and SMU model-based. Dashed lines: DL, REML, MP, SSC, SMC “always”; SSU and SMU naïve.

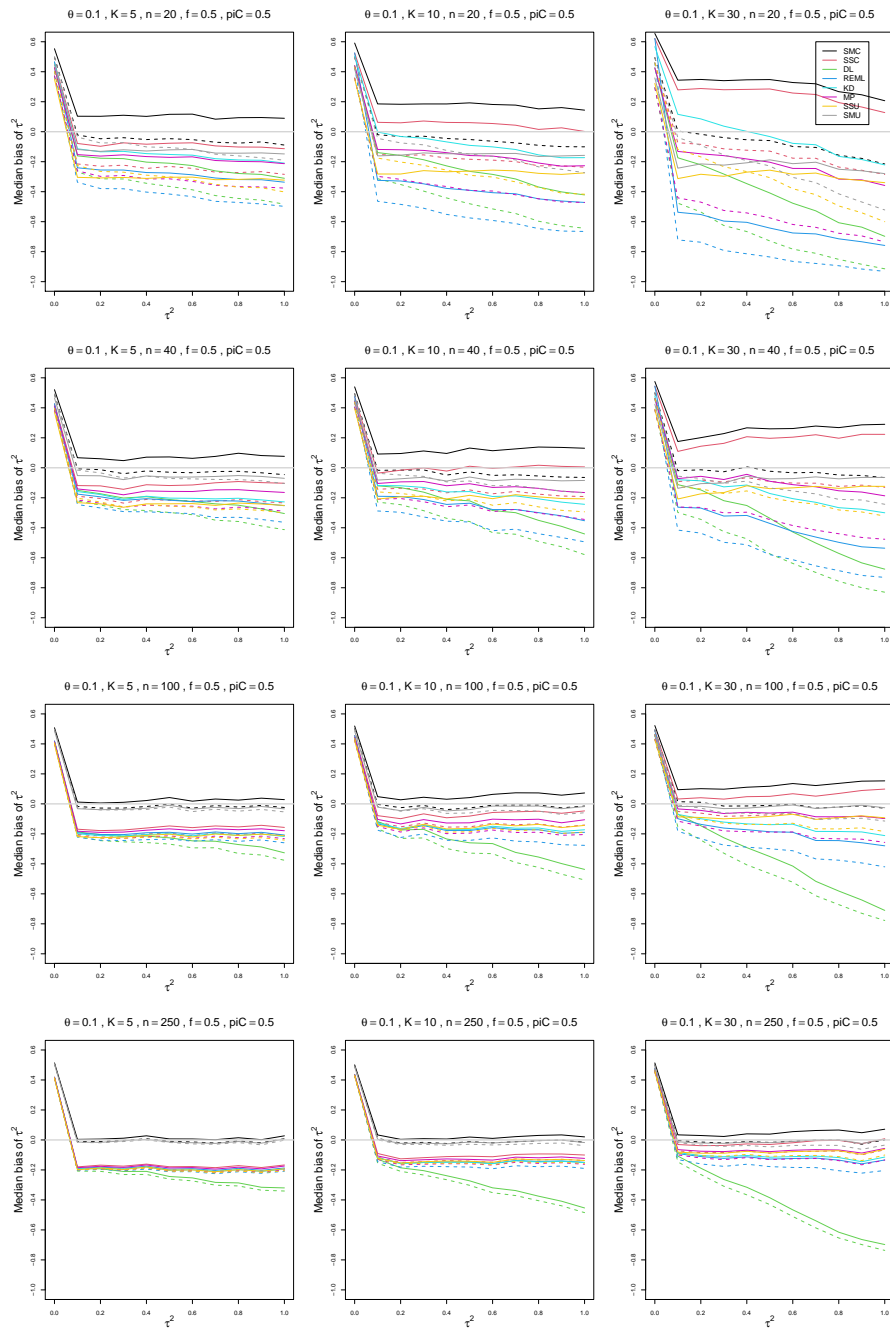


Figure B.27: Median bias of estimators of between-study variance of LOR (DL, REML, KD, MP, SMC, SSC, SMU, and SSU) vs τ^2 , for equal sample sizes $n = 20, 40, 100$ and 250 , $p_{iC} = .5$, $\theta = 0.1$ and $f = 0.5$. Solid lines: DL, REML, MP, SSC, SMC “only”; KD; SSU and SMU model-based. Dashed lines: DL, REML, MP, SSC, SMC “always”; SSU and SMU naïve.

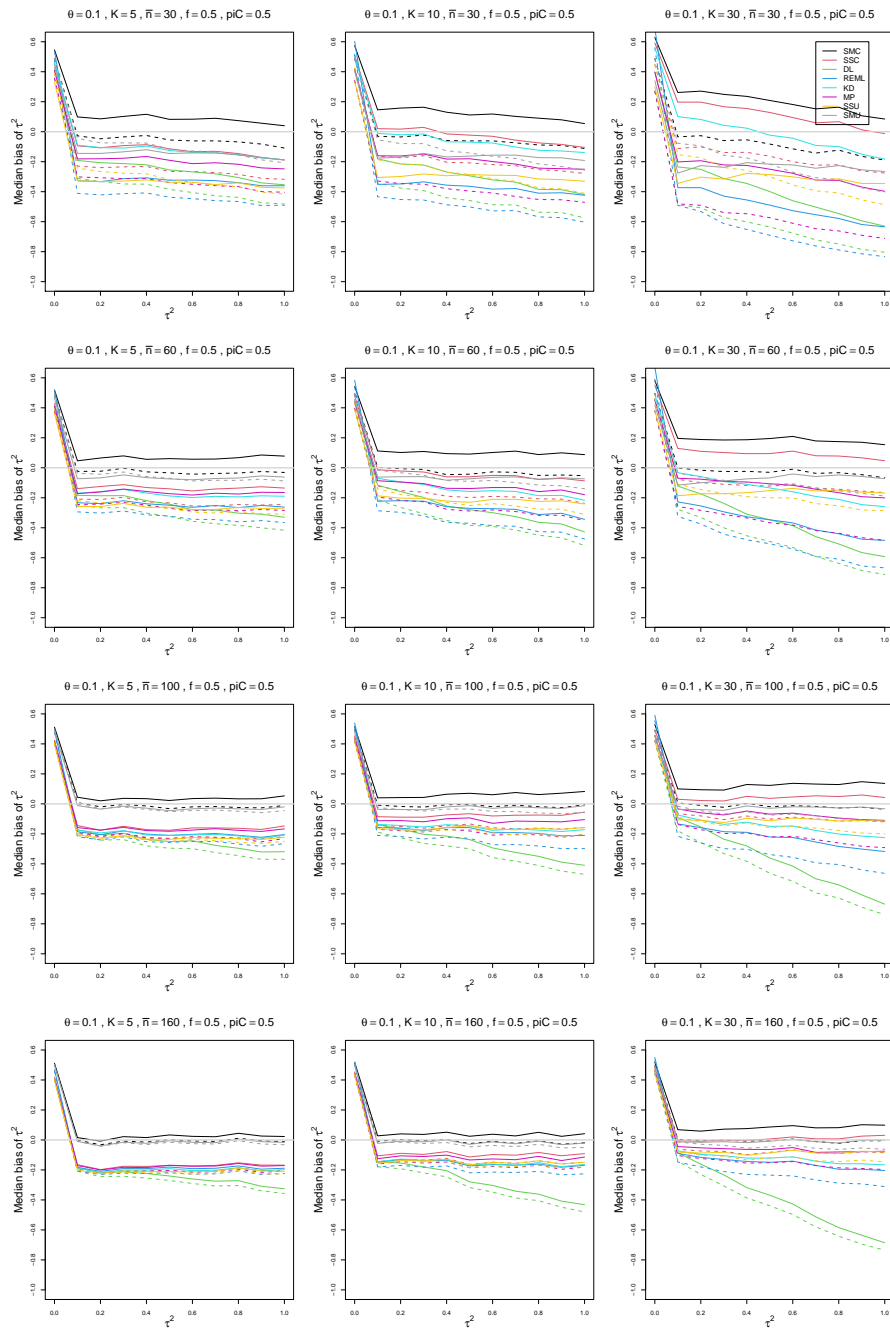


Figure B.28: Median bias of estimators of between-study variance of LOR (DL, REML, KD, MP, SMC, SSC, SMU, and SSU) vs τ^2 , for unequal sample sizes $\bar{n} = 30, 60, 100$ and 160 , $p_{iC} = .5$, $\theta = 0.1$ and $f = 0.5$. Solid lines: DL, REML, MP, SSC, SMC “only”; KD; SSU and SMU model-based. Dashed lines: DL, REML, MP, SSC, SMC “always”; SSU and SMU naïve.

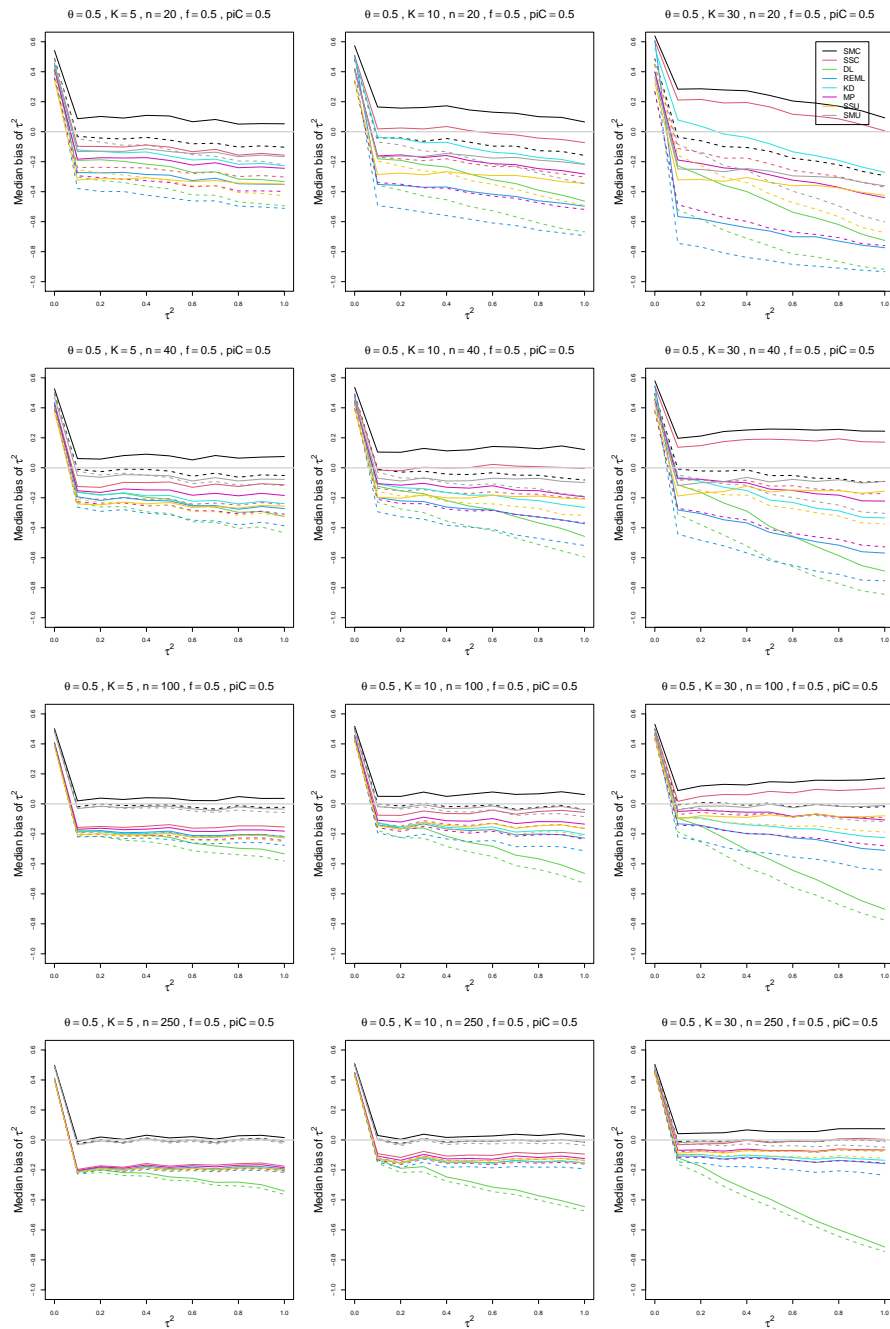


Figure B.29: Median bias of estimators of between-study variance of LOR (DL, REML, KD, MP, SMC, SSC, SMU, and SSU) vs τ^2 , for equal sample sizes $n = 20, 40, 100$ and 250 , $p_{iC} = .5$, $\theta = 0.5$ and $f = 0.5$. Solid lines: DL, REML, MP, SSC, SMC “only”; KD; SSU and SMU model-based. Dashed lines: DL, REML, MP, SSC, SMC “always”; SSU and SMU naïve.

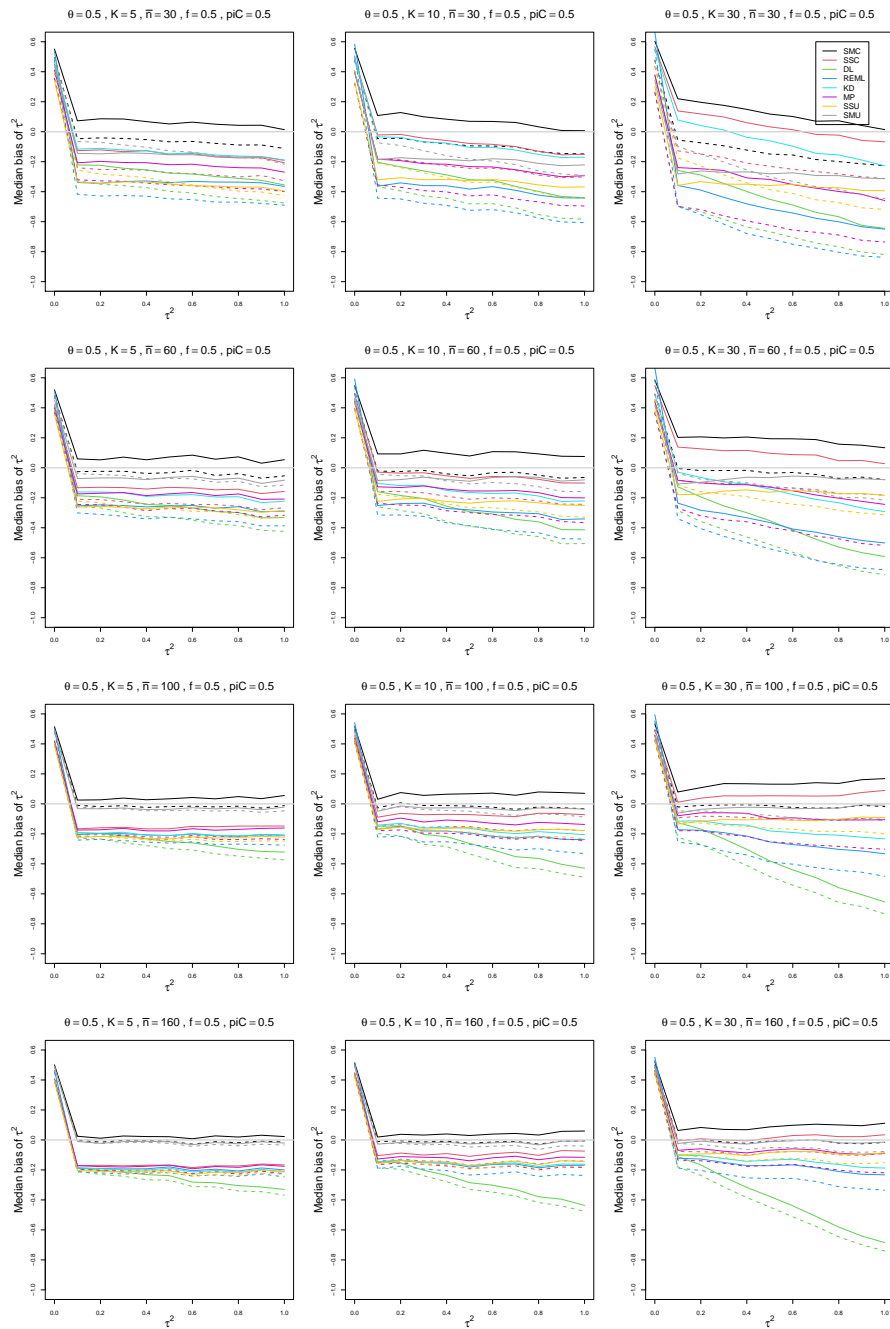


Figure B.30: Median bias of estimators of between-study variance of LOR (DL, REML, KD, MP, SMC, SSC, SMU, and SSU) vs τ^2 , for unequal sample sizes $\bar{n} = 30, 60, 100$ and 160 , $p_{iC} = .5$, $\theta = 0.5$ and $f = 0.5$. Solid lines: DL, REML, MP, SSC, SMC “only”; KD; SSU and SMU model-based. Dashed lines: DL, REML, MP, SSC, SMC “always”; SSU and SMU naïve.

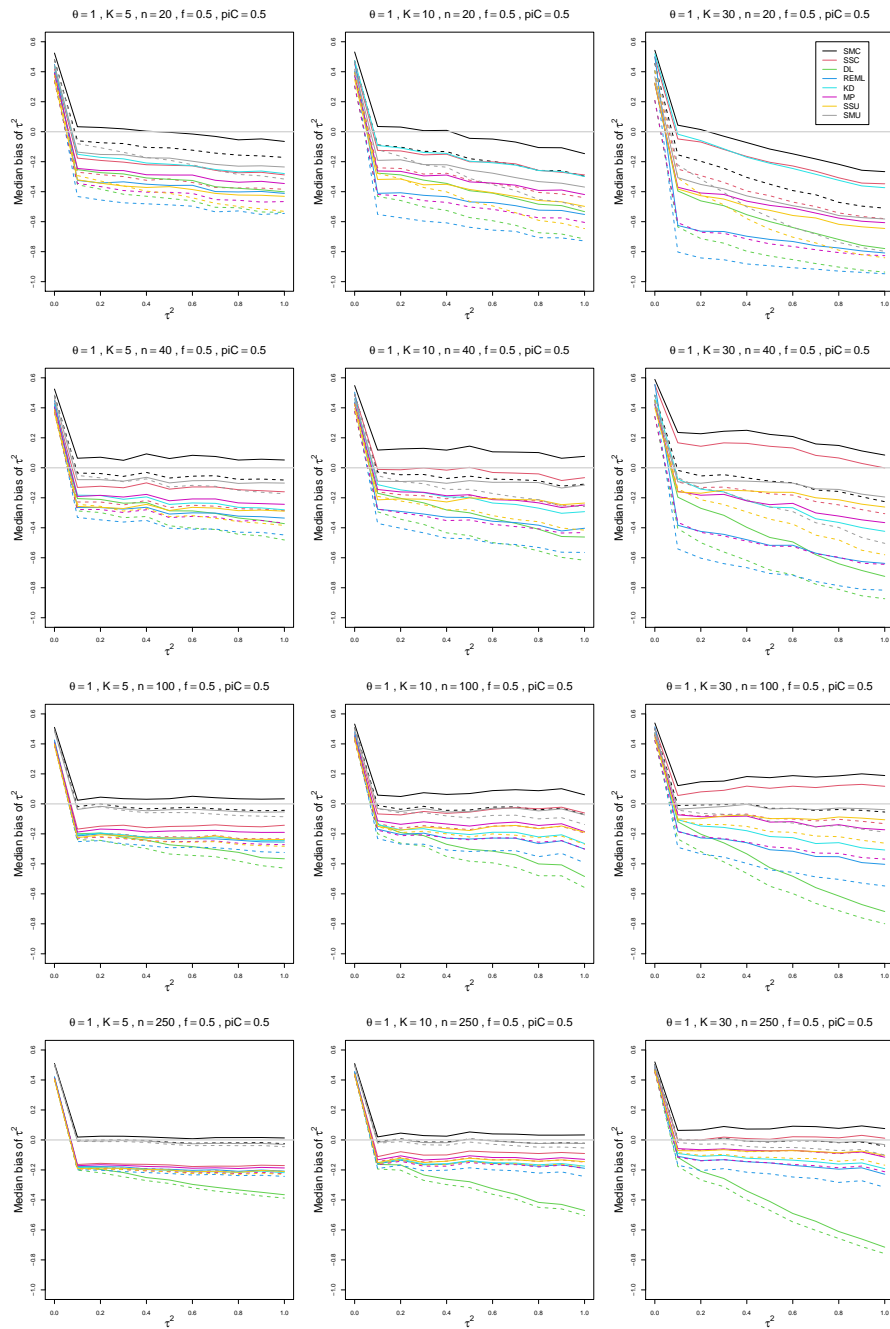


Figure B.31: Median bias of estimators of between-study variance of LOR (DL, REML, KD, MP, SMC, SSC, SMU, and SSU) vs τ^2 , for equal sample sizes $n = 20, 40, 100$ and 250 , $p_{iC} = .5$, $\theta = 1$ and $f = 0.5$. Solid lines: DL, REML, MP, SSC, SMC “only”; KD; SSU and SMU model-based. Dashed lines: DL, REML, MP, SSC, SMC “always”; SSU and SMU naïve.

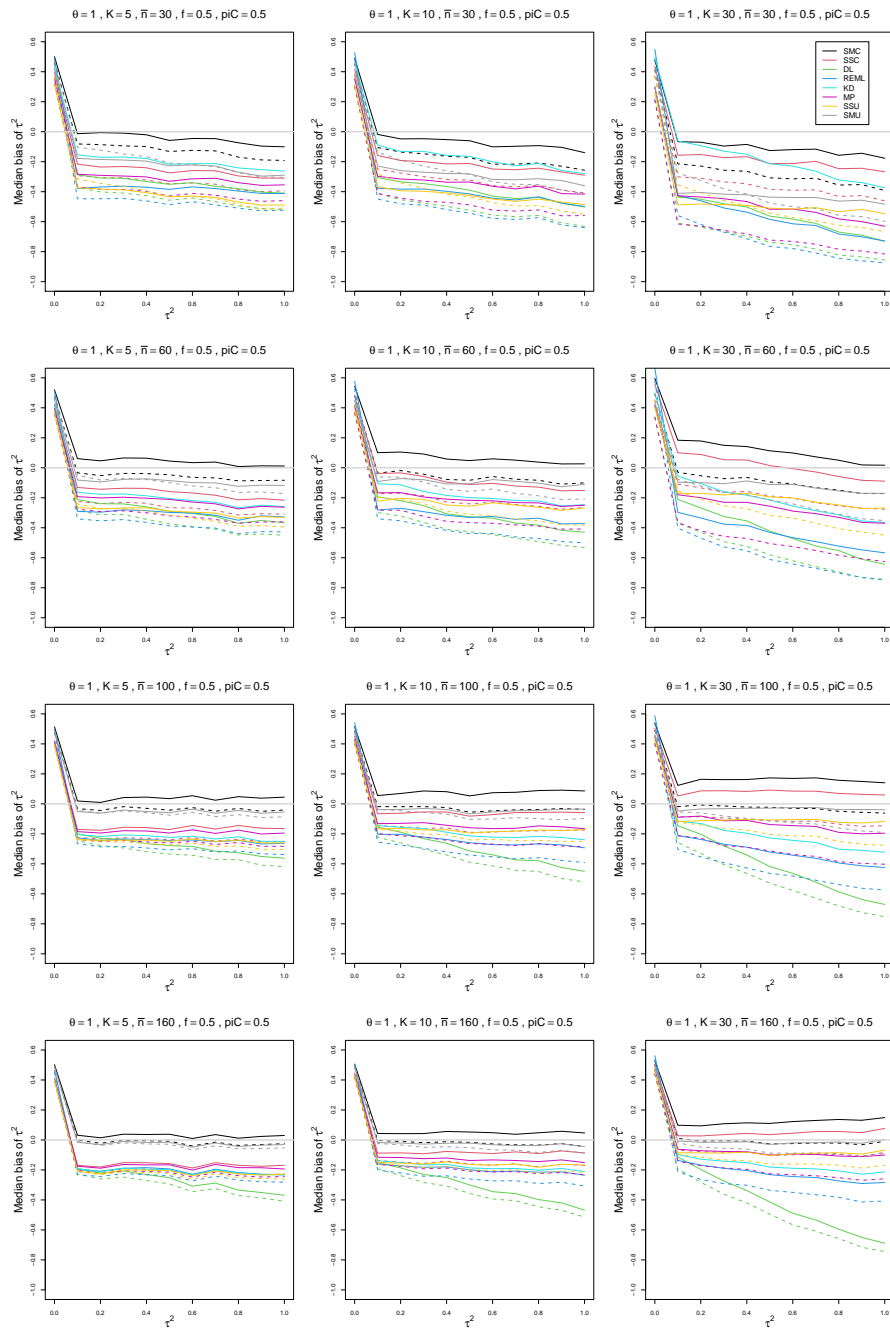


Figure B.32: Median bias of estimators of between-study variance of LOR (DL, REML, KD, MP, SMC, SSC, SMU, and SSU) vs τ^2 , for unequal sample sizes $\bar{n} = 30, 60, 100$ and 160 , $p_{iC} = .5$, $\theta = 1$ and $f = 0.5$. Solid lines: DL, REML, MP, SSC, SMC “only”; KD; SSU and SMU model-based. Dashed lines: DL, REML, MP, SSC, SMC “always”; SSU and SMU naïve.

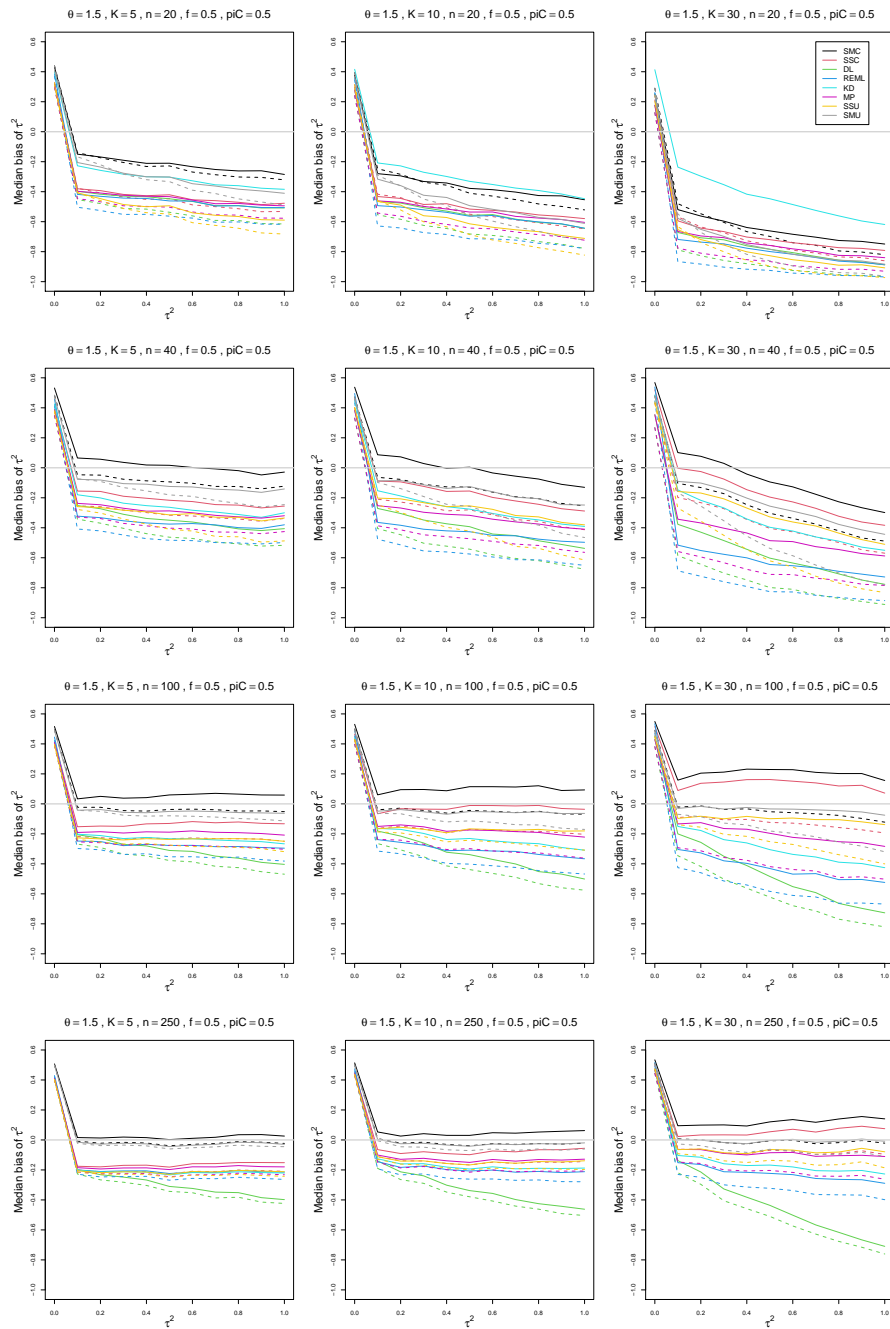


Figure B.33: Median bias of estimators of between-study variance of LOR (DL, REML, KD, MP, SMC, SSC, SMU, and SSU) vs τ^2 , for equal sample sizes $n = 20, 40, 100$ and 250 , $p_{iC} = .5$, $\theta = 1.5$ and $f = 0.5$. Solid lines: DL, REML, MP, SSC, SMC “only”; KD; SSU and SMU model-based. Dashed lines: DL, REML, MP, SSC, SMC “always”; SSU and SMU naïve.

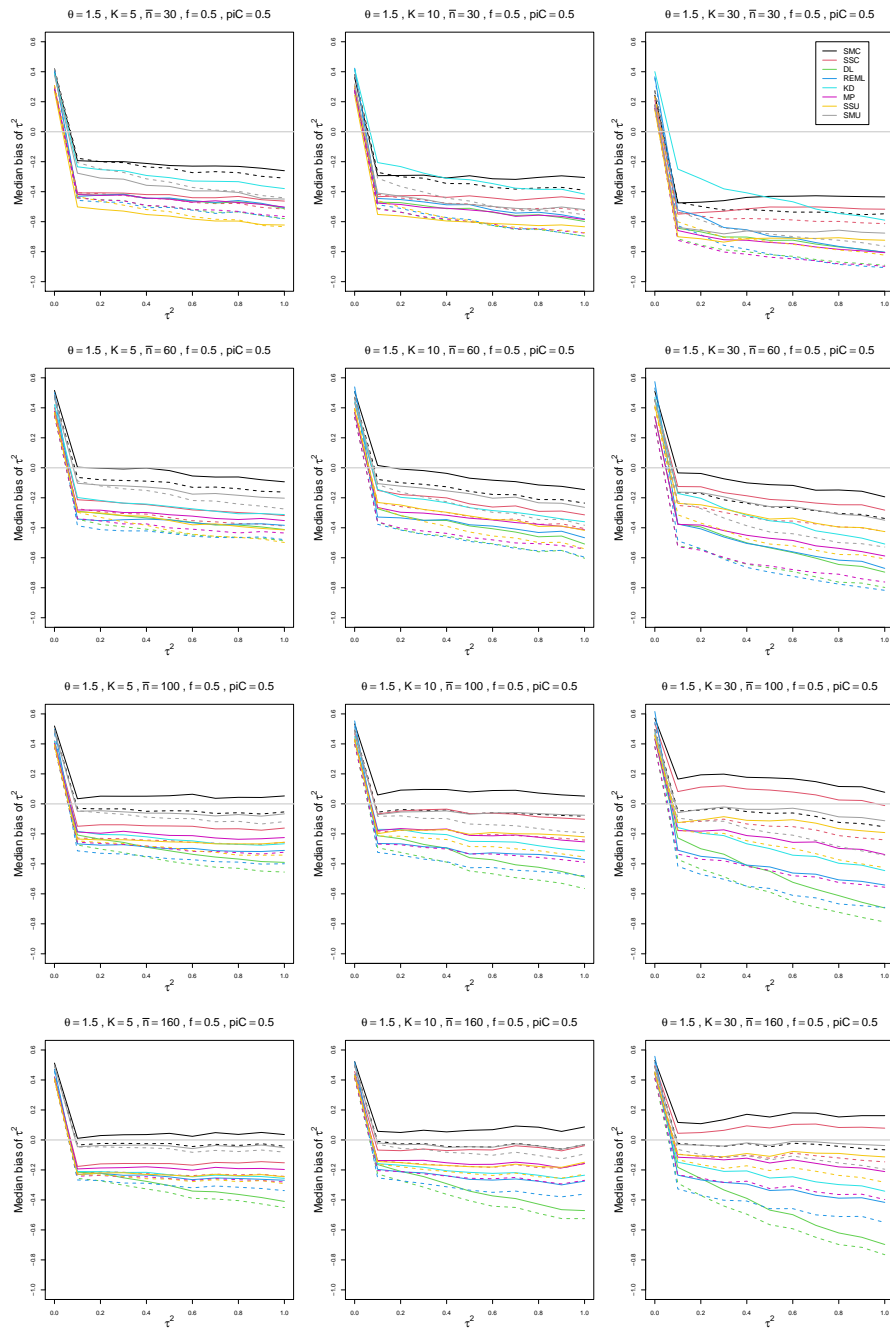


Figure B.34: Median bias of estimators of between-study variance of LOR (DL, REML, KD, MP, SMC, SSC, SMU, and SSU) vs τ^2 , for unequal sample sizes $\bar{n} = 30, 60, 100$ and 160 , $p_{iC} = .5$, $\theta = 1.5$ and $f = 0.5$. Solid lines: DL, REML, MP, SSC, SMC “only”; KD; SSU and SMU model-based. Dashed lines: DL, REML, MP, SSC, SMC “always”; SSU and SMU naïve.

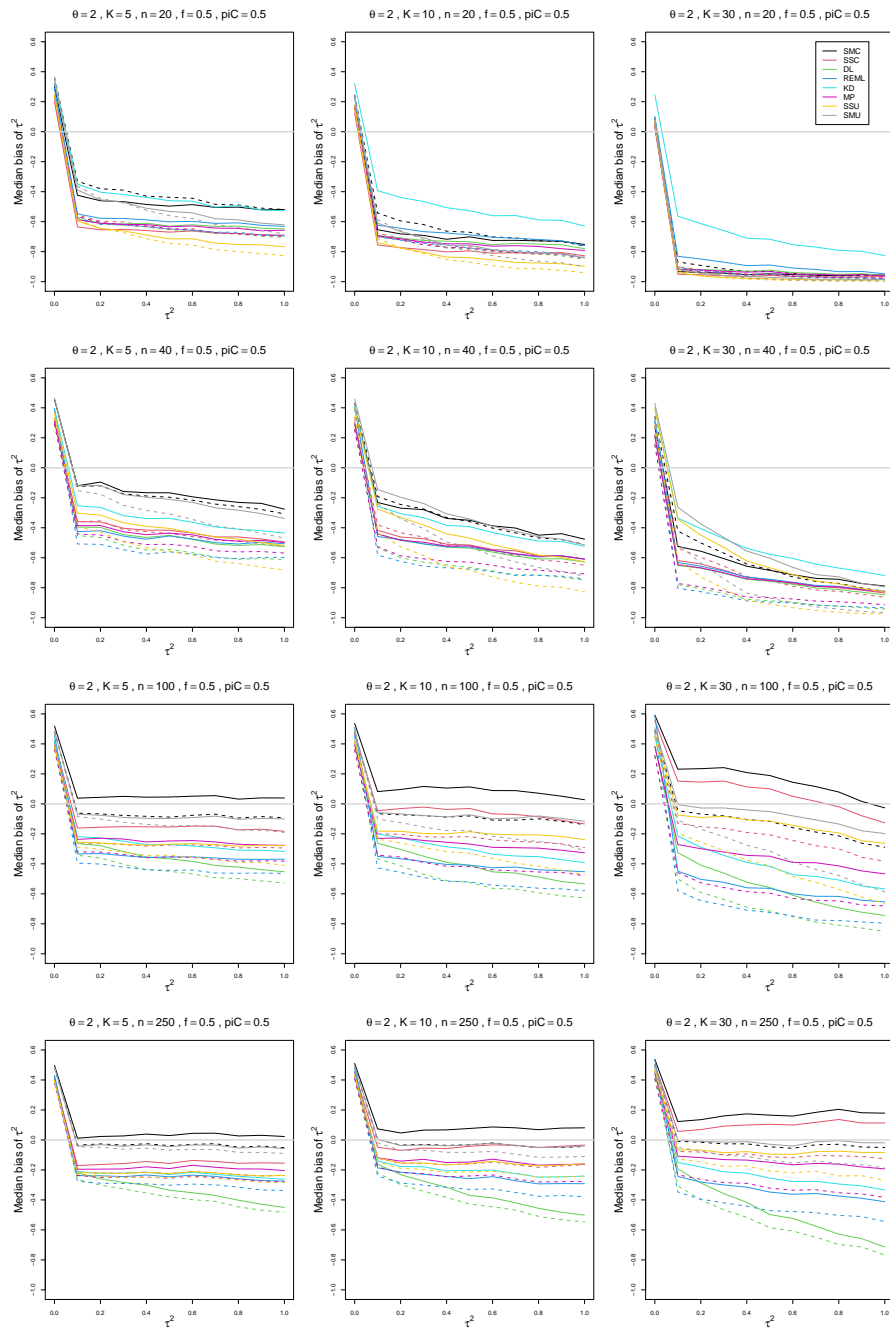


Figure B.35: Median bias of estimators of between-study variance of LOR (DL, REML, KD, MP, SMC, SSC, SMU, and SSU) vs τ^2 , for equal sample sizes $n = 20, 40, 100$ and 250 , $p_{iC} = .5$, $\theta = 2$ and $f = 0.5$. Solid lines: DL, REML, MP, SSC, SMC “only”; KD; SSU and SMU model-based. Dashed lines: DL, REML, MP, SSC, SMC “always”; SSU and SMU naïve.

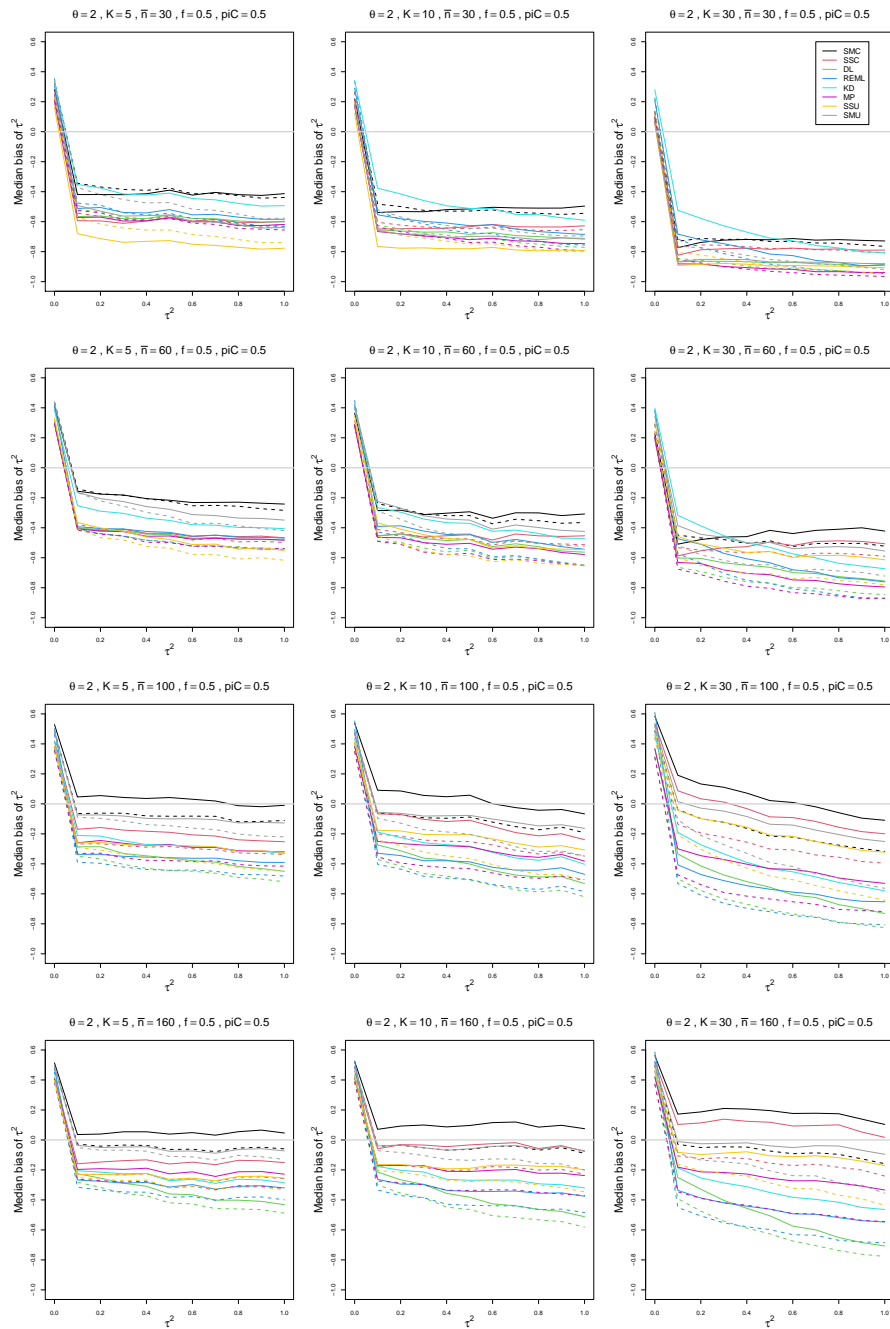


Figure B.36: Median bias of estimators of between-study variance of LOR (DL, REML, KD, MP, SMC, SSC, SMU, and SSU) vs τ^2 , for unequal sample sizes $\bar{n} = 30, 60, 100$ and 160 , $p_{iC} = .5$, $\theta = 2$ and $f = 0.5$. Solid lines: DL, REML, MP, SSC, SMC “only”; KD; SSU and SMU model-based. Dashed lines: DL, REML, MP, SSC, SMC “always”; SSU and SMU naïve.

Appendix C: Coverage of 95% confidence intervals for between-study variance

Each figure corresponds to a value of the probability of an event in the Control arm p_{iC} ($= .1, .2, .5$).

The fraction of each study's sample size in the Control arm (f) is held constant at 0.5. For each combination of a value of n ($= 20, 40, 100, 250$) or \bar{n} ($= 30, 60, 100, 160$) and a value of K ($= 5, 10, 30$), a panel plots coverage of 95% confidence intervals versus τ^2 ($= 0.0(0.1)1$).

The confidence intervals for τ^2 are

- PL (Profile likelihood), inverse-variance weights)
- QP (Q-profile, inverse-variance weights)
- KD (based on Kulinskaya-Dollinger (2015) approximation, inverse-variance weights)
- FPC (based on Farebrother approximation, effective-sample-size weights, conditional variance of LOR)
- FPU (based on Farebrother approximation, effective-sample-size weights, unconditional variance of LOR)

The plots include two versions of PL, QP, and FPC: adding 1/2 to all four of X_{iT} , X_{iC} , $n_{iT} - X_{iT}$, $n_{iC} - X_{iC}$ only when one of these is zero (solid lines) or always (dashed lines).

The plots also include two versions of FPU: model-based estimation of p_{iT} (solid lines) or naïve estimation (dashed lines).

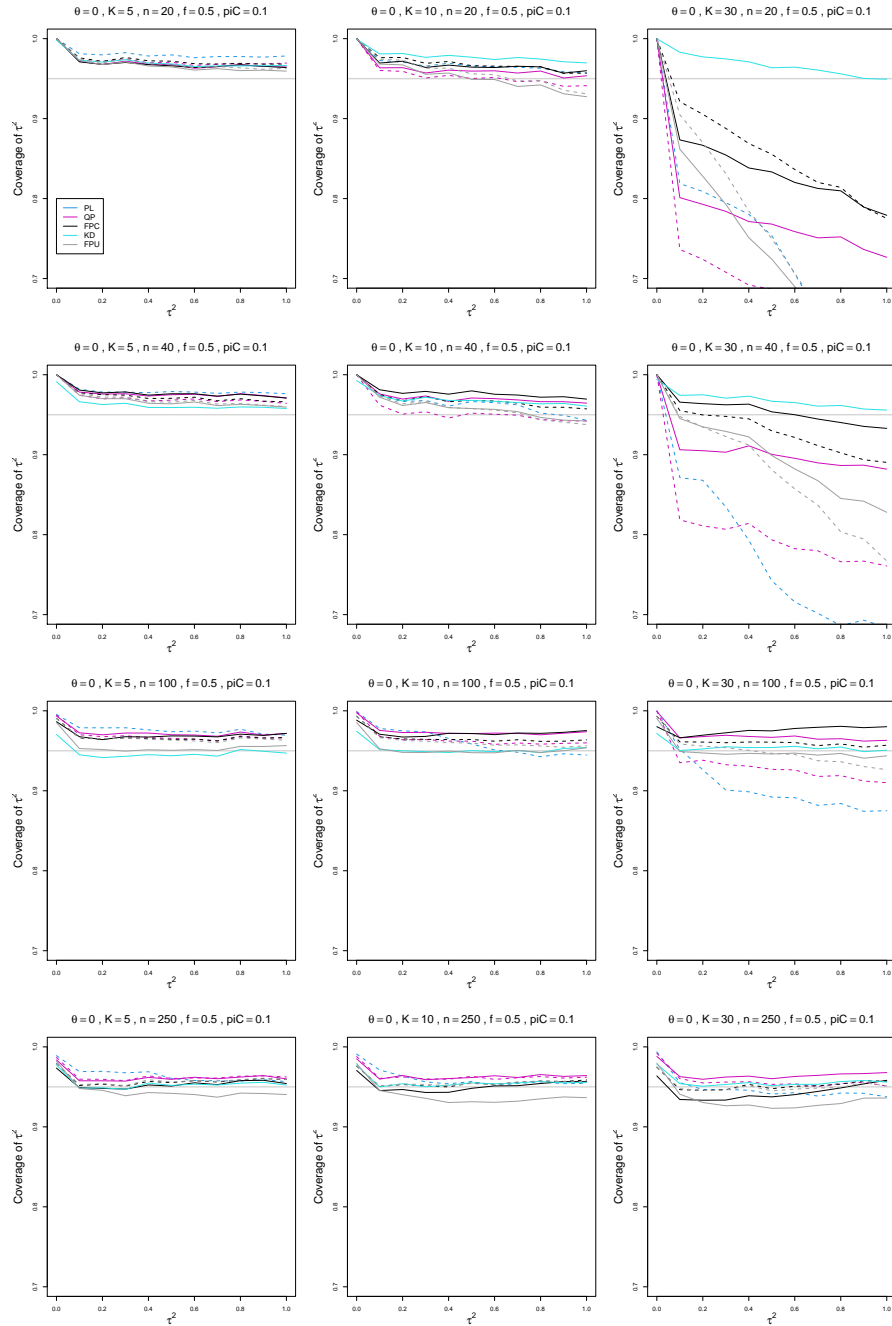


Figure C.1: Coverage of PL, QP, KD, FPC, and FPU 95% confidence intervals for between-study variance of LOR vs τ^2 , for equal sample sizes $n = 20, 40, 100$ and 250 , $p_{iC} = .1$, $\theta = 0$ and $f = 0.5$. Solid lines: PL, QP, and FPC “only”, FPU model-based, and KD. Dashed lines: PL, QP, and FPC “always” and FPU naïve.

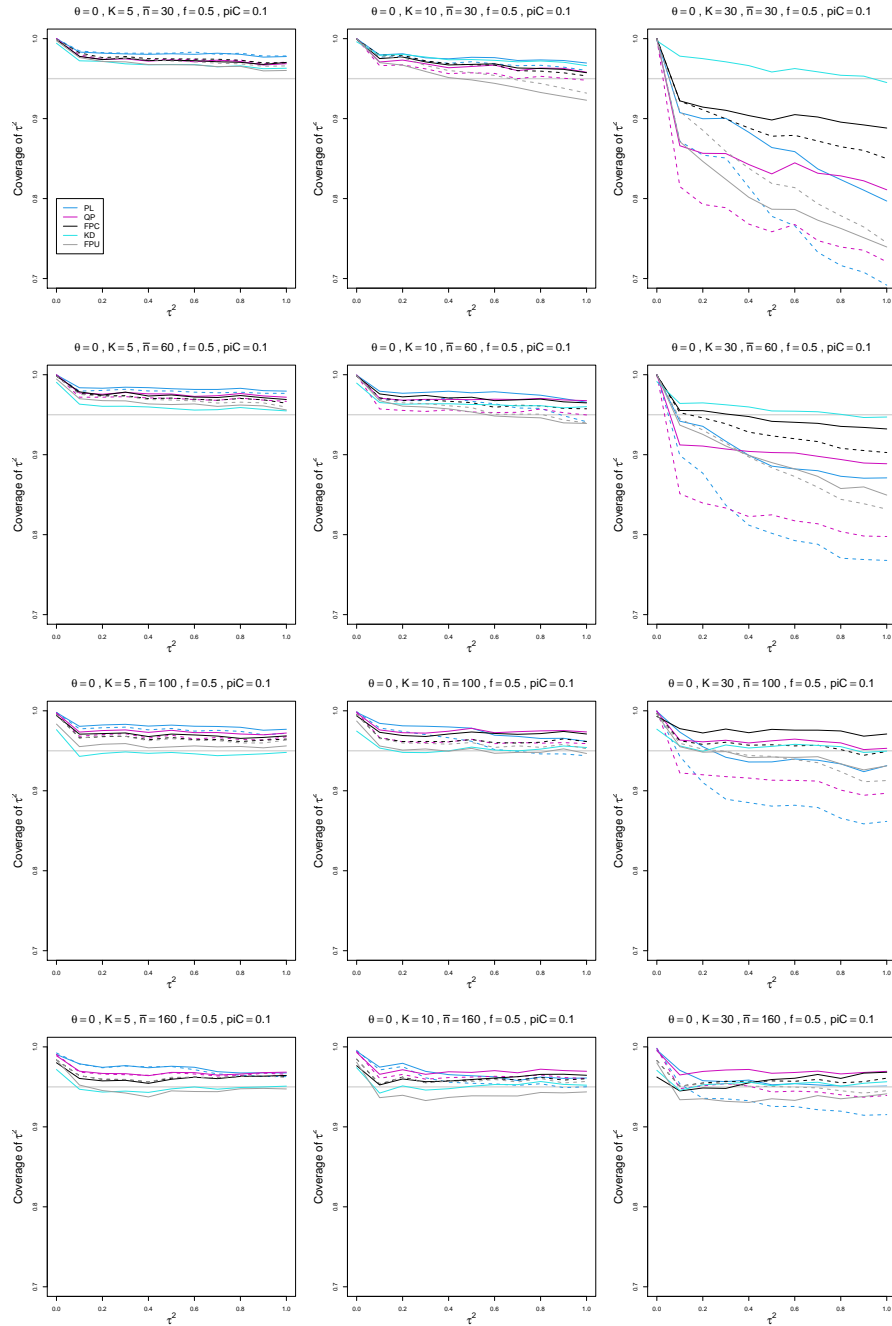


Figure C.2: Coverage of PL, QP, KD, FPC, and FPU 95% confidence intervals for between-study variance of LOR vs τ^2 , for unequal sample sizes $\bar{n} = 30, 60, 100$ and 160 , $p_{iC} = .1$, $\theta = 0$ and $f = 0.5$. Solid lines: PL, QP, and FPC “only”, FPU model-based, and KD. Dashed lines: PL, QP, and FPC “always” and FPU naïve.

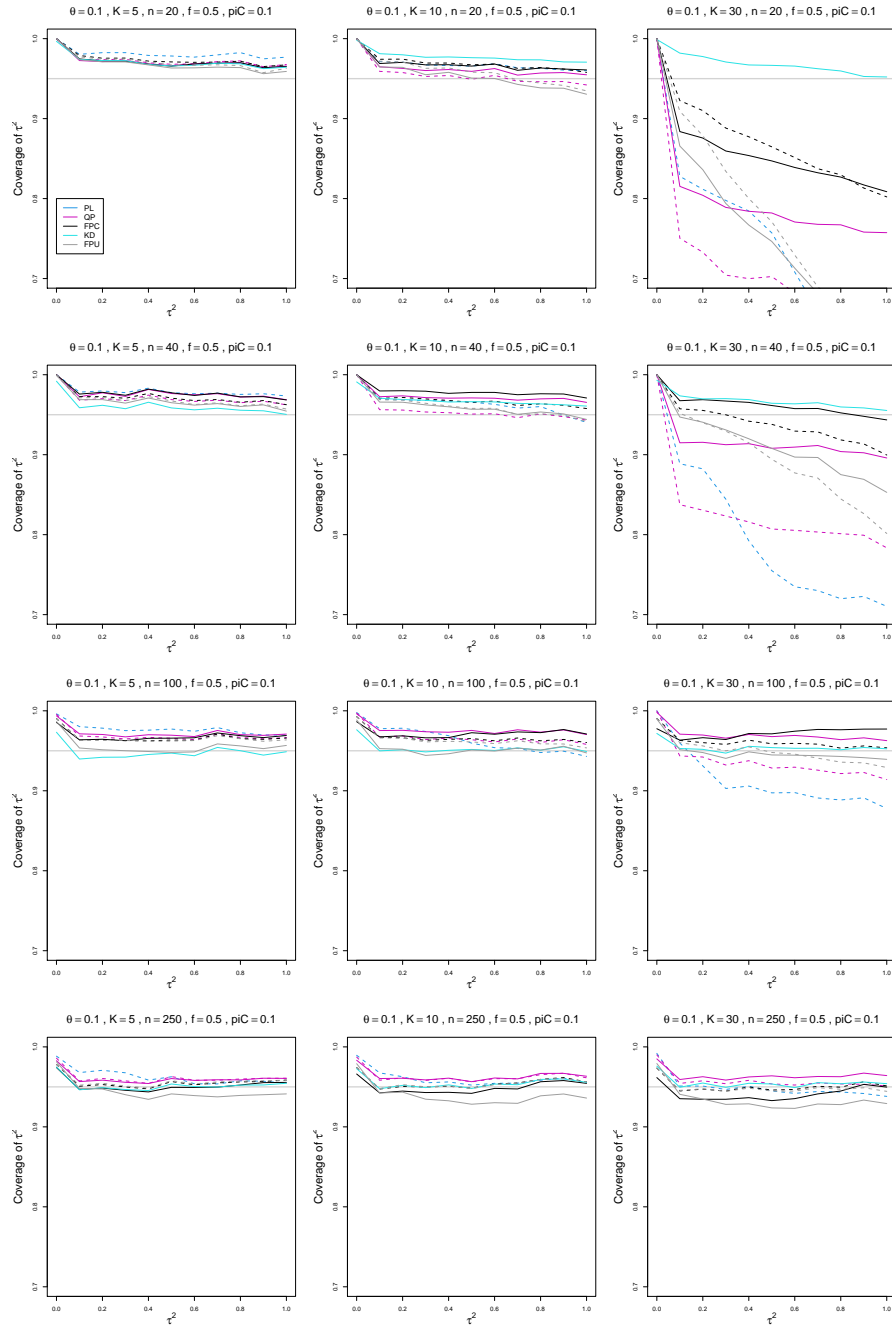


Figure C.3: Coverage of PL, QP, KD, FPC, and FPU 95% confidence intervals for between-study variance of LOR vs τ^2 , for equal sample sizes $n = 20, 40, 100$ and 250 , $p_{iC} = .1$, $\theta = 0.1$ and $f = 0.5$. Solid lines: PL, QP, and FPC “only”, FPU model-based, and KD. Dashed lines: PL, QP, and FPC “always” and FPU naïve.

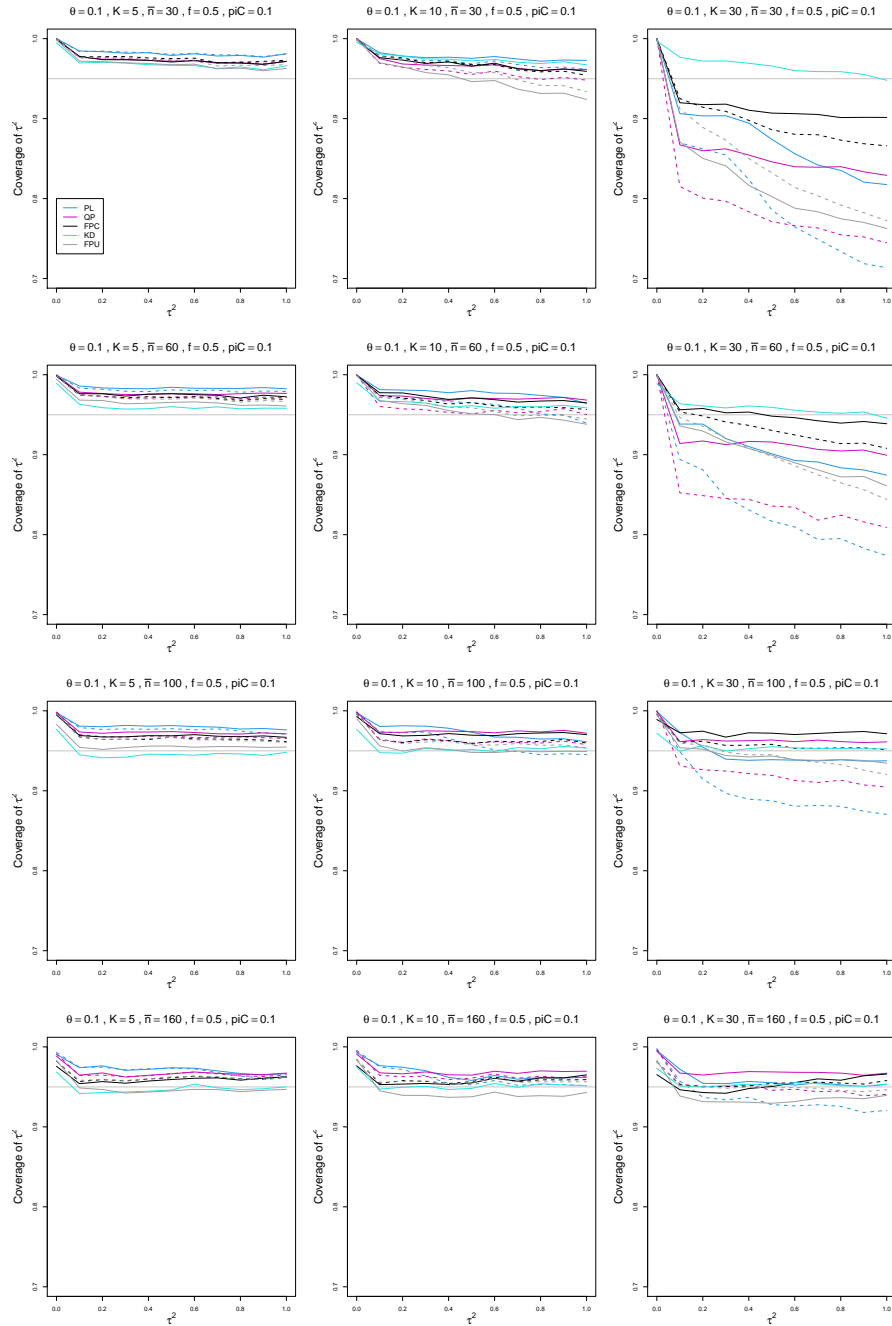


Figure C.4: Coverage of PL, QP, KD, FPC, and FPU 95% confidence intervals for between-study variance of LOR vs τ^2 , for unequal sample sizes $\bar{n} = 30, 60, 100$ and 160 , $p_{iC} = .1$, $\theta = 0.1$ and $f = 0.5$. Solid lines: PL, QP, and FPC “only”, FPU model-based, and KD. Dashed lines: PL, QP, and FPC “always” and FPU naïve.

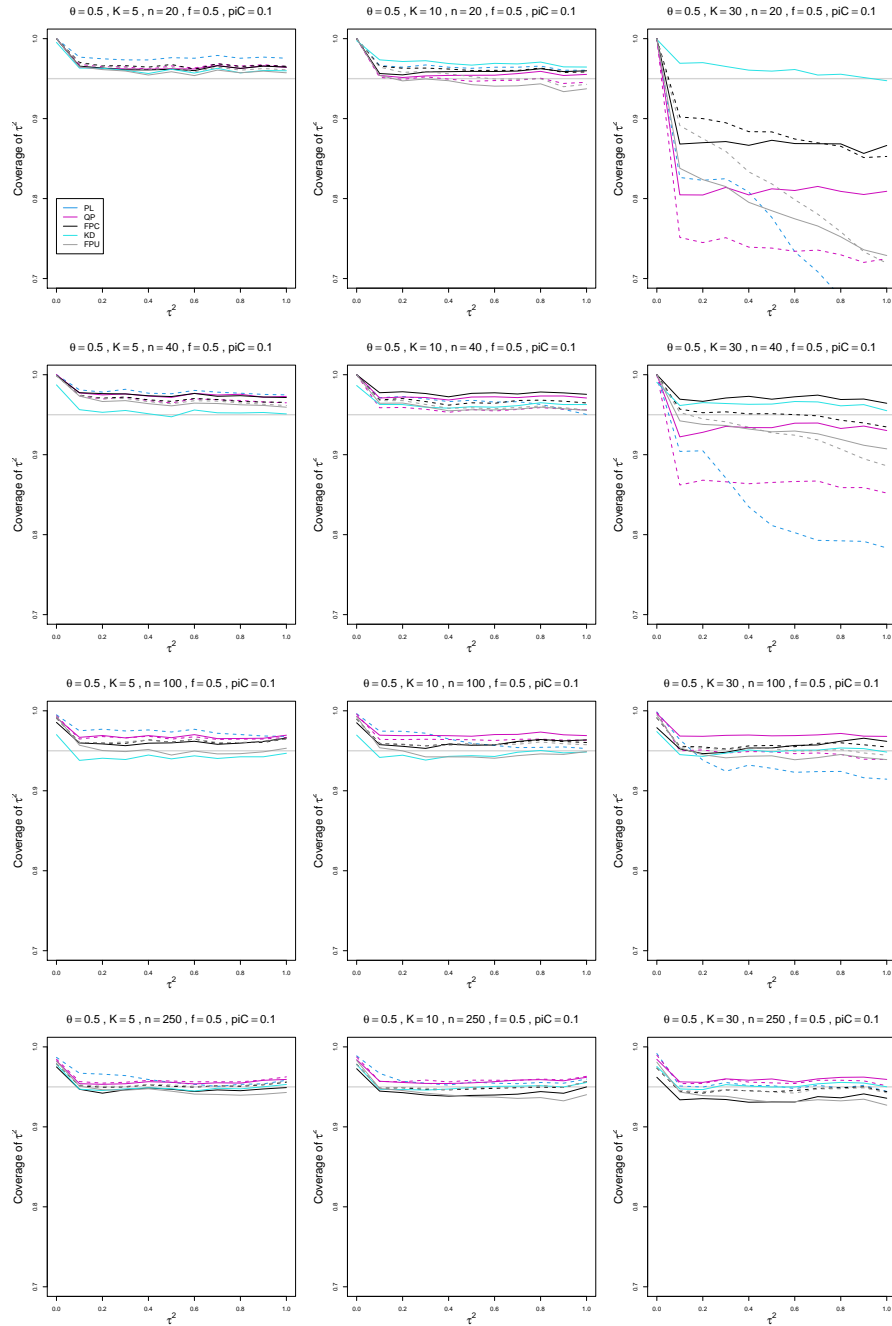


Figure C.5: Coverage of PL, QP, KD, FPC, and FPU 95% confidence intervals for between-study variance of LOR vs τ^2 , for equal sample sizes $n = 20, 40, 100$ and 250 , $p_{iC} = .1$, $\theta = 0.5$ and $f = 0.5$. Solid lines: PL, QP, and FPC “only”, FPU model-based, and KD. Dashed lines: PL, QP, and FPC “always” and FPU naïve.

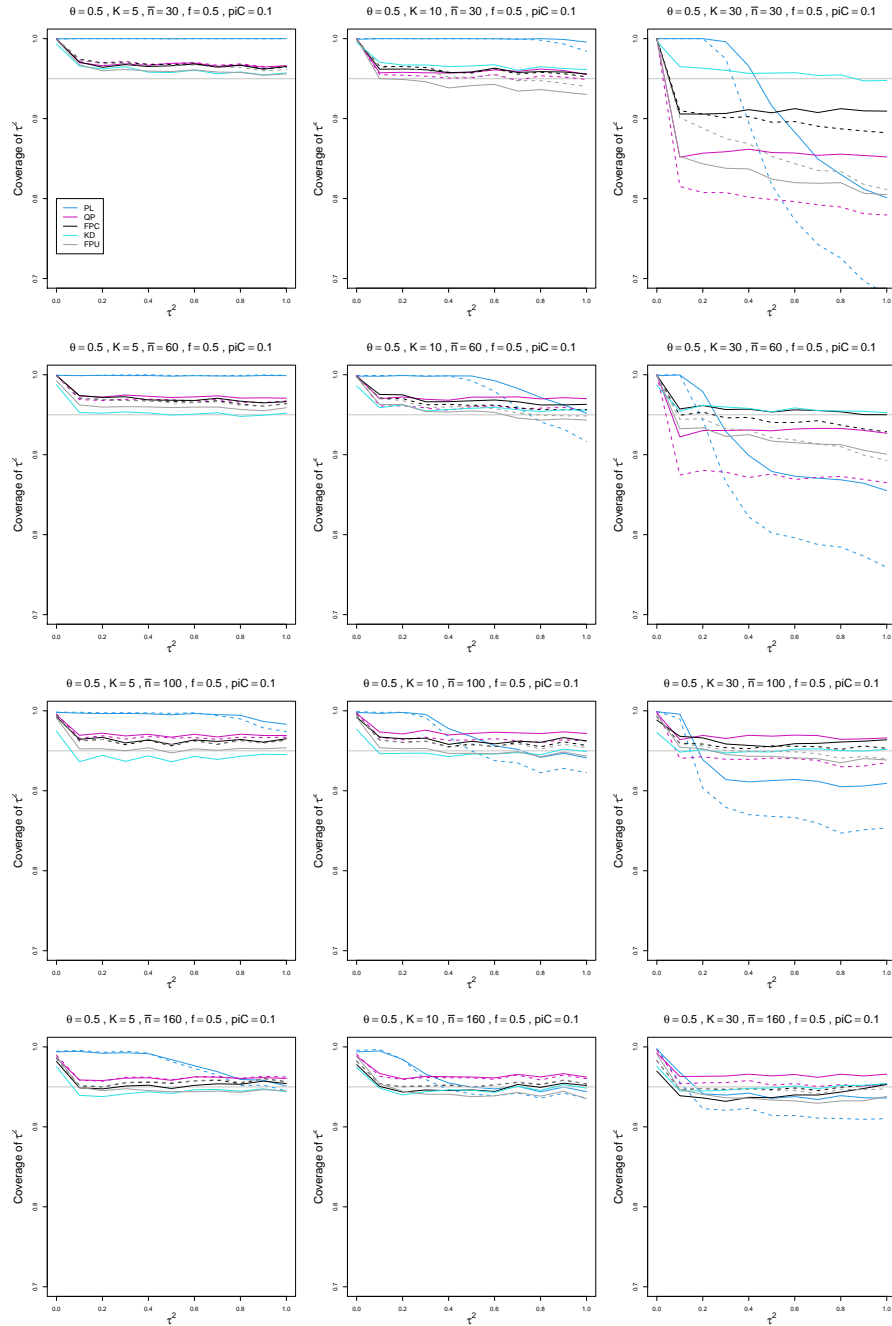


Figure C.6: Coverage of PL, QP, KD, FPC, and FPU 95% confidence intervals for between-study variance of LOR vs τ^2 , for unequal sample sizes $\bar{n} = 30, 60, 100$ and 160 , $p_{iC} = .1$, $\theta = 0.5$ and $f = 0.5$. Solid lines: PL, QP, and FPC “only”, FPU model-based, and KD. Dashed lines: PL, QP, and FPC “always” and FPU naïve.

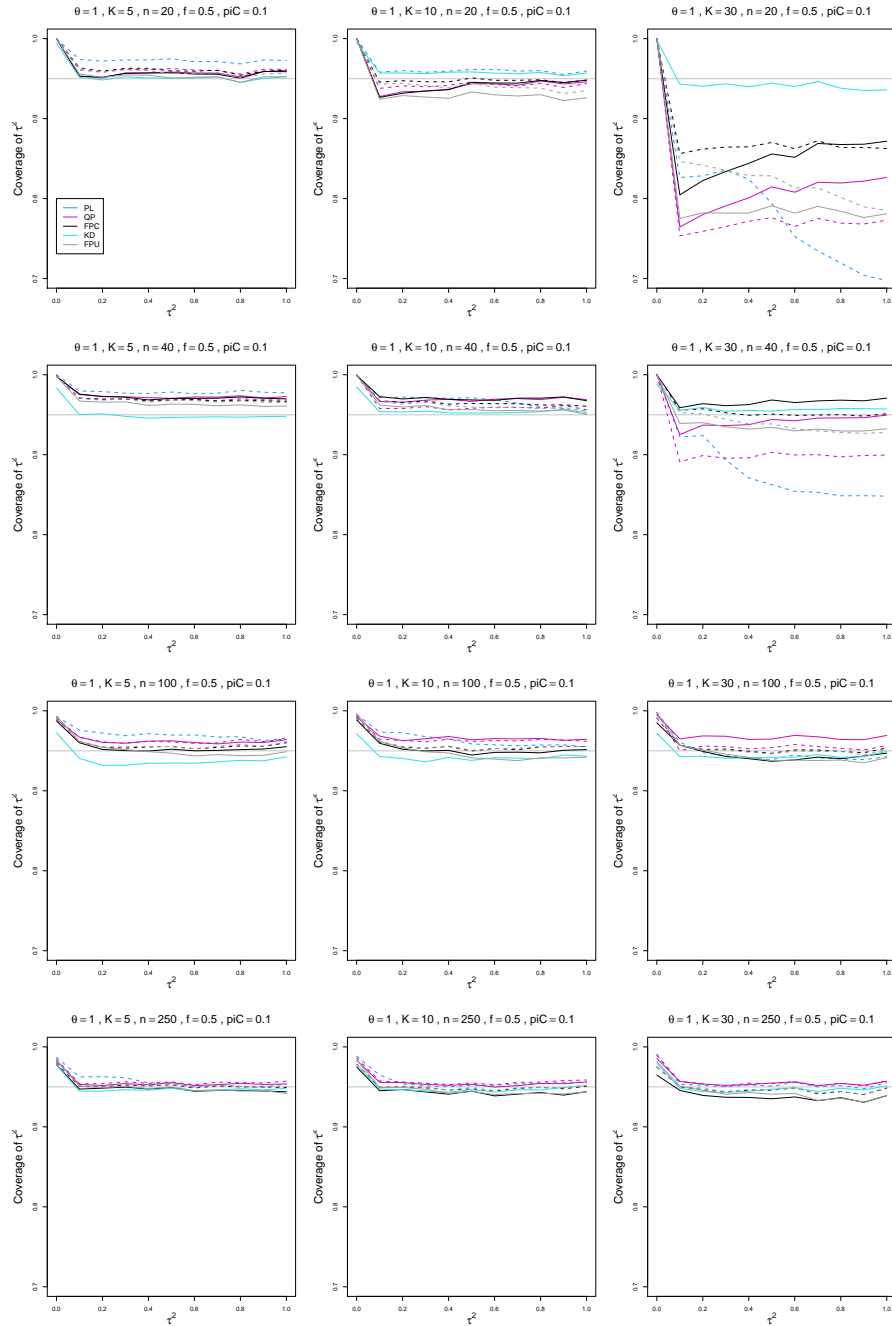


Figure C.7: Coverage of PL, QP, KD, FPC, and FPU 95% confidence intervals for between-study variance of LOR vs τ^2 , for equal sample sizes $n = 20, 40, 100$ and 250 , $p_{iC} = .1$, $\theta = 1$ and $f = 0.5$. Solid lines: PL, QP, and FPC “only”, FPU model-based, and KD. Dashed lines: PL, QP, and FPC “always” and FPU naïve.

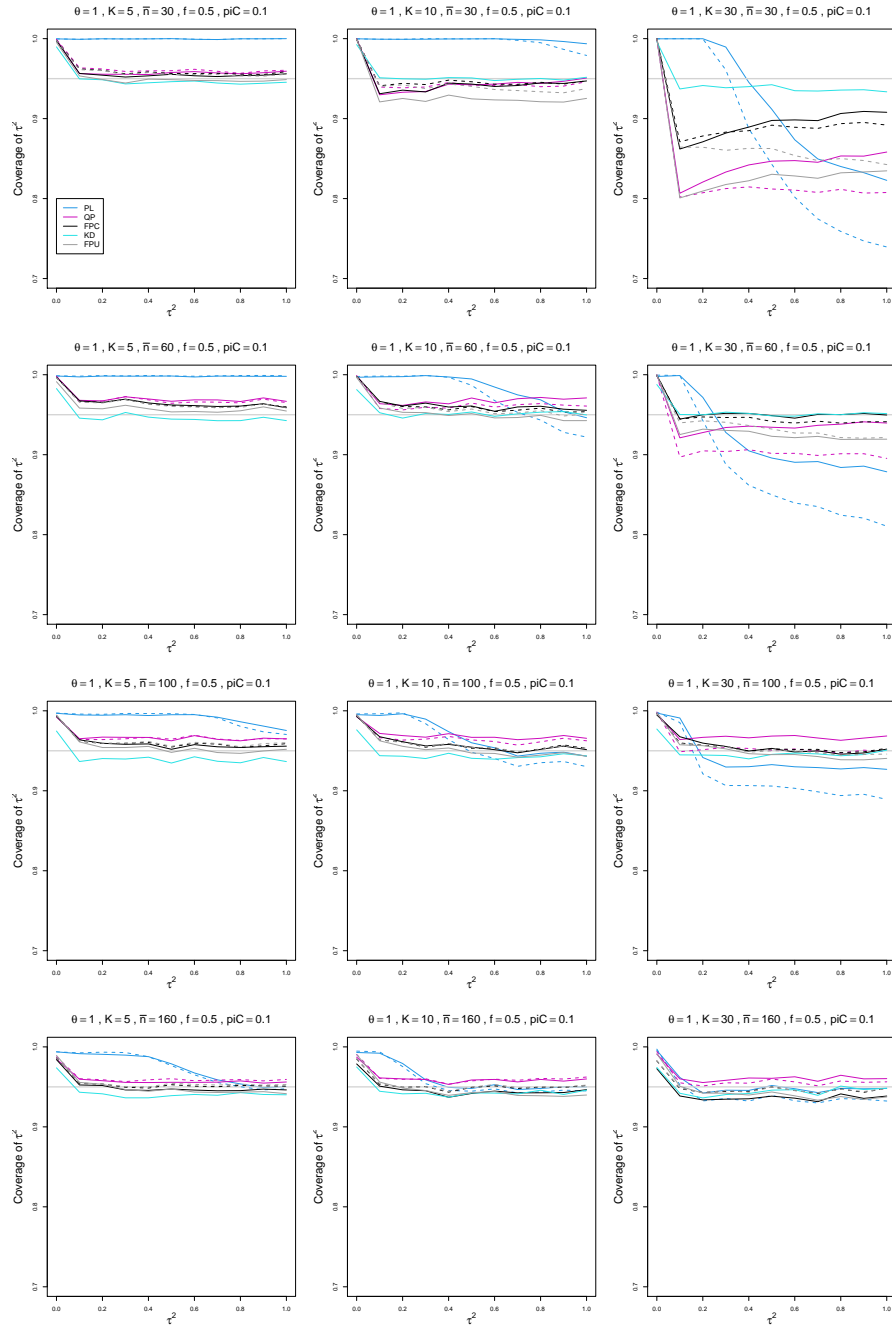


Figure C.8: Coverage of PL, QP, KD, FPC, and FPU 95% confidence intervals for between-study variance of LOR vs τ^2 , for unequal sample sizes $\bar{n} = 30, 60, 100$ and 160 , $p_{iC} = .1$, $\theta = 1$ and $f = 0.5$. Solid lines: PL, QP, and FPC “only”, FPU model-based, and KD. Dashed lines: PL, QP, and FPC “always” and FPU naive.

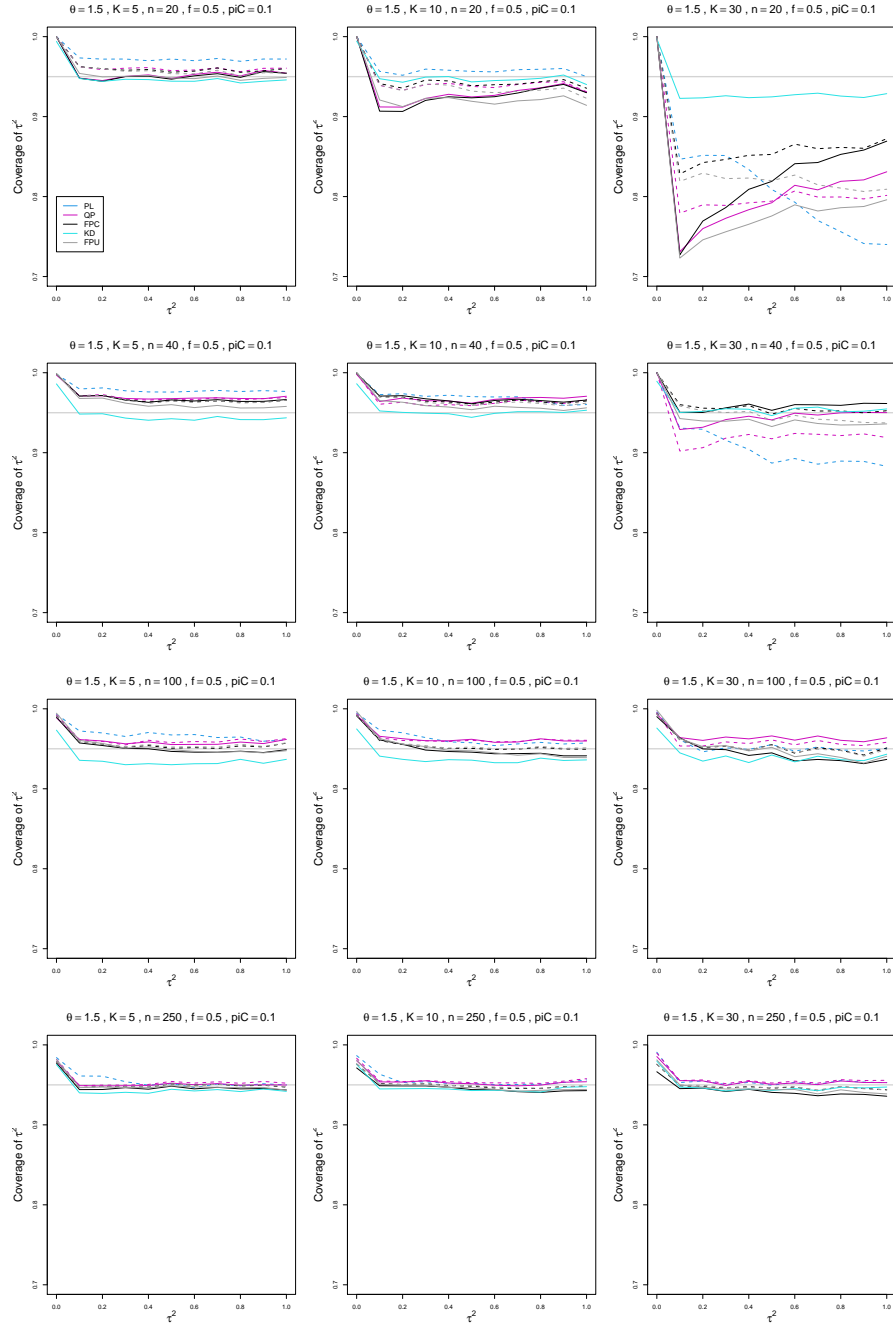


Figure C.9: Coverage of PL, QP, KD, FPC, and FPU 95% confidence intervals for between-study variance of LOR vs τ^2 , for equal sample sizes $n = 20, 40, 100$ and 250 , $p_{iC} = .1$, $\theta = 1.5$ and $f = 0.5$. Solid lines: PL, QP, and FPC “only”, FPU model-based, and KD. Dashed lines: PL, QP, and FPC “always” and FPU naïve.

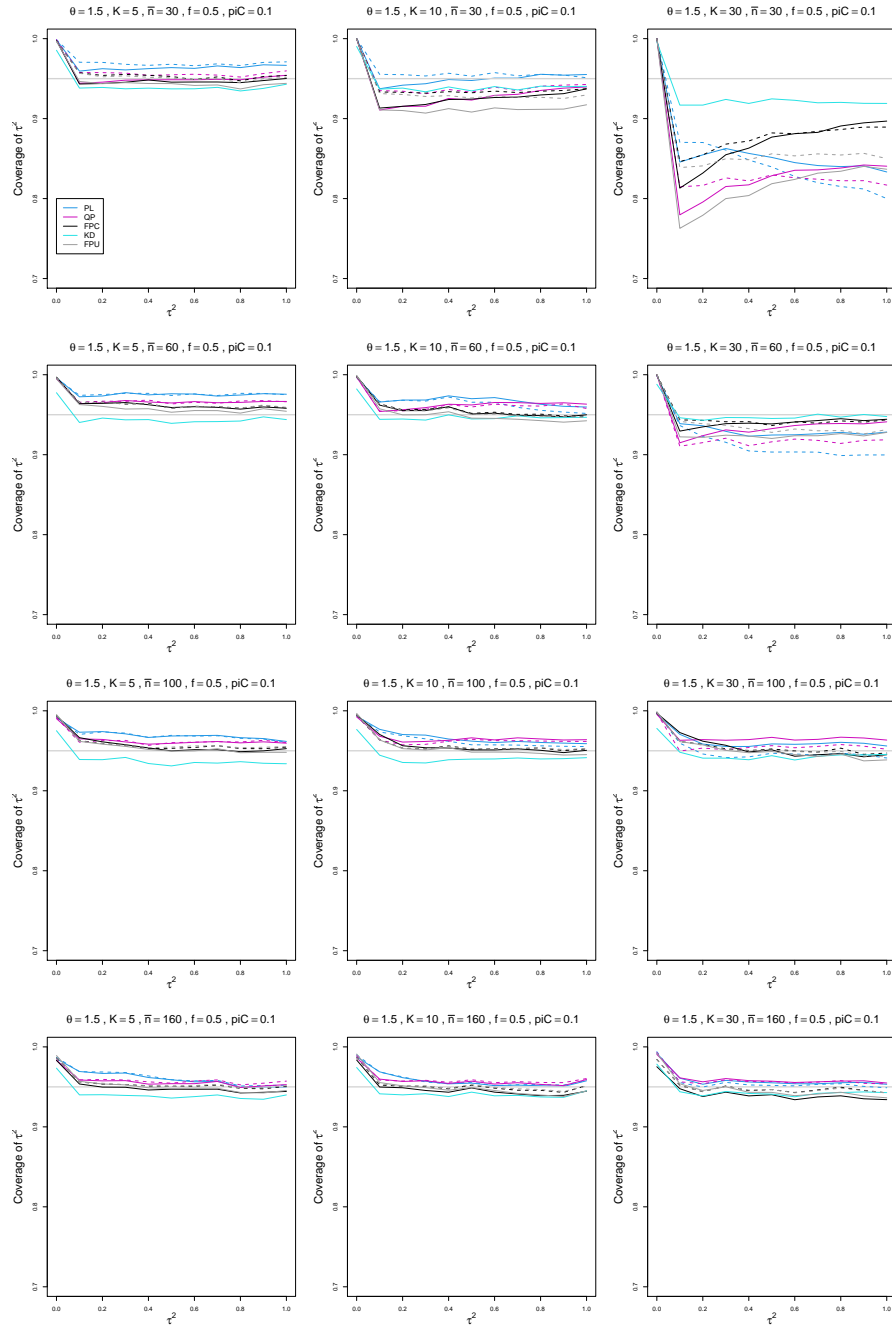


Figure C.10: Coverage of PL, QP, KD, FPC, and FPU 95% confidence intervals for between-study variance of LOR vs τ^2 , for unequal sample sizes $\bar{n} = 30, 60, 100$ and 160 , $p_{iC} = .1$, $\theta = 1.5$ and $f = 0.5$. Solid lines: PL, QP, and FPC “only”, FPU model-based, and KD. Dashed lines: PL, QP, and FPC “always” and FPU naïve.

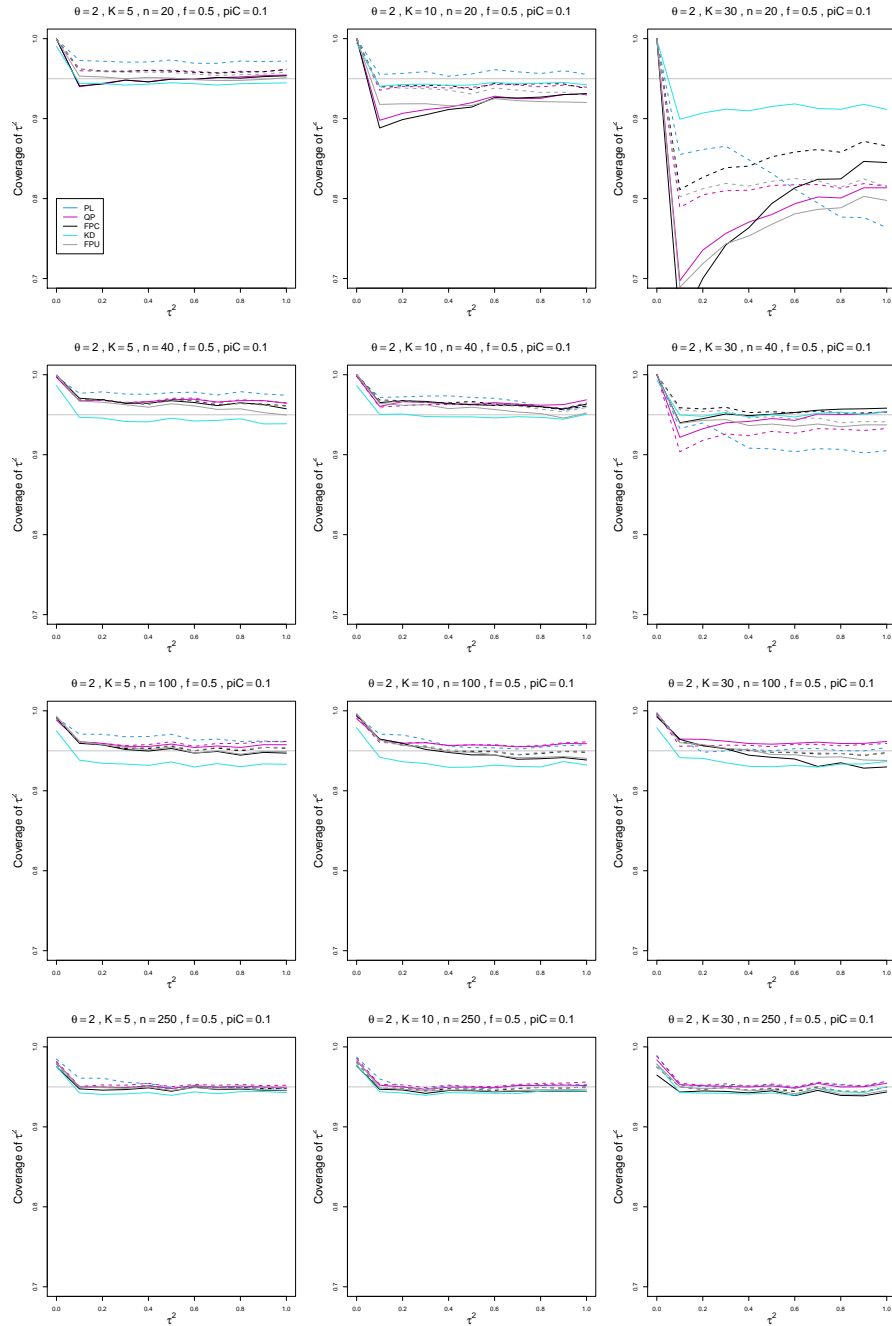


Figure C.11: Coverage of PL, QP, KD, FPC, and FPU 95% confidence intervals for between-study variance of LOR vs τ^2 , for equal sample sizes $n = 20, 40, 100$ and 250 , $p_{iC} = .1$, $\theta = 2$ and $f = 0.5$. Solid lines: PL, QP, and FPC “only”, FPU model-based, and KD. Dashed lines: PL, QP, and FPC “always” and FPU naïve.

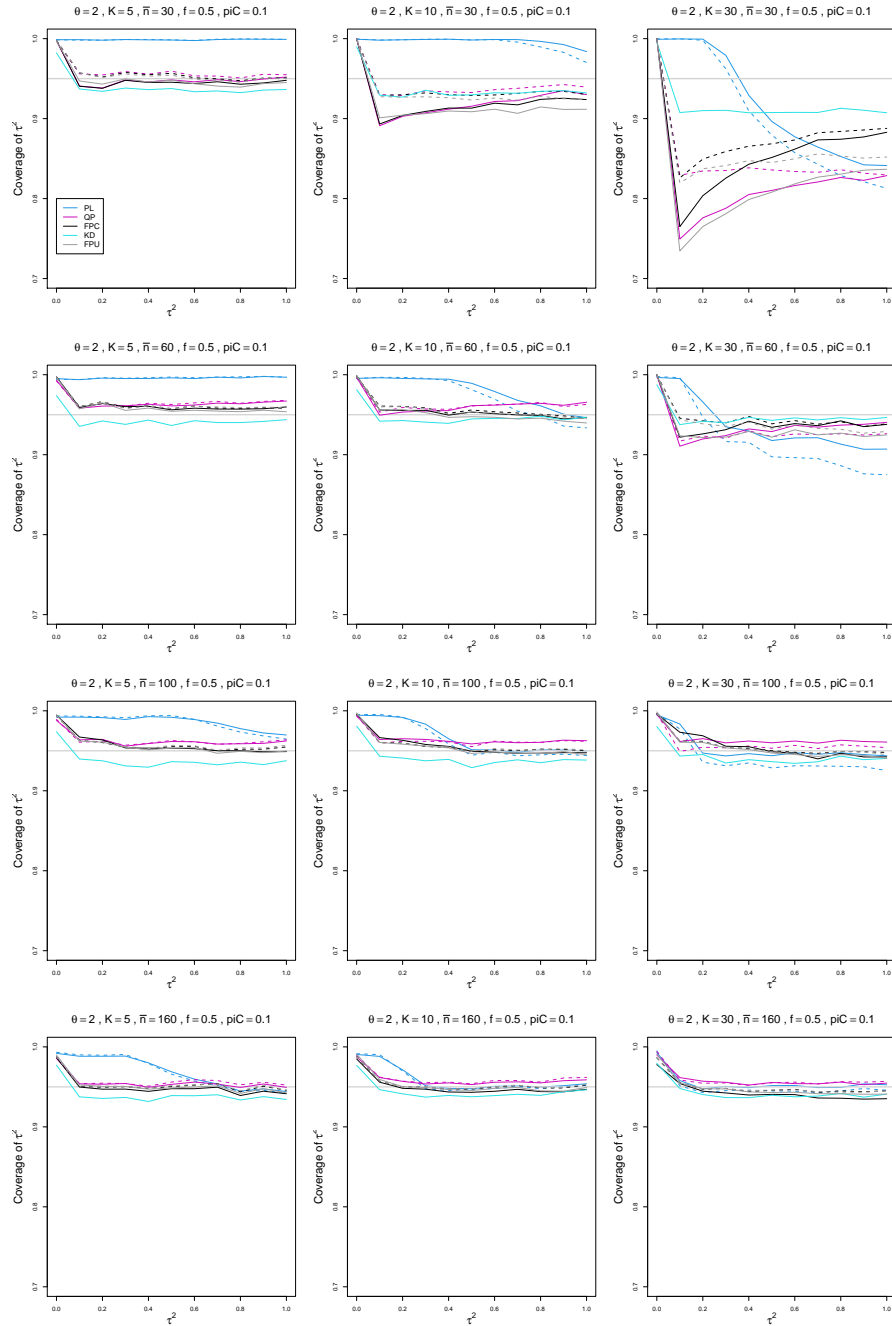


Figure C.12: Coverage of PL, QP, KD, FPC, and FPU 95% confidence intervals for between-study variance of LOR vs τ^2 , for unequal sample sizes $\bar{n} = 30, 60, 100$ and 160 , $p_{iC} = .1$, $\theta = 2$ and $f = 0.5$. Solid lines: PL, QP, and FPC “only”, FPU model-based, and KD. Dashed lines: PL, QP, and FPC “always” and FPU naïve.

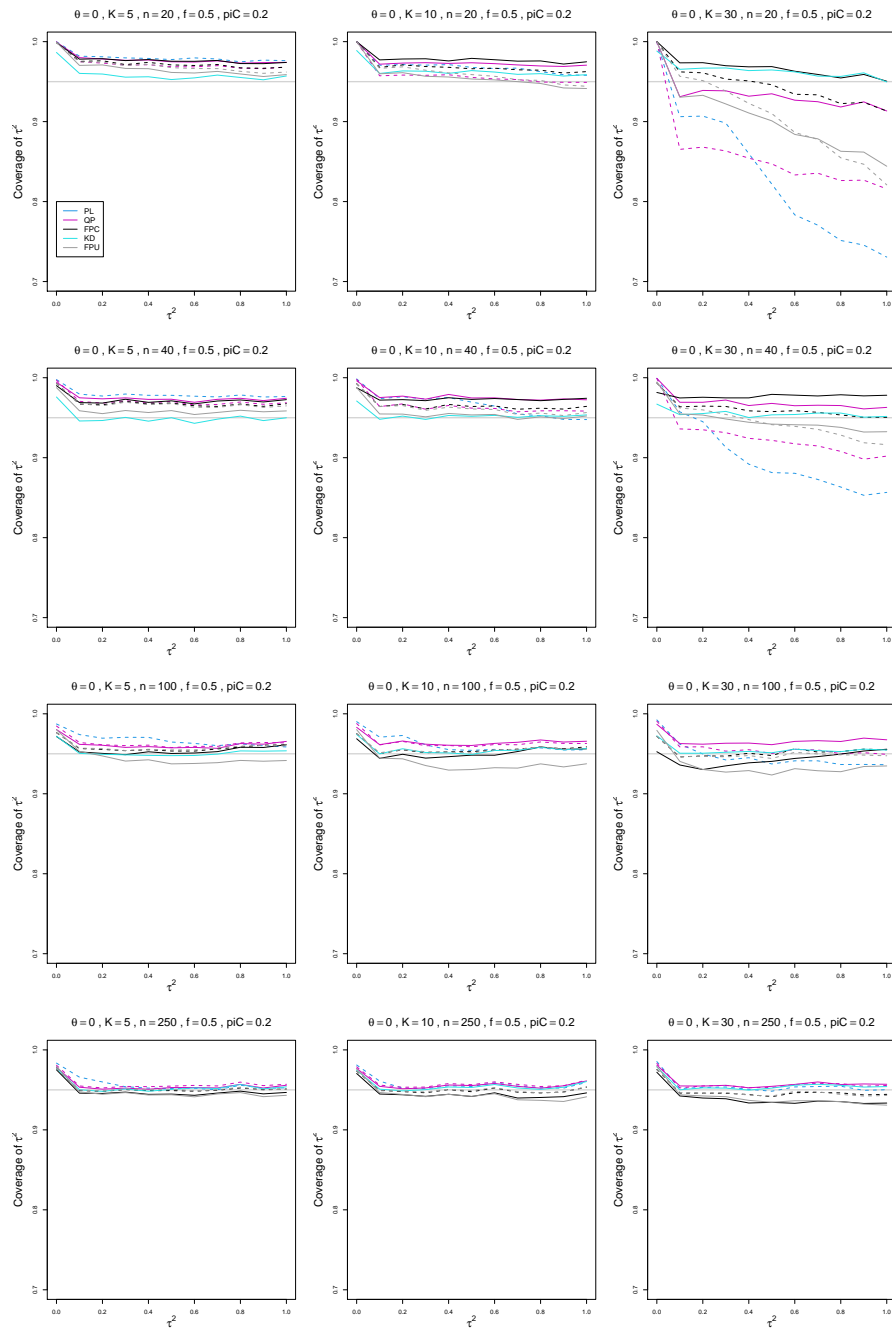


Figure C.13: Coverage of PL, QP, KD, FPC, and FPU 95% confidence intervals for between-study variance of LOR vs τ^2 , for equal sample sizes $n = 20, 40, 100$ and 250 , $p_{iC} = .2$, $\theta = 0$ and $f = 0.5$. Solid lines: PL, QP, and FPC “only”, FPU model-based, and KD. Dashed lines: PL, QP, and FPC “always” and FPU naïve.

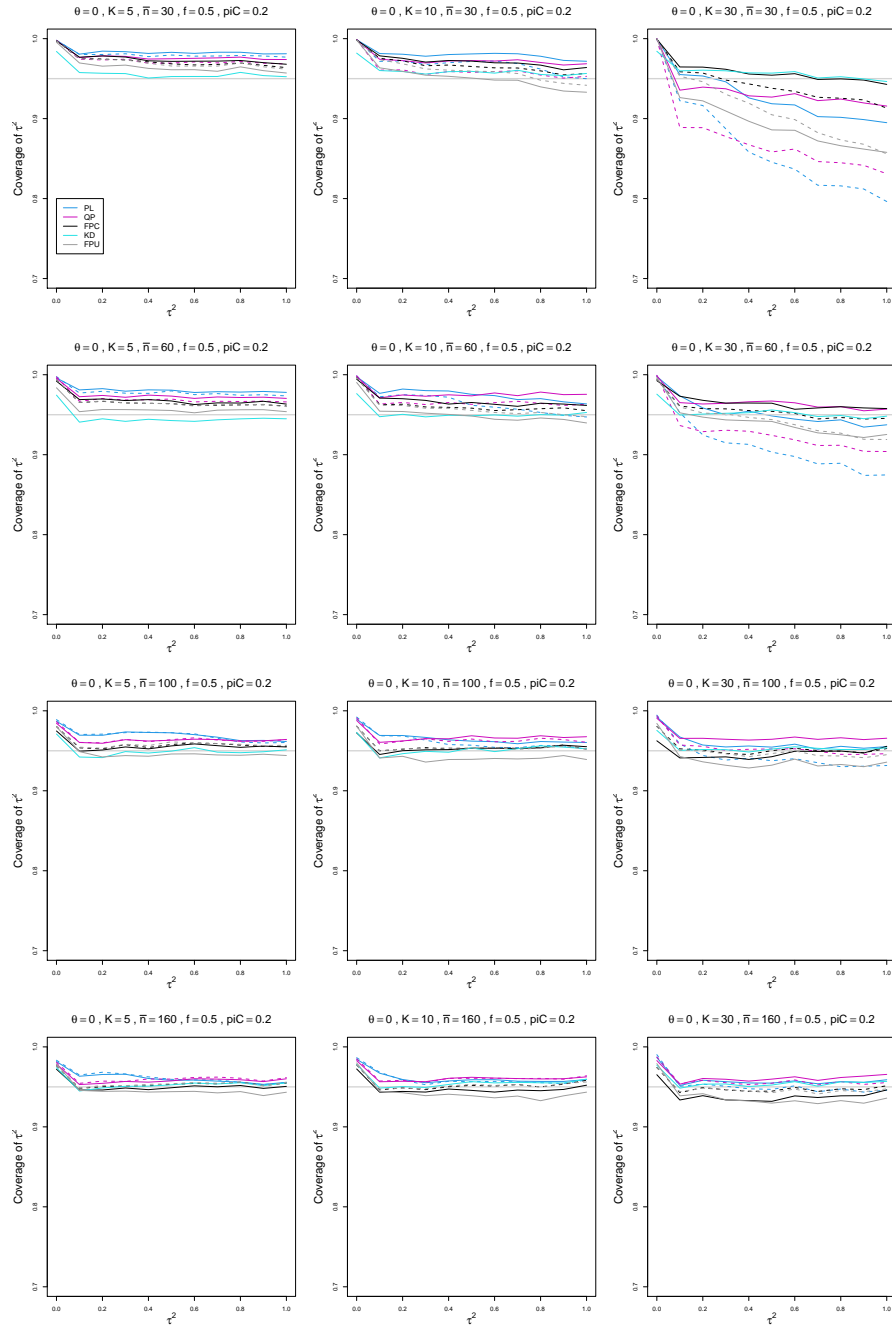


Figure C.14: Coverage of PL, QP, KD, FPC, and FPU 95% confidence intervals for between-study variance of LOR vs τ^2 , for unequal sample sizes $\bar{n} = 30, 60, 100$ and 160 , $p_{iC} = .2$, $\theta = 0$ and $f = 0.5$. Solid lines: PL, QP, and FPC “only”, FPU model-based, and KD. Dashed lines: PL, QP, and FPC “always” and FPU naïve.

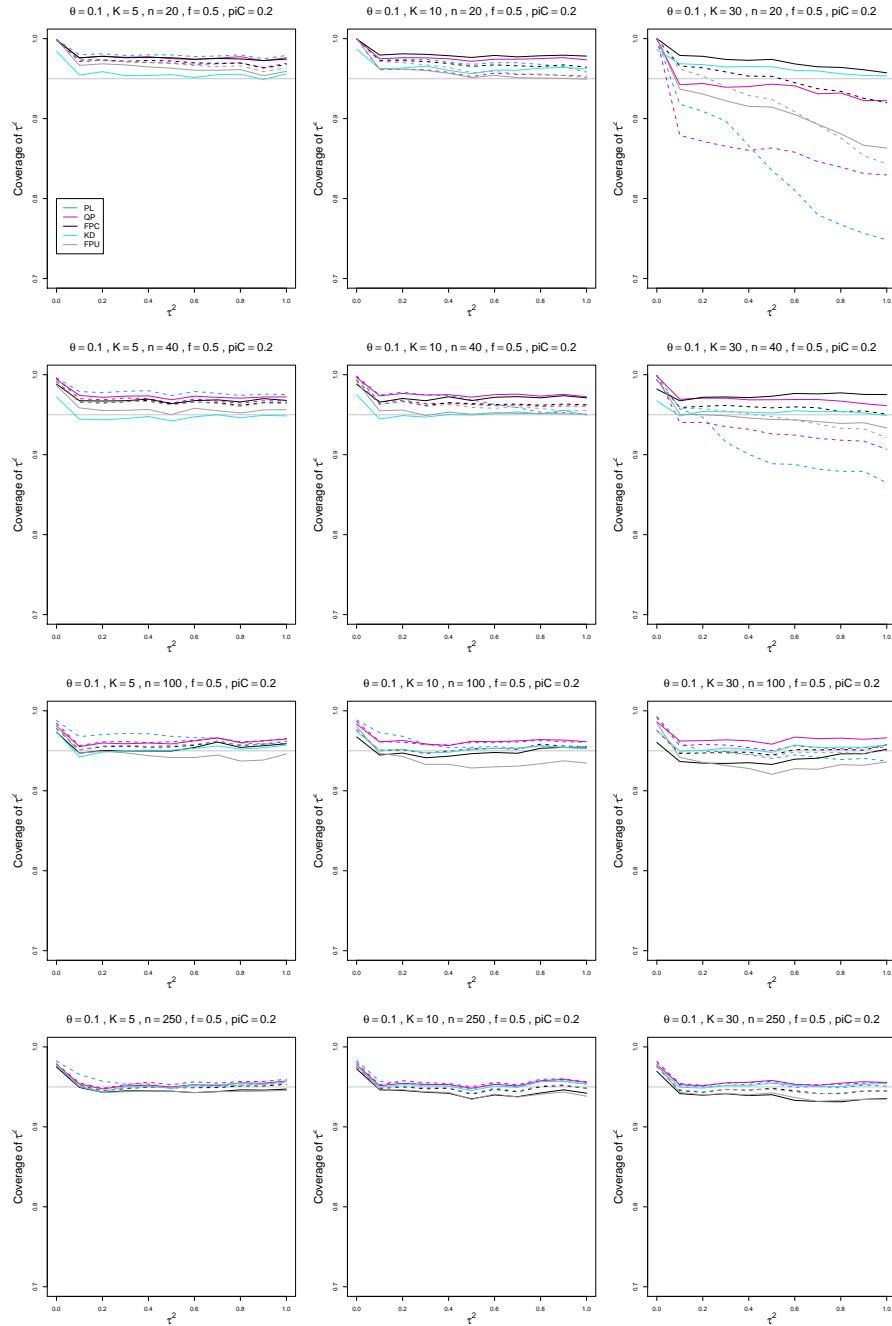


Figure C.15: Coverage of PL, QP, KD, FPC, and FPU 95% confidence intervals for between-study variance of LOR vs τ^2 , for equal sample sizes $n = 20, 40, 100$ and 250 , $p_{iC} = .2$, $\theta = 0.1$ and $f = 0.5$. Solid lines: PL, QP, and FPC “only”, FPU model-based, and KD. Dashed lines: PL, QP, and FPC “always” and FPU naïve.

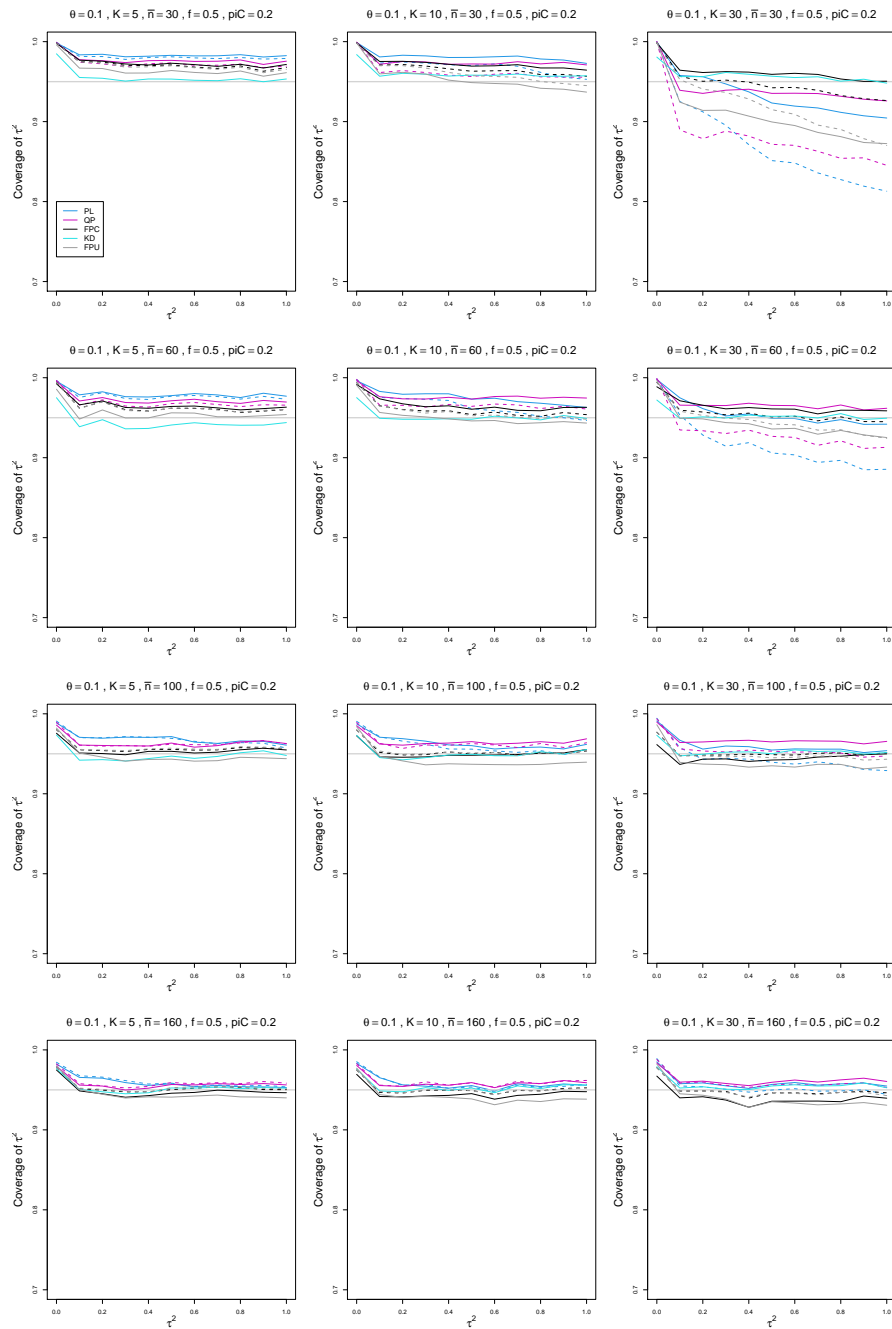


Figure C.16: Coverage of PL, QP, KD, FPC, and FPU 95% confidence intervals for between-study variance of LOR vs τ^2 , for unequal sample sizes $\bar{n} = 30, 60, 100$ and 160 , $p_{iC} = .2$, $\theta = 0.1$ and $f = 0.5$. Solid lines: PL, QP, and FPC “only”, FPU model-based, and KD. Dashed lines: PL, QP, and FPC “always” and FPU naïve.

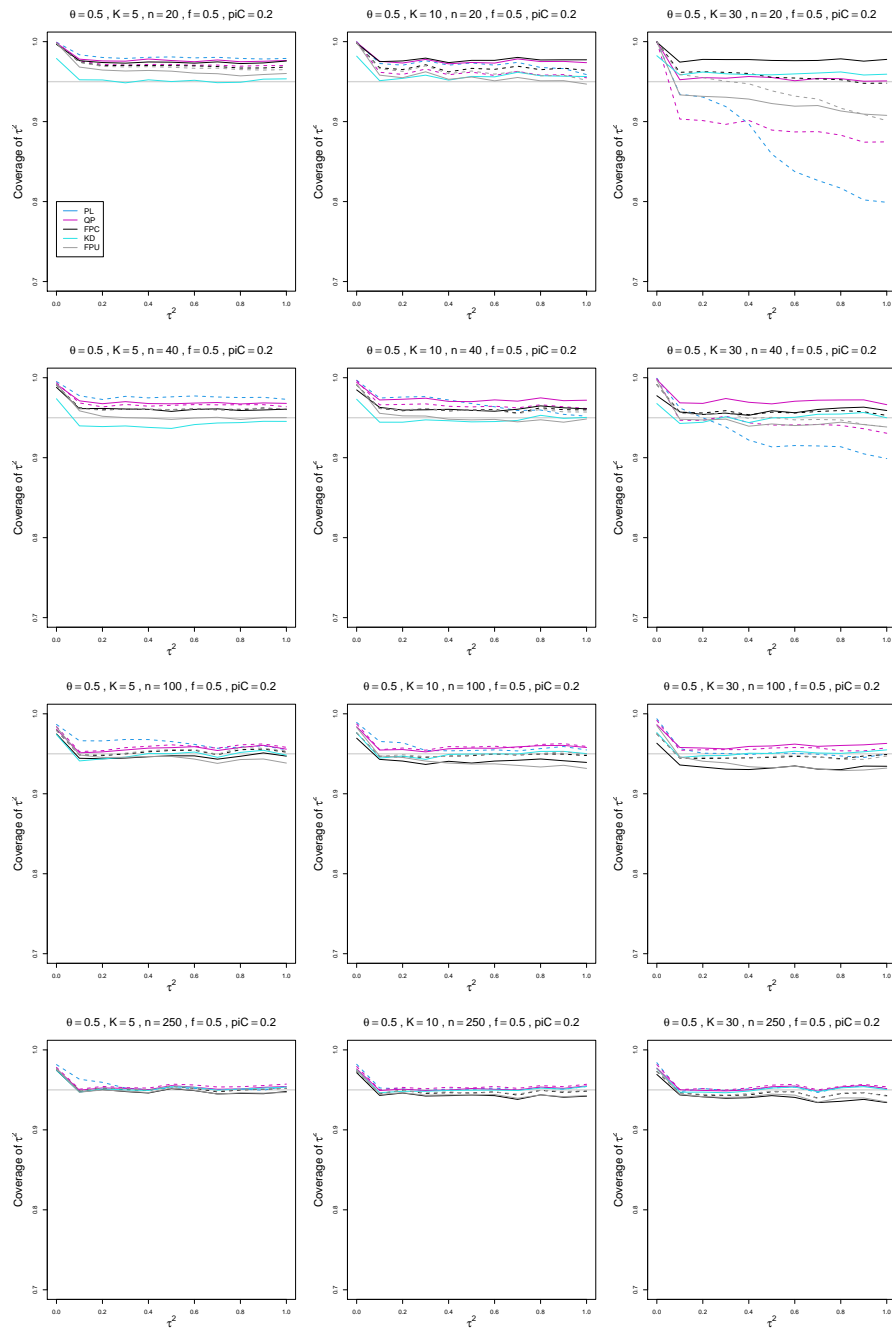


Figure C.17: Coverage of PL, QP, KD, FPC, and FPU 95% confidence intervals for between-study variance of LOR vs τ^2 , for equal sample sizes $n = 20, 40, 100$ and 250 , $p_{iC} = .2$, $\theta = 0.5$ and $f = 0.5$. Solid lines: PL, QP, and FPC “only”, FPU model-based, and KD. Dashed lines: PL, QP, and FPC “always” and FPU naïve.

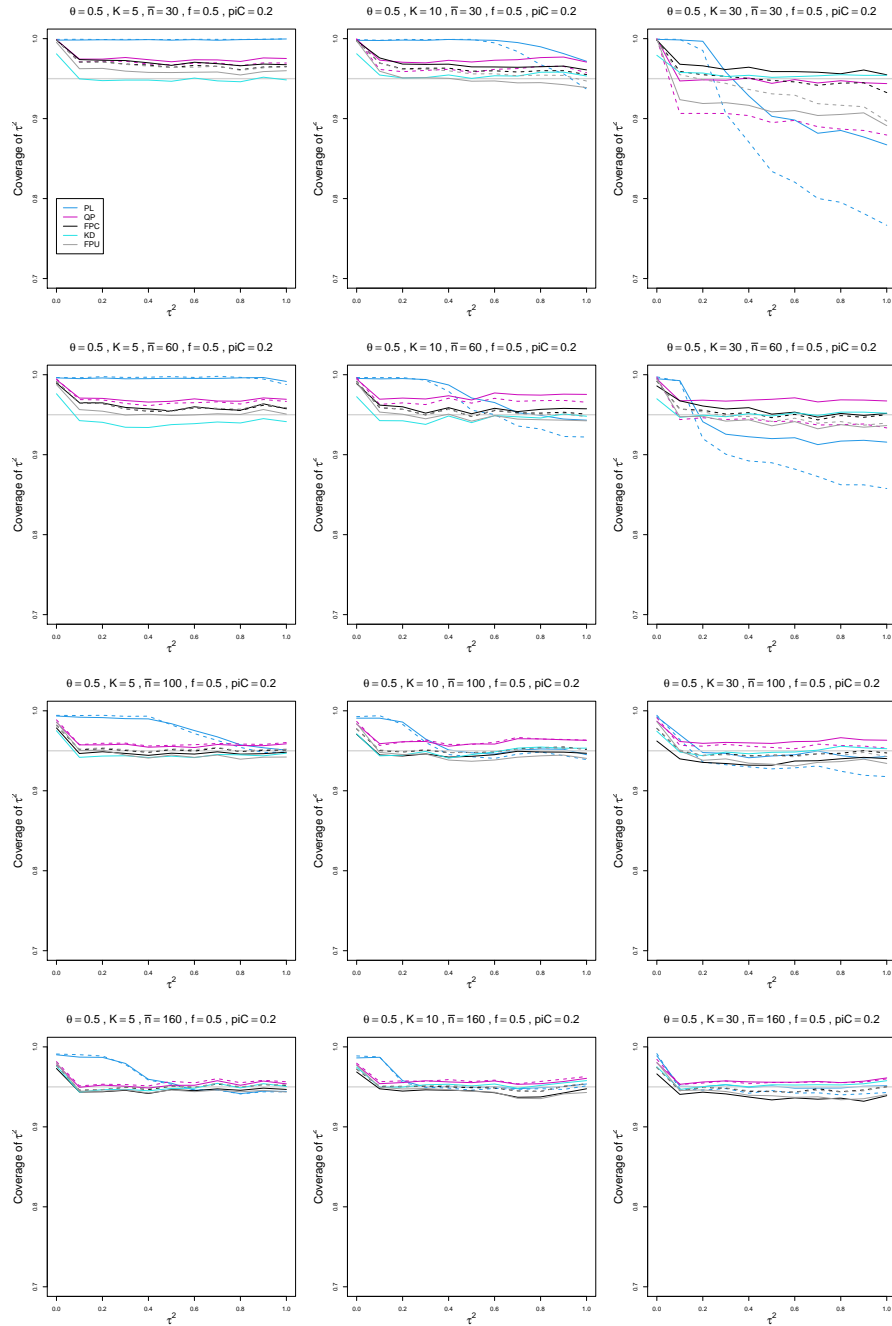


Figure C.18: Coverage of PL, QP, KD, FPC, and FPU 95% confidence intervals for between-study variance of LOR vs τ^2 , for unequal sample sizes $\bar{n} = 30, 60, 100$ and 160 , $p_{iC} = .2$, $\theta = 0.5$ and $f = 0.5$. Solid lines: PL, QP, and FPC “only”, FPU model-based, and KD. Dashed lines: PL, QP, and FPC “always” and FPU naïve.

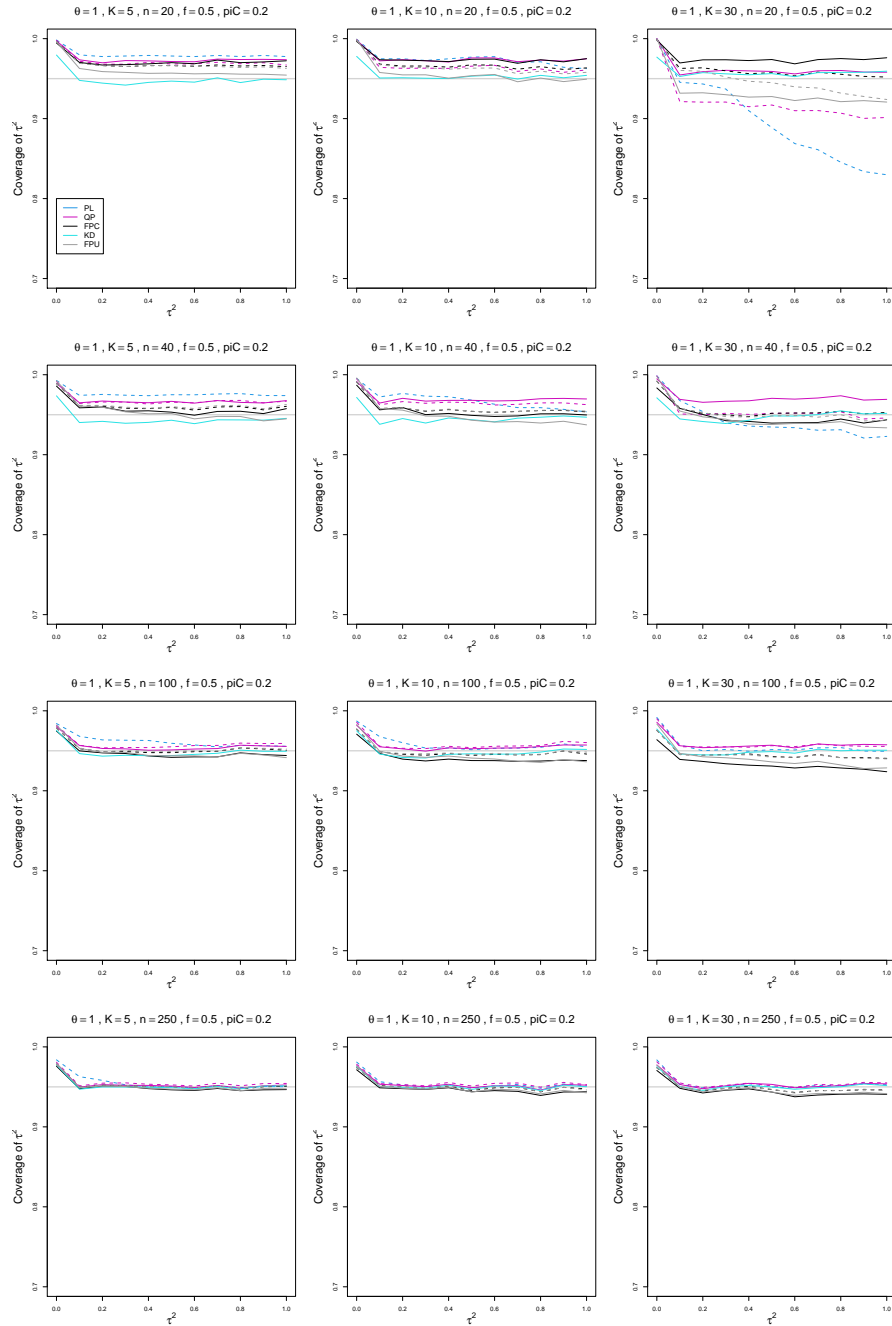


Figure C.19: Coverage of PL, QP, KD, FPC, and FPU 95% confidence intervals for between-study variance of LOR vs τ^2 , for equal sample sizes $n = 20, 40, 100$ and 250 , $p_{iC} = .2$, $\theta = 1$ and $f = 0.5$. Solid lines: PL, QP, and FPC “only”, FPU model-based, and KD. Dashed lines: PL, QP, and FPC “always” and FPU naïve.

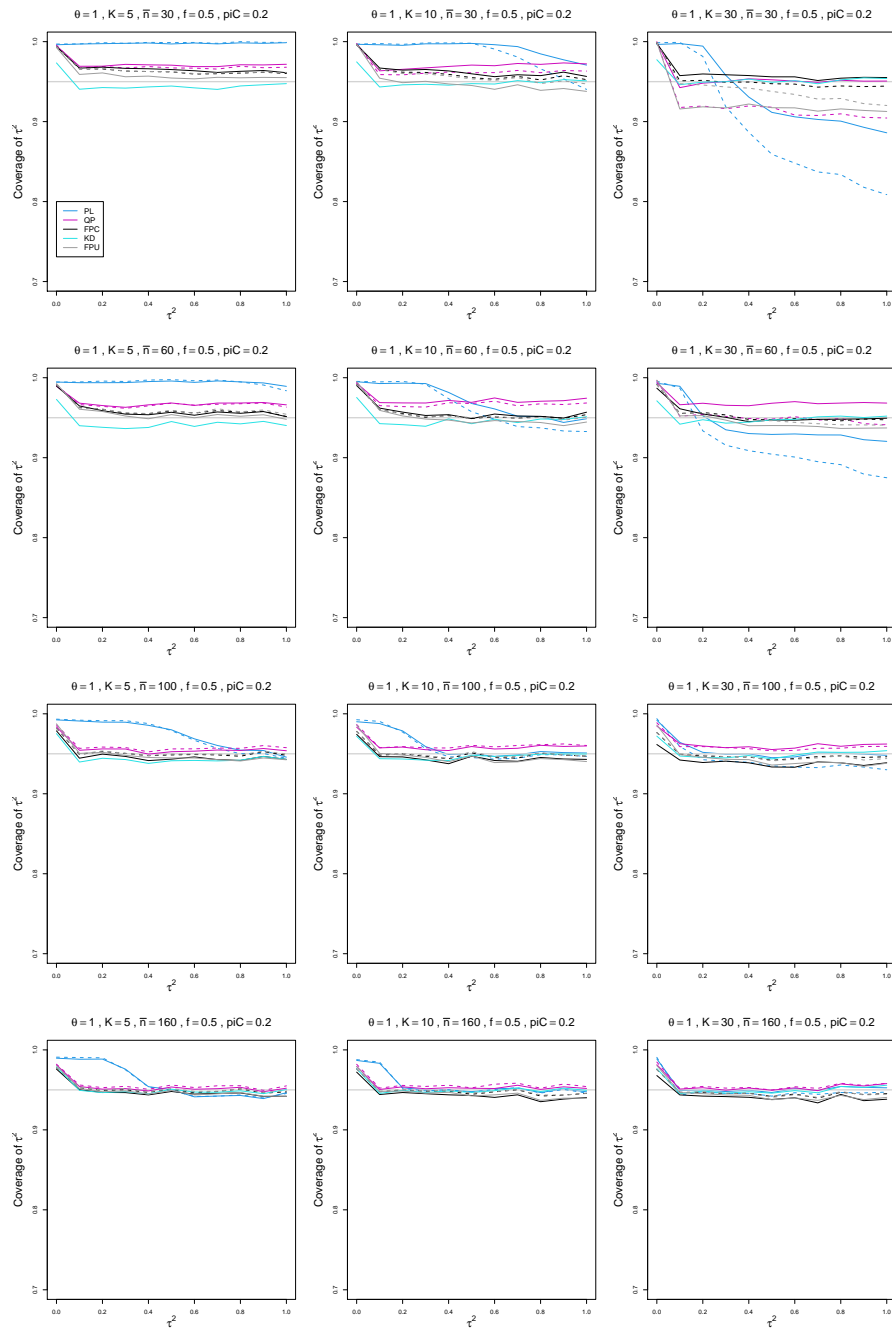


Figure C.20: Coverage of PL, QP, KD, FPC, and FPU 95% confidence intervals for between-study variance of LOR vs τ^2 , for unequal sample sizes $\bar{n} = 30, 60, 100$ and 160 , $p_{iC} = .2$, $\theta = 1$ and $f = 0.5$. Solid lines: PL, QP, and FPC “only”, FPU model-based, and KD. Dashed lines: PL, QP, and FPC “always” and FPU naïve.

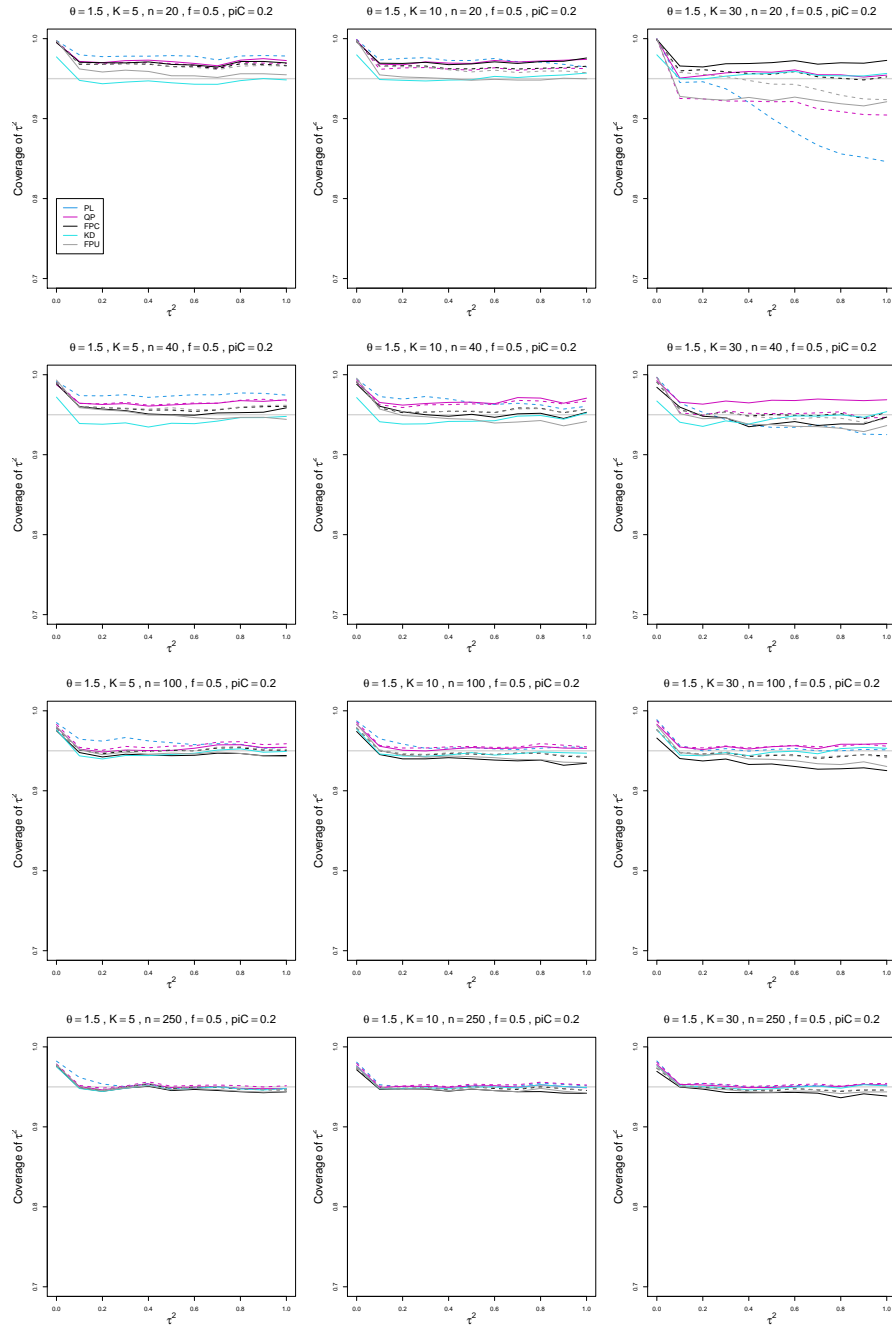


Figure C.21: Coverage of PL, QP, KD, FPC, and FPU 95% confidence intervals for between-study variance of LOR vs τ^2 , for equal sample sizes $n = 20, 40, 100$ and 250 , $p_{iC} = .2$, $\theta = 1.5$ and $f = 0.5$. Solid lines: PL, QP, and FPC “only”, FPU model-based, and KD. Dashed lines: PL, QP, and FPC “always” and FPU naïve.

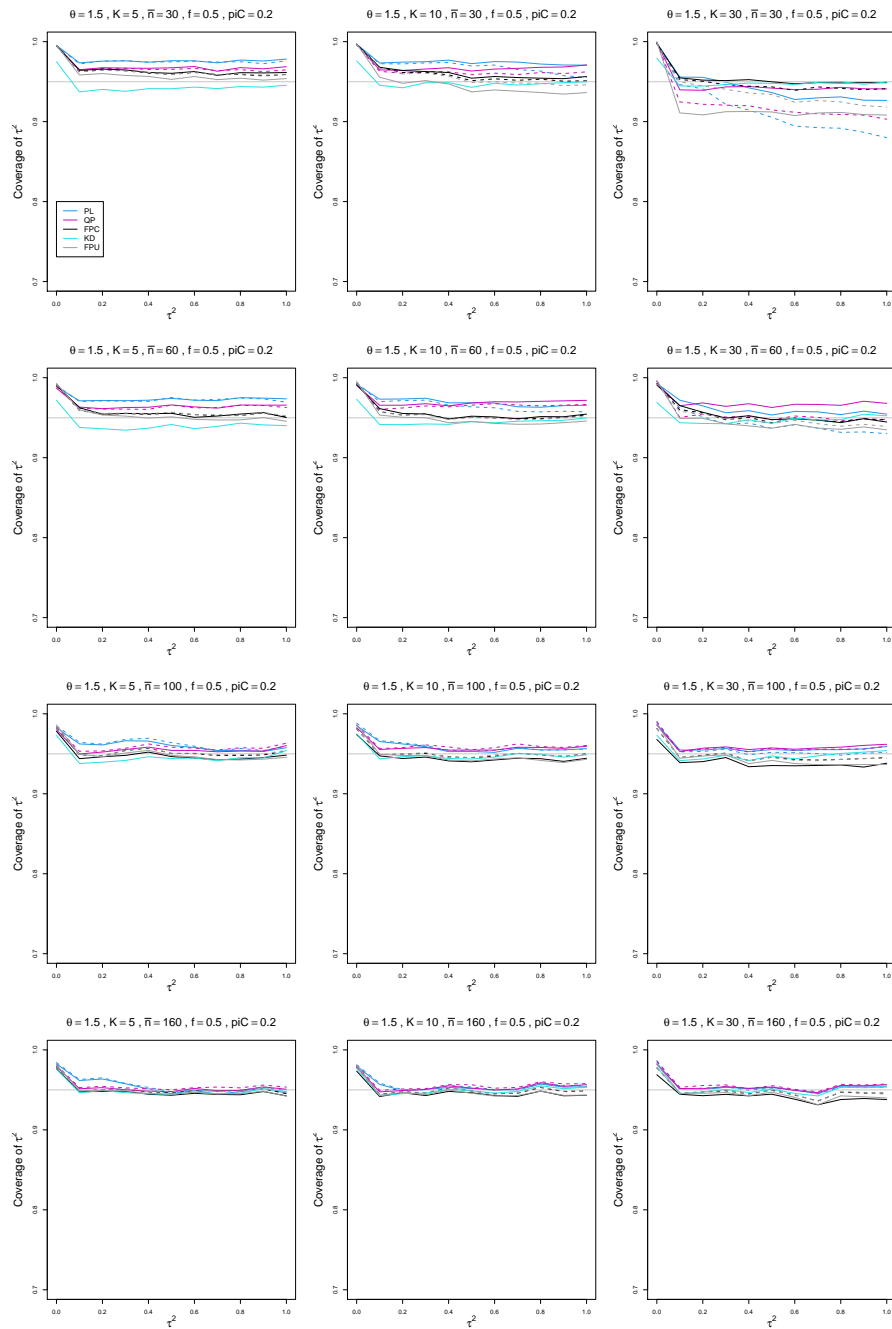


Figure C.22: Coverage of PL, QP, KD, FPC, and FPU 95% confidence intervals for between-study variance of LOR vs τ^2 , for unequal sample sizes $\bar{n} = 30, 60, 100$ and 160 , $p_{iC} = .2$, $\theta = 1.5$ and $f = 0.5$. Solid lines: PL, QP, and FPC “only”, FPU model-based, and KD. Dashed lines: PL, QP, and FPC “always” and FPU naïve.

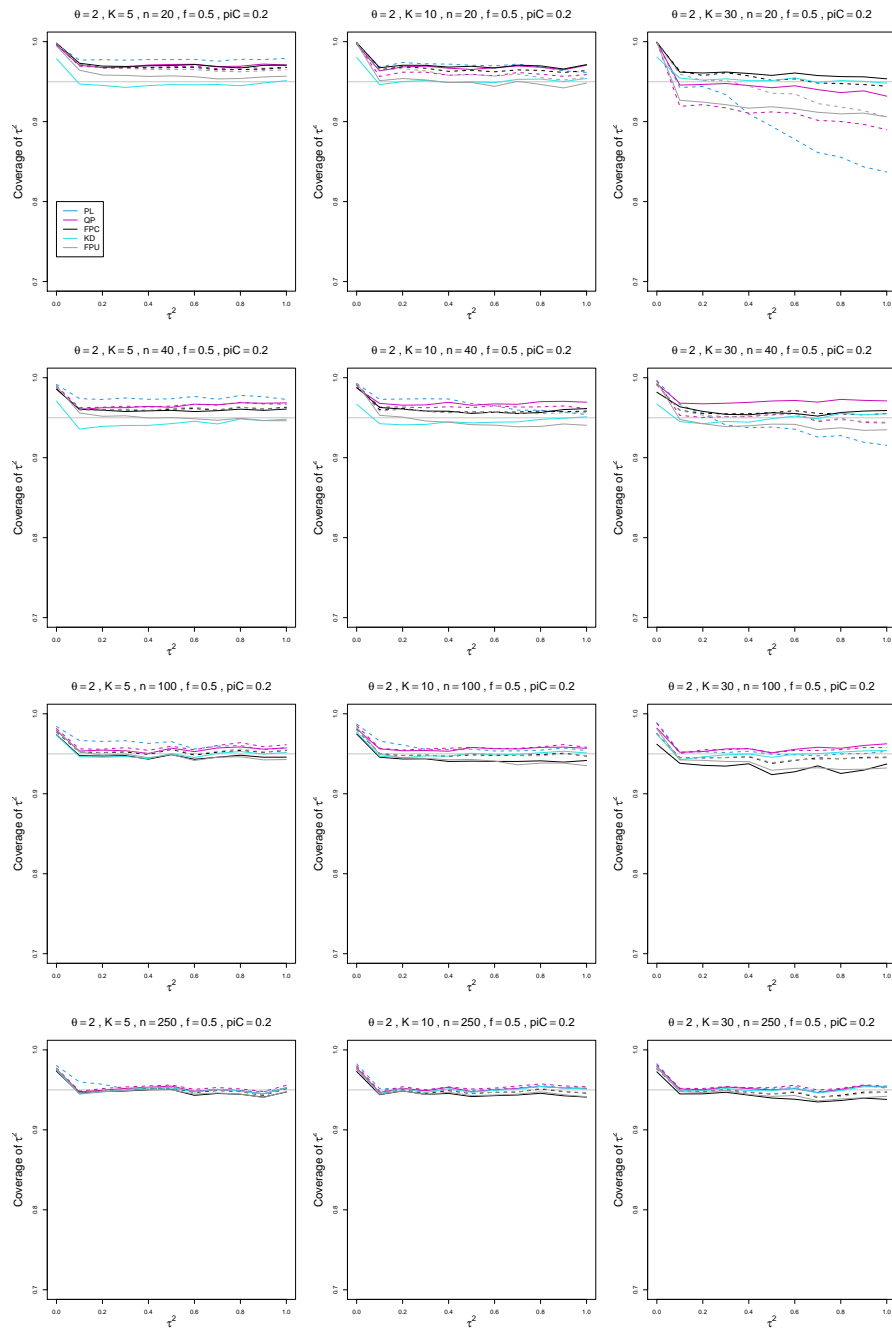


Figure C.23: Coverage of PL, QP, KD, FPC, and FPU 95% confidence intervals for between-study variance of LOR vs τ^2 , for equal sample sizes $n = 20, 40, 100$ and 250 , $p_{iC} = .2$, $\theta = 2$ and $f = 0.5$. Solid lines: PL, QP, and FPC “only”, FPU model-based, and KD. Dashed lines: PL, QP, and FPC “always” and FPU naïve.

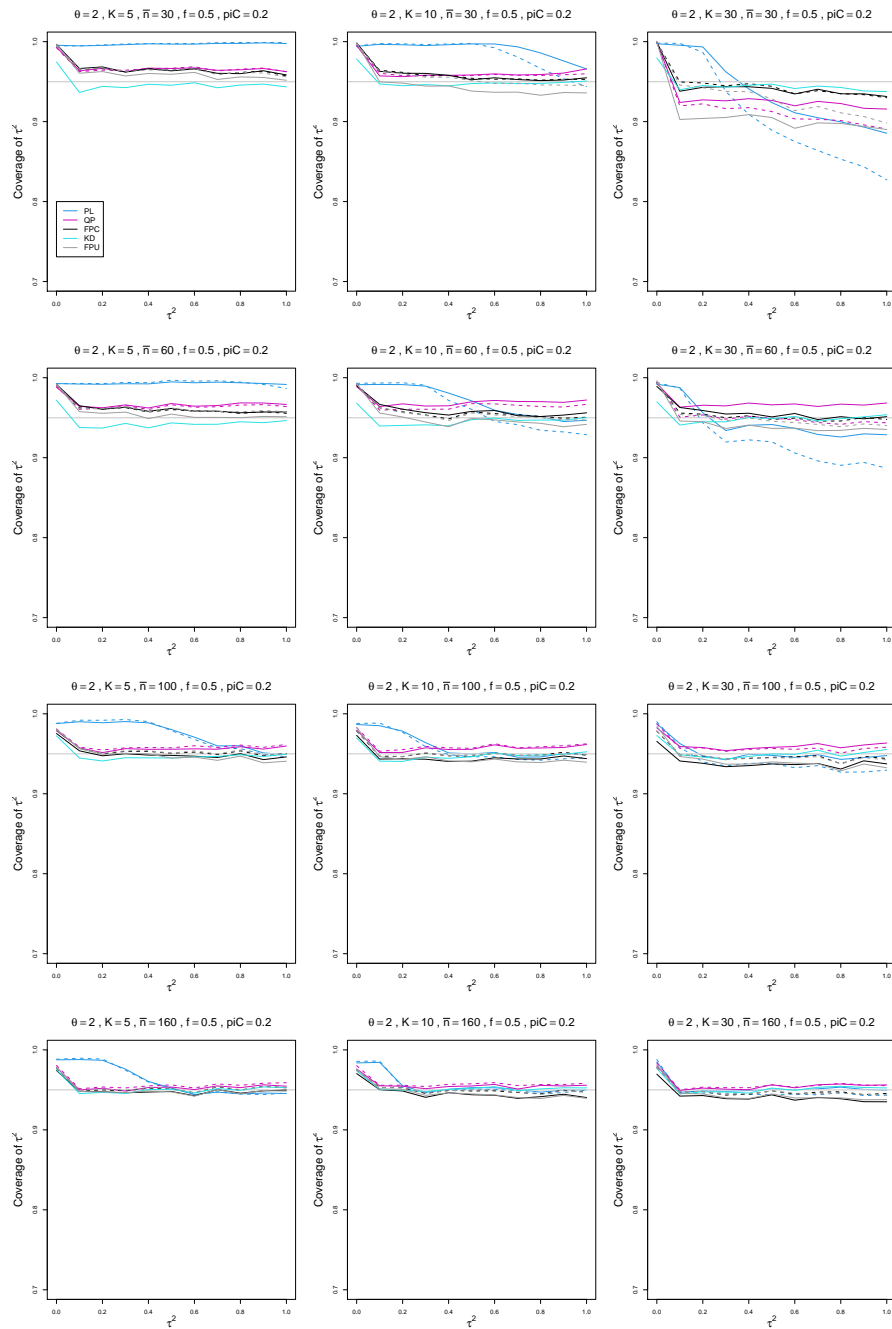


Figure C.24: Coverage of PL, QP, KD, FPC, and FPU 95% confidence intervals for between-study variance of LOR vs τ^2 , for unequal sample sizes $\bar{n} = 30, 60, 100$ and 160 , $p_{iC} = .2$, $\theta = 2$ and $f = 0.5$. Solid lines: PL, QP, and FPC “only”, FPU model-based, and KD. Dashed lines: PL, QP, and FPC “always” and FPU naïve.

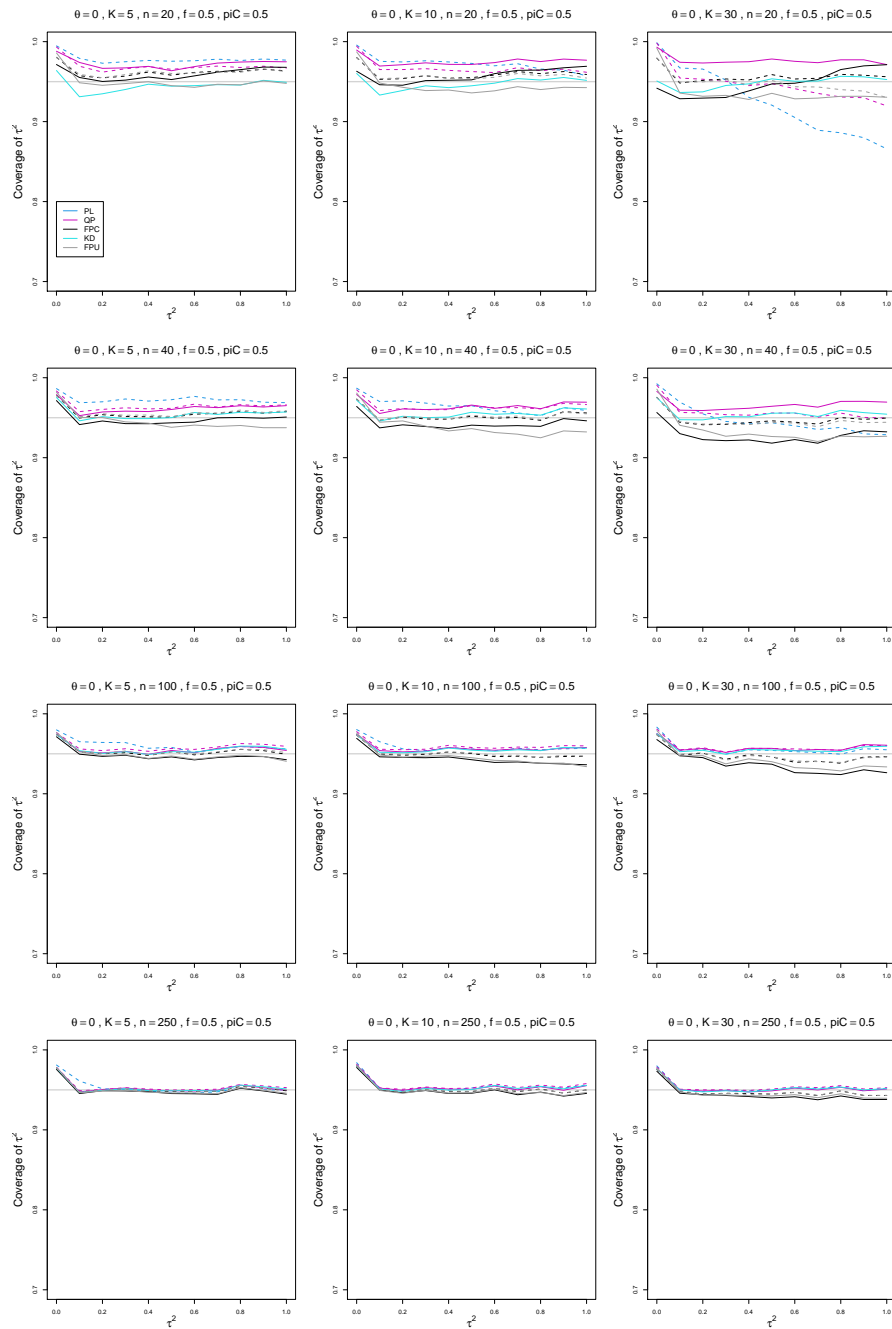


Figure C.25: Coverage of PL, QP, KD, FPC, and FPU 95% confidence intervals for between-study variance of LOR vs τ^2 , for equal sample sizes $n = 20, 40, 100$ and 250 , $p_{iC} = .5$, $\theta = 0$ and $f = 0.5$. Solid lines: PL, QP, and FPC “only”, FPU model-based, and KD. Dashed lines: PL, QP, and FPC “always” and FPU naïve.

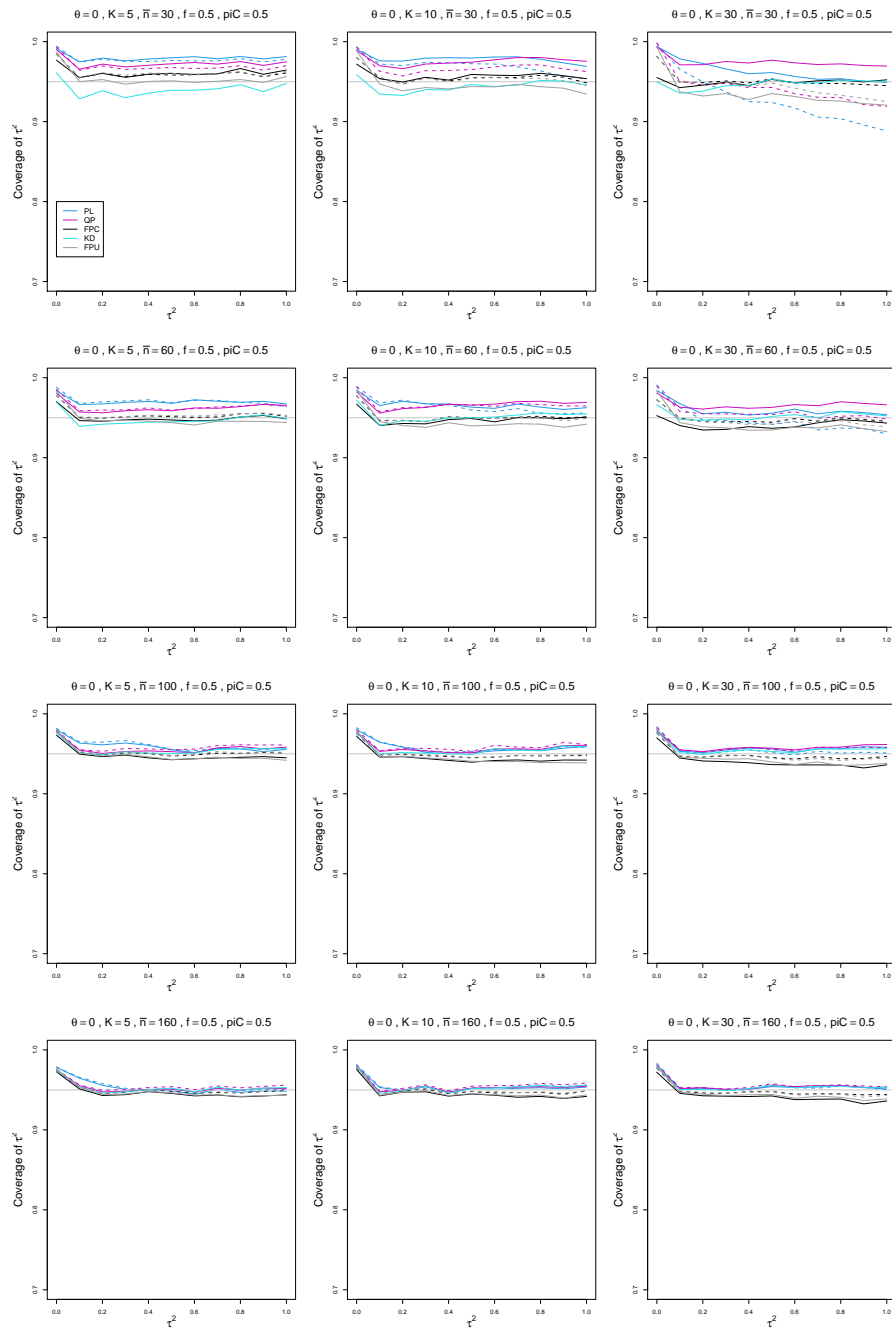


Figure C.26: Coverage of PL, QP, KD, FPC, and FPU 95% confidence intervals for between-study variance of LOR vs τ^2 , for unequal sample sizes $\bar{n} = 30, 60, 100$ and 160 , $p_{iC} = .5$, $\theta = 0$ and $f = 0.5$. Solid lines: PL, QP, and FPC “only”, FPU model-based, and KD. Dashed lines: PL, QP, and FPC “always” and FPU naïve.

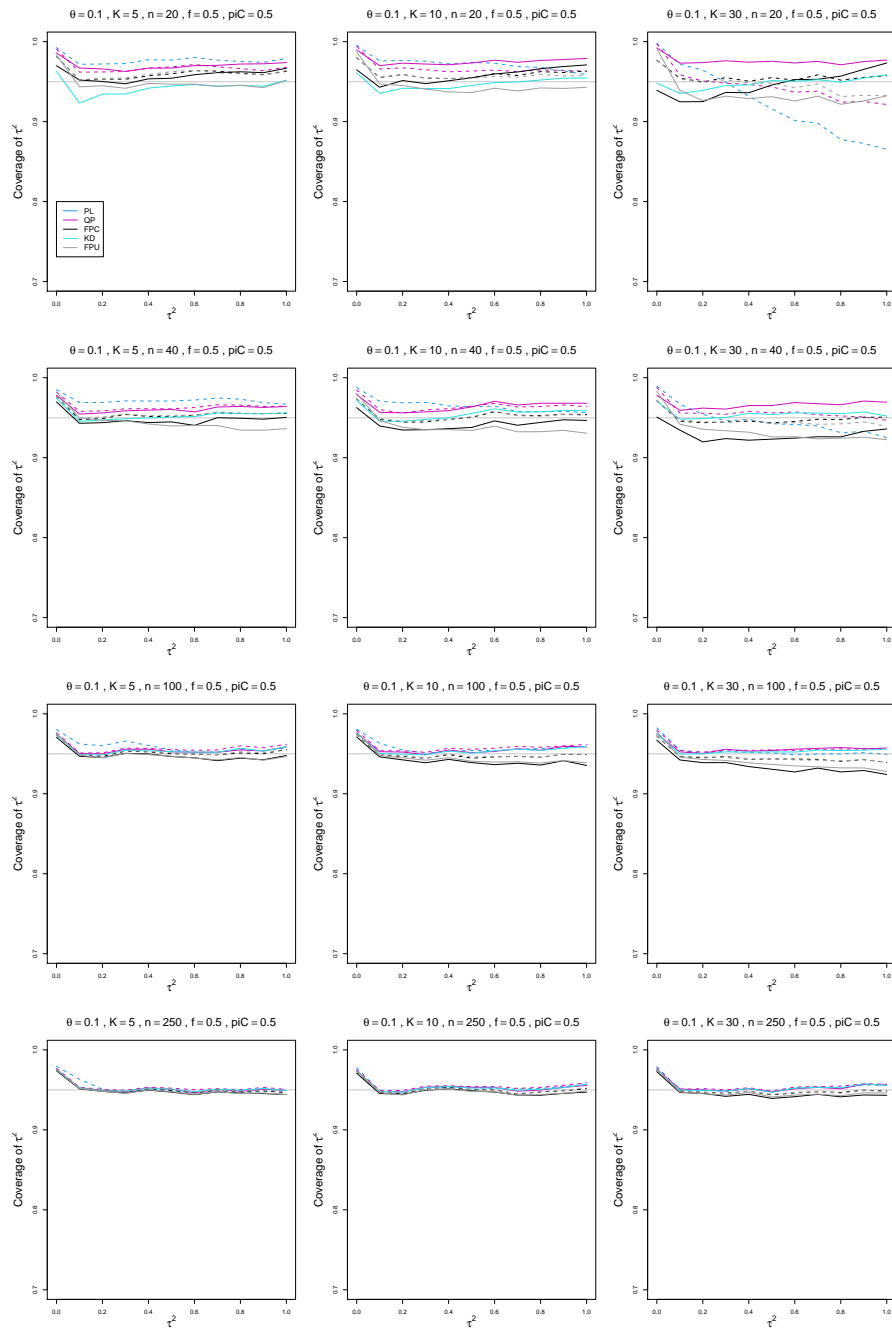


Figure C.27: Coverage of PL, QP, KD, FPC, and FPU 95% confidence intervals for between-study variance of LOR vs τ^2 , for equal sample sizes $n = 20, 40, 100$ and 250 , $p_{iC} = .5$, $\theta = 0.1$ and $f = 0.5$. Solid lines: PL, QP, and FPC “only”, FPU model-based, and KD. Dashed lines: PL, QP, and FPC “always” and FPU naïve.

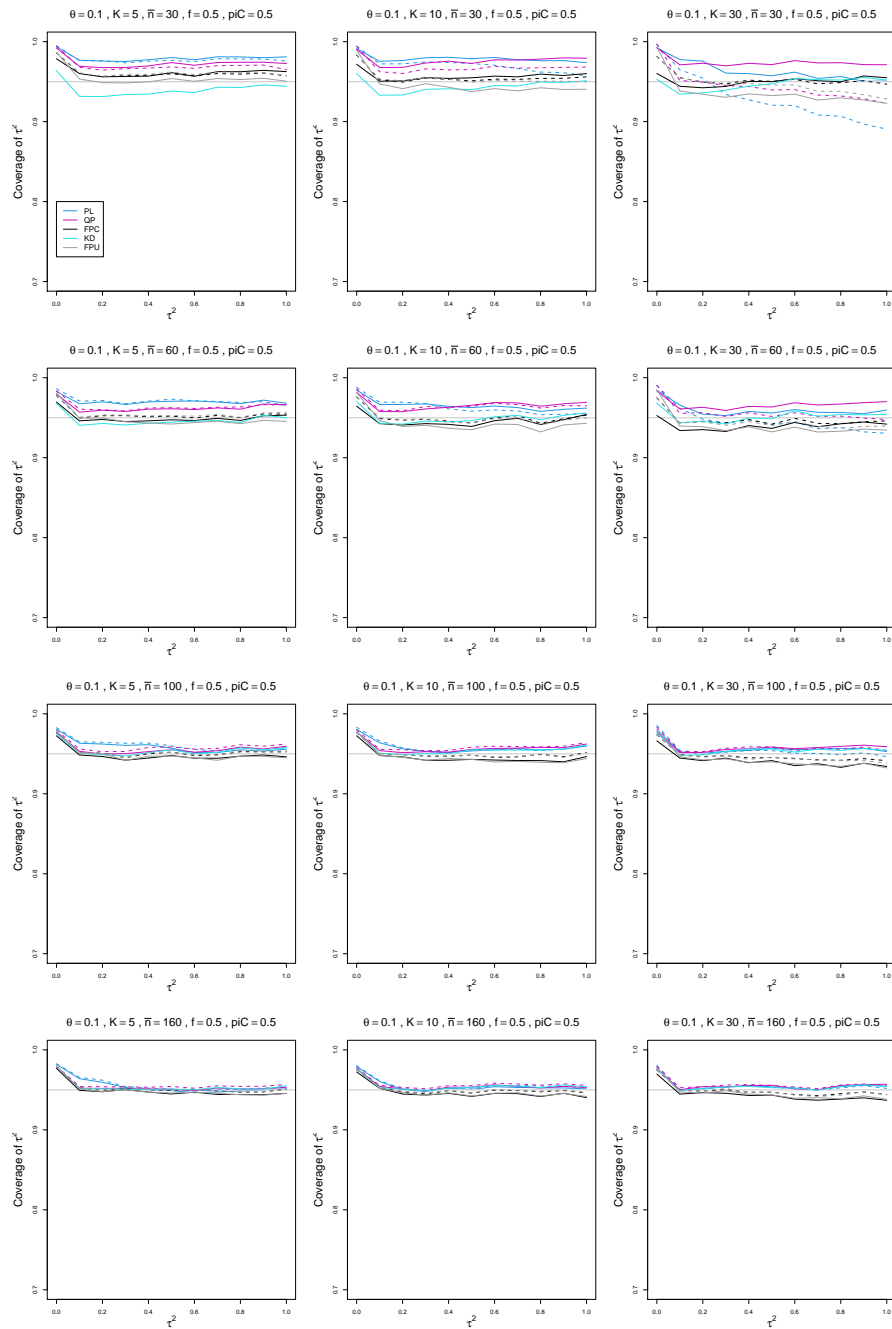


Figure C.28: Coverage of PL, QP, KD, FPC, and FPU 95% confidence intervals for between-study variance of LOR vs τ^2 , for unequal sample sizes $\bar{n} = 30, 60, 100$ and 160 , $p_{iC} = .5$, $\theta = 0.1$ and $f = 0.5$. Solid lines: PL, QP, and FPC “only”, FPU model-based, and KD. Dashed lines: PL, QP, and FPC “always” and FPU naïve.

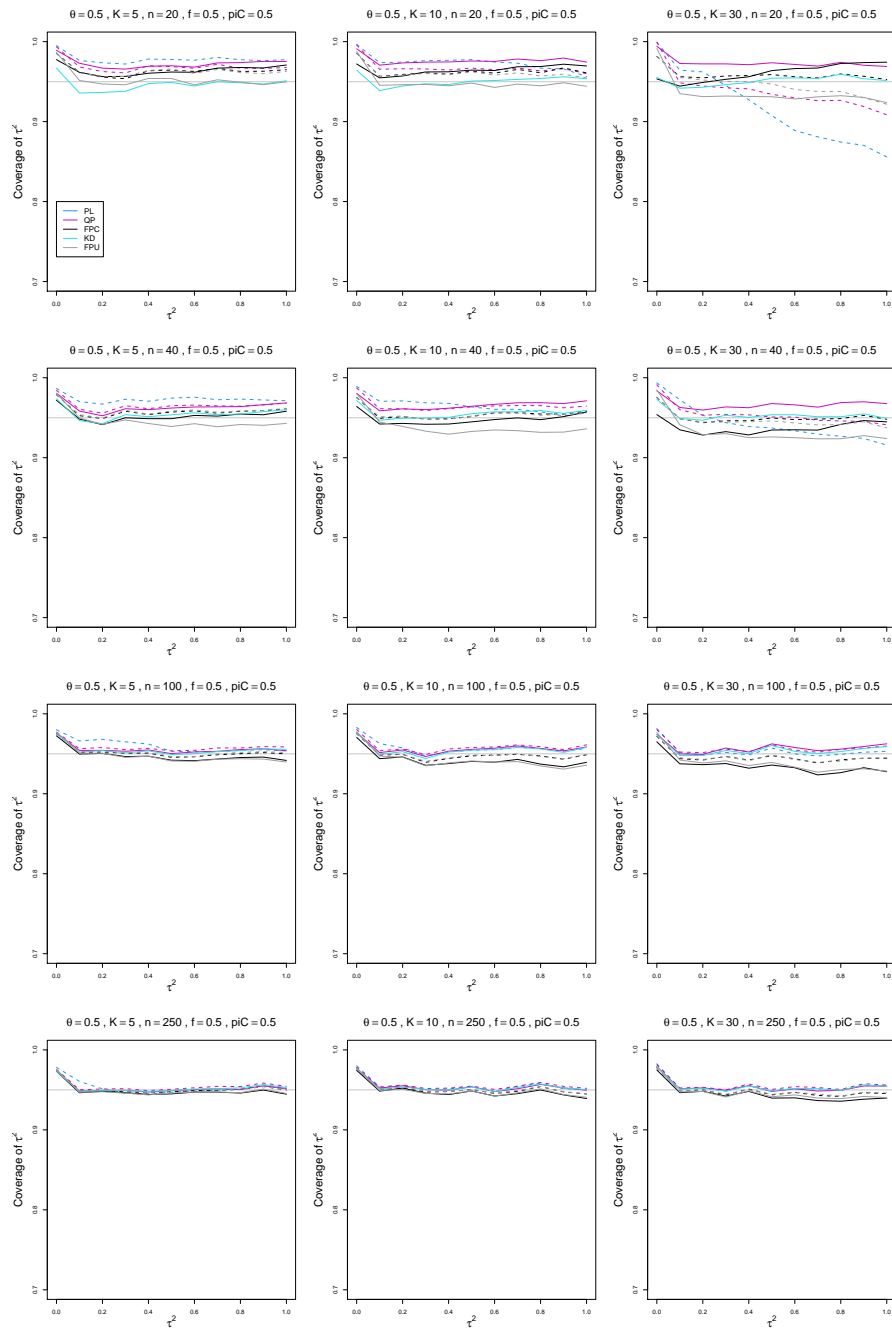


Figure C.29: Coverage of PL, QP, KD, FPC, and FPU 95% confidence intervals for between-study variance of LOR vs τ^2 , for equal sample sizes $n = 20, 40, 100$ and 250 , $p_{iC} = .5$, $\theta = 0.5$ and $f = 0.5$. Solid lines: PL, QP, and FPC “only”, FPU model-based, and KD. Dashed lines: PL, QP, and FPC “always” and FPU naïve.

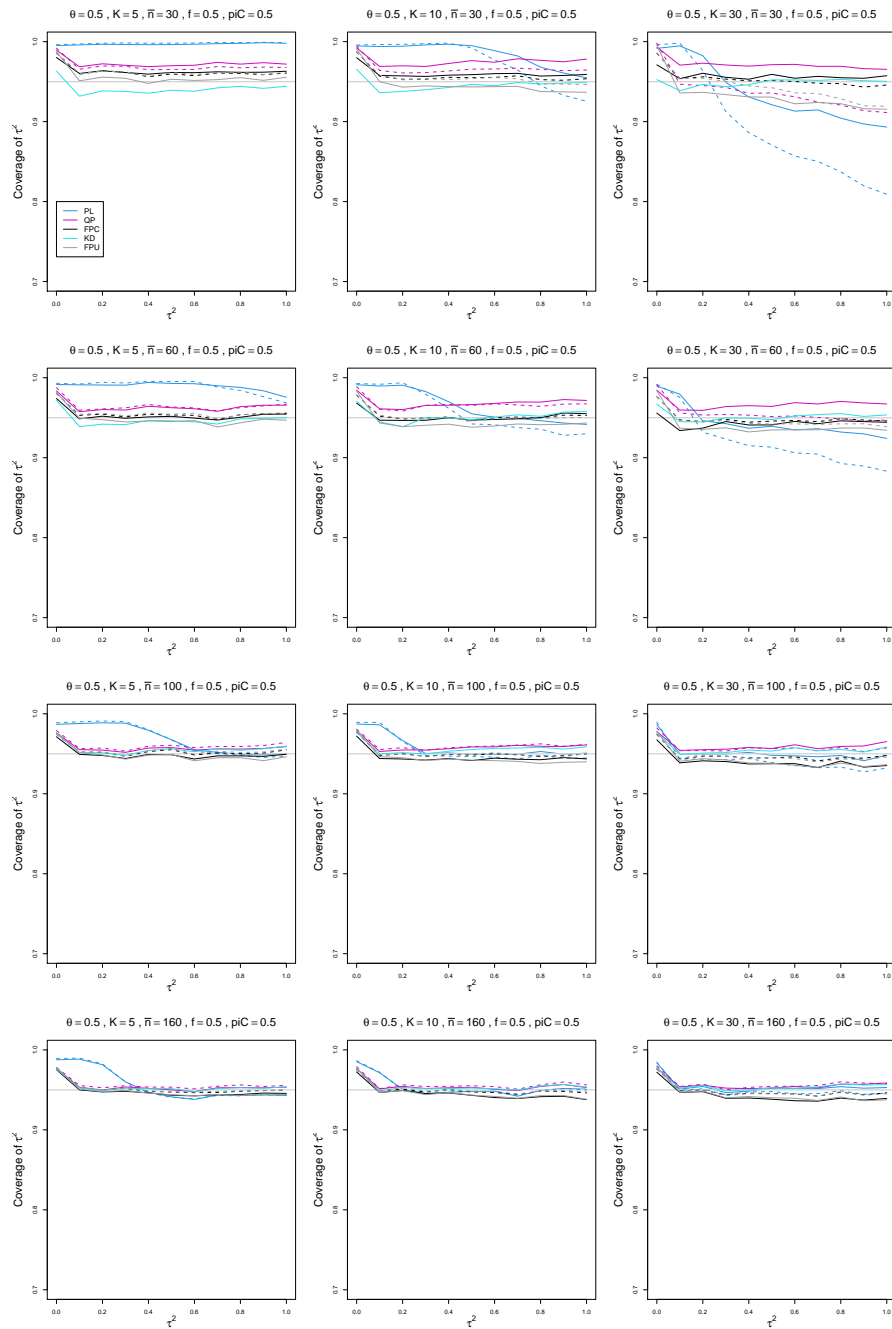


Figure C.30: Coverage of PL, QP, KD, FPC, and FPU 95% confidence intervals for between-study variance of LOR vs τ^2 , for unequal sample sizes $\bar{n} = 30, 60, 100$ and 160 , $p_{iC} = .5$, $\theta = 0.5$ and $f = 0.5$. Solid lines: PL, QP, and FPC “only”, FPU model-based, and KD. Dashed lines: PL, QP, and FPC “always” and FPU naïve.

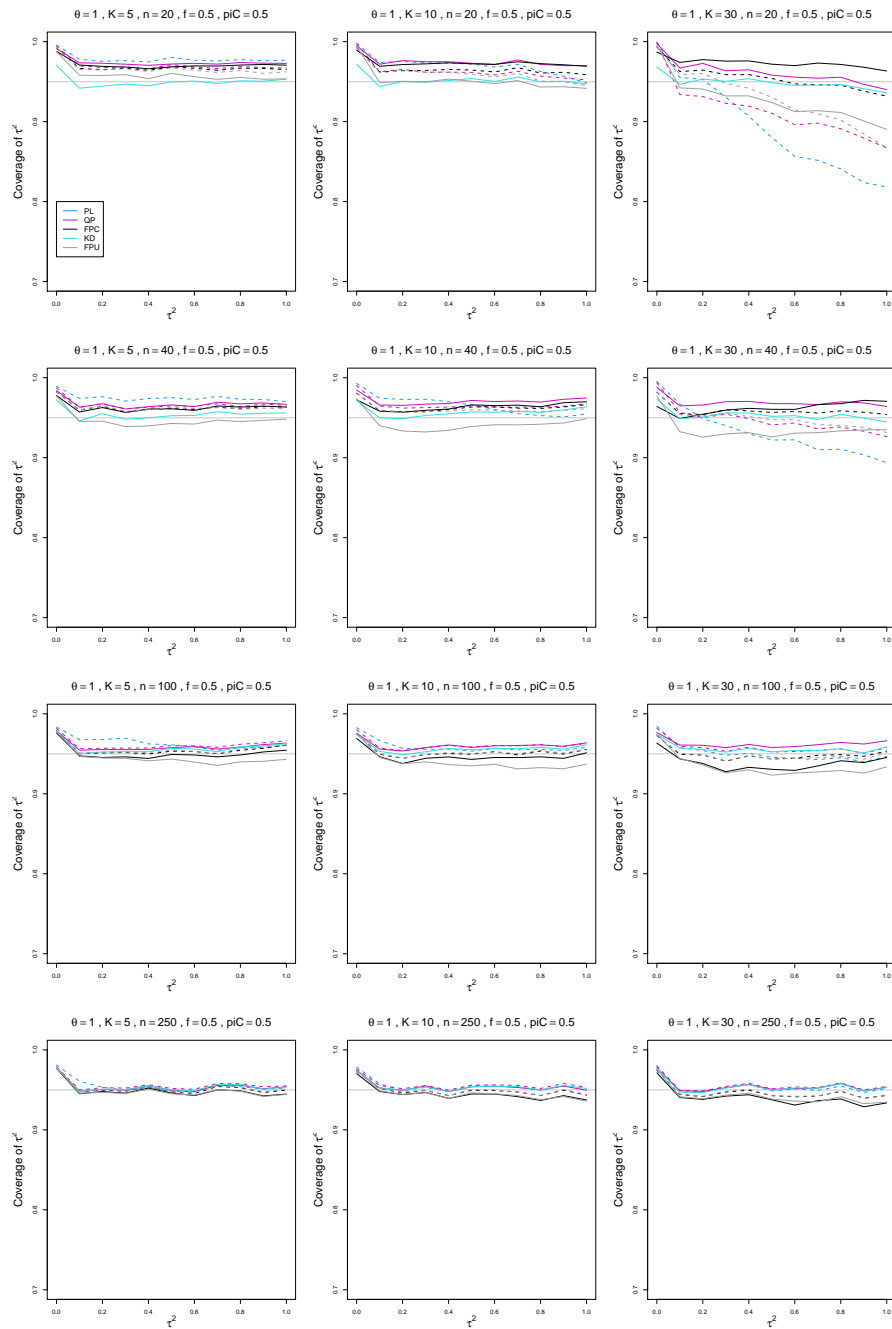


Figure C.31: Coverage of PL, QP, KD, FPC, and FPU 95% confidence intervals for between-study variance of LOR vs τ^2 , for equal sample sizes $n = 20, 40, 100$ and 250 , $p_{iC} = .5$, $\theta = 1$ and $f = 0.5$. Solid lines: PL, QP, and FPC “only”, FPU model-based, and KD. Dashed lines: PL, QP, and FPC “always” and FPU naïve.

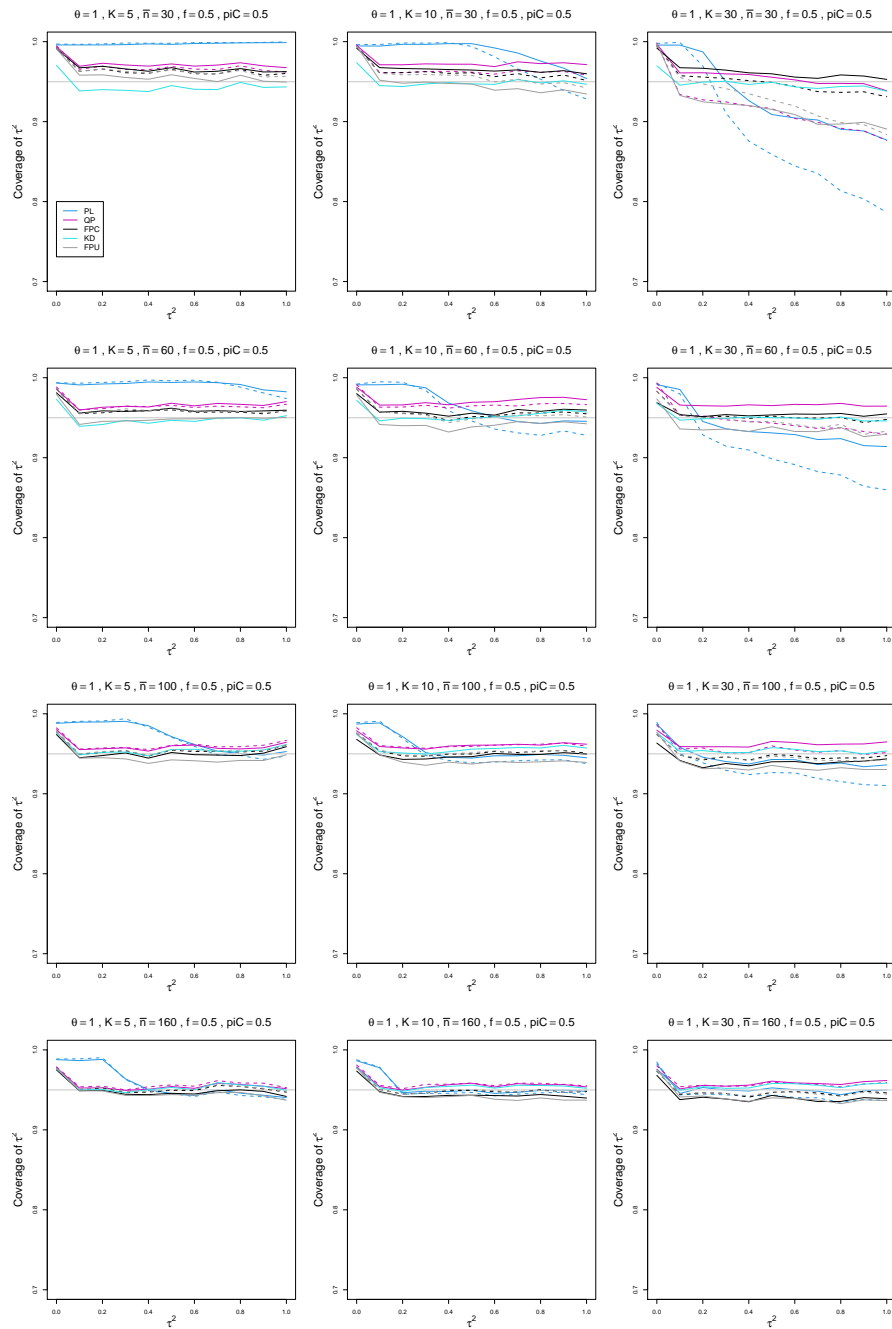


Figure C.32: Coverage of PL, QP, KD, FPC, and FPU 95% confidence intervals for between-study variance of LOR vs τ^2 , for unequal sample sizes $\bar{n} = 30, 60, 100$ and 160 , $p_{iC} = .5$, $\theta = 1$ and $f = 0.5$. Solid lines: PL, QP, and FPC “only”, FPU model-based, and KD. Dashed lines: PL, QP, and FPC “always” and FPU naïve.

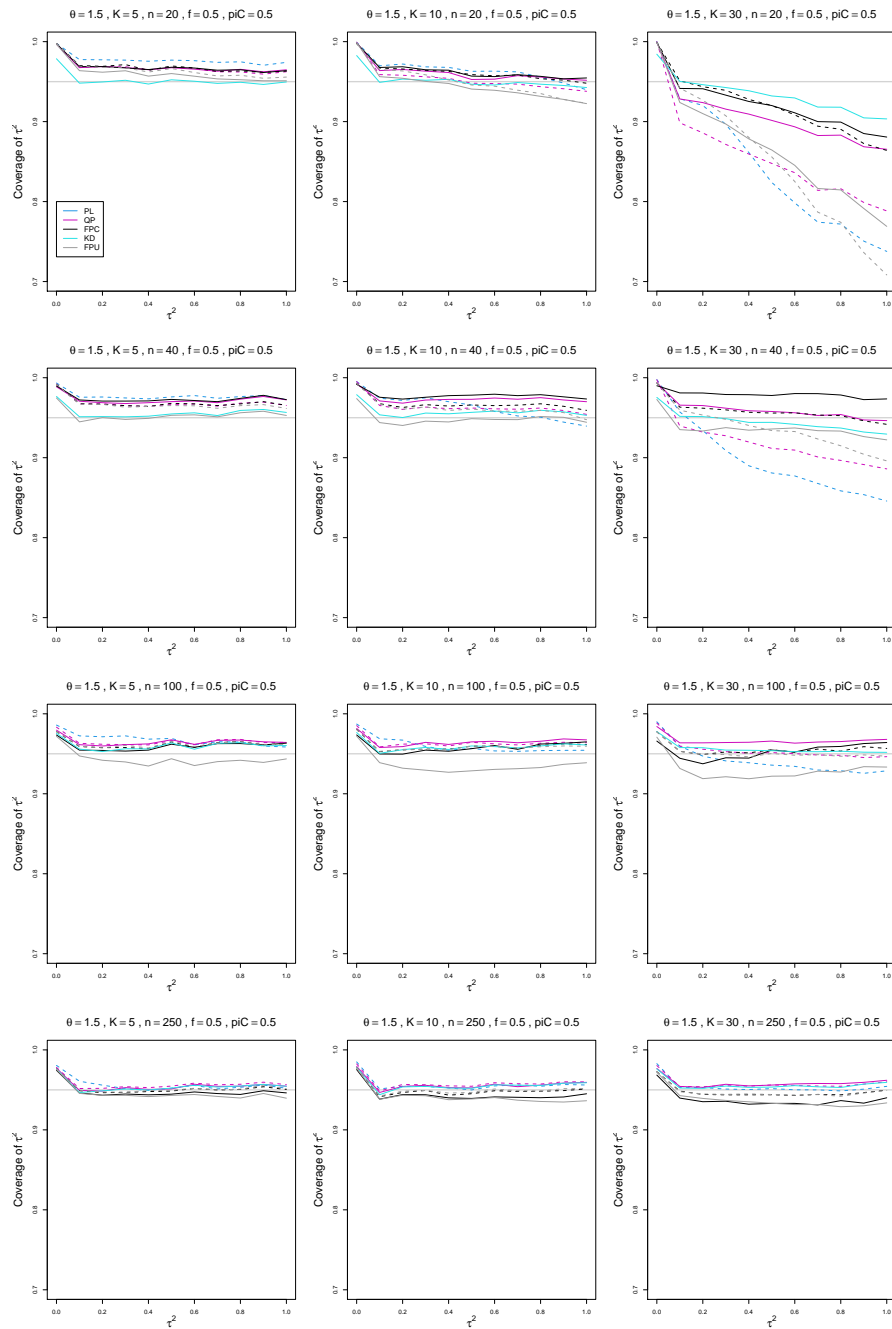


Figure C.33: Coverage of PL, QP, KD, FPC, and FPU 95% confidence intervals for between-study variance of LOR vs τ^2 , for equal sample sizes $n = 20, 40, 100$ and 250 , $p_{iC} = .5$, $\theta = 1.5$ and $f = 0.5$. Solid lines: PL, QP, and FPC “only”, FPU model-based, and KD. Dashed lines: PL, QP, and FPC “always” and FPU naïve.

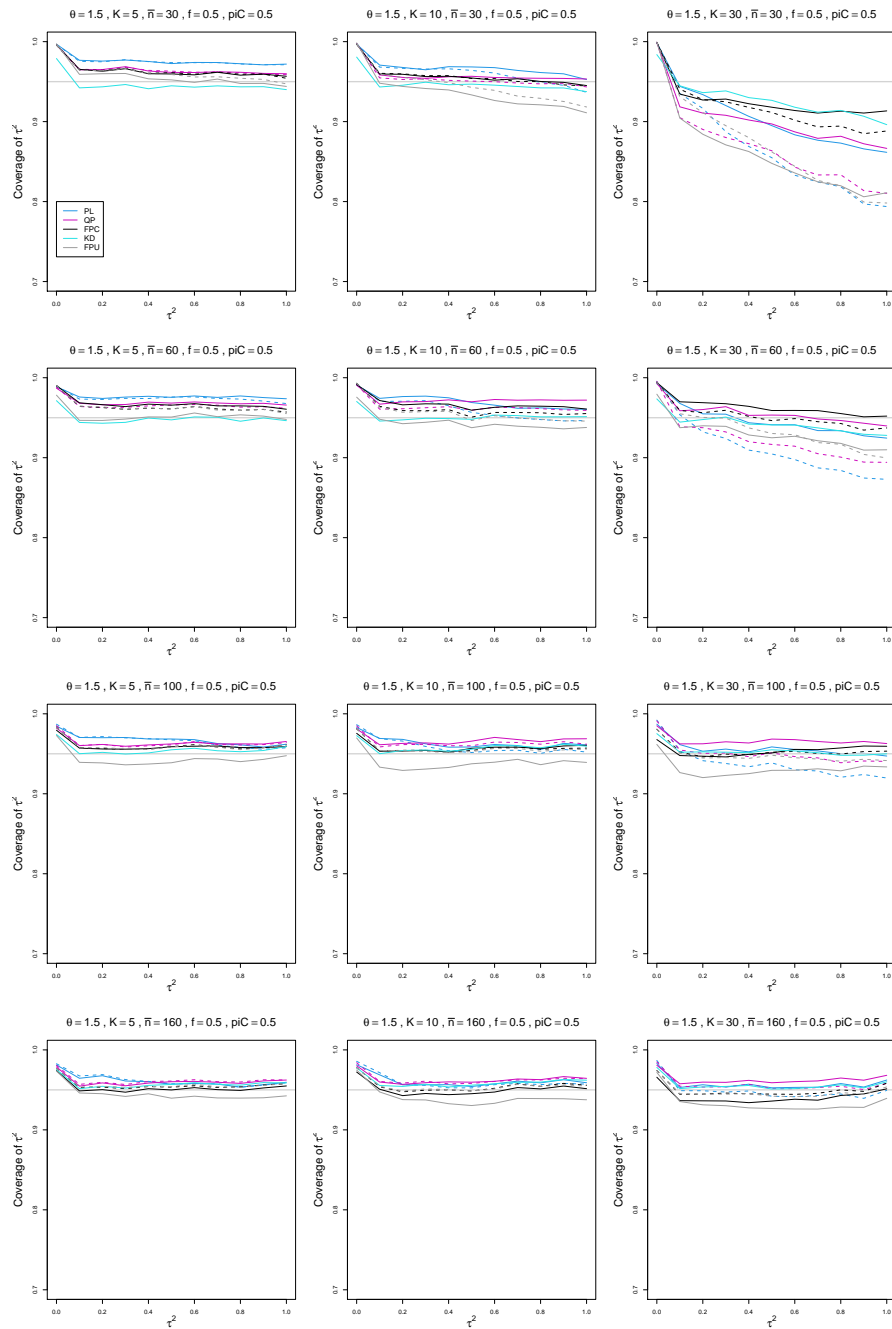


Figure C.34: Coverage of PL, QP, KD, FPC, and FPU 95% confidence intervals for between-study variance of LOR vs τ^2 , for unequal sample sizes $\bar{n} = 30, 60, 100$ and 160 , $p_{iC} = .5$, $\theta = 1.5$ and $f = 0.5$. Solid lines: PL, QP, and FPC “only”, FPU model-based, and KD. Dashed lines: PL, QP, and FPC “always” and FPU naïve.

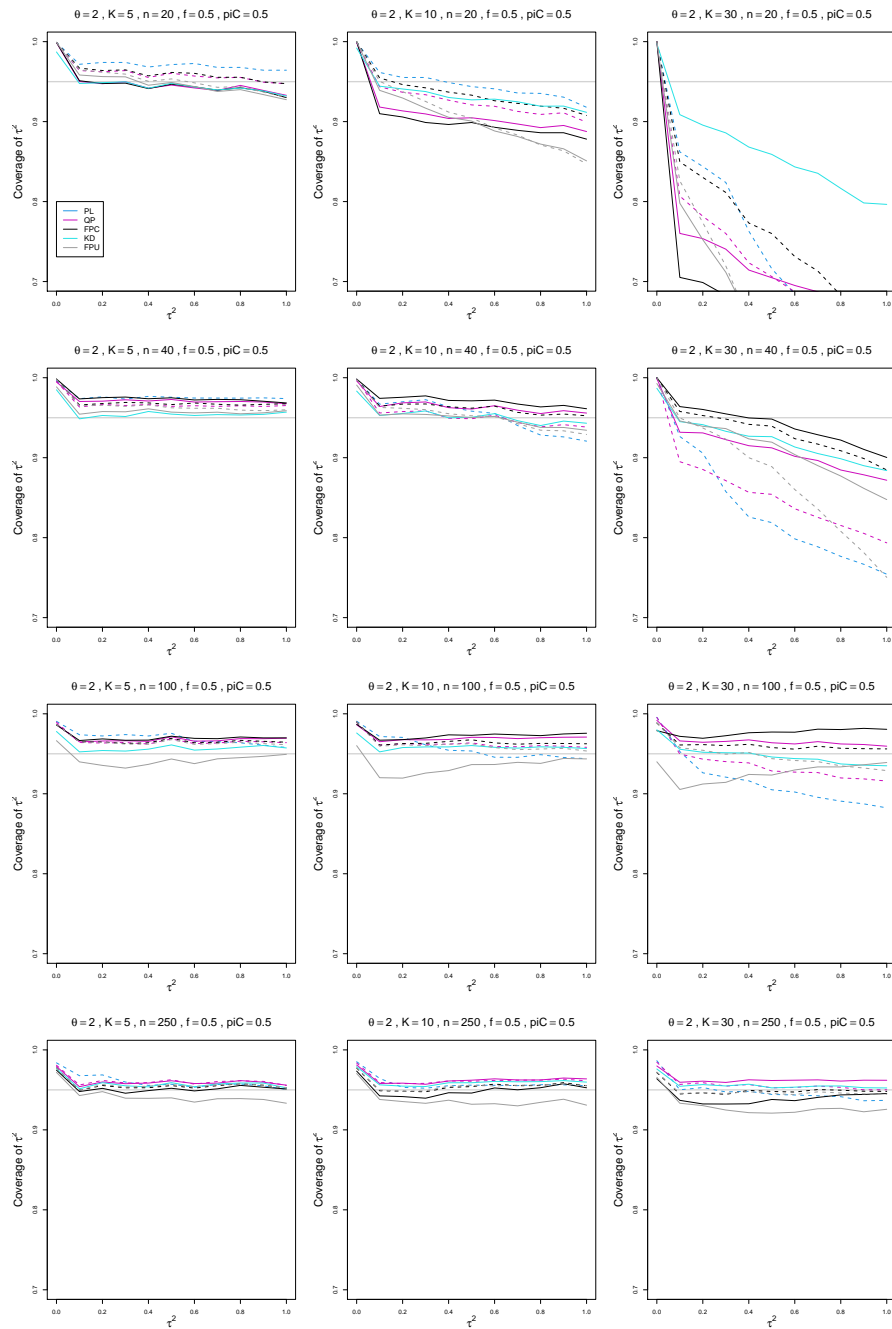


Figure C.35: Coverage of PL, QP, KD, FPC, and FPU 95% confidence intervals for between-study variance of LOR vs τ^2 , for equal sample sizes $n = 20, 40, 100$ and 250 , $p_{iC} = .5$, $\theta = 2$ and $f = 0.5$. Solid lines: PL, QP, and FPC “only”, FPU model-based, and KD. Dashed lines: PL, QP, and FPC “always” and FPU naïve.

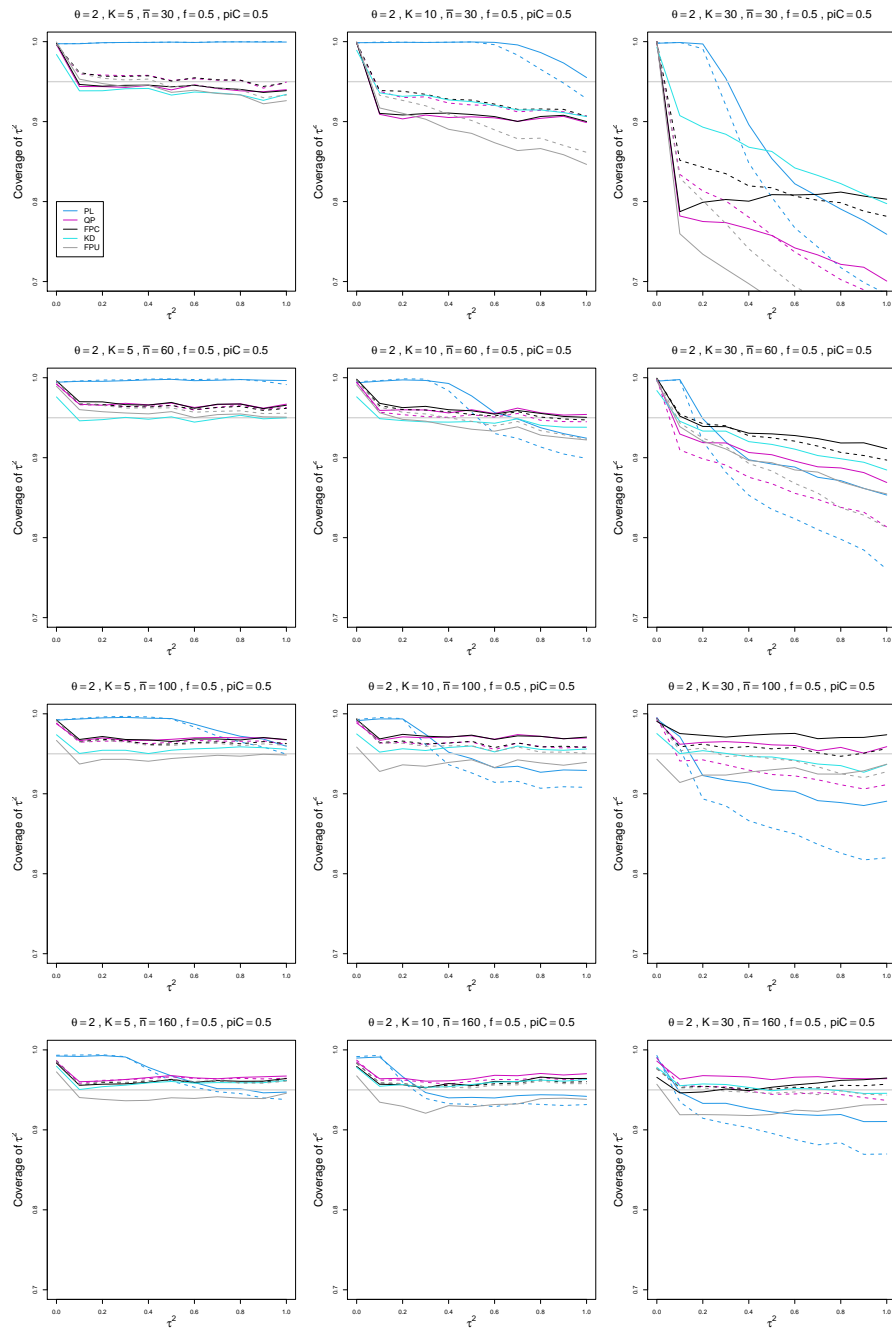


Figure C.36: Coverage of PL, QP, KD, FPC, and FPU 95% confidence intervals for between-study variance of LOR vs τ^2 , for unequal sample sizes $\bar{n} = 30, 60, 100$ and 160 , $p_{iC} = .5$, $\theta = 2$ and $f = 0.5$. Solid lines: PL, QP, and FPC “only”, FPU model-based, and KD. Dashed lines: PL, QP, and FPC “always” and FPU naïve.

Appendix D: Sample miss-left probability for 95% confidence intervals for between-study variance

Each figure corresponds to a value of the probability of an event in the Control arm p_{iC} ($= .1, .2, .5$).

The fraction of each study's sample size in the Control arm f is held constant at 0.5. For each combination of a value of n ($= 20, 40, 100, 250$) or \bar{n} ($= 30, 60, 100, 160$) and a value of K ($= 5, 10, 30$), a panel plots the probability that the parameter is to the left of the lower confidence limit of the confidence interval versus τ^2 ($= 0.0(0.1)1$).

The confidence intervals for τ^2 are

- PL (Profile Likelihood), inverse-variance weights)
- QP (Q profile, inverse-variance weights)
- KD (based on Kulinskaya-Dollinger (2015) approximation, inverse-variance weights)
- FPC (based on Farebrother approximation, effective-sample-size weights, conditional variance of LOR)
- FPU (based on Farebrother approximation, effective-sample-size weights, unconditional variance of LOR)

The plots include two versions of PL, QP, and FPC: adding $1/2$ to all four of X_{iT} , X_{iC} , $n_{iT} - X_{iT}$, $n_{iC} - X_{iC}$ only when one of these is zero (solid lines) or always (dashed lines).

The plots also include two versions of FPU: model-based estimation of p_{iT} (solid lines) or naïve estimation (dashed lines).

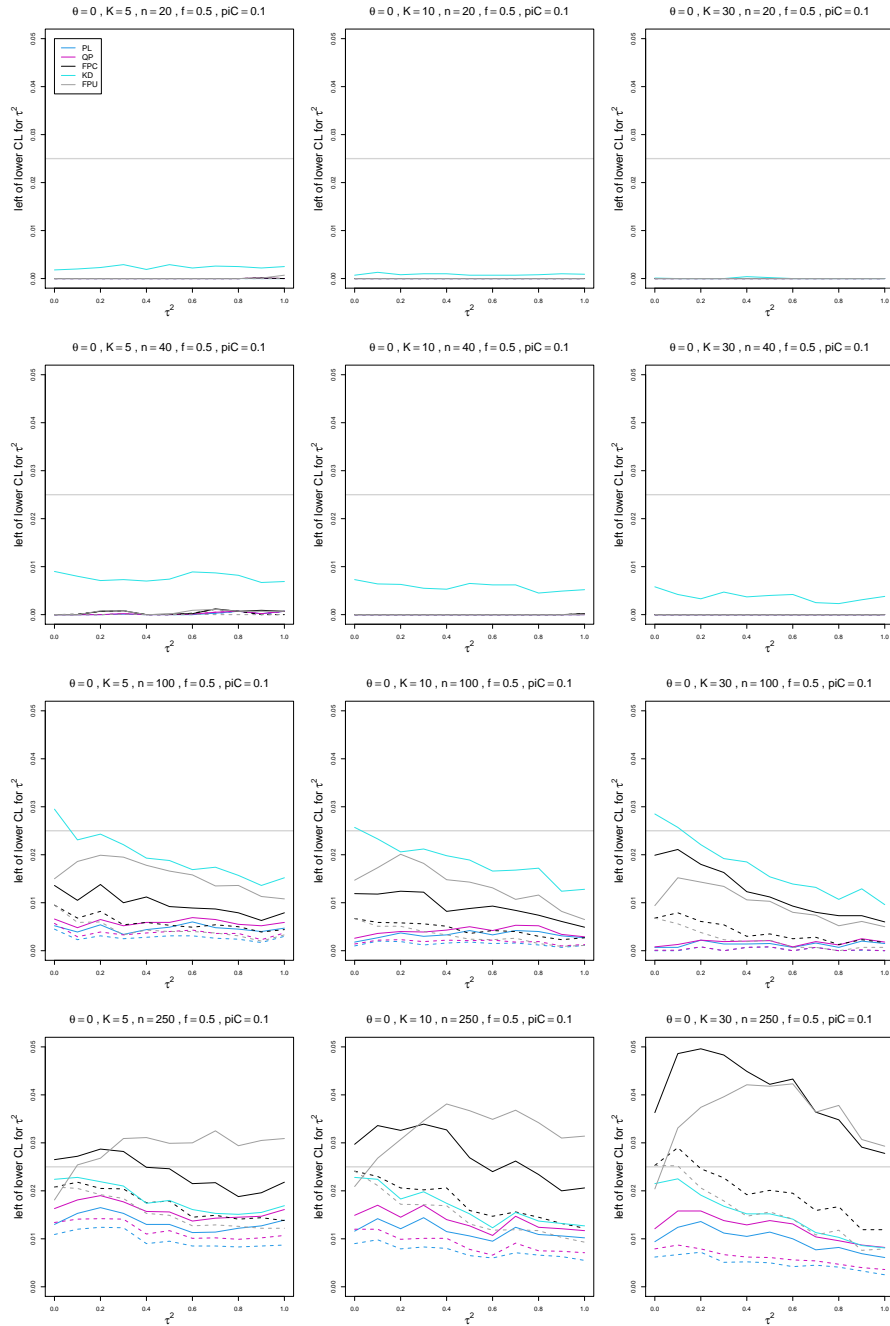


Figure D.1: Miss-left probability of PL, QP, KD, FPC, and FPU 95% confidence intervals for between-study variance of LOR vs τ^2 , for equal sample sizes $n = 20, 40, 100$ and 250 , $p_{iC} = .1$, $\theta = 0$ and $f = 0.5$. Solid lines: PL, QP, and FPC “only”, FPU model-based, and KD. Dashed lines: PL, QP, and FPC “always” and FPU naïve.

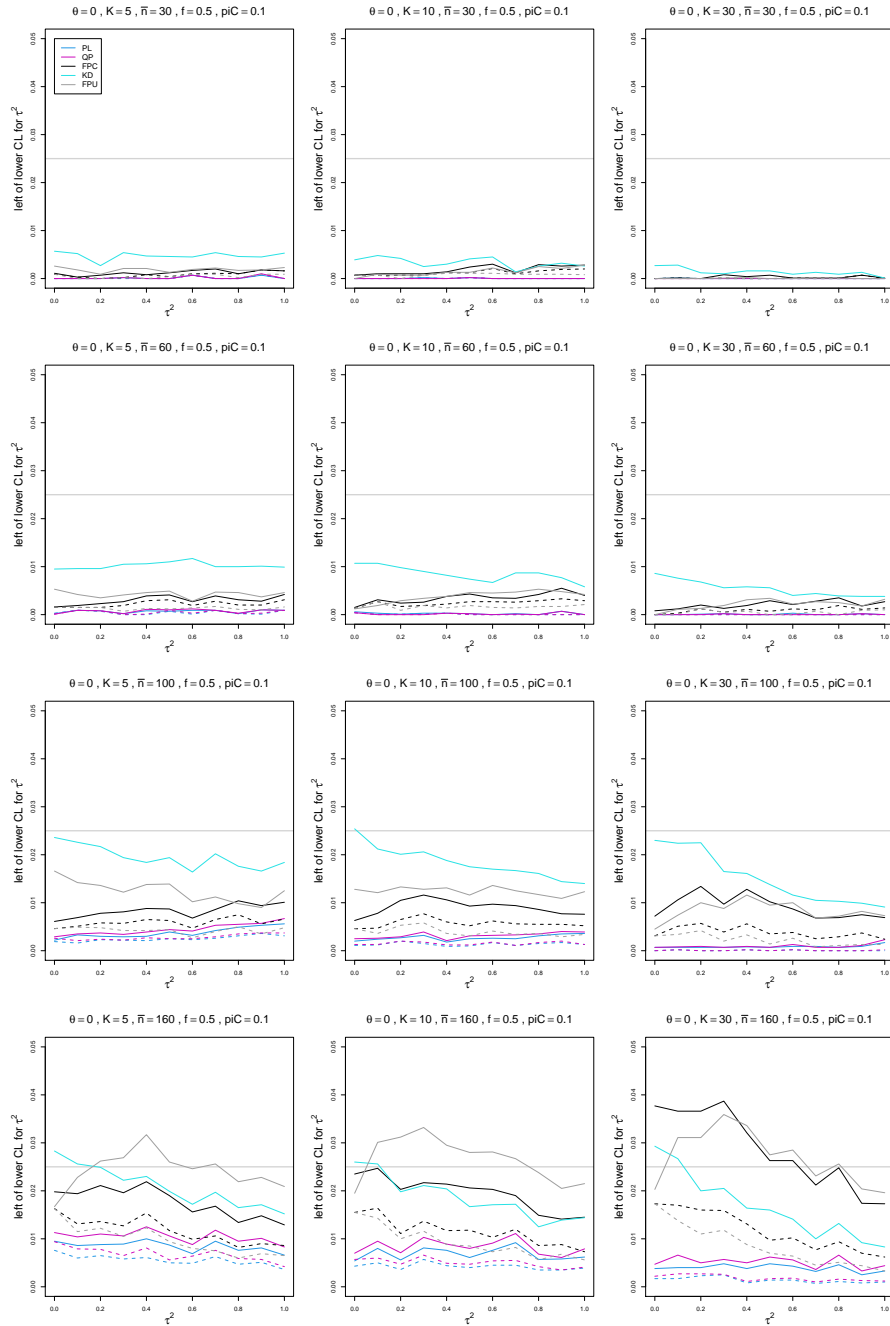


Figure D.2: Miss-left probability of PL, QP, KD, FPC, and FPU 95% confidence intervals for between-study variance of LOR vs τ^2 , for unequal sample sizes $\bar{n} = 30, 60, 100$ and 160 , $p_{iC} = .1$, $\theta = 0$ and $f = 0.5$. Solid lines: PL, QP, and FPC “only”, FPU model-based, and KD. Dashed lines: PL, QP, and FPC “always” and FPU naïve.

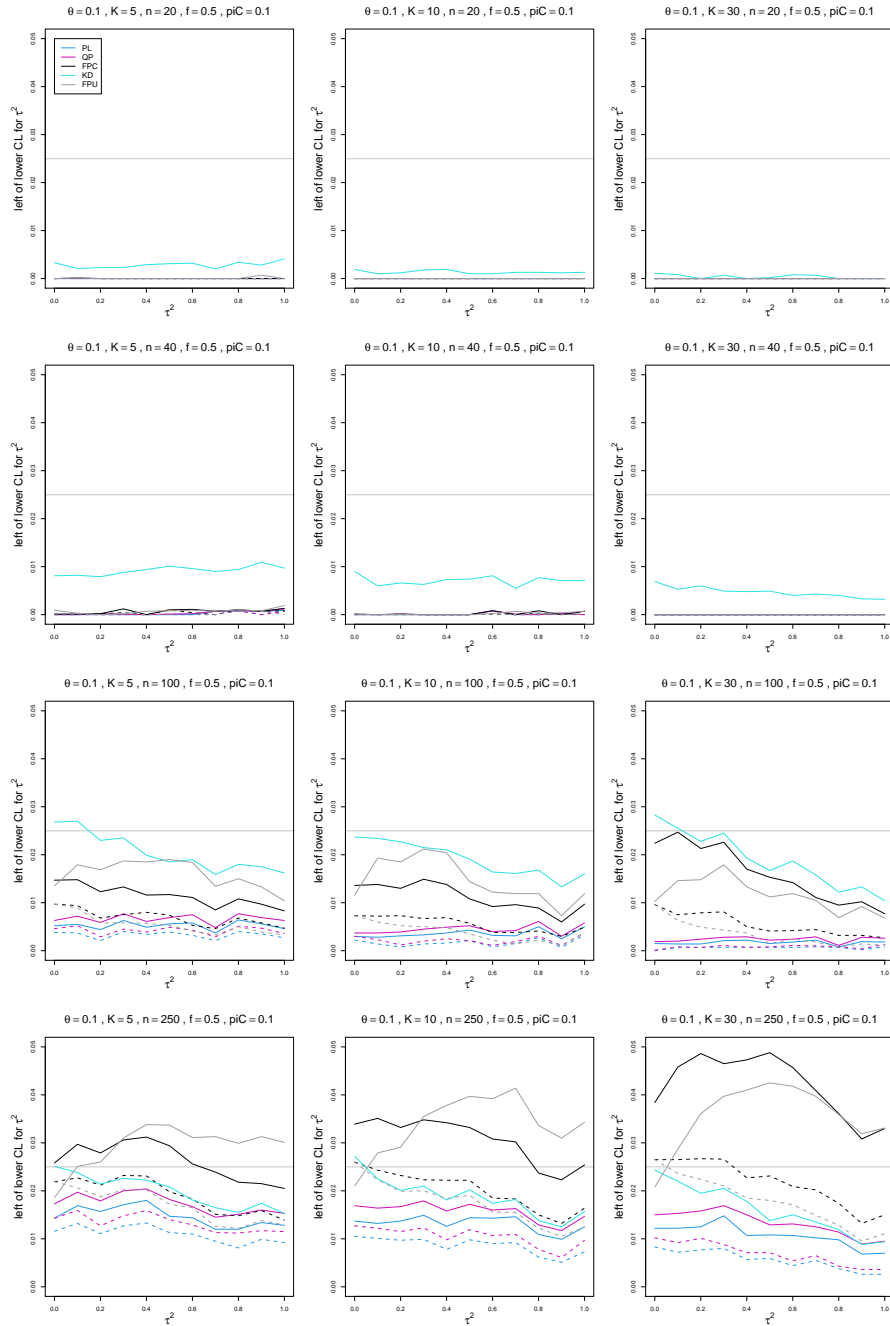


Figure D.3: Miss-left probability of PL, QP, KD, FPC, and FPU 95% confidence intervals for between-study variance of LOR vs τ^2 , for equal sample sizes $n = 20, 40, 100$ and 250 , $piC = .1$, $\theta = 0.1$ and $f = 0.5$. Solid lines: PL, QP, and FPC “only”, FPU model-based, and KD. Dashed lines: PL, QP, and FPC “always” and FPU naïve.

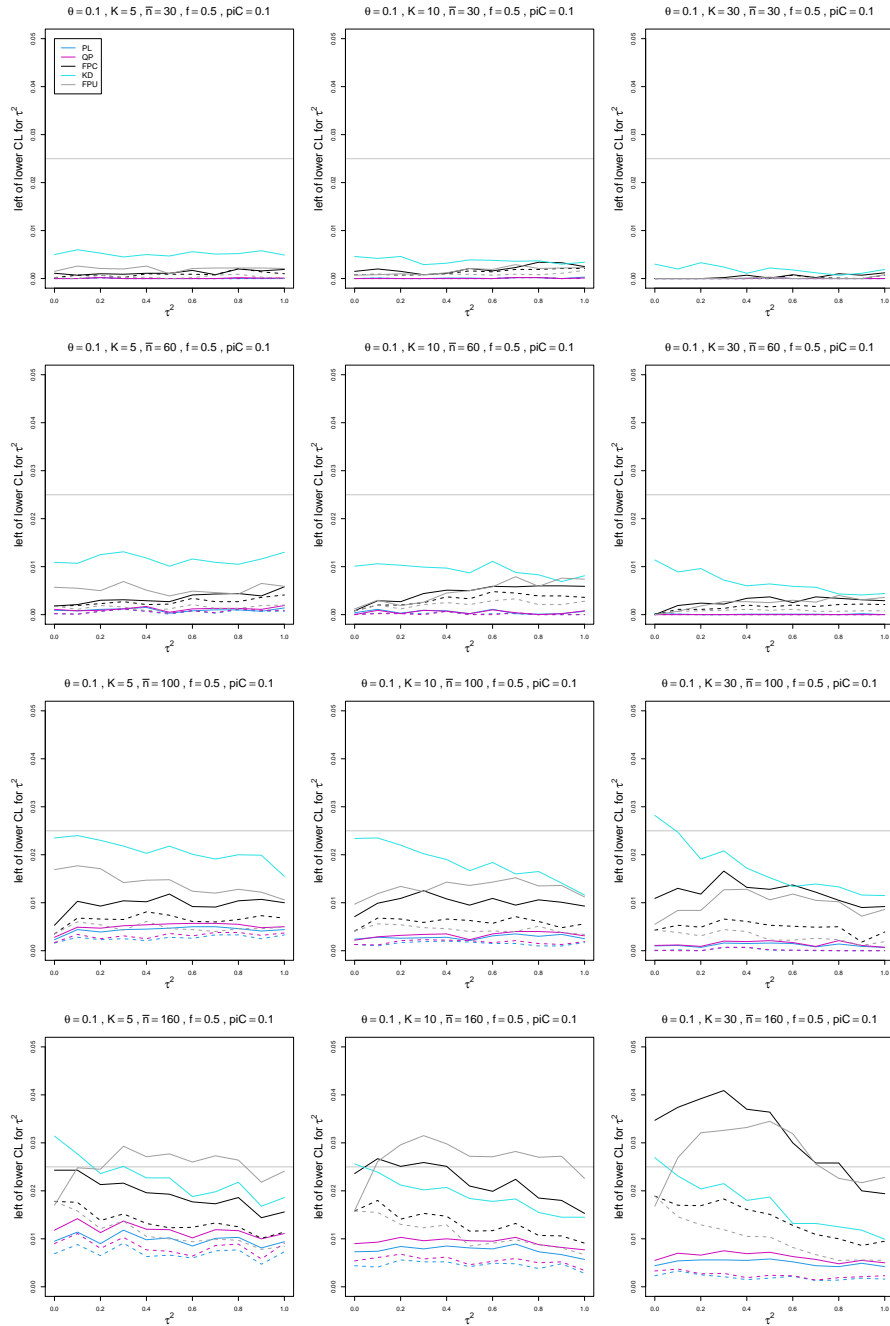


Figure D.4: Miss-left probability of PL, QP, KD, FPC, and FPU 95% confidence intervals for between-study variance of LOR vs τ^2 , for unequal sample sizes $\bar{n} = 30, 60, 100$ and 160 , $p_{iC} = .1$, $\theta = 0.1$ and $f = 0.5$. Solid lines: PL, QP, and FPC “only”, FPU model-based, and KD. Dashed lines: PL, QP, and FPC “always” and FPU naïve.

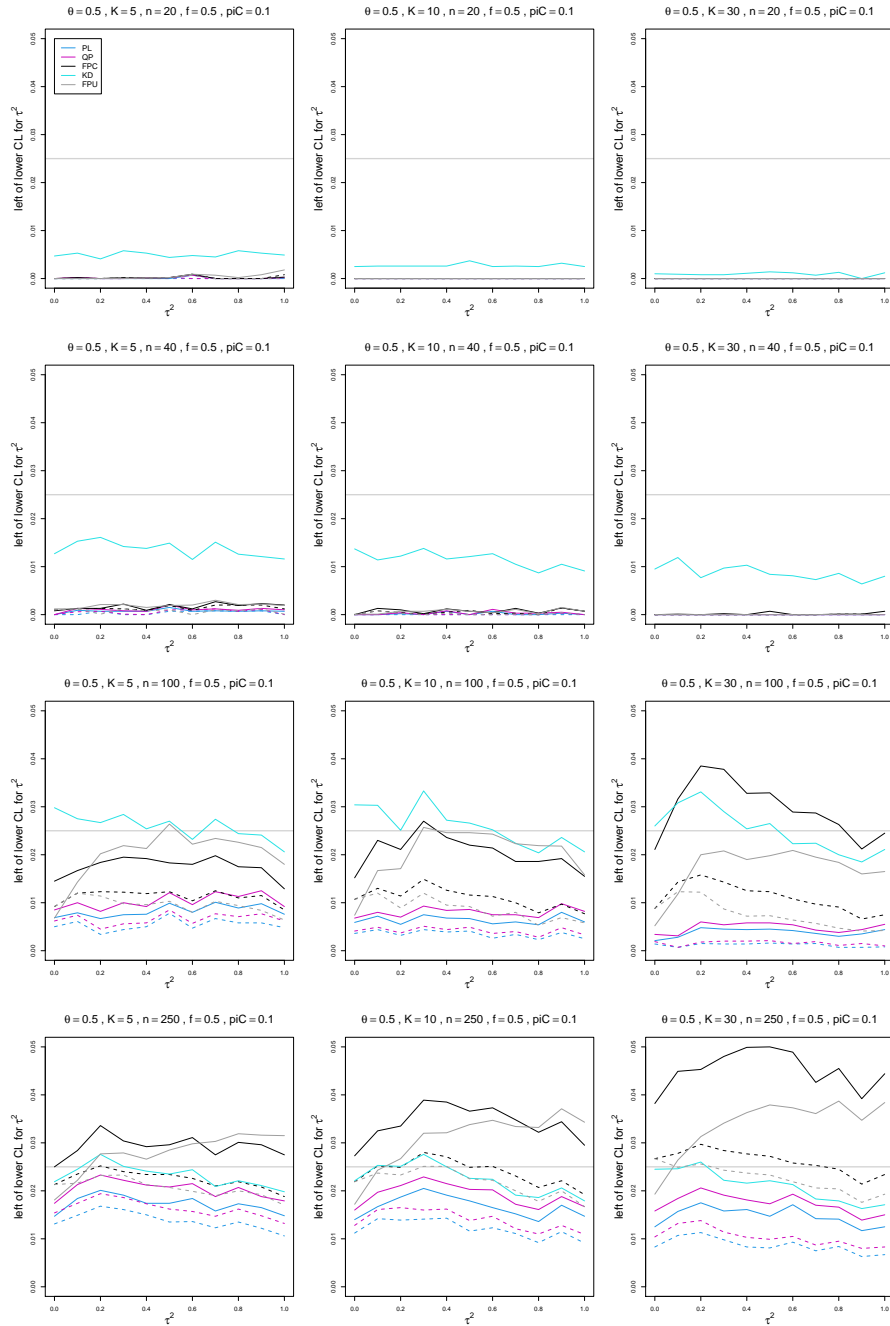


Figure D.5: Miss-left probability of PL, QP, KD, FPC, and FPU 95% confidence intervals for between-study variance of LOR vs τ^2 , for equal sample sizes $n = 20, 40, 100$ and 250 , $p_{iC} = .1$, $\theta = 0.5$ and $f = 0.5$. Solid lines: PL, QP, and FPC “only”, FPU model-based, and KD. Dashed lines: PL, QP, and FPC “always” and FPU naïve.

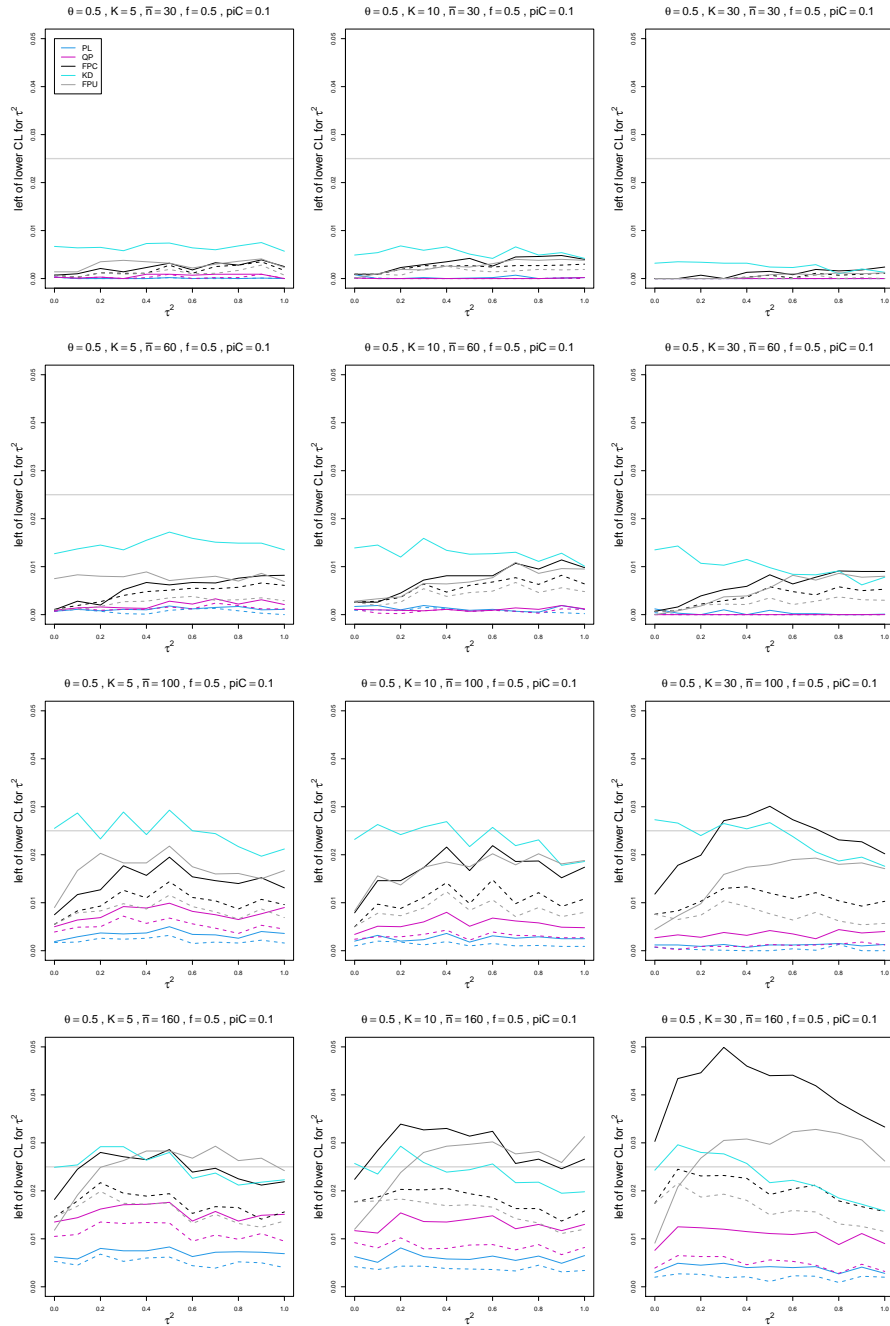


Figure D.6: Miss-left probability of PL, QP, KD, FPC, and FPU 95% confidence intervals for between-study variance of LOR vs τ^2 , for unequal sample sizes $\bar{n} = 30, 60, 100$ and 160 , $p_{iC} = .1$, $\theta = 0.5$ and $f = 0.5$. Solid lines: PL, QP, and FPC “only”, FPU model-based, and KD. Dashed lines: PL, QP, and FPC “always” and FPU naïve.

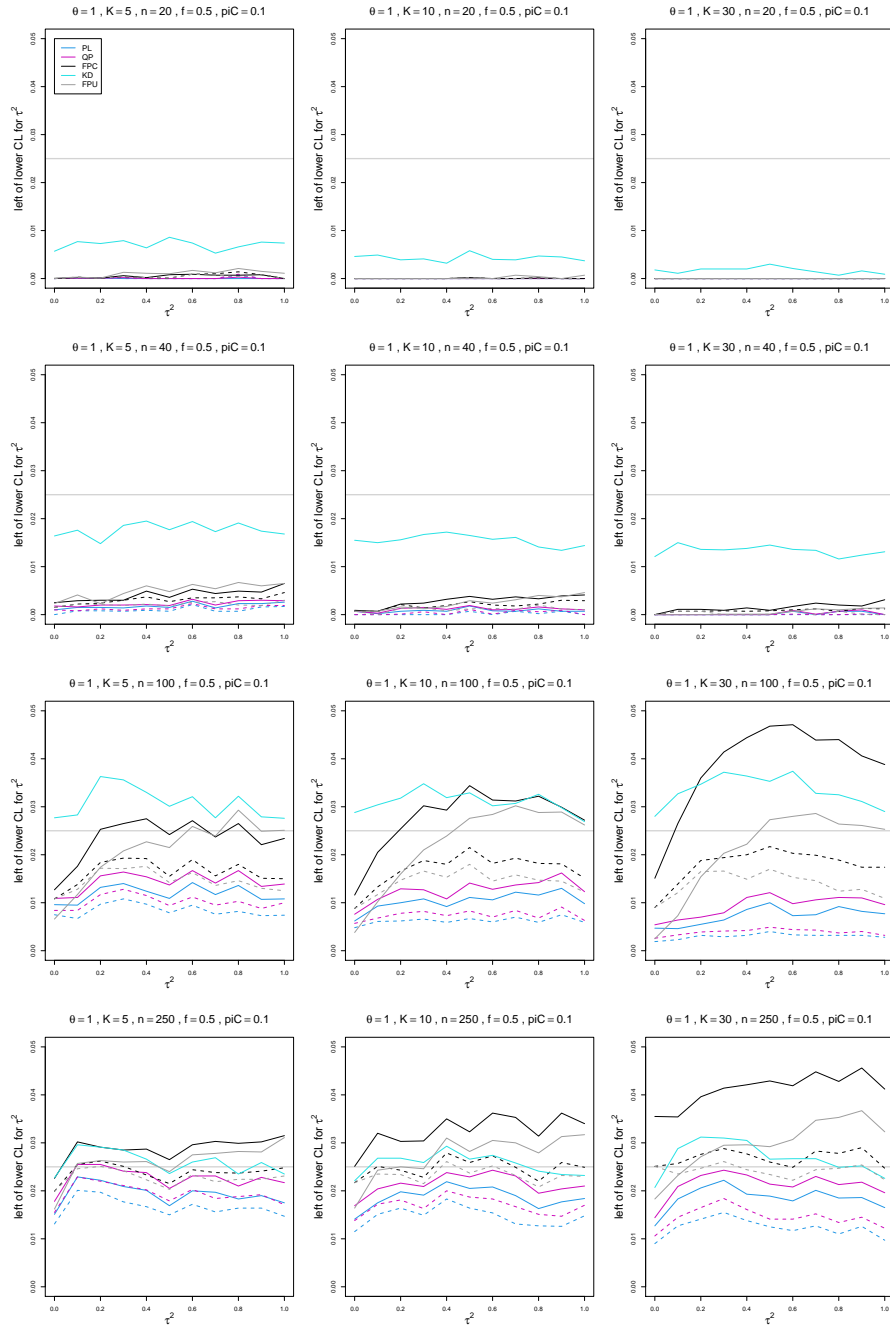


Figure D.7: Miss-left probability of PL, QP, KD, FPC, and FPU 95% confidence intervals for between-study variance of LOR vs τ^2 , for equal sample sizes $n = 20, 40, 100$ and 250 , $p_{iC} = .1$, $\theta = 1$ and $f = 0.5$. Solid lines: PL, QP, and FPC “only”, FPU model-based, and KD. Dashed lines: PL, QP, and FPC “always” and FPU naïve.

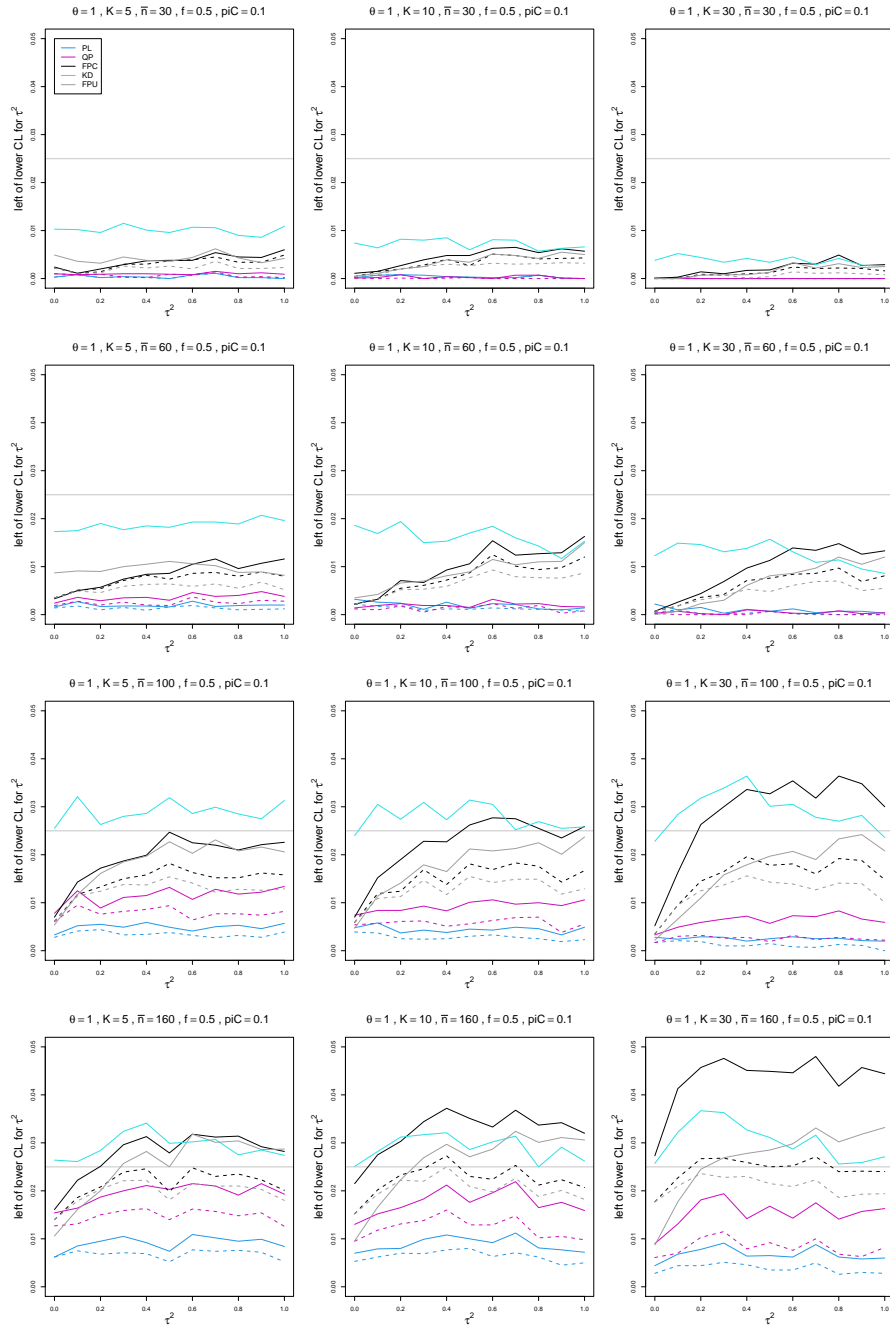


Figure D.8: Miss-left probability of PL, QP, KD, FPC, and FPU 95% confidence intervals for between-study variance of LOR vs τ^2 , for unequal sample sizes $\bar{n} = 30, 60, 100$ and 160 , $p_{iC} = .1$, $\theta = 1$ and $f = 0.5$. Solid lines: PL, QP, and FPC “only”, FPU model-based, and KD. Dashed lines: PL, QP, and FPC “always” and FPU naïve.

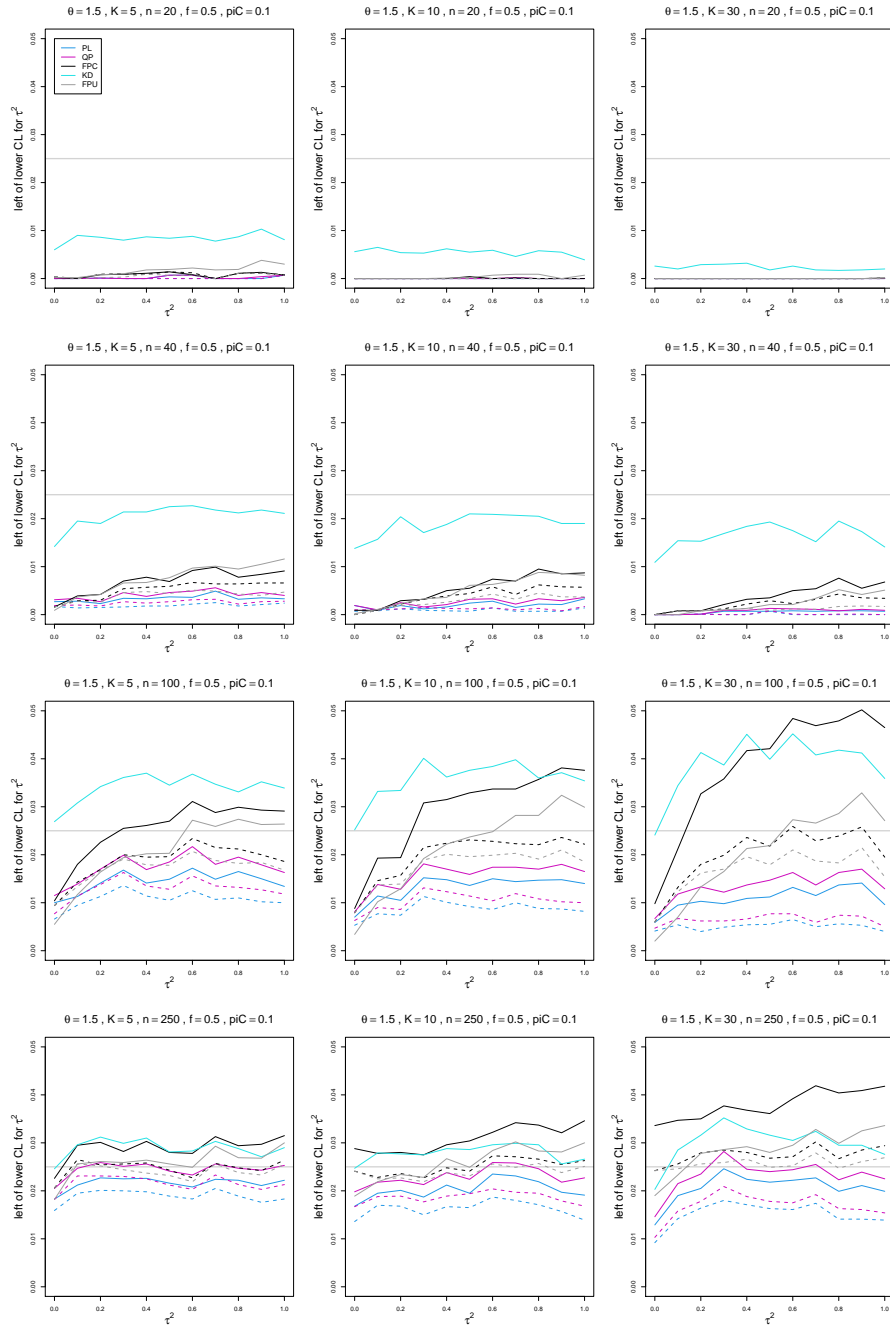


Figure D.9: Miss-left probability of PL, QP, KD, FPC, and FPU 95% confidence intervals for between-study variance of LOR vs τ^2 , for equal sample sizes $n = 20, 40, 100$ and 250 , $p_{iC} = .1$, $\theta = 1.5$ and $f = 0.5$. Solid lines: PL, QP, and FPC “only”, FPU model-based, and KD. Dashed lines: PL, QP, and FPC “always” and FPU naïve.

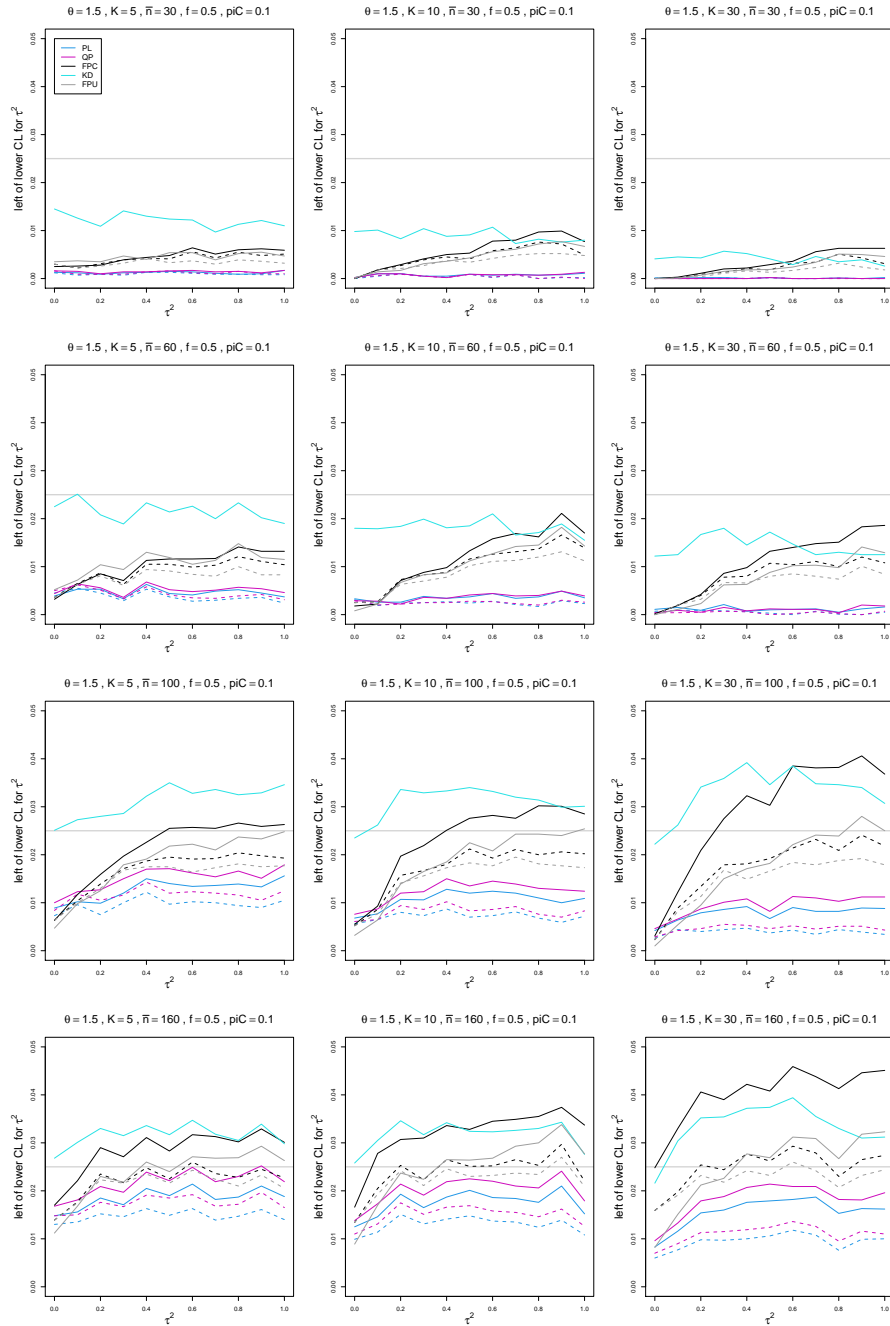


Figure D.10: Miss-left probability of PL, QP, KD, FPC, and FPU 95% confidence intervals for between-study variance of LOR vs τ^2 , for unequal sample sizes $\bar{n} = 30, 60, 100$ and 160 , $piC = .1$, $\theta = 1.5$ and $f = 0.5$. Solid lines: PL, QP, and FPC “only”, FPU model-based, and KD. Dashed lines: PL, QP, and FPC “always” and FPU naïve.

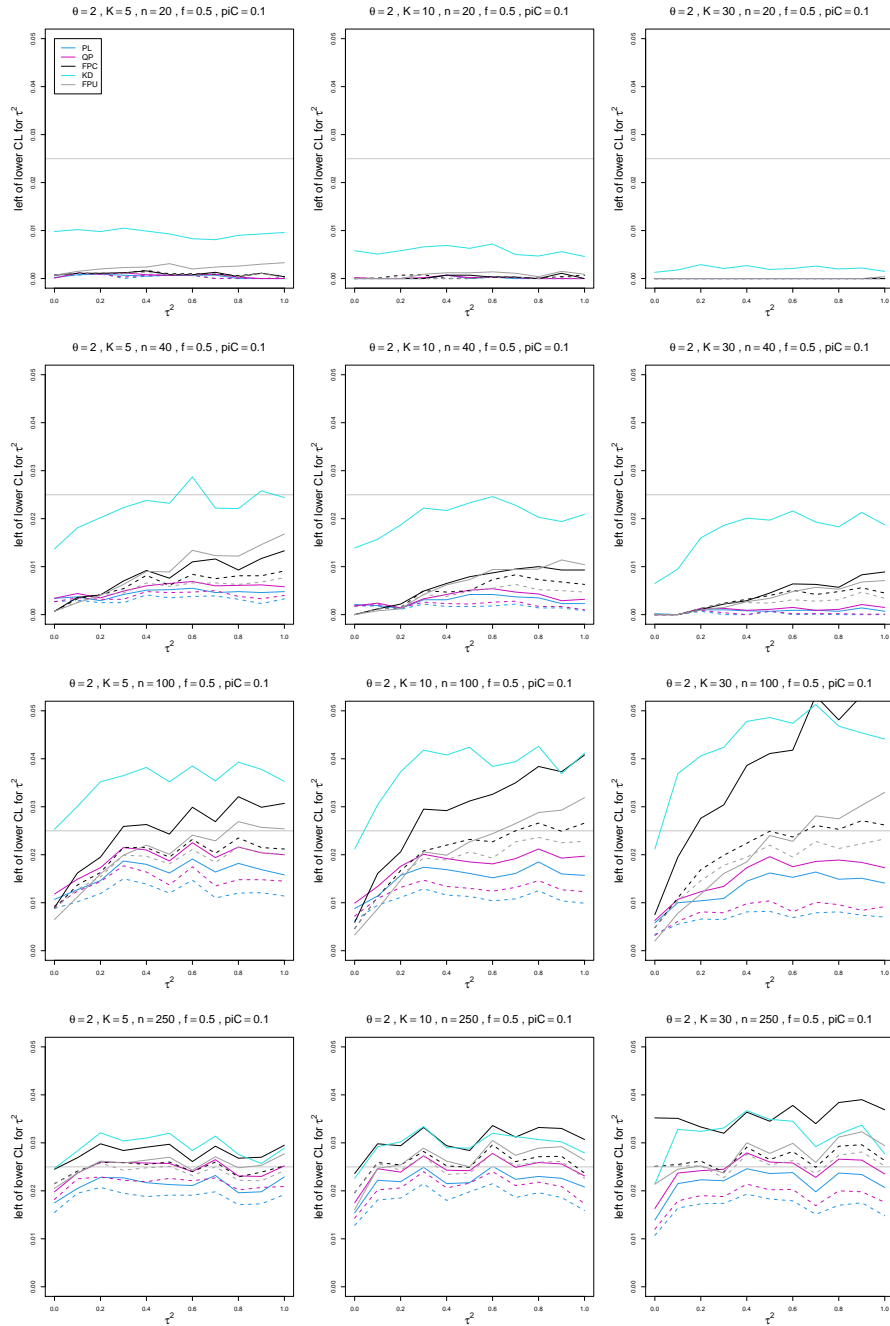


Figure D.11: Miss-left probability of PL, QP, KD, FPC, and FPU 95% confidence intervals for between-study variance of LOR vs τ^2 , for equal sample sizes $n = 20, 40, 100$ and 250 , $p_{iC} = .1$, $\theta = 2$ and $f = 0.5$. Solid lines: PL, QP, and FPC “only”, FPU model-based, and KD. Dashed lines: PL, QP, and FPC “always” and FPU naïve.

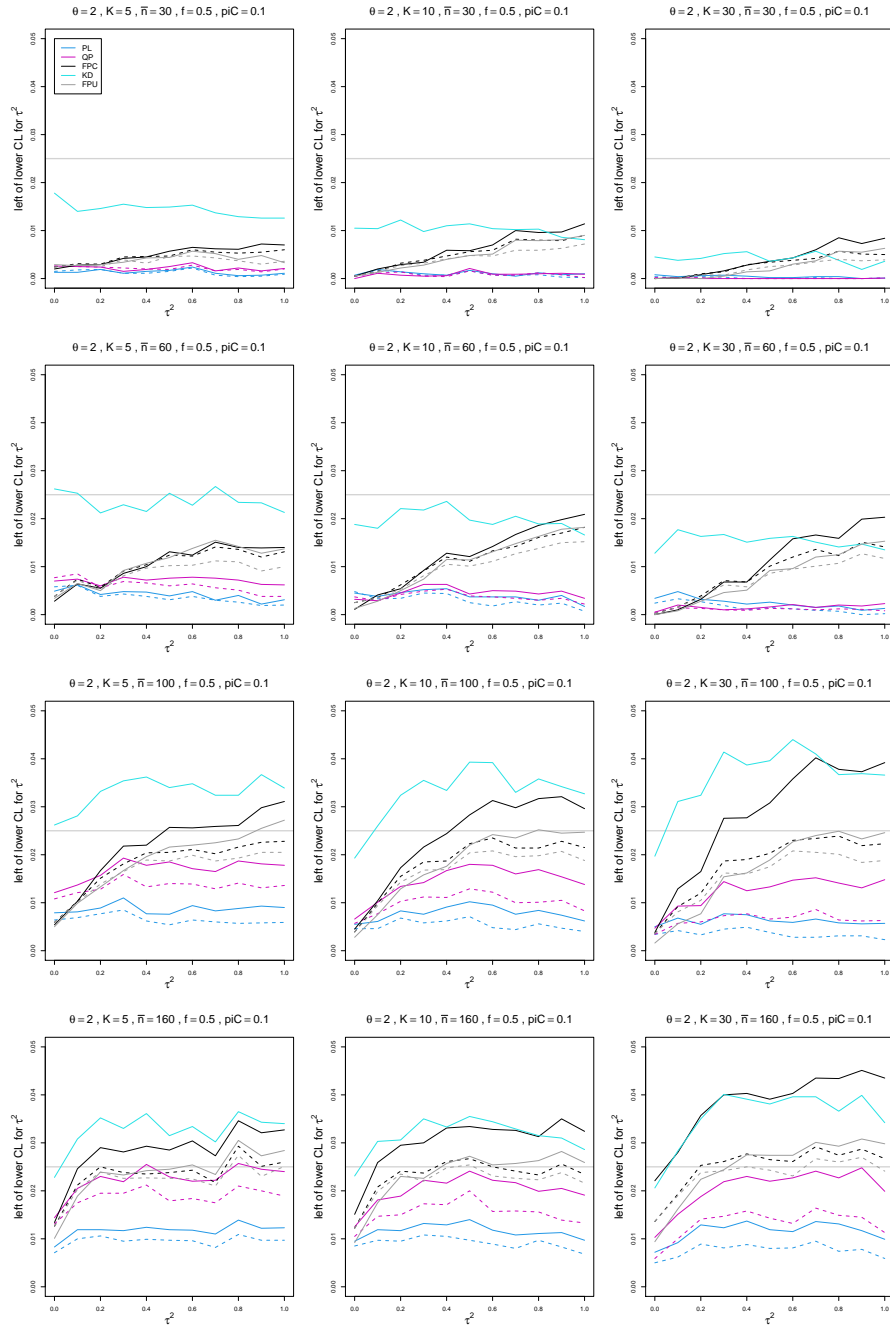


Figure D.12: Miss-left probability of PL, QP, KD, FPC, and FPU 95% confidence intervals for between-study variance of LOR vs τ^2 , for unequal sample sizes $\bar{n} = 30, 60, 100$ and 160 , $p_{iC} = .1$, $\theta = 2$ and $f = 0.5$. Solid lines: PL, QP, and FPC “only”, FPU model-based, and KD. Dashed lines: PL, QP, and FPC “always” and FPU naïve.

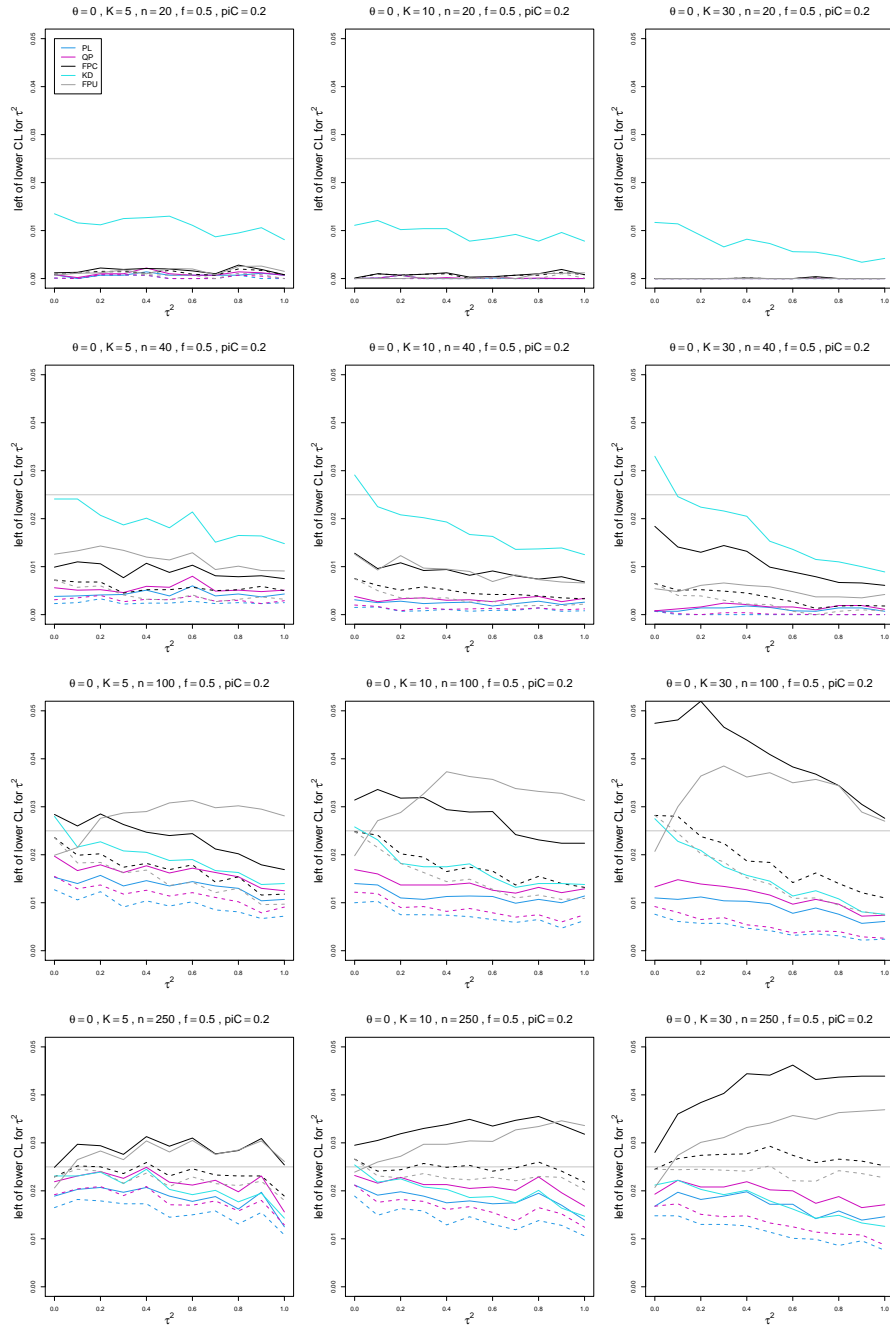


Figure D.13: Miss-left probability of PL, QP, KD, FPC, and FPU 95% confidence intervals for between-study variance of LOR vs τ^2 , for equal sample sizes $n = 20, 40, 100$ and 250 , $p_{iC} = .2$, $\theta = 0$ and $f = 0.5$. Solid lines: PL, QP, and FPC “only”, FPU model-based, and KD. Dashed lines: PL, QP, and FPC “always” and FPU naïve.

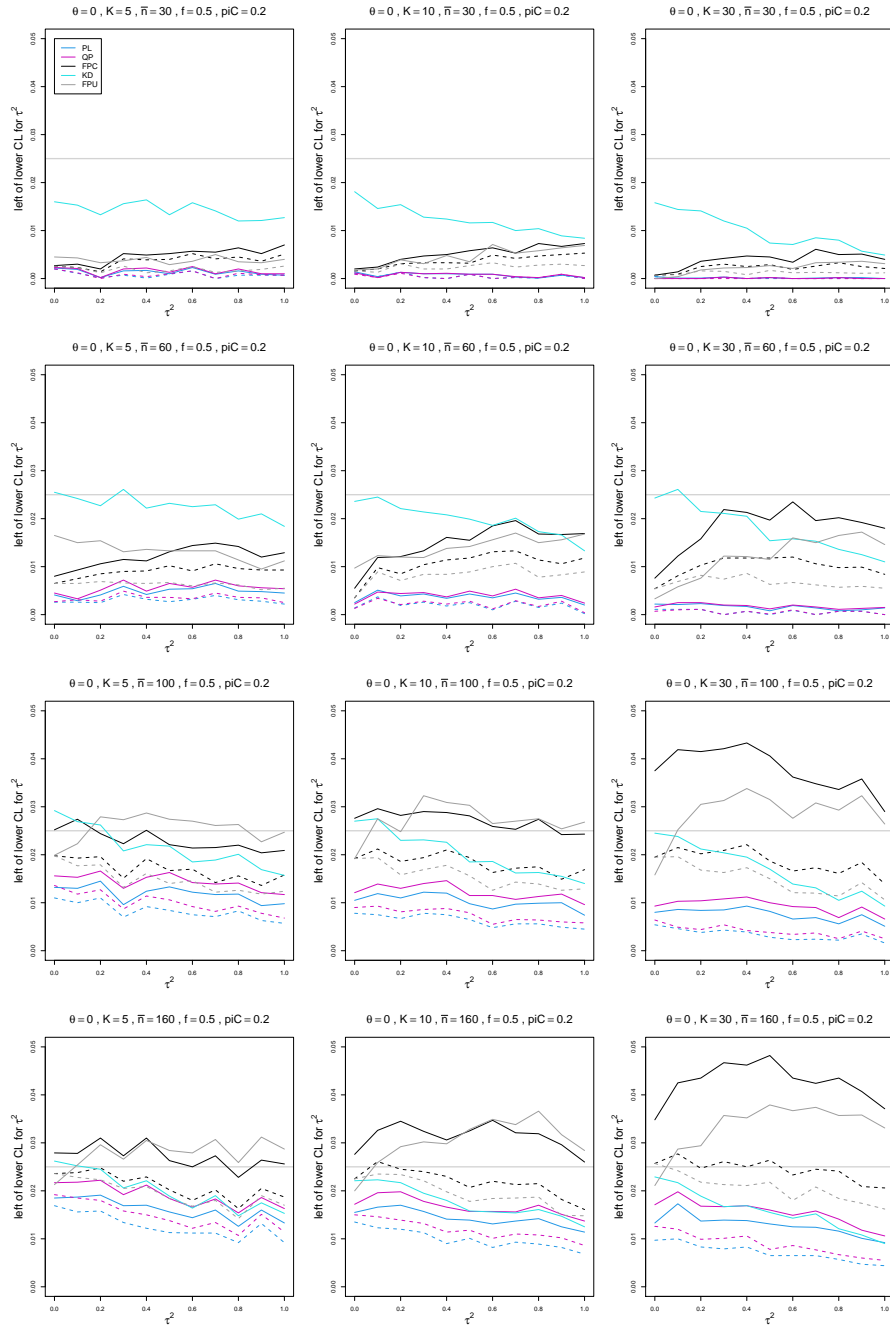


Figure D.14: Miss-left probability of PL, QP, KD, FPC, and FPU 95% confidence intervals for between-study variance of LOR vs τ^2 , for unequal sample sizes $\bar{n} = 30, 60, 100$ and 160 , $p_{iC} = .2$, $\theta = 0$ and $f = 0.5$. Solid lines: PL, QP, and FPC “only”, FPU model-based, and KD. Dashed lines: PL, QP, and FPC “always” and FPU naïve.

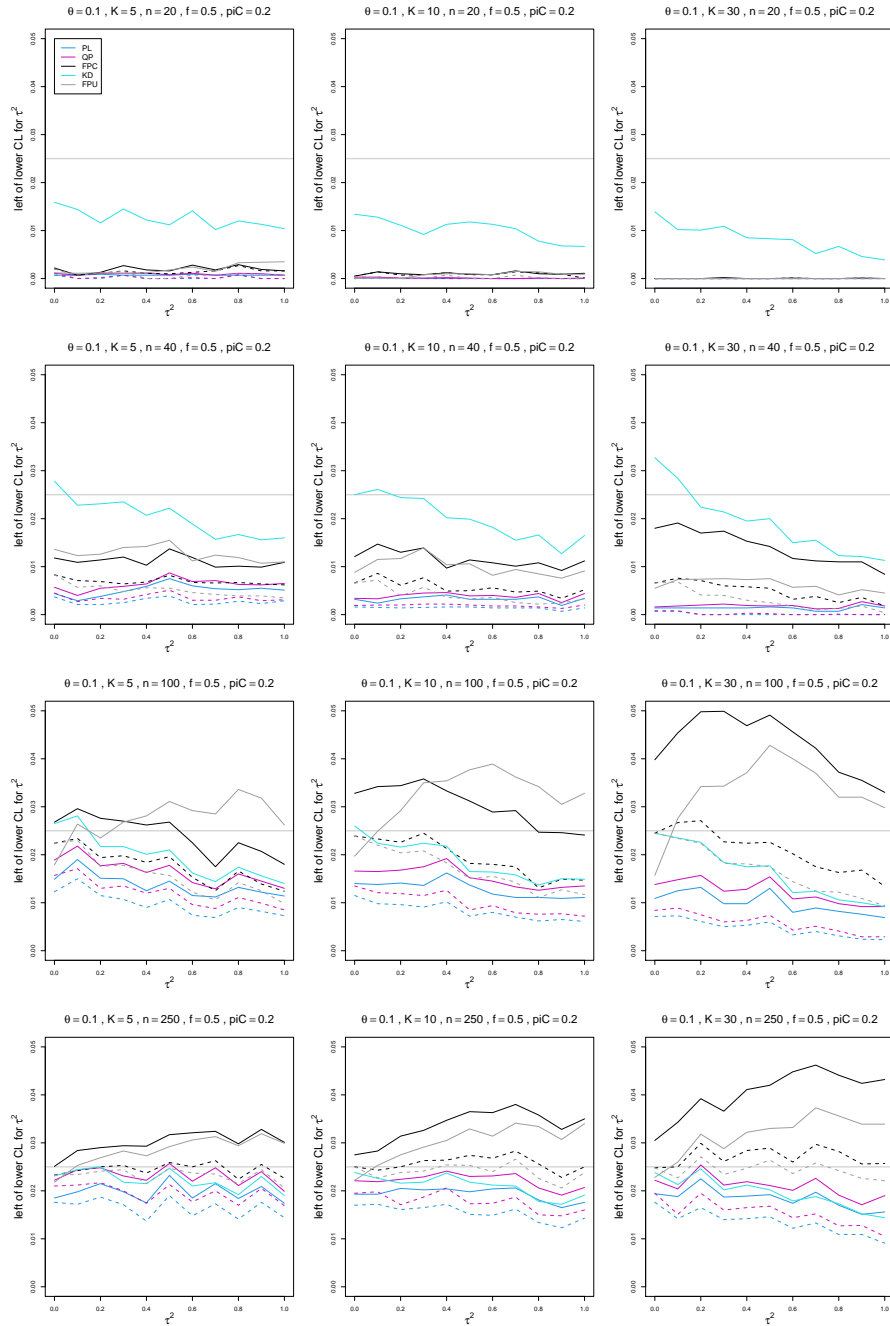


Figure D.15: Miss-left probability of PL, QP, KD, FPC, and FPU 95% confidence intervals for between-study variance of LOR vs τ^2 , for equal sample sizes $n = 20, 40, 100$ and 250 , $p_{iC} = .2$, $\theta = 0.1$ and $f = 0.5$. Solid lines: PL, QP, and FPC “only”, FPU model-based, and KD. Dashed lines: PL, QP, and FPC “always” and FPU naïve.

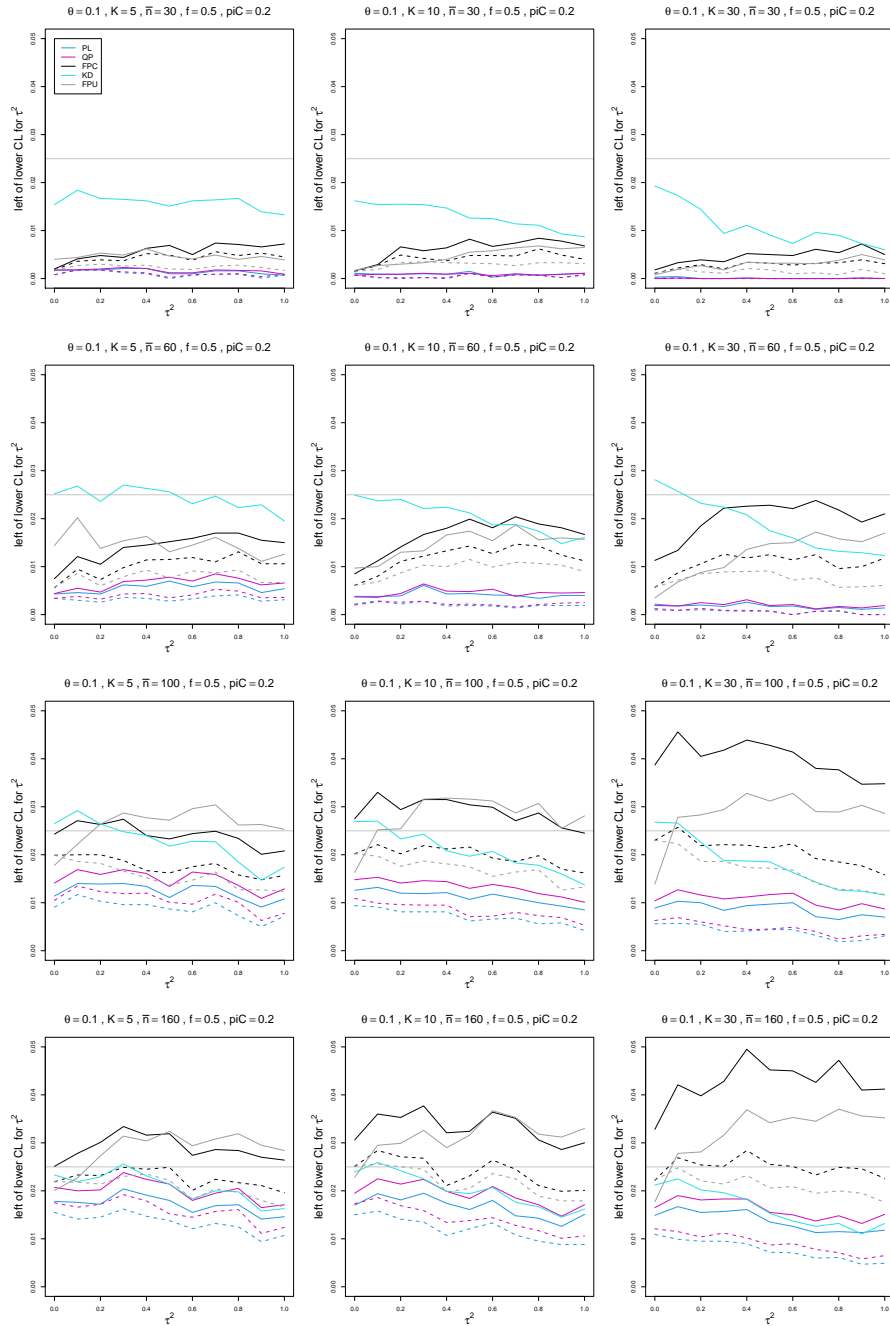


Figure D.16: Miss-left probability of PL, QP, KD, FPC, and FPU 95% confidence intervals for between-study variance of LOR vs τ^2 , for unequal sample sizes $\bar{n} = 30, 60, 100$ and 160 , $p_{iC} = .2$, $\theta = 0.1$ and $f = 0.5$. Solid lines: PL, QP, and FPC “only”, FPU model-based, and KD. Dashed lines: PL, QP, and FPC “always” and FPU naïve.

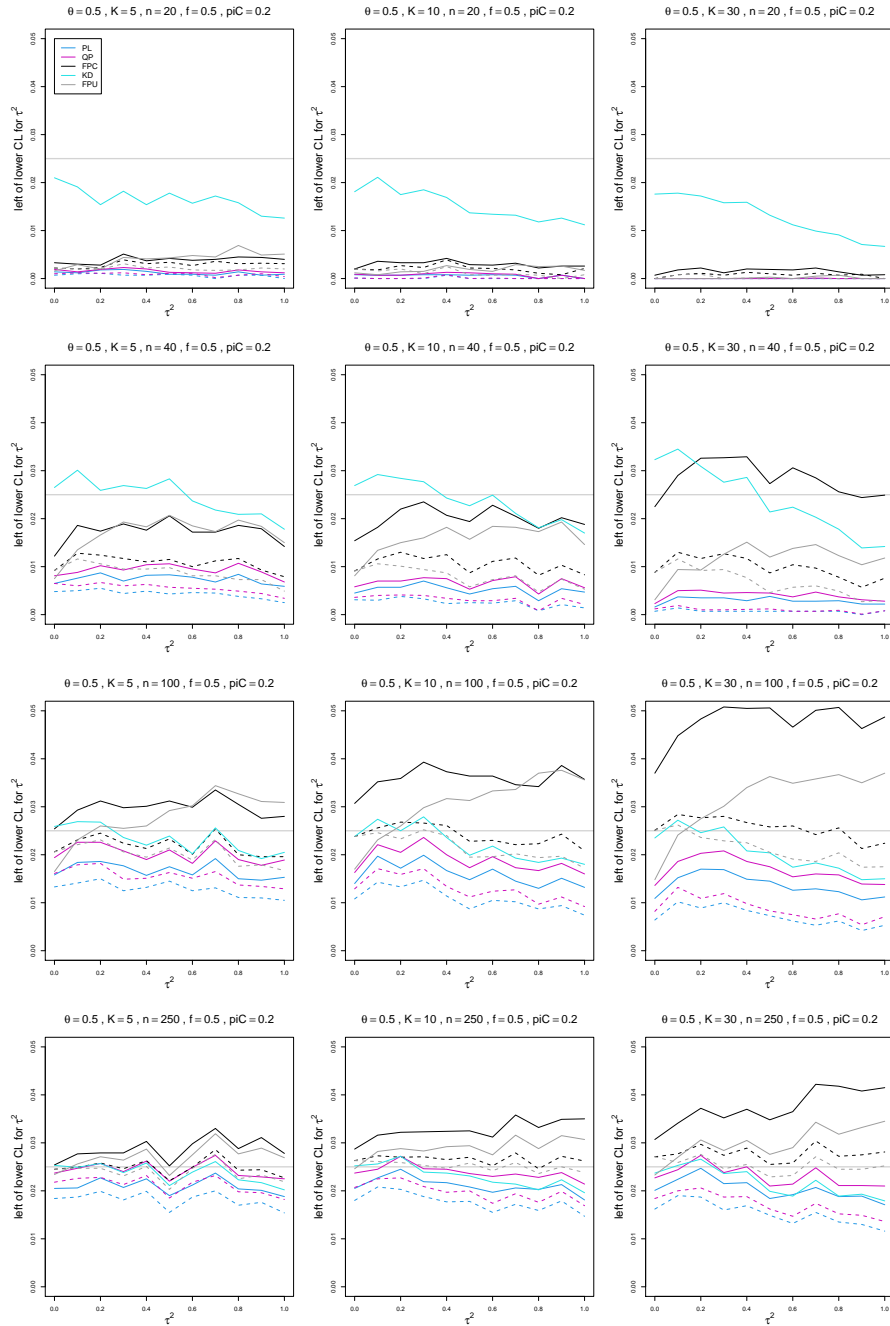


Figure D.17: Miss-left probability of PL, QP, KD, FPC, and FPU 95% confidence intervals for between-study variance of LOR vs τ^2 , for equal sample sizes $n = 20, 40, 100$ and 250 , $p_{iC} = .2$, $\theta = 0.5$ and $f = 0.5$. Solid lines: PL, QP, and FPC “only”, FPU model-based, and KD. Dashed lines: PL, QP, and FPC “always” and FPU naïve.

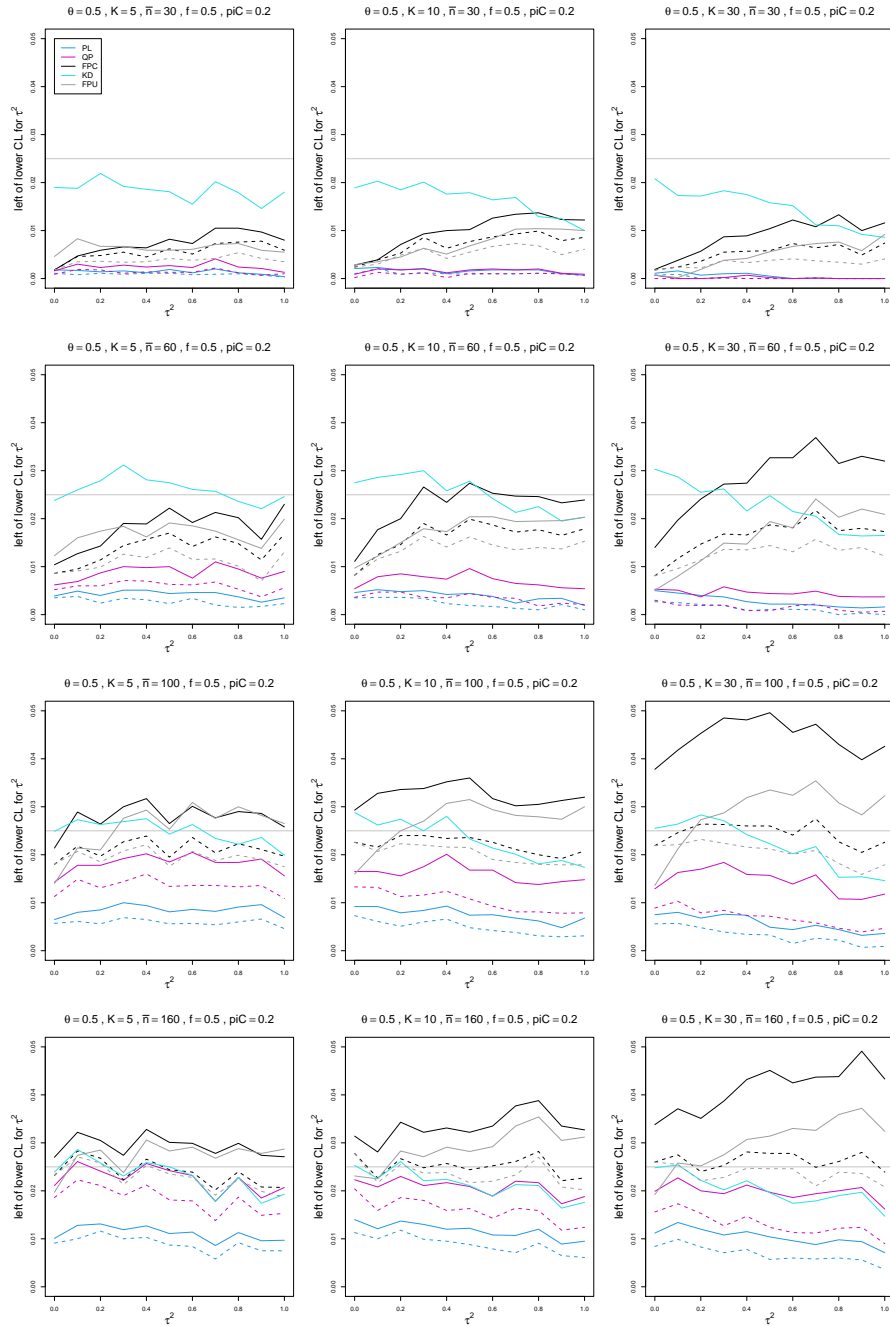


Figure D.18: Miss-left probability of PL, QP, KD, FPC, and FPU 95% confidence intervals for between-study variance of LOR vs τ^2 , for unequal sample sizes $\bar{n} = 30, 60, 100$ and 160 , $\pi C = .2$, $\theta = 0.5$ and $f = 0.5$. Solid lines: PL, QP, and FPC “only”, FPU model-based, and KD. Dashed lines: PL, QP, and FPC “always” and FPU naïve.

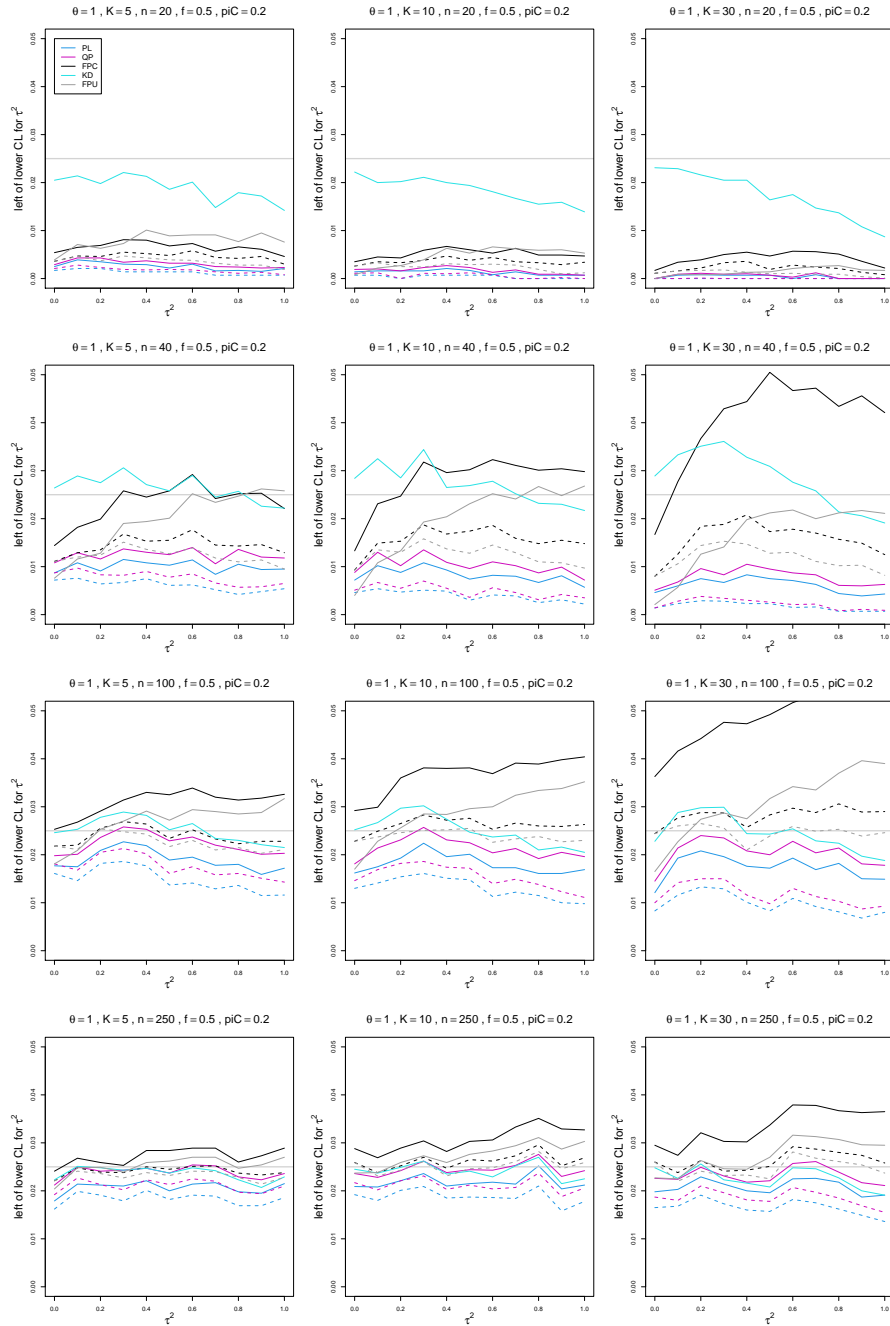


Figure D.19: Miss-left probability of PL, QP, KD, FPC, and FPU 95% confidence intervals for between-study variance of LOR vs τ^2 , for equal sample sizes $n = 20, 40, 100$ and 250 , $p_{iC} = .2$, $\theta = 1$ and $f = 0.5$. Solid lines: PL, QP, and FPC “only”, FPU model-based, and KD. Dashed lines: PL, QP, and FPC “always” and FPU naïve.

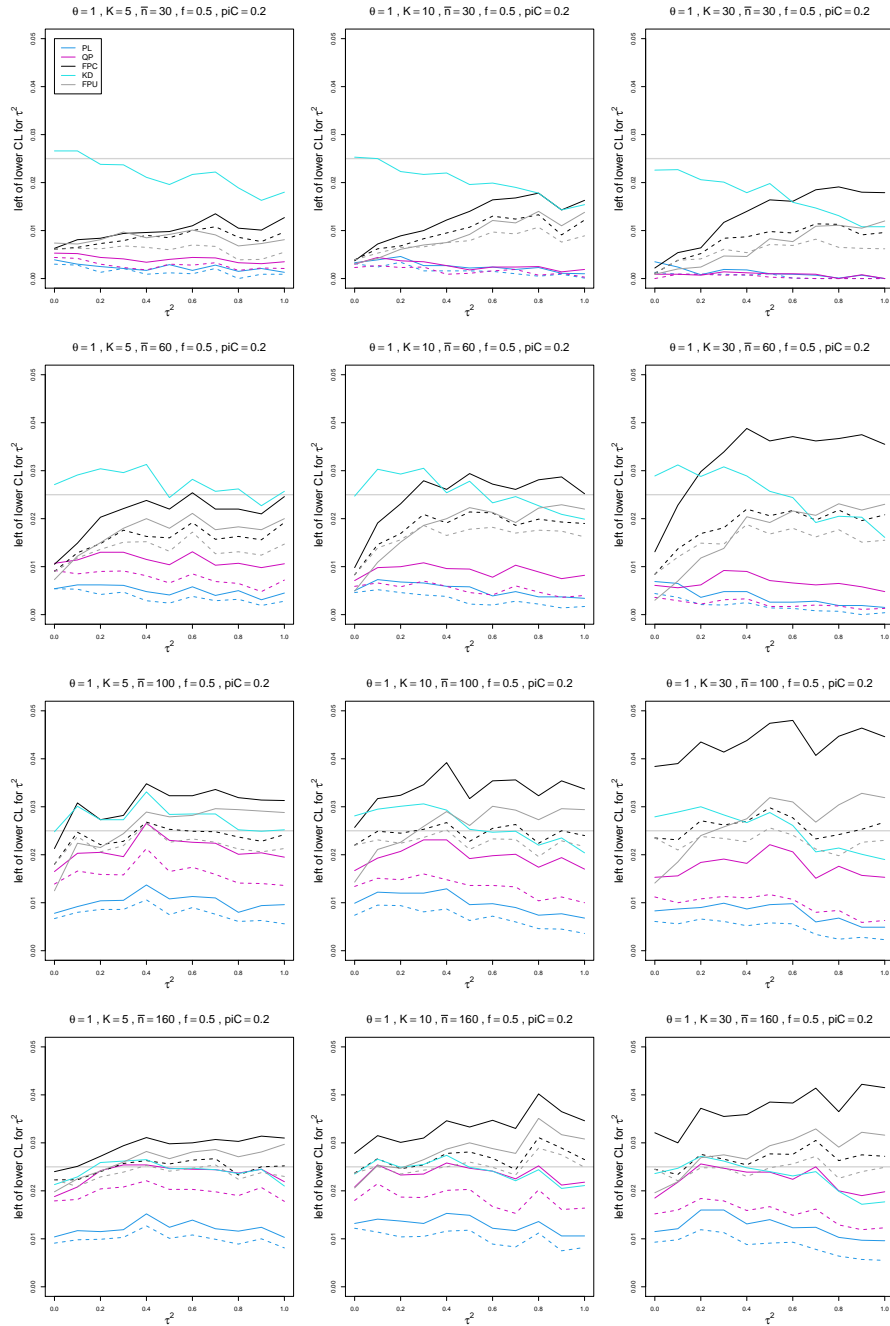


Figure D.20: Miss-left probability of PL, QP, KD, FPC, and FPU 95% confidence intervals for between-study variance of LOR vs τ^2 , for unequal sample sizes $\bar{n} = 30, 60, 100$ and 160 , $p_{iC} = .2$, $\theta = 1$ and $f = 0.5$. Solid lines: PL, QP, and FPC “only”, FPU model-based, and KD. Dashed lines: PL, QP, and FPC “always” and FPU naïve.

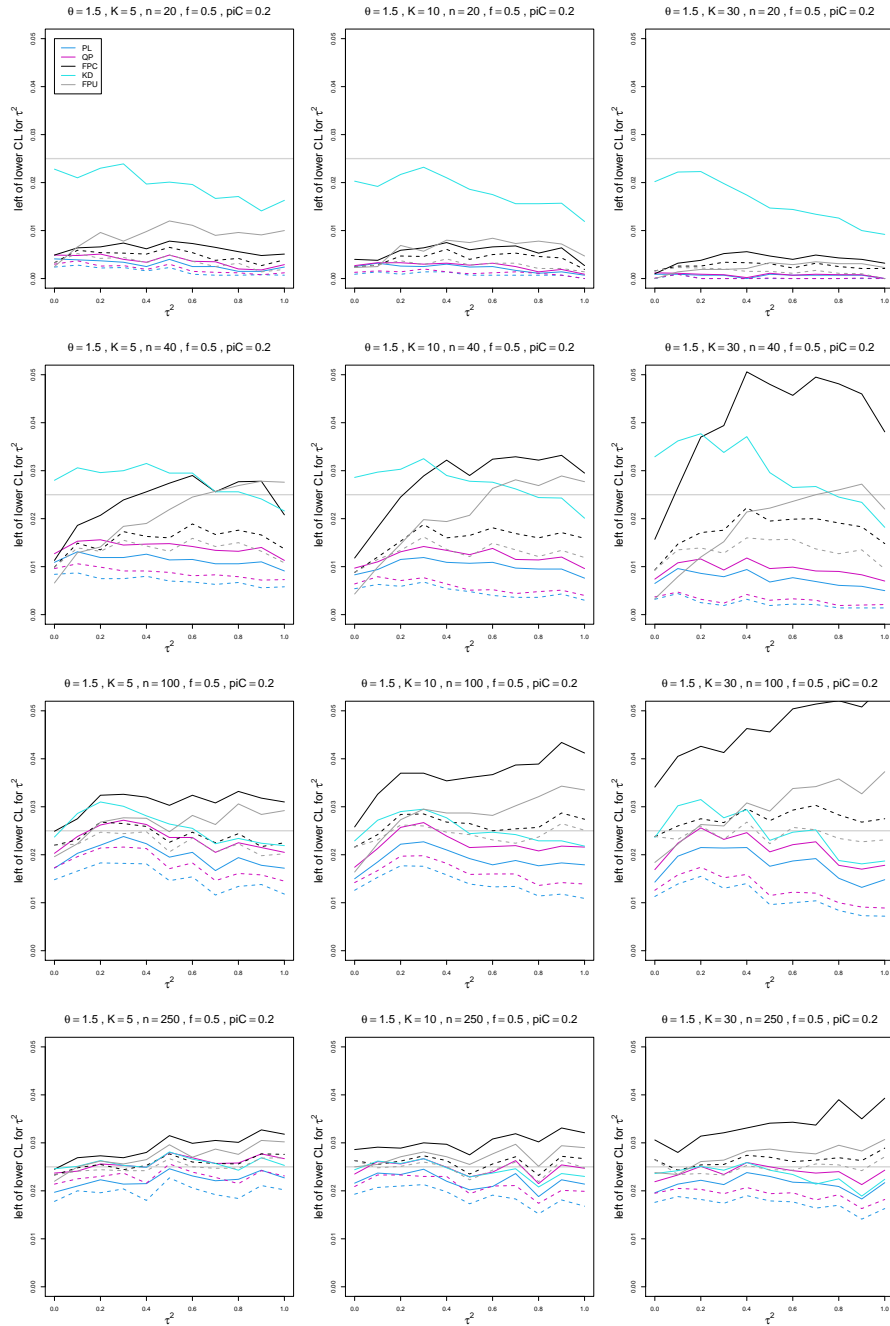


Figure D.21: Miss-left probability of PL, QP, KD, FPC, and FPU 95% confidence intervals for between-study variance of LOR vs τ^2 , for equal sample sizes $n = 20, 40, 100$ and 250 , $p_{iC} = .2$, $\theta = 1.5$ and $f = 0.5$. Solid lines: PL, QP, and FPC “only”, FPU model-based, and KD. Dashed lines: PL, QP, and FPC “always” and FPU naïve.

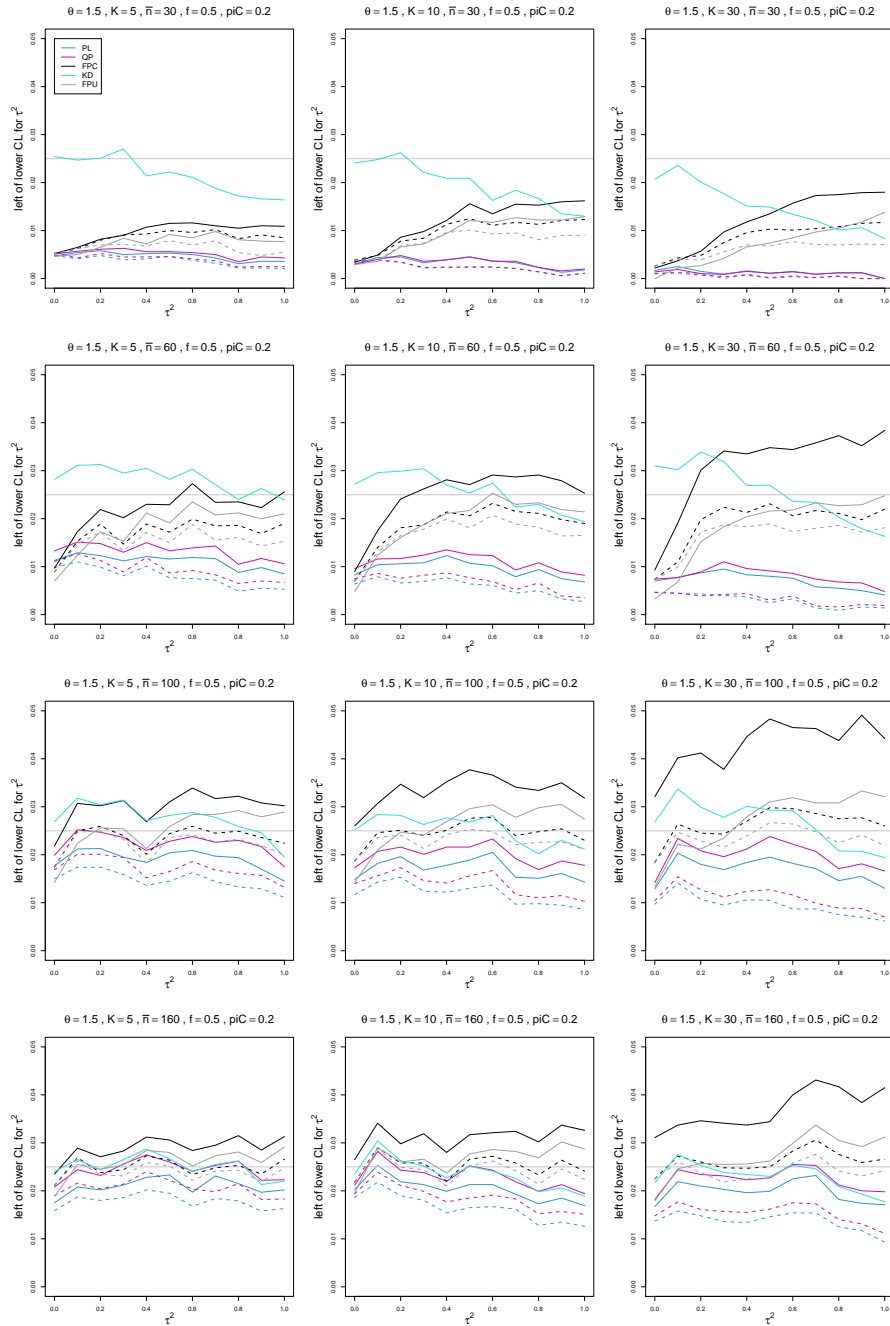


Figure D.22: Miss-left probability of PL, QP, KD, FPC, and FPU 95% confidence intervals for between-study variance of LOR vs τ^2 , for unequal sample sizes $\bar{n} = 30, 60, 100$ and 160 , $piC = .2$, $\theta = 1.5$ and $f = 0.5$. Solid lines: PL, QP, and FPC “only”, FPU model-based, and KD. Dashed lines: PL, QP, and FPC “always” and FPU naïve.

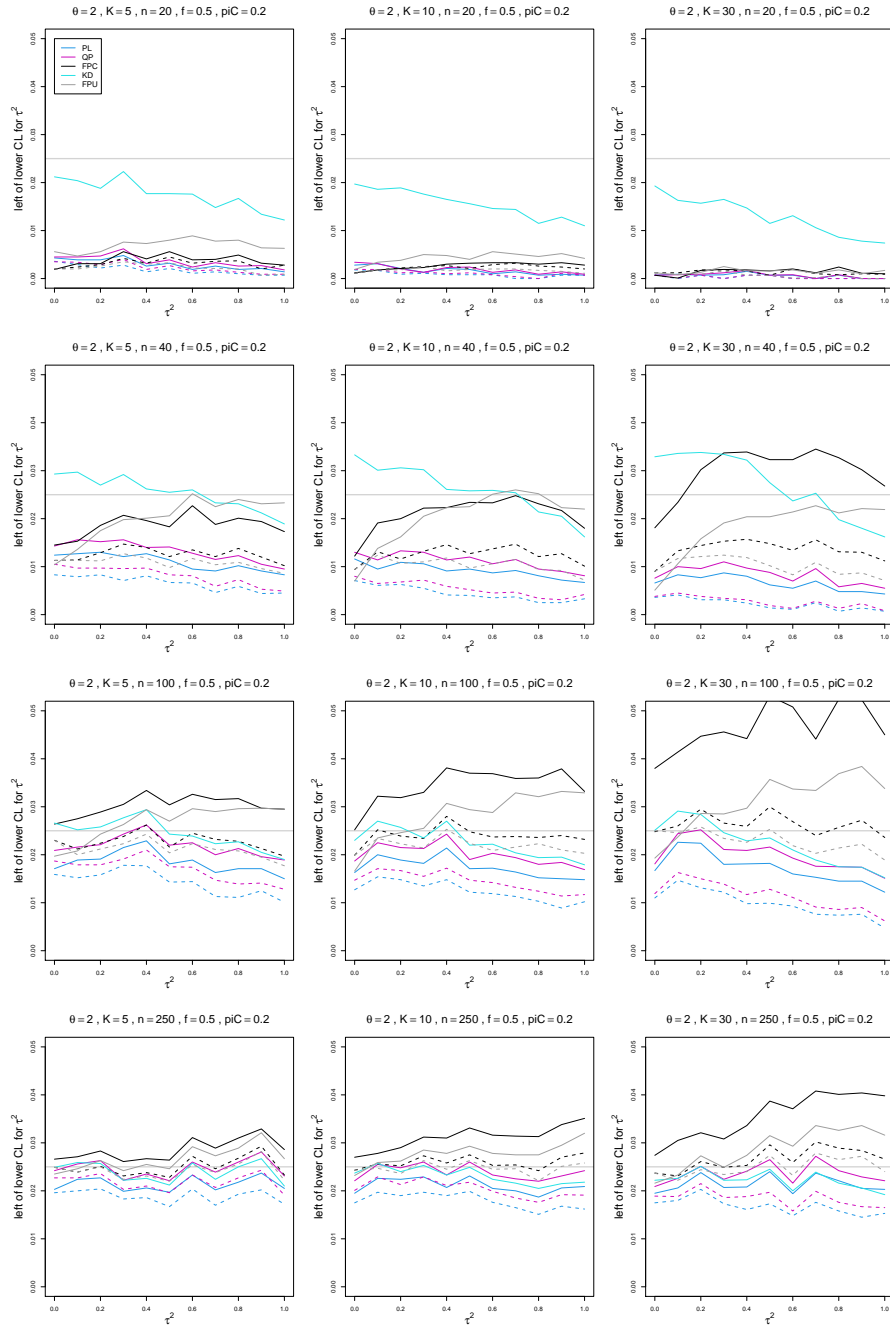


Figure D.23: Miss-left probability of PL, QP, KD, FPC, and FPU 95% confidence intervals for between-study variance of LOR vs τ^2 , for equal sample sizes $n = 20, 40, 100$ and 250 , $p_{iC} = .2$, $\theta = 2$ and $f = 0.5$. Solid lines: PL, QP, and FPC “only”, FPU model-based, and KD. Dashed lines: PL, QP, and FPC “always” and FPU naïve.

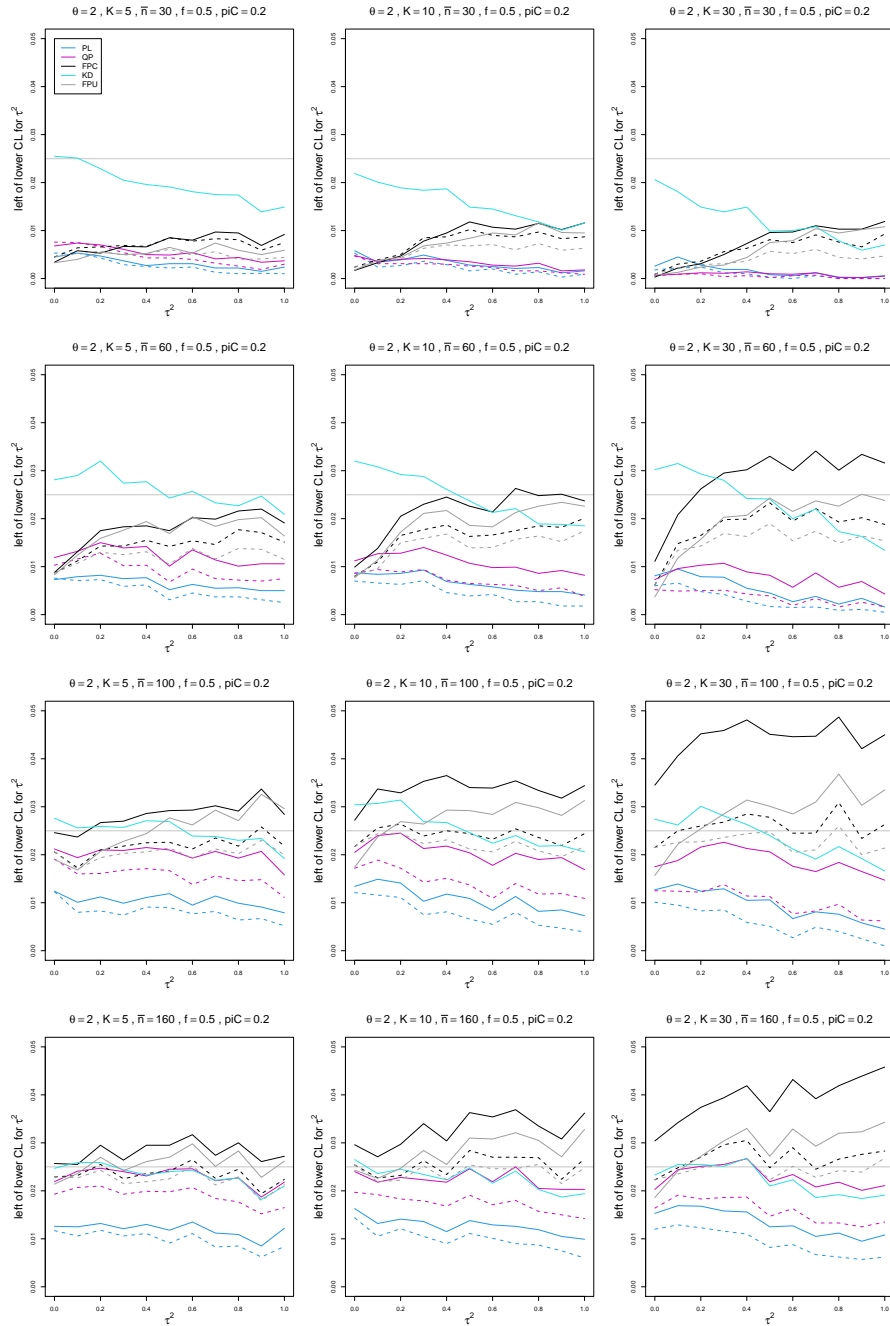


Figure D.24: Miss-left probability of PL, QP, KD, FPC, and FPU 95% confidence intervals for between-study variance of LOR vs τ^2 , for unequal sample sizes $\bar{n} = 30, 60, 100$ and 160 , $p_{iC} = .2$, $\theta = 2$ and $f = 0.5$. Solid lines: PL, QP, and FPC “only”, FPU model-based, and KD. Dashed lines: PL, QP, and FPC “always” and FPU naïve.

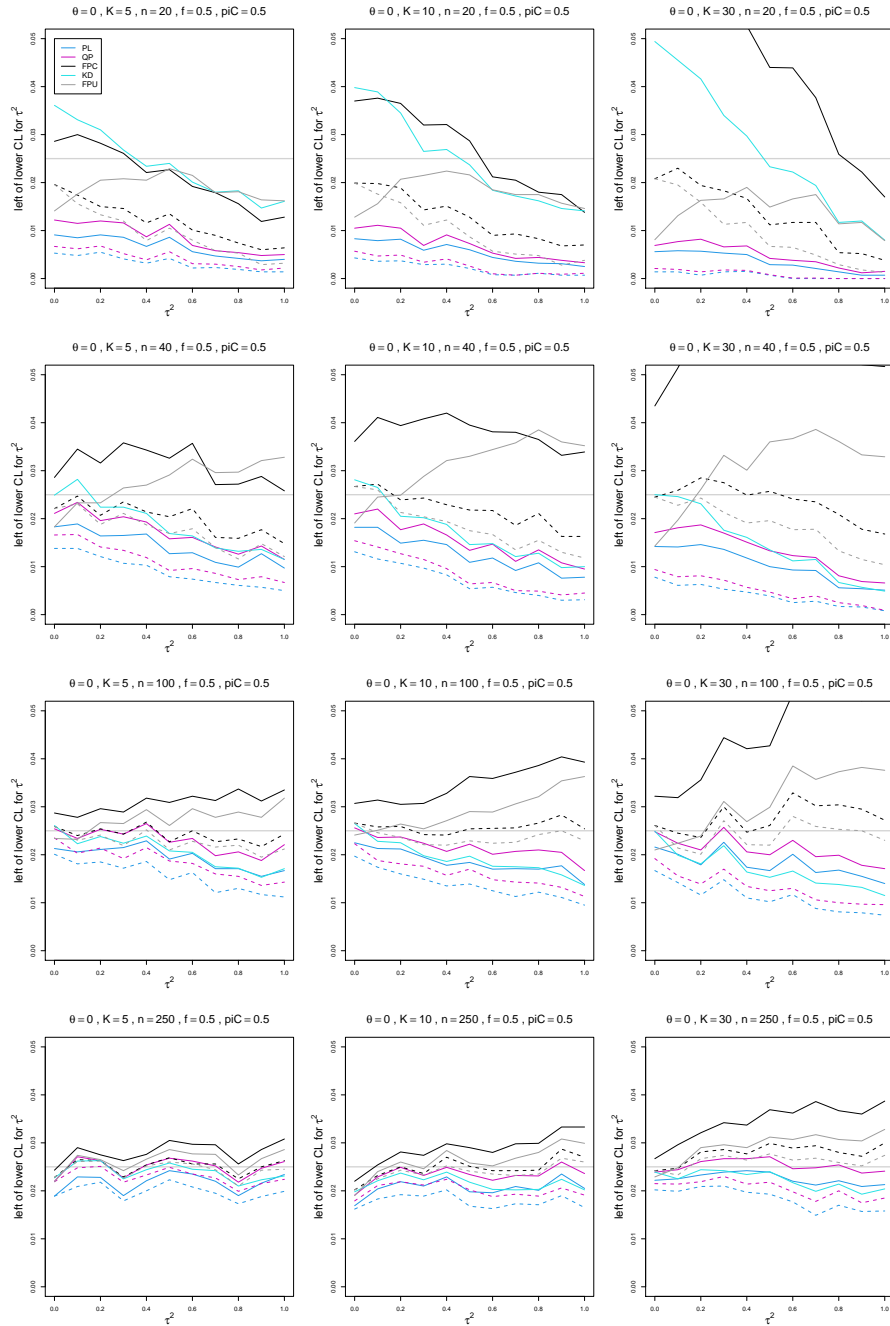


Figure D.25: Miss-left probability of PL, QP, KD, FPC, and FPU 95% confidence intervals for between-study variance of LOR vs τ^2 , for equal sample sizes $n = 20, 40, 100$ and 250 , $piC = .5$, $\theta = 0$ and $f = 0.5$. Solid lines: PL, QP, and FPC “only”, FPU model-based, and KD. Dashed lines: PL, QP, and FPC “always” and FPU naïve.

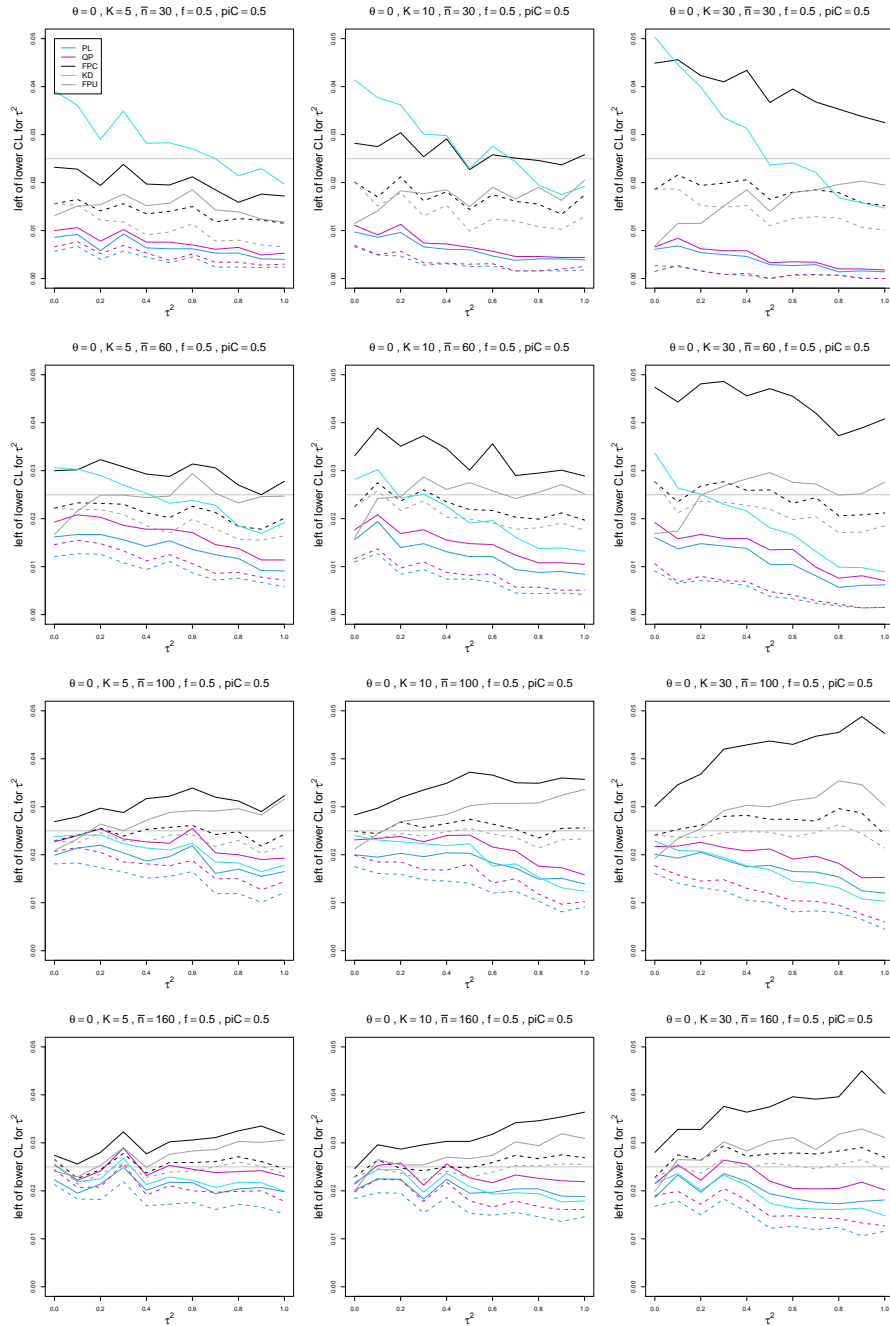


Figure D.26: Miss-left probability of PL, QP, KD, FPC, and FPU 95% confidence intervals for between-study variance of LOR vs τ^2 , for unequal sample sizes $\bar{n} = 30, 60, 100$ and 160 , $p_{iC} = .5$, $\theta = 0$ and $f = 0.5$. Solid lines: PL, QP, and FPC “only”, FPU model-based, and KD. Dashed lines: PL, QP, and FPC “always” and FPU naïve.

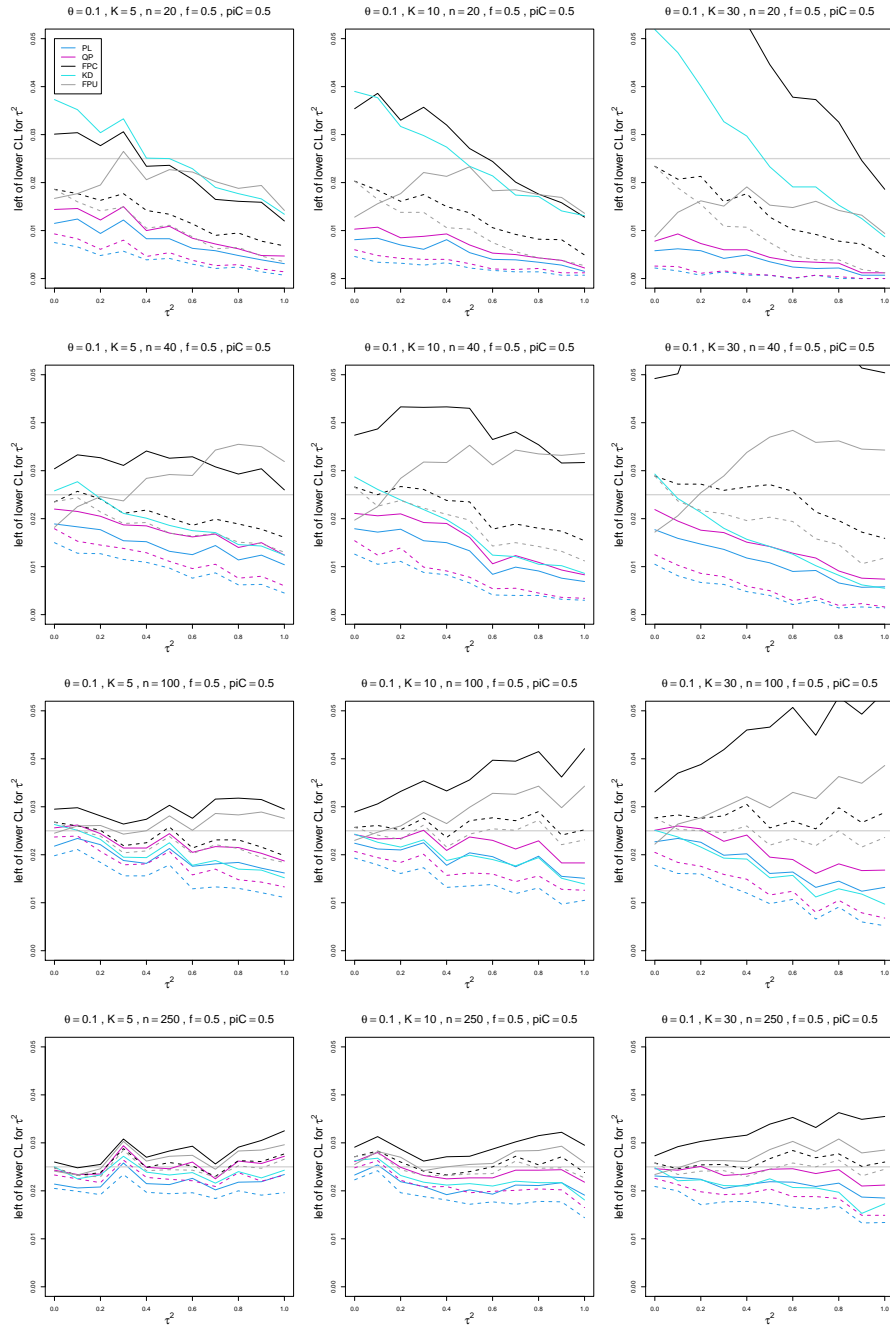


Figure D.27: Miss-left probability of PL, QP, KD, FPC, and FPU 95% confidence intervals for between-study variance of LOR vs τ^2 , for equal sample sizes $n = 20, 40, 100$ and 250 , $piC = .5$, $\theta = 0.1$ and $f = 0.5$. Solid lines: PL, QP, and FPC “only”, FPU model-based, and KD. Dashed lines: PL, QP, and FPC “always” and FPU naïve.

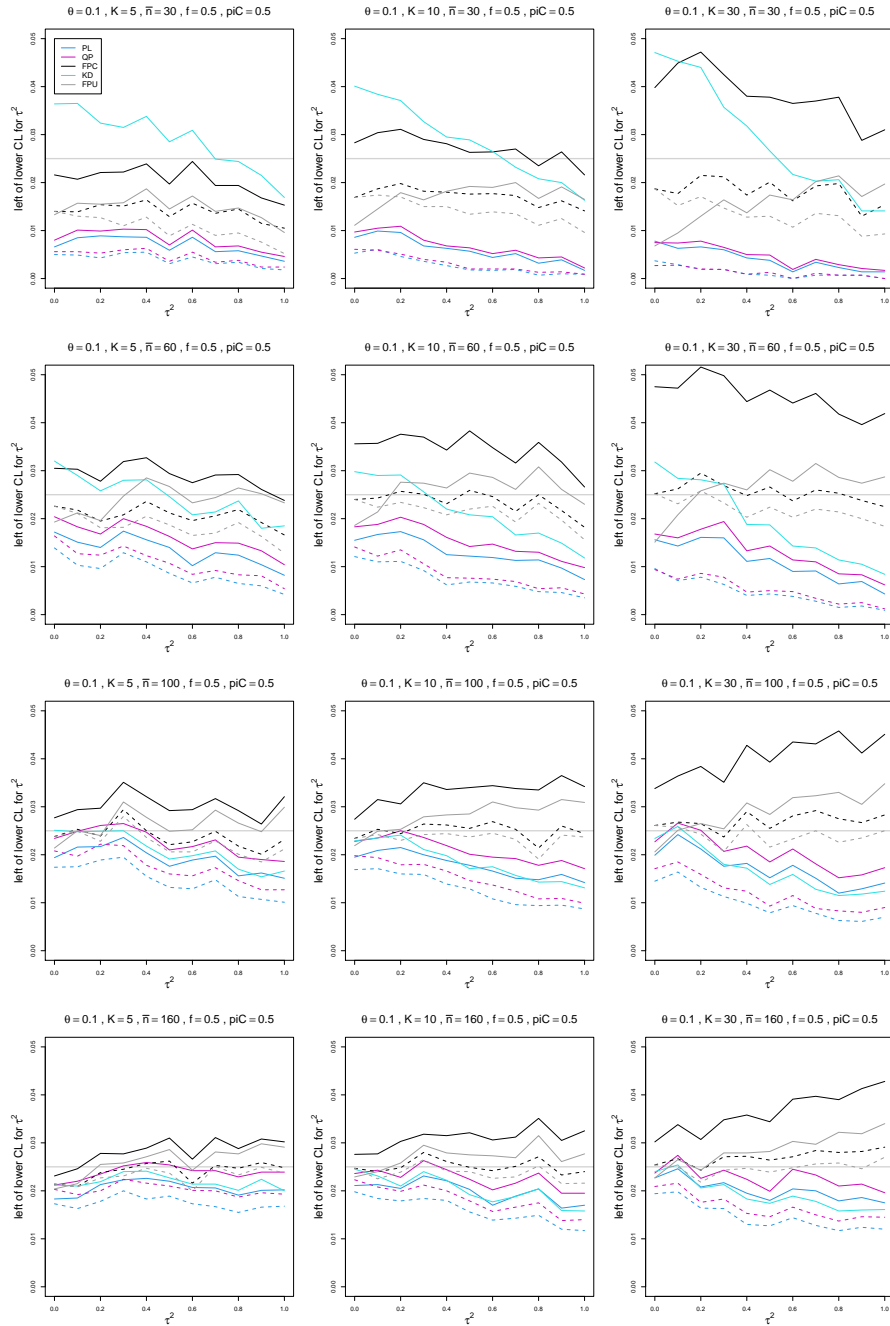


Figure D.28: Miss-left probability of PL, QP, KD, FPC, and FPU 95% confidence intervals for between-study variance of LOR vs τ^2 , for unequal sample sizes $\bar{n} = 30, 60, 100$ and 160 , $p_{iC} = .5$, $\theta = 0.1$ and $f = 0.5$. Solid lines: PL, QP, and FPC “only”, FPU model-based, and KD. Dashed lines: PL, QP, and FPC “always” and FPU naïve.

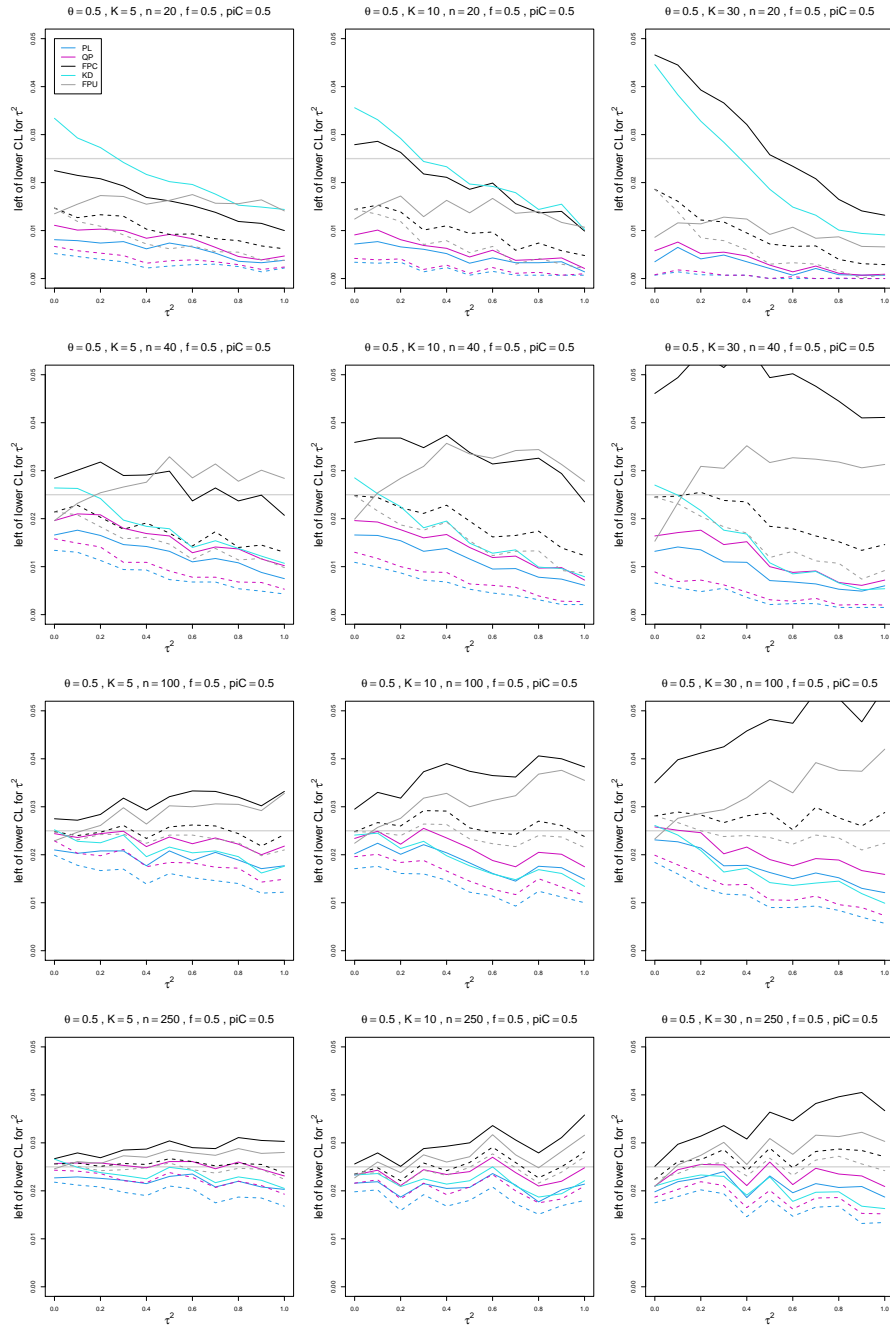


Figure D.29: Miss-left probability of PL, QP, KD, FPC, and FPU 95% confidence intervals for between-study variance of LOR vs τ^2 , for equal sample sizes $n = 20, 40, 100$ and 250 , $p_{iC} = .5$, $\theta = 0.5$ and $f = 0.5$. Solid lines: PL, QP, and FPC “only”, FPU model-based, and KD. Dashed lines: PL, QP, and FPC “always” and FPU naïve.

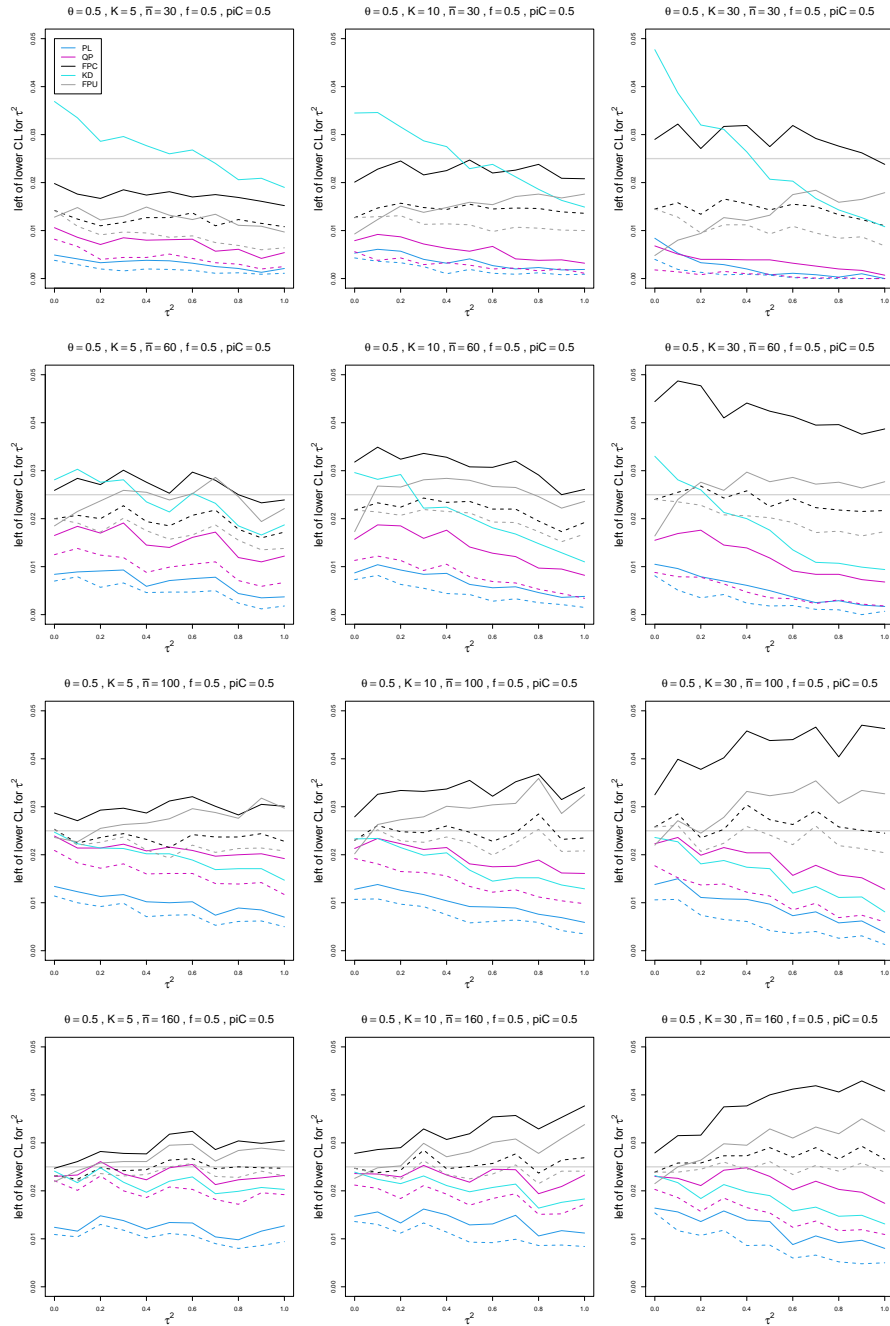


Figure D.30: Miss-left probability of PL, QP, KD, FPC, and FPU 95% confidence intervals for between-study variance of LOR vs τ^2 , for unequal sample sizes $\bar{n} = 30, 60, 100$ and 160 , $piC = .5$, $\theta = 0.5$ and $f = 0.5$. Solid lines: PL, QP, and FPC “only”, FPU model-based, and KD. Dashed lines: PL, QP, and FPC “always” and FPU naïve.

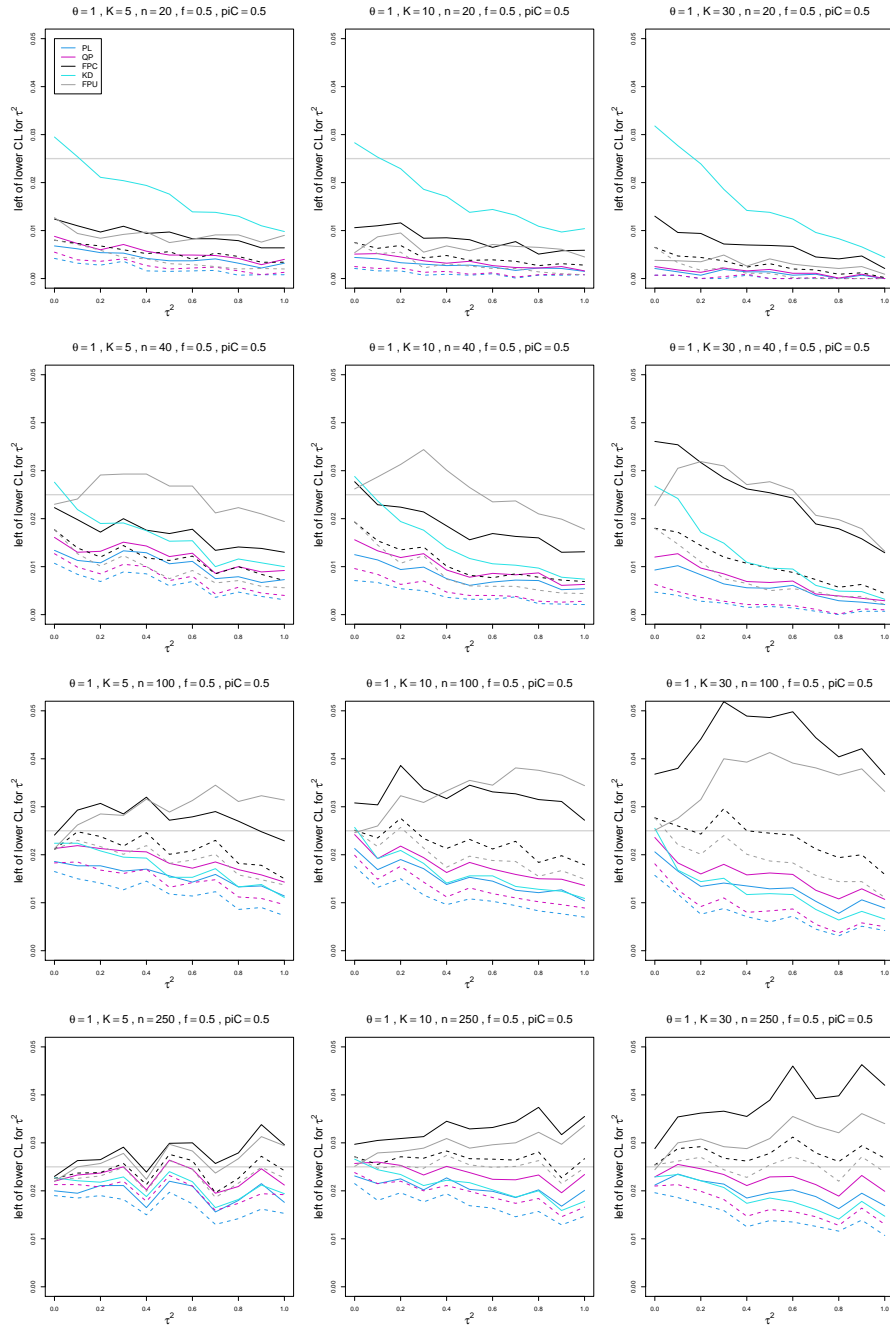


Figure D.31: Miss-left probability of PL, QP, KD, FPC, and FPU 95% confidence intervals for between-study variance of LOR vs τ^2 , for equal sample sizes $n = 20, 40, 100$ and 250 , $p_{iC} = .5$, $\theta = 1$ and $f = 0.5$. Solid lines: PL, QP, and FPC “only”, FPU model-based, and KD. Dashed lines: PL, QP, and FPC “always” and FPU naïve.

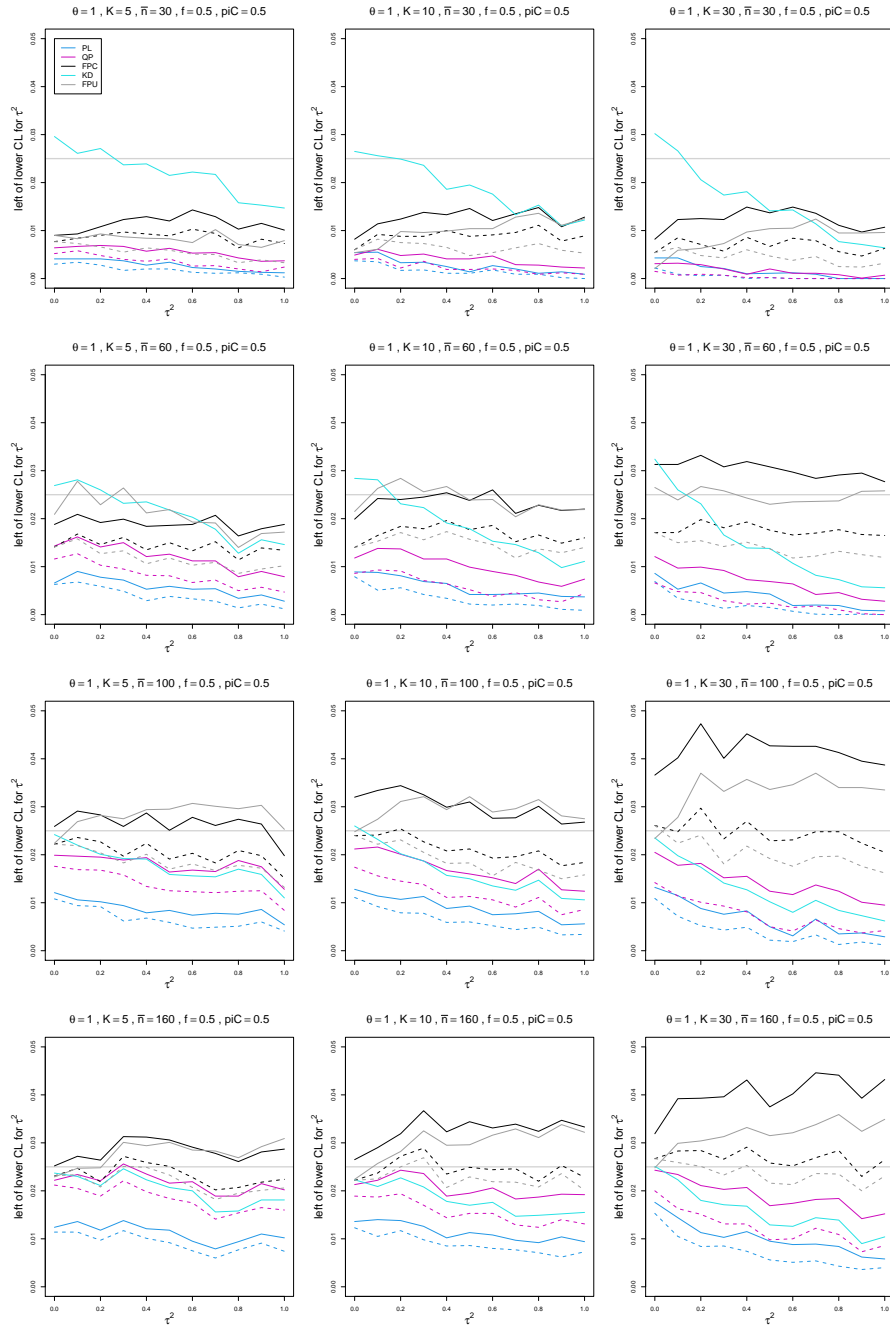


Figure D.32: Miss-left probability of PL, QP, KD, FPC, and FPU 95% confidence intervals for between-study variance of LOR vs τ^2 , for unequal sample sizes $\bar{n} = 30, 60, 100$ and 160 , $p_{iC} = .5$, $\theta = 1$ and $f = 0.5$. Solid lines: PL, QP, and FPC “only”, FPU model-based, and KD. Dashed lines: PL, QP, and FPC “always” and FPU naïve.

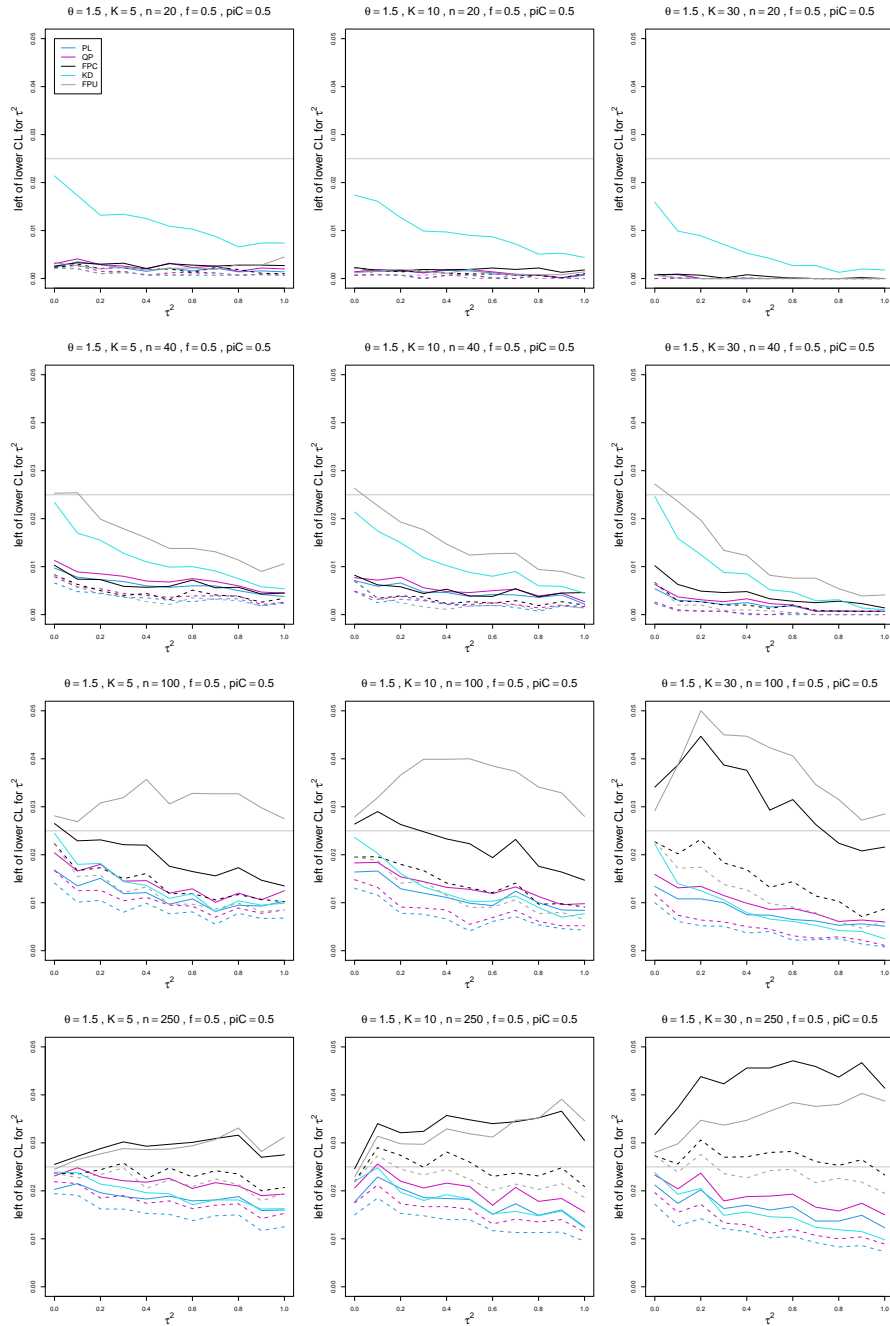


Figure D.33: Miss-left probability of PL, QP, KD, FPC, and FPU 95% confidence intervals for between-study variance of LOR vs τ^2 , for equal sample sizes $n = 20, 40, 100$ and 250 , $piC = .5$, $\theta = 1.5$ and $f = 0.5$. Solid lines: PL, QP, and FPC “only”, FPU model-based, and KD. Dashed lines: PL, QP, and FPC “always” and FPU naïve.

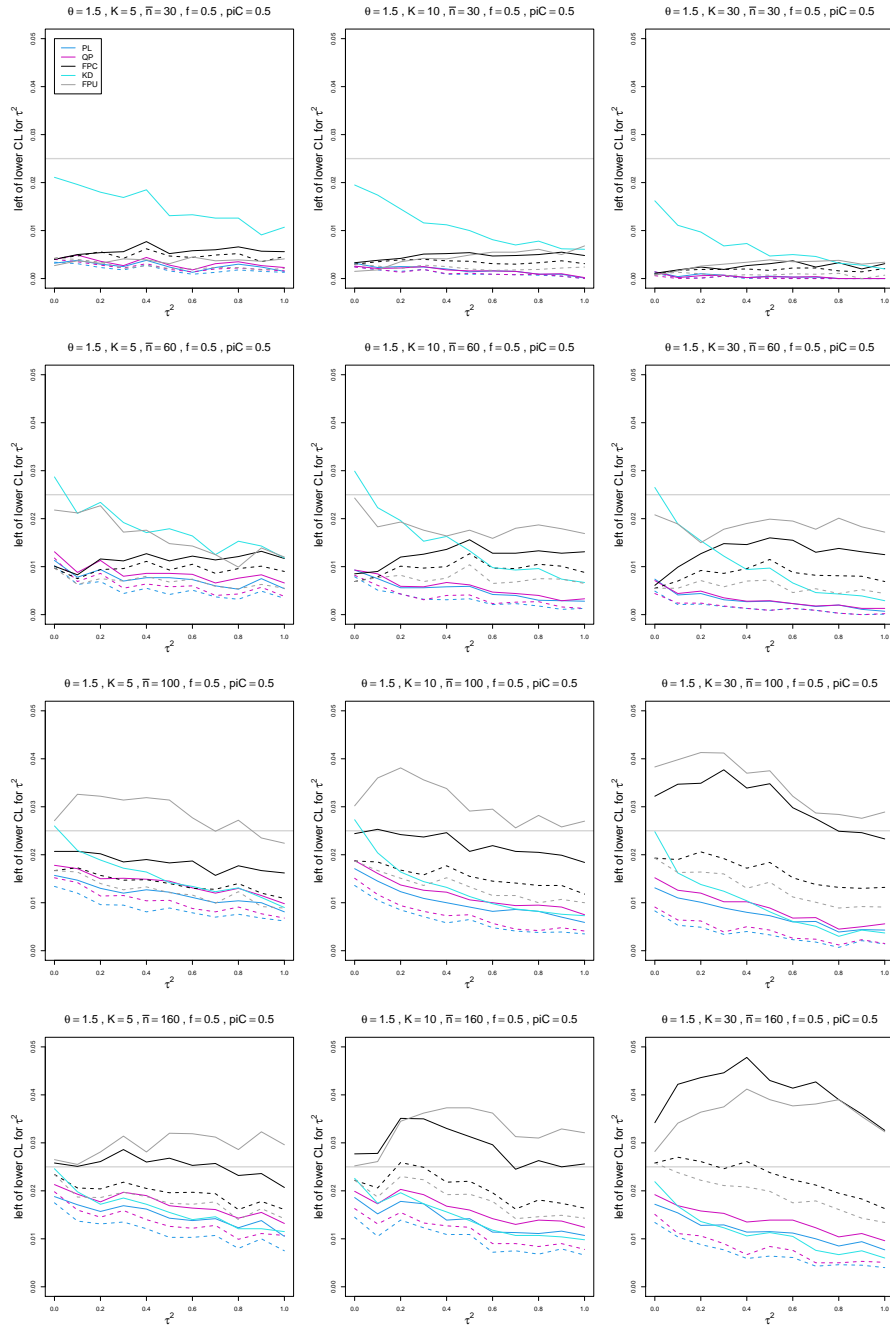


Figure D.34: Miss-left probability of PL, QP, KD, FPC, and FPU 95% confidence intervals for between-study variance of LOR vs τ^2 , for unequal sample sizes $\bar{n} = 30, 60, 100$ and 160 , $piC = .5$, $\theta = 1.5$ and $f = 0.5$. Solid lines: PL, QP, and FPC “only”, FPU model-based, and KD. Dashed lines: PL, QP, and FPC “always” and FPU naïve.

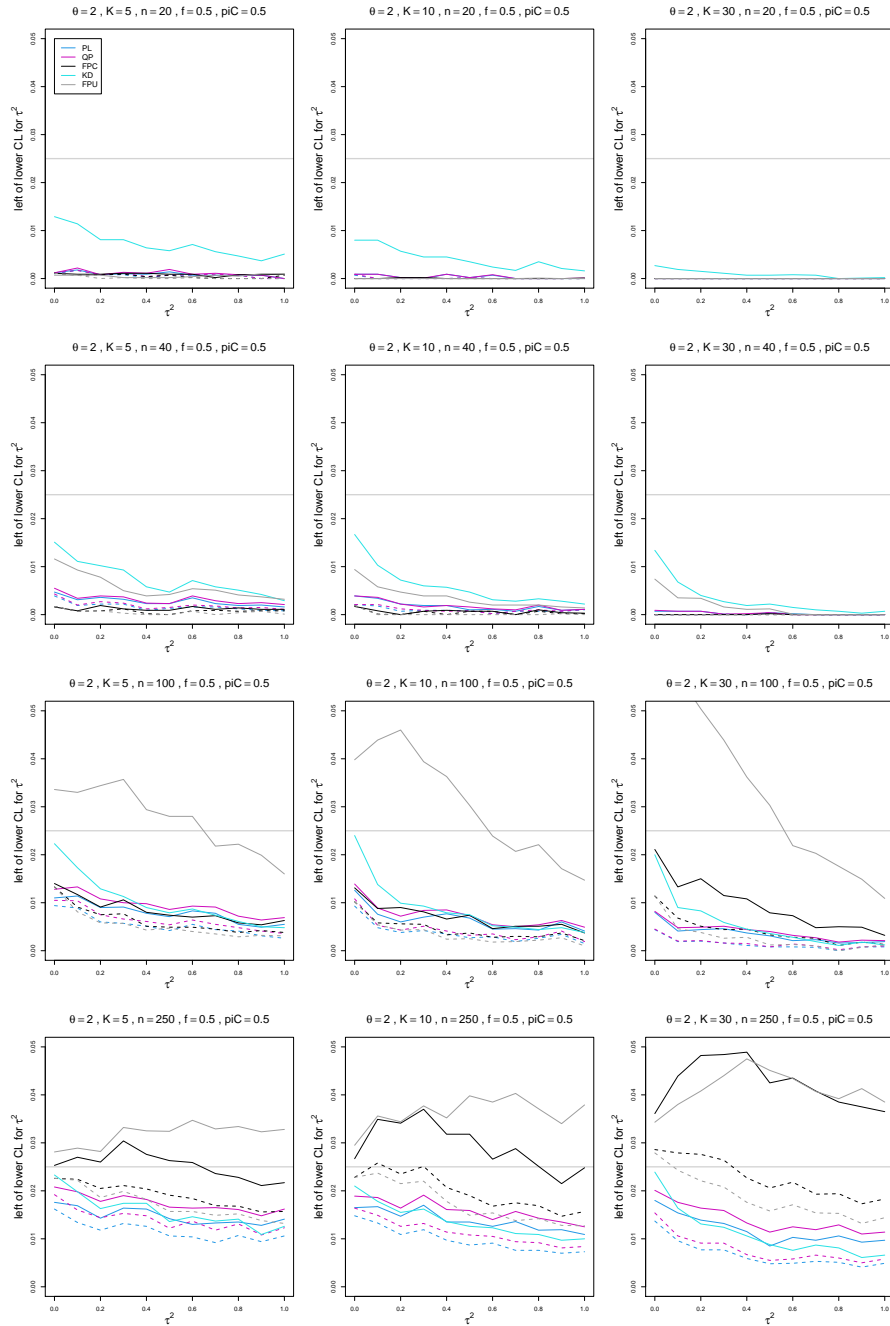


Figure D.35: Miss-left probability of PL, QP, KD, FPC, and FPU 95% confidence intervals for between-study variance of LOR vs τ^2 , for equal sample sizes $n = 20, 40, 100$ and 250 , $p_{iC} = .5$, $\theta = 2$ and $f = 0.5$. Solid lines: PL, QP, and FPC “only”, FPU model-based, and KD. Dashed lines: PL, QP, and FPC “always” and FPU naïve.

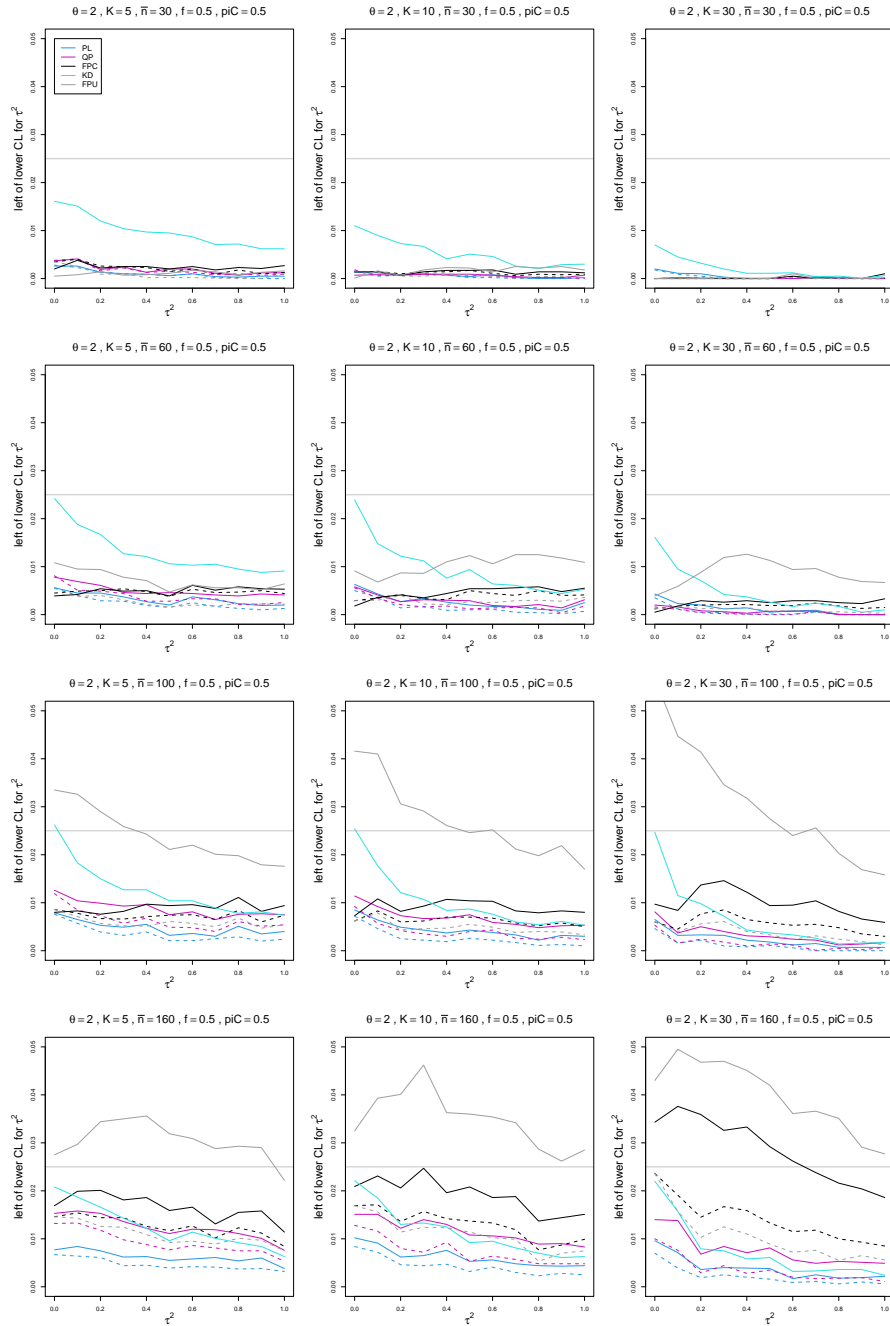


Figure D.36: Miss-left probability of PL, QP, KD, FPC, and FPU 95% confidence intervals for between-study variance of LOR vs τ^2 , for unequal sample sizes $\bar{n} = 30, 60, 100$ and 160 , $p_{iC} = .5$, $\theta = 2$ and $f = 0.5$. Solid lines: PL, QP, and FPC “only”, FPU model-based, and KD. Dashed lines: PL, QP, and FPC “always” and FPU naïve.

Appendix E: Sample miss-right probability for 95% confidence intervals for between-study variance

Each figure corresponds to a value of the probability of an event in the Control arm p_{iC} ($= .1, .2, .5$).

The fraction of each study's sample size in the Control arm f is held constant at 0.5. For each combination of a value of n ($= 20, 40, 100, 250$) or \bar{n} ($= 30, 60, 100, 160$) and a value of K ($= 5, 10, 30$), a panel plots the probability that the parameter is to the right of the upper confidence limit of the confidence interval versus τ^2 ($= 0.0(0.1)1$).

The confidence intervals are

- PL (Profile Likelihood), inverse-variance weights)
- QP (Q profile, inverse-variance weights)
- KD (based on Kulinskaya-Dollinger (2015) approximation, inverse-variance weights)
- FPC (based on Farebrother approximation, effective-sample-size weights, conditional variance of LOR)
- FPU (based on Farebrother approximation, effective-sample-size weights, unconditional variance of LOR)

The plots include two versions of PL, QP, and FPC: adding 1/2 to all four of X_{iT} , X_{iC} , $n_{iT} - X_{iT}$, $n_{iC} - X_{iC}$ only when one of these is zero (solid lines) or always (dashed lines).

The plots also include two versions of FPU: model-based estimation of p_{iT} (solid lines) or naïve estimation (dashed lines).

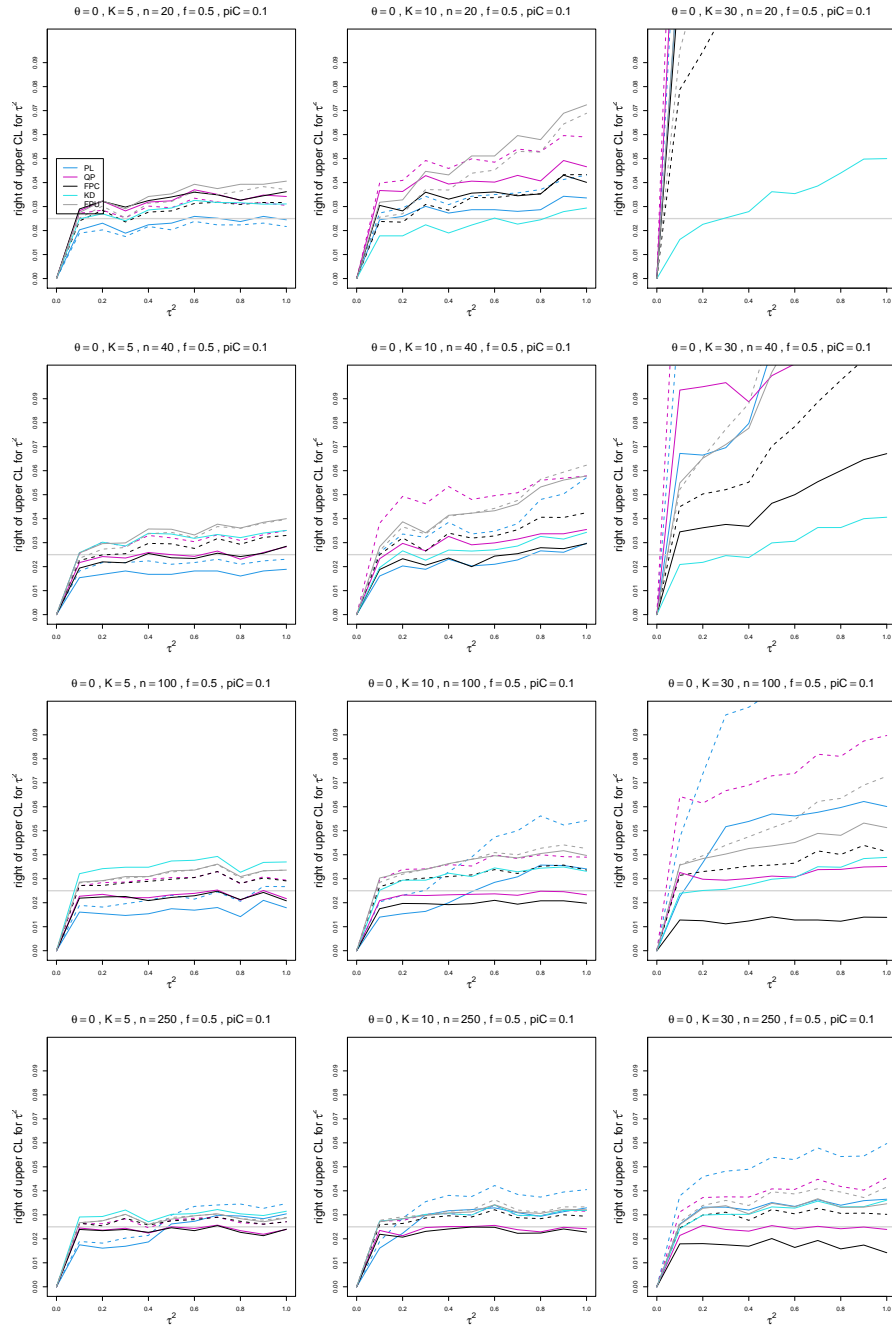


Figure E.1: Miss-right probability of PL, QP, KD, FPC, and FPU 95% confidence intervals for between-study variance of LOR vs τ^2 , for equal sample sizes $n = 20, 40, 100$ and 250 , $p_{iC} = .1$, $\theta = 0$ and $f = 0.5$. Solid lines: PL, QP, and FPC “only”, FPU model-based, and KD. Dashed lines: PL, QP and FPC “always” and FPU naïve.

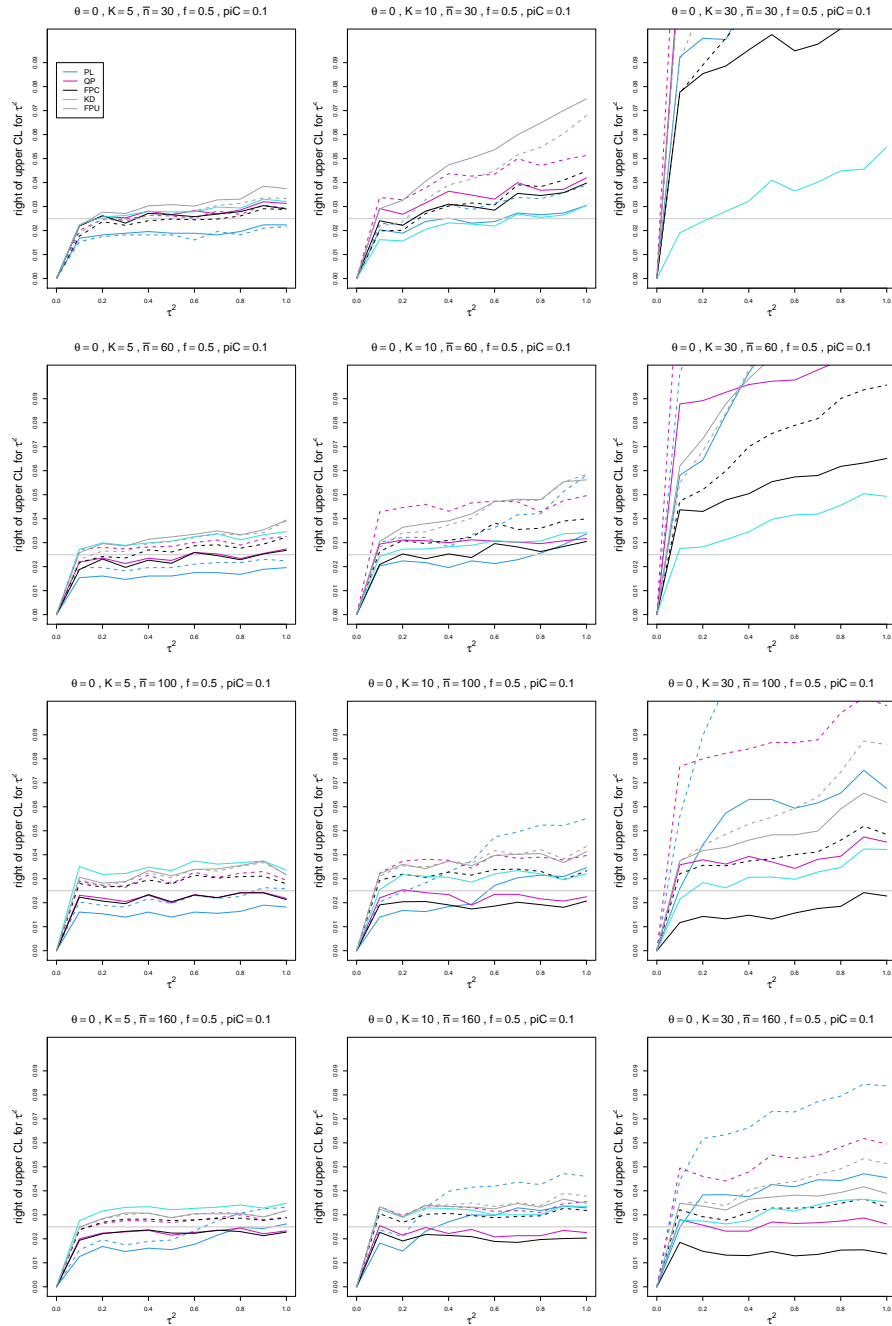


Figure E.2: Miss-right probability of PL, QP, KD, FPC, and FPU 95% confidence intervals for between-study variance of LOR vs τ^2 , for unequal sample sizes $\bar{n} = 30, 60, 100$ and 160 , $p_{iC} = .1$, $\theta = 0$ and $f = 0.5$. Solid lines: PL, QP, and FPC “only”, FPU model-based, and KD. Dashed lines: PL, QP, and FPC “always” and FPU naïve.

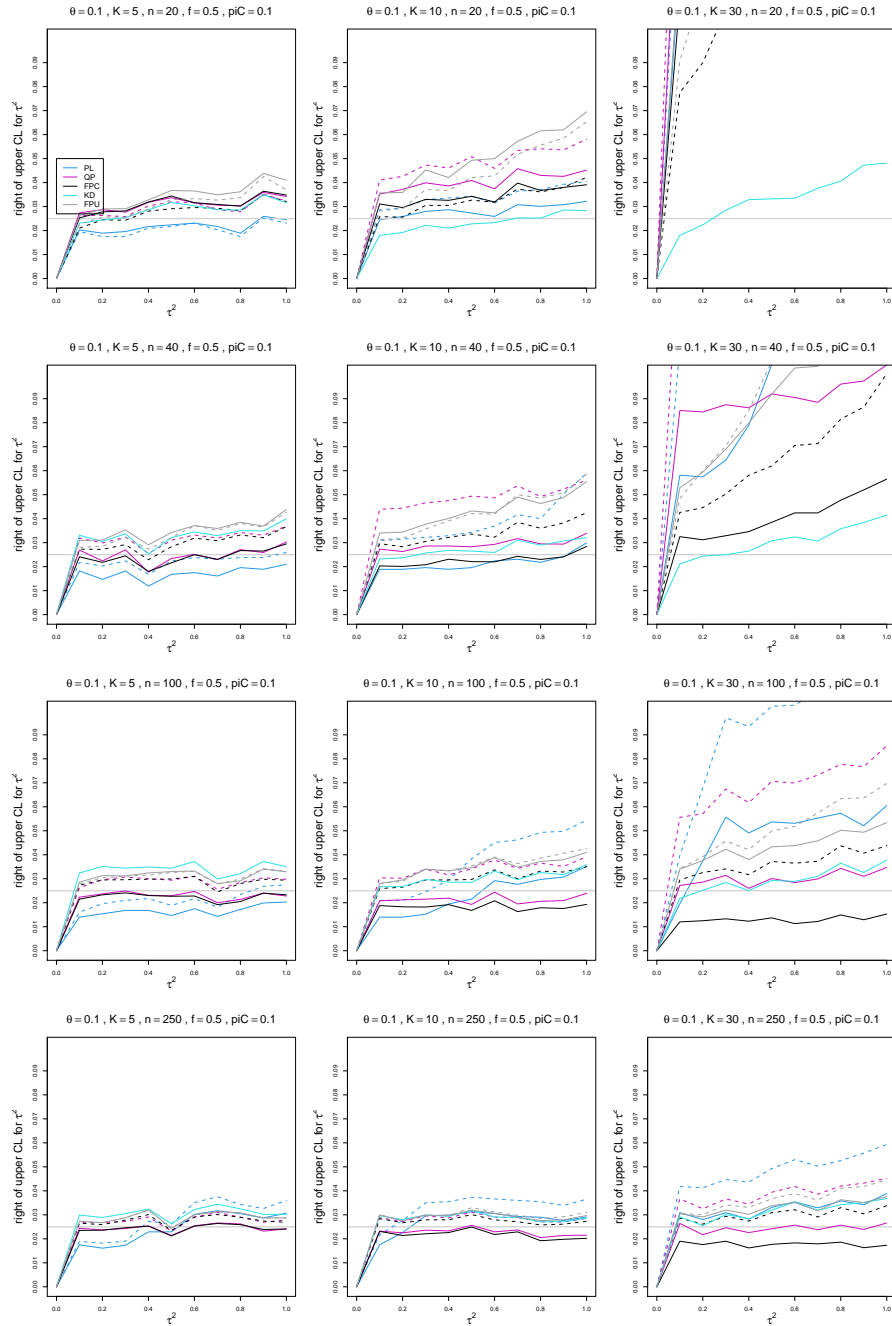


Figure E.3: Miss-right probability of PL, QP, KD, FPC, and FPU 95% confidence intervals for between-study variance of LOR vs τ^2 , for equal sample sizes $n = 20, 40, 100$ and 250 , $\pi_{iC} = .1$, $\theta = 0.1$ and $f = 0.5$. Solid lines: PL, QP, and FPC “only”, FPU model-based, and KD. Dashed lines: PL, QP and FPC “always” and FPU naïve.

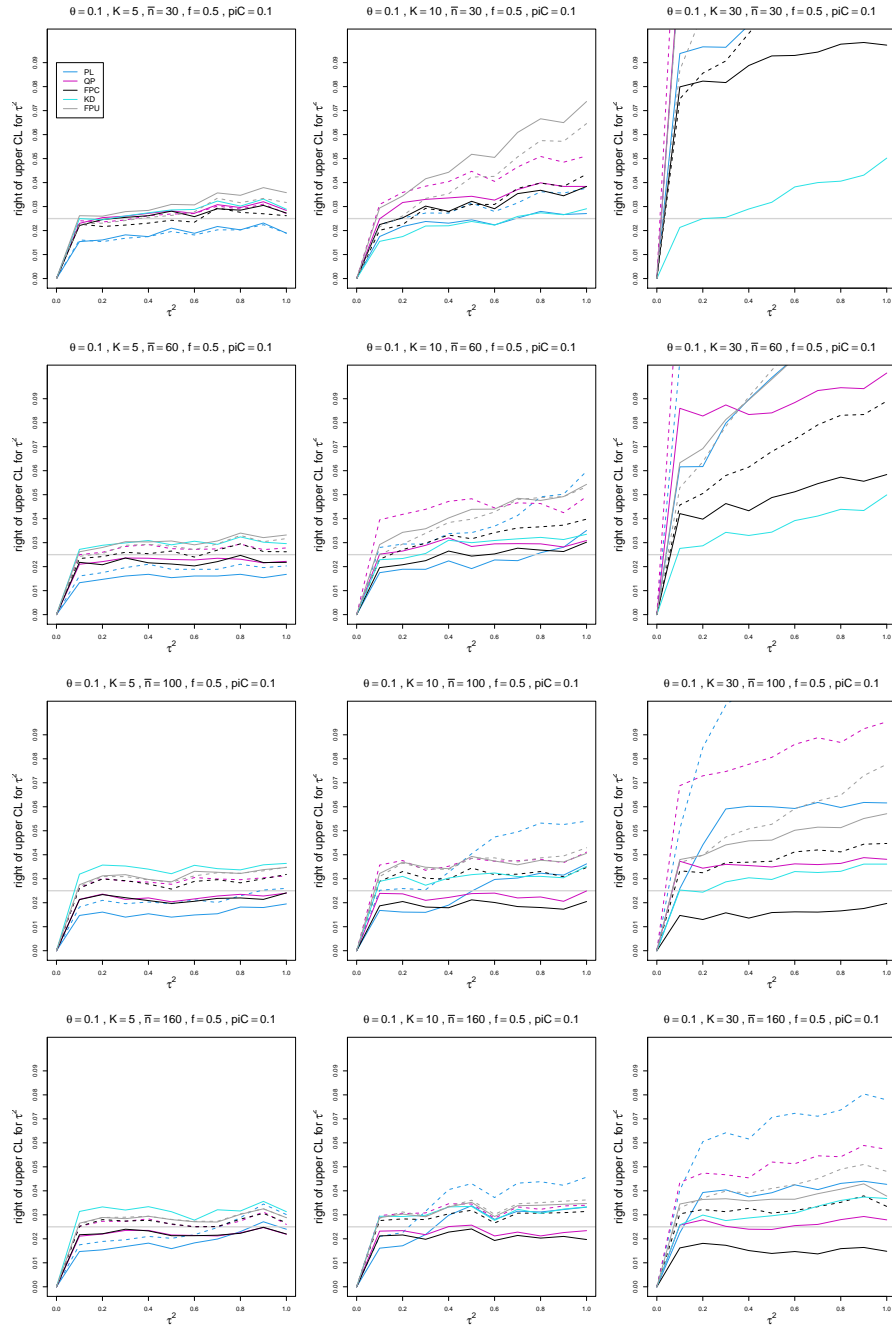


Figure E.4: Miss-right probability of PL, QP, KD, FPC, and FPU 95% confidence intervals for between-study variance of LOR vs τ^2 , for unequal sample sizes $\bar{n} = 30, 60, 100$ and 160 , $p_{iC} = .1$, $\theta = 0.1$ and $f = 0.5$. Solid lines: PL, QP, and FPC “only”, FPU model-based, and KD. Dashed lines: PL, QP, and FPC “always” and FPU naïve.

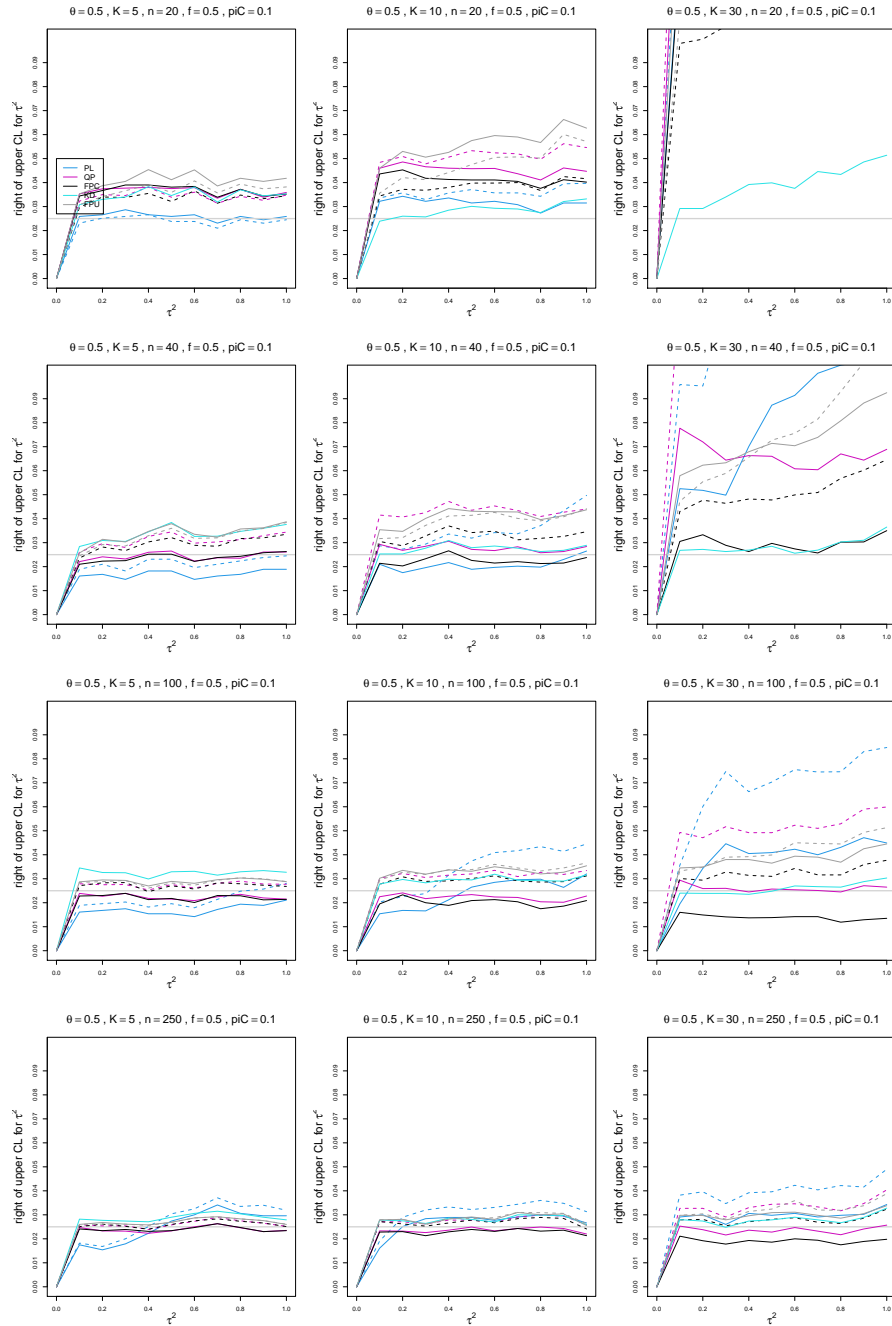


Figure E.5: Miss-right probability of PL, QP, KD, FPC, and FPU 95% confidence intervals for between-study variance of LOR vs τ^2 , for equal sample sizes $n = 20, 40, 100$ and 250 , $\pi_C = .1$, $\theta = 0.5$ and $f = 0.5$. Solid lines: PL, QP, and FPC “only”, FPU model-based, and KD. Dashed lines: PL, QP and FPC “always” and FPU naïve.

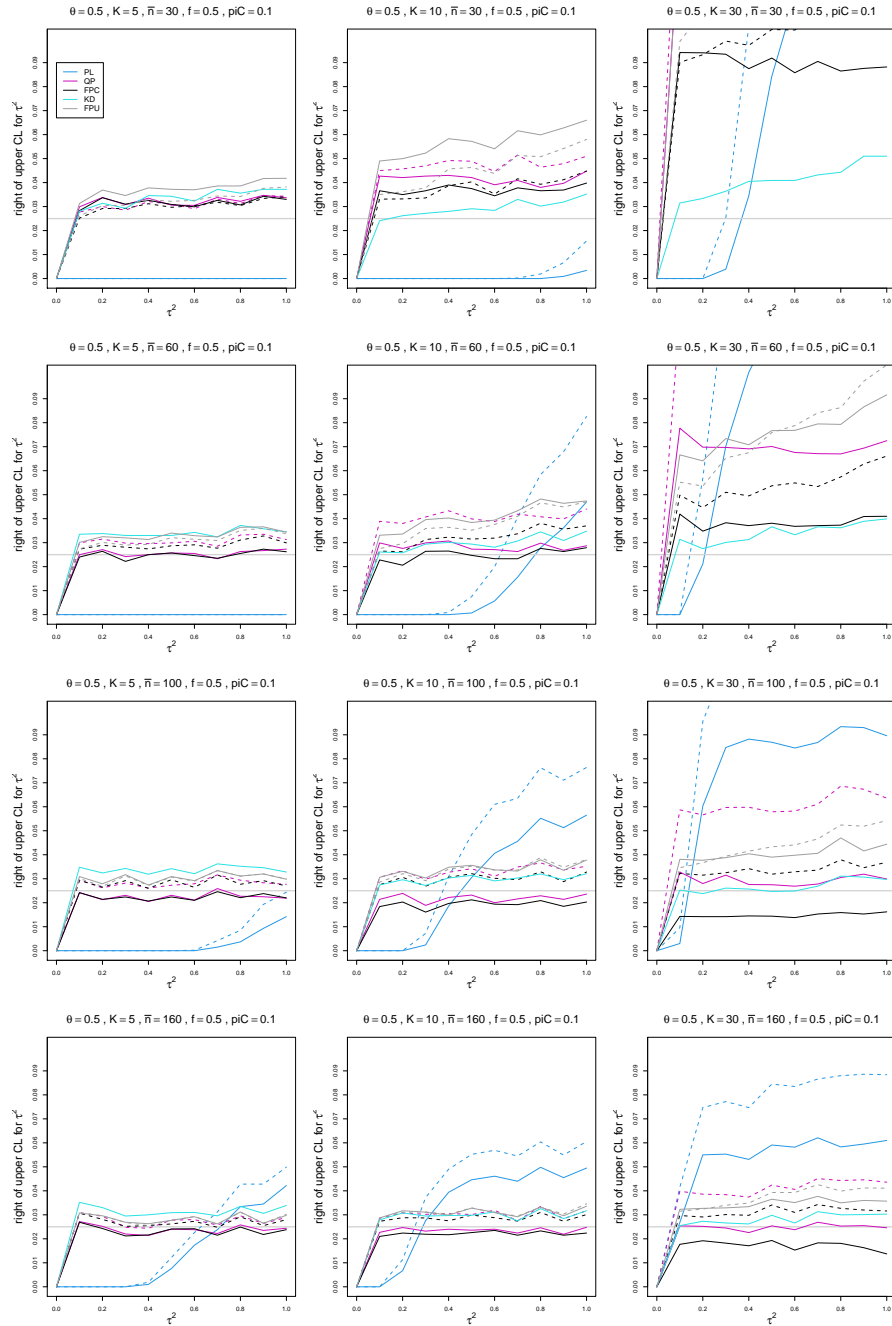


Figure E.6: Miss-right probability of PL, QP, KD, FPC, and FPU 95% confidence intervals for between-study variance of LOR vs τ^2 , for unequal sample sizes $\bar{n} = 30, 60, 100$ and 160 , $\pi_C = .1$, $\theta = 0.5$ and $f = 0.5$. Solid lines: PL, QP, and FPC “only”, FPU model-based, and KD. Dashed lines: PL, QP, and FPC “always” and FPU naïve.

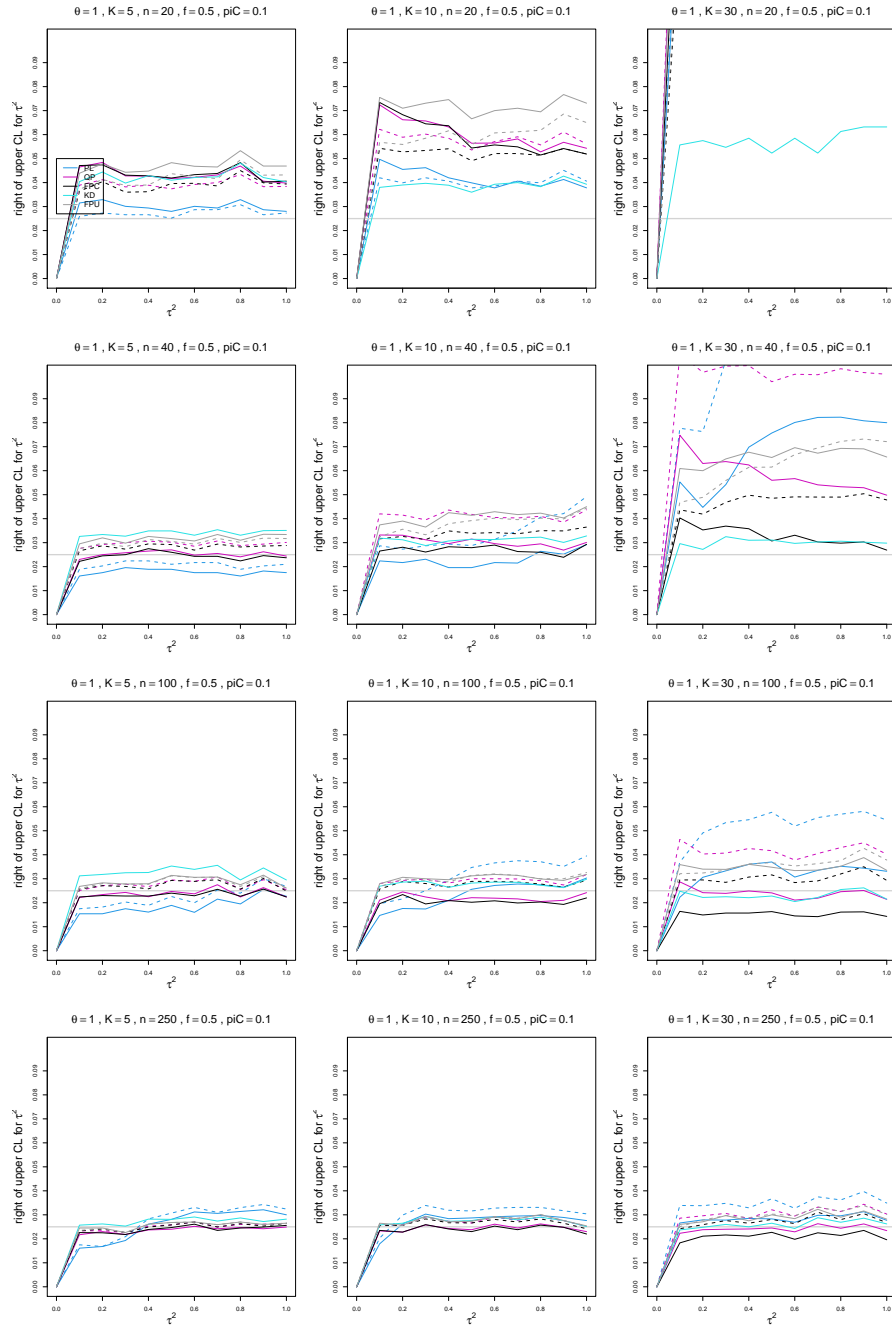


Figure E.7: Miss-right probability of PL, QP, KD, FPC, and FPU 95% confidence intervals for between-study variance of LOR vs τ^2 , for equal sample sizes $n = 20, 40, 100$ and 250 , $p_{iC} = .1$, $\theta = 1$ and $f = 0.5$. Solid lines: PL, QP, and FPC “only”, FPU model-based, and KD. Dashed lines: PL, QP and FPC “always” and FPU naïve.

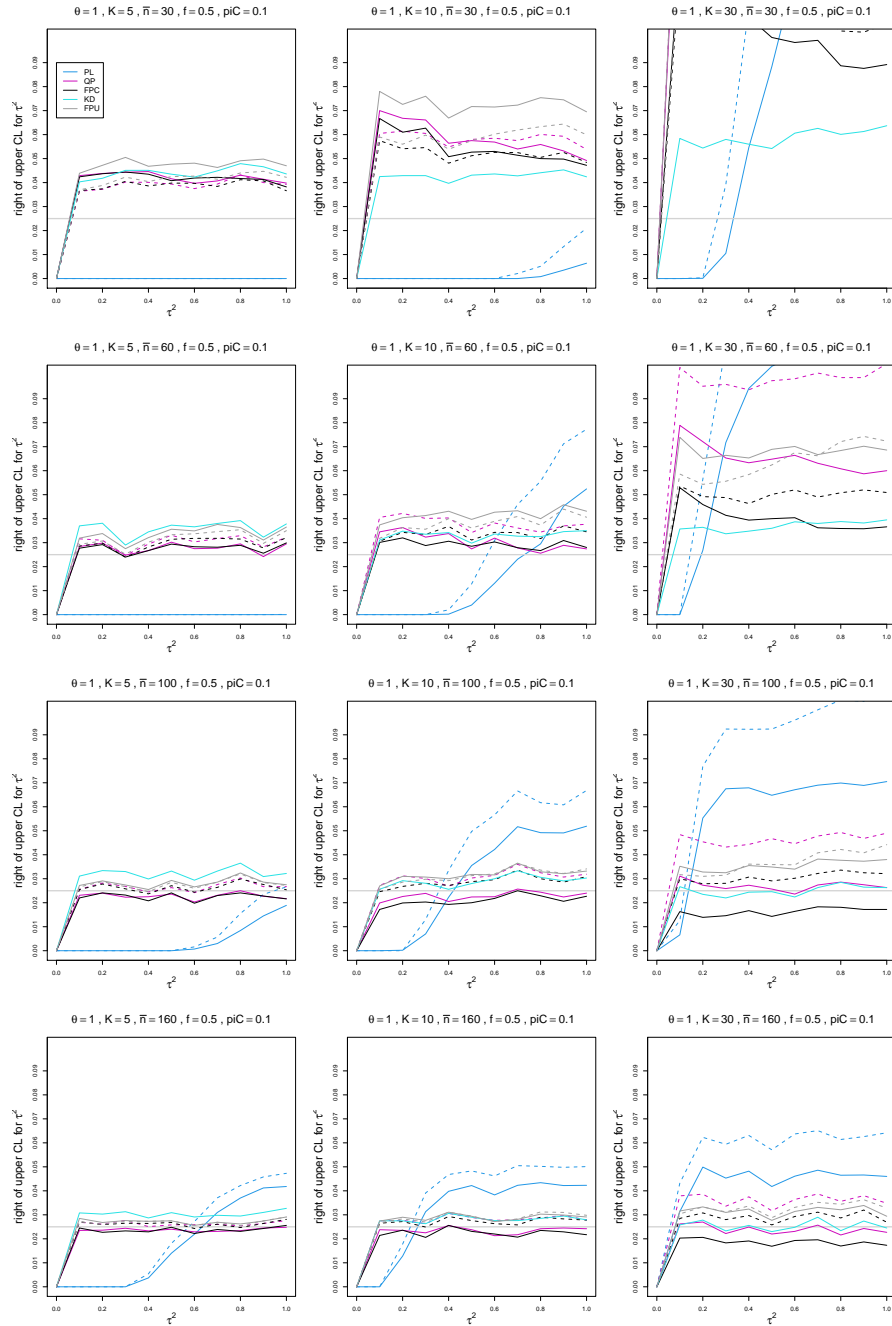


Figure E.8: Miss-right probability of PL, QP, KD, FPC, and FPU 95% confidence intervals for between-study variance of LOR vs τ^2 , for unequal sample sizes $\bar{n} = 30, 60, 100$ and 160 , $p_{iC} = .1$, $\theta = 1$ and $f = 0.5$. Solid lines: PL, QP, and FPC “only”, FPU model-based, and KD. Dashed lines: PL, QP, and FPC “always” and FPU naïve.

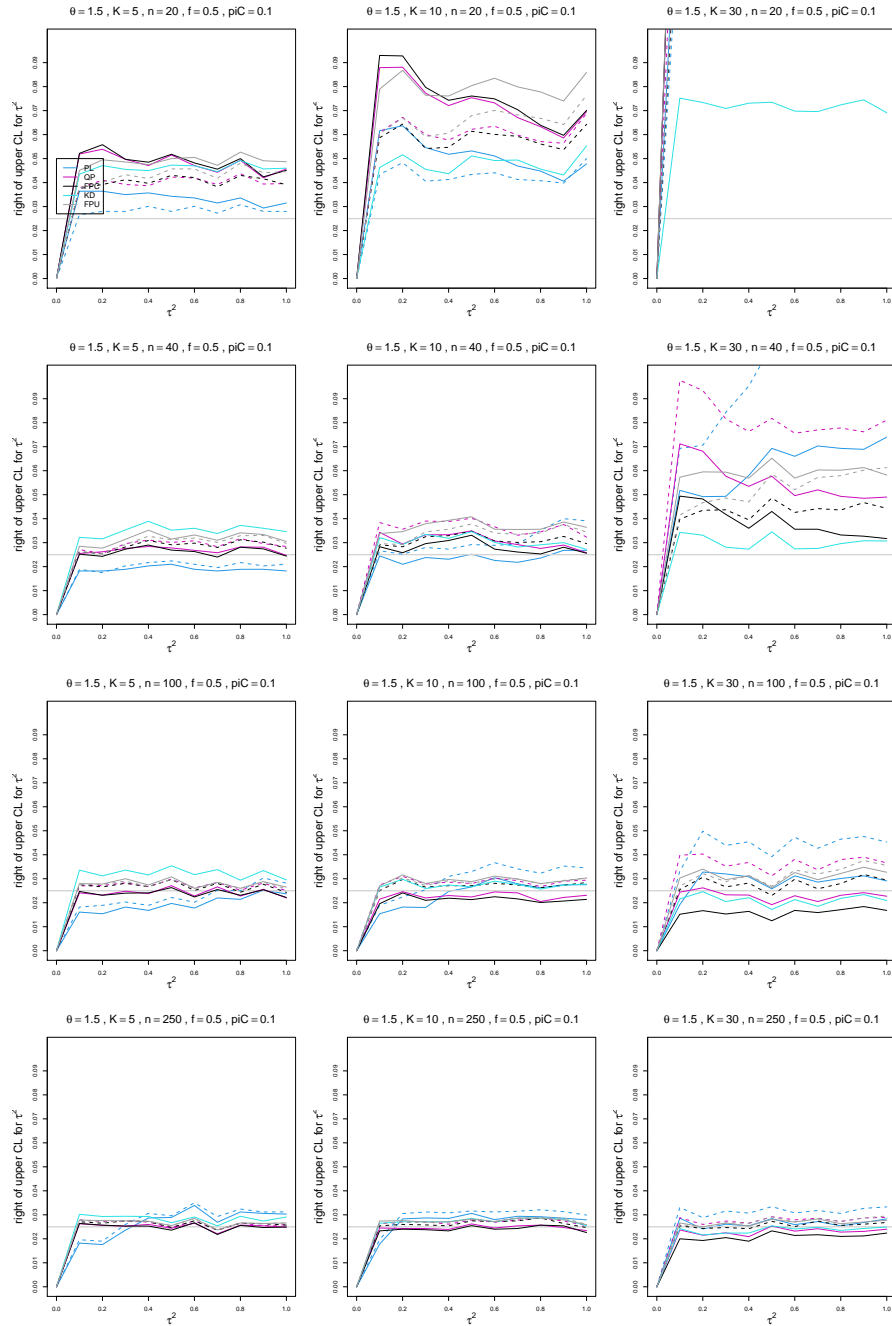


Figure E.9: Miss-right probability of PL, QP, KD, FPC, and FPU 95% confidence intervals for between-study variance of LOR vs τ^2 , for equal sample sizes $n = 20, 40, 100$ and 250 , $p_{iC} = .1$, $\theta = 1.5$ and $f = 0.5$. Solid lines: PL, QP, and FPC “only”, FPU model-based, and KD. Dashed lines: PL, QP and FPC “always” and FPU naïve.

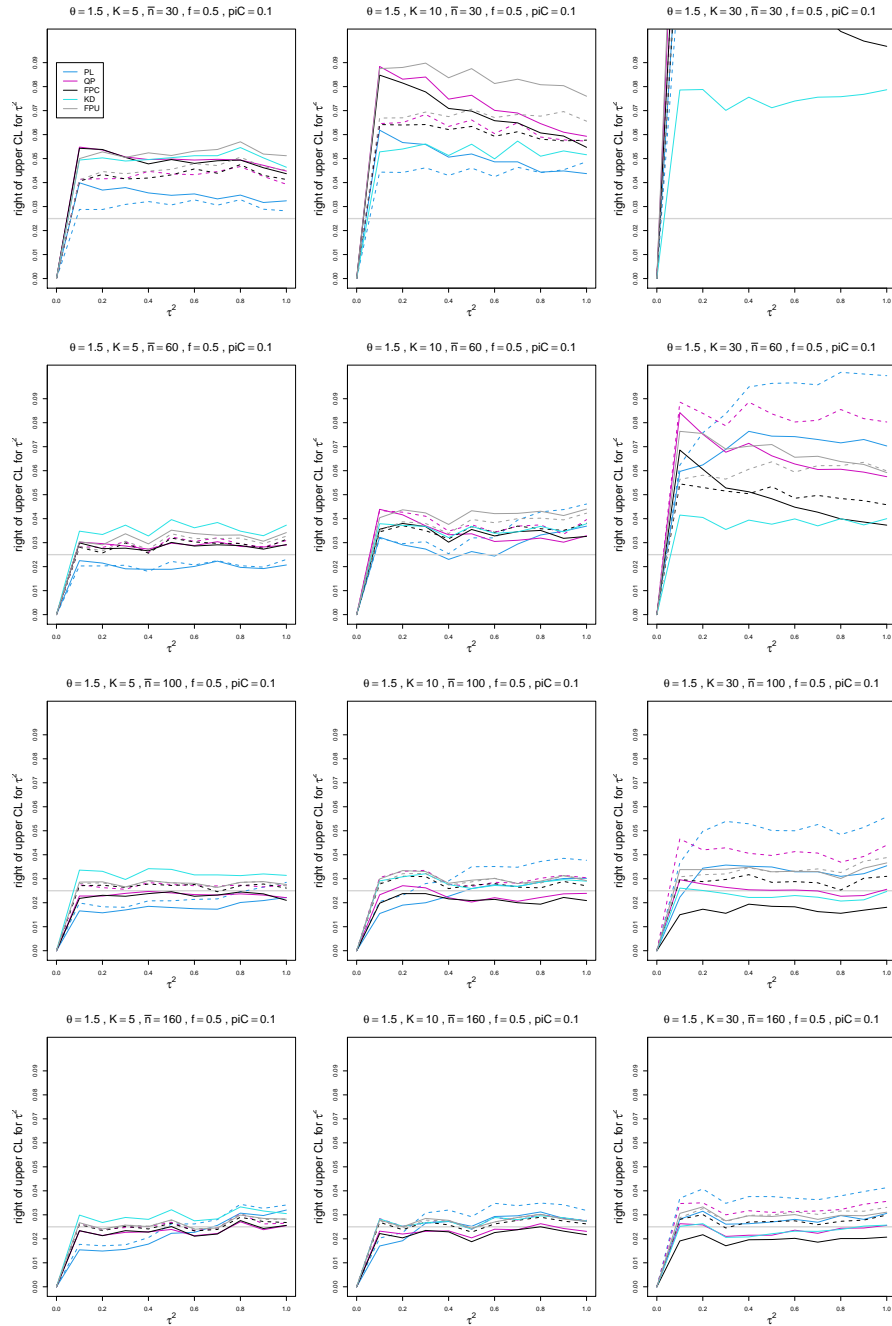


Figure E.10: Miss-right probability of PL, QP, KD, FPC, and FPU 95% confidence intervals for between-study variance of LOR vs τ^2 , for unequal sample sizes $\bar{n} = 30, 60, 100$ and 160 , $p_{iC} = .1$, $\theta = 1.5$ and $f = 0.5$. Solid lines: PL, QP, and FPC “only”, FPU model-based, and KD. Dashed lines: PL, QP, and FPC “always” and FPU naïve.

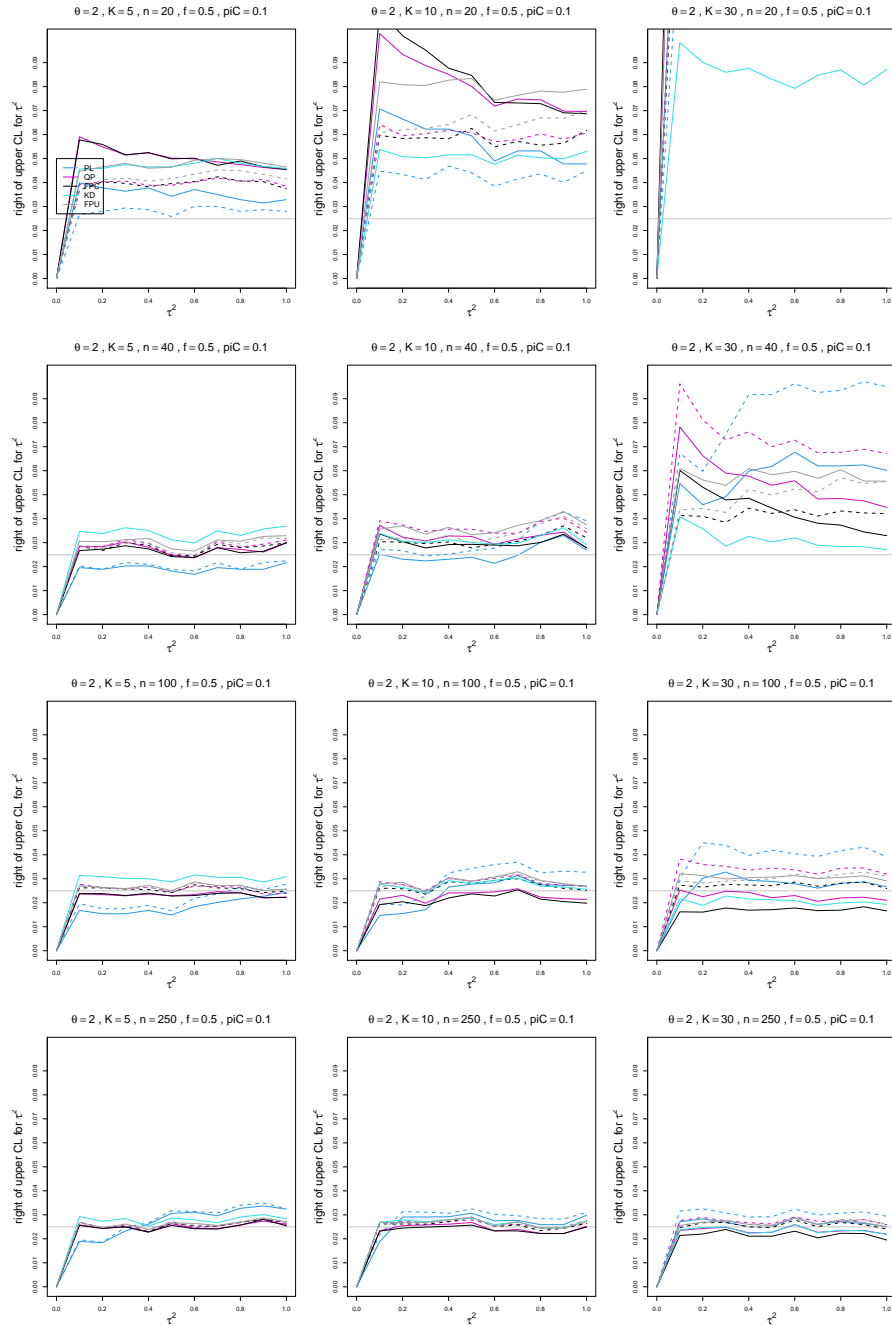


Figure E.11: Miss-right probability of PL, QP, KD, FPC, and FPU 95% confidence intervals for between-study variance of LOR vs τ^2 , for equal sample sizes $n = 20, 40, 100$ and 250 , $p_{iC} = .1$, $\theta = 2$ and $f = 0.5$. Solid lines: PL, QP, and FPC “only”, FPU model-based, and KD. Dashed lines: PL, QP and FPC “always” and FPU naïve.

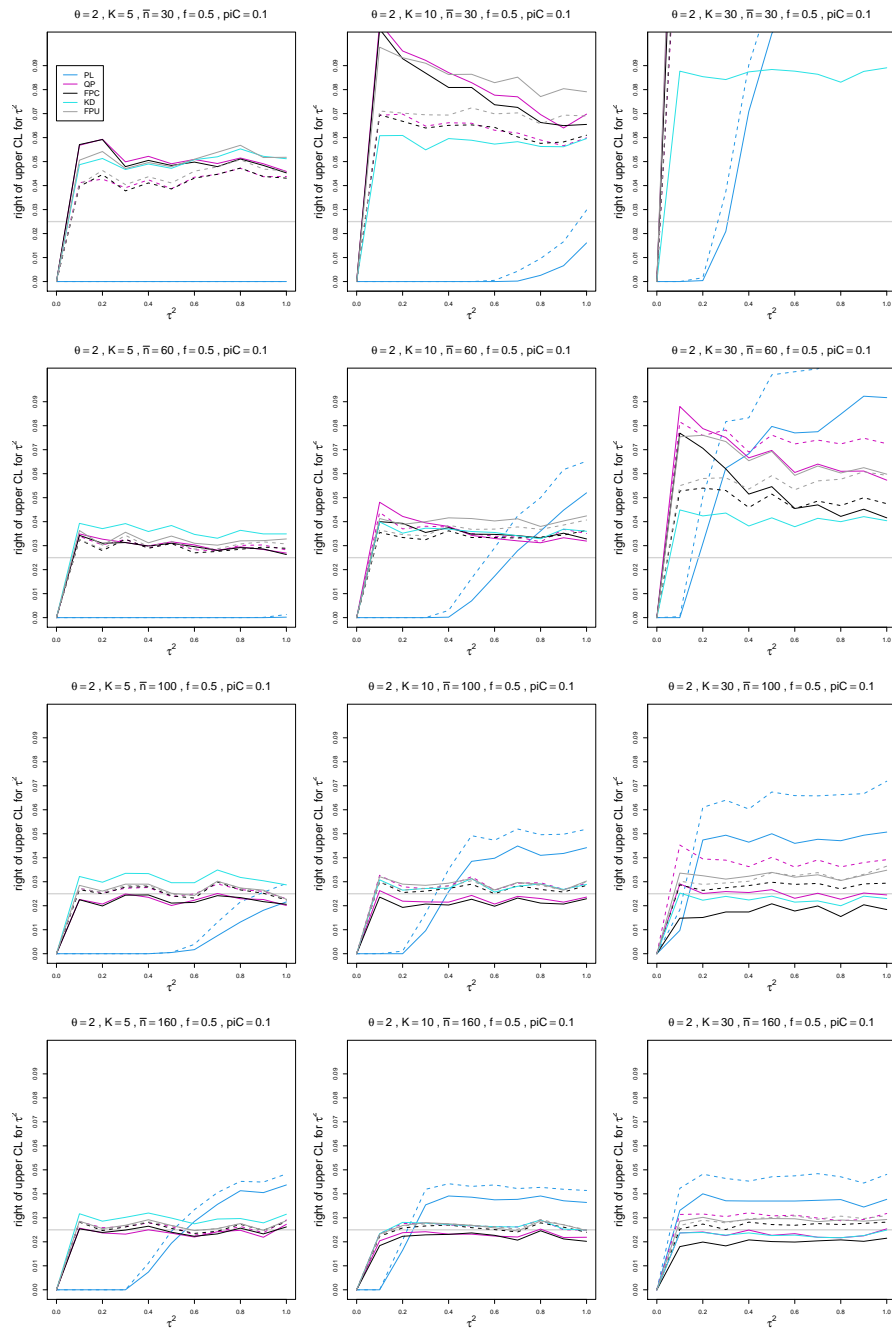


Figure E.12: Miss-right probability of PL, QP, KD, FPC, and FPU 95% confidence intervals for between-study variance of LOR vs τ^2 , for unequal sample sizes $\bar{n} = 30, 60, 100$ and 160 , $p_{iC} = .1$, $\theta = 2$ and $f = 0.5$. Solid lines: PL, QP, and FPC “only”, FPU model-based, and KD. Dashed lines: PL, QP, and FPC “always” and FPU naïve.

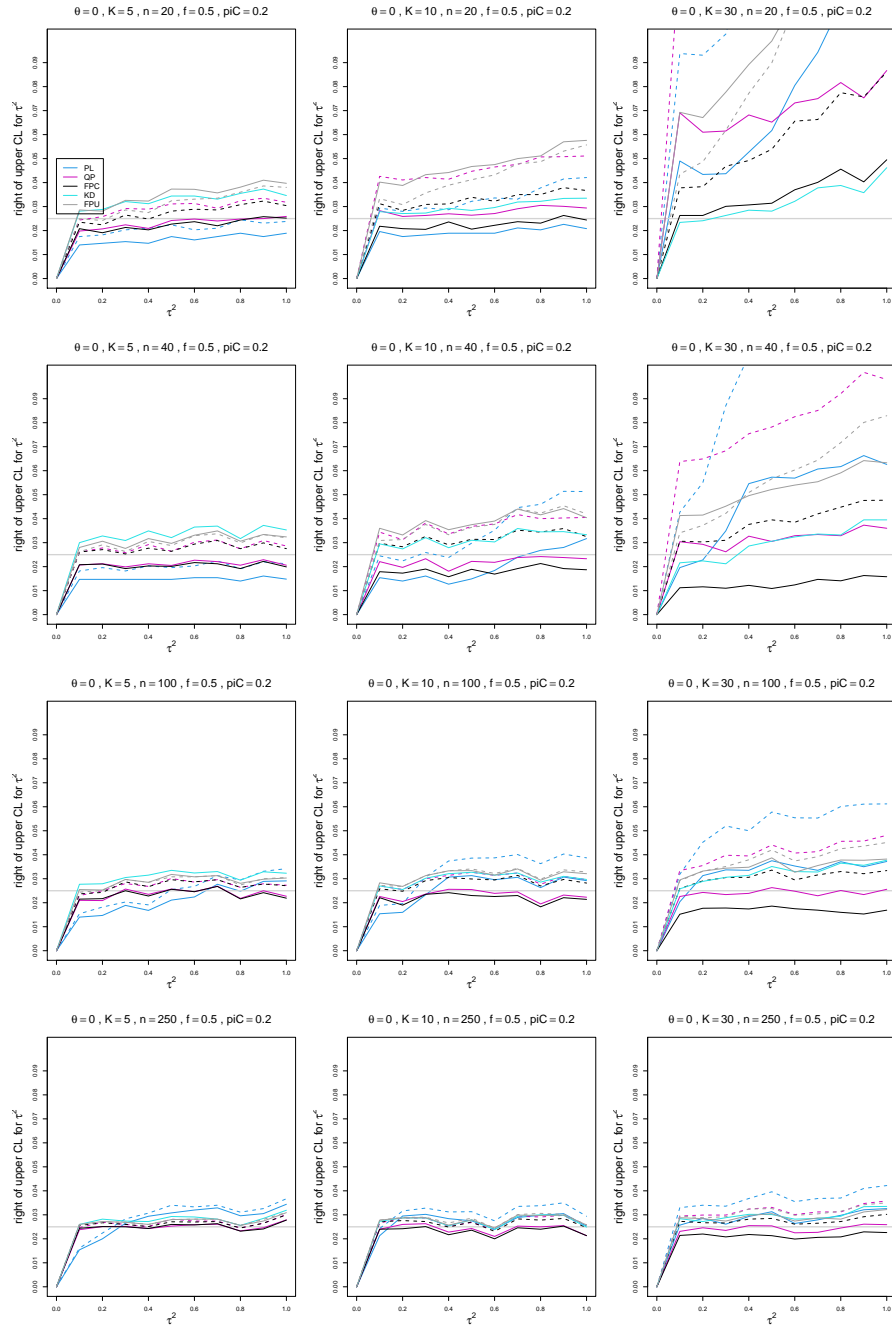


Figure E.13: Miss-right probability of PL, QP, KD, FPC, and FPU 95% confidence intervals for between-study variance of LOR vs τ^2 , for equal sample sizes $n = 20, 40, 100$ and 250 , $\text{piC} = .2$, $\theta = 0$ and $f = 0.5$. Solid lines: PL, QP, and FPC “only”, FPU model-based, and KD. Dashed lines: PL, QP and FPC “always” and FPU naïve.

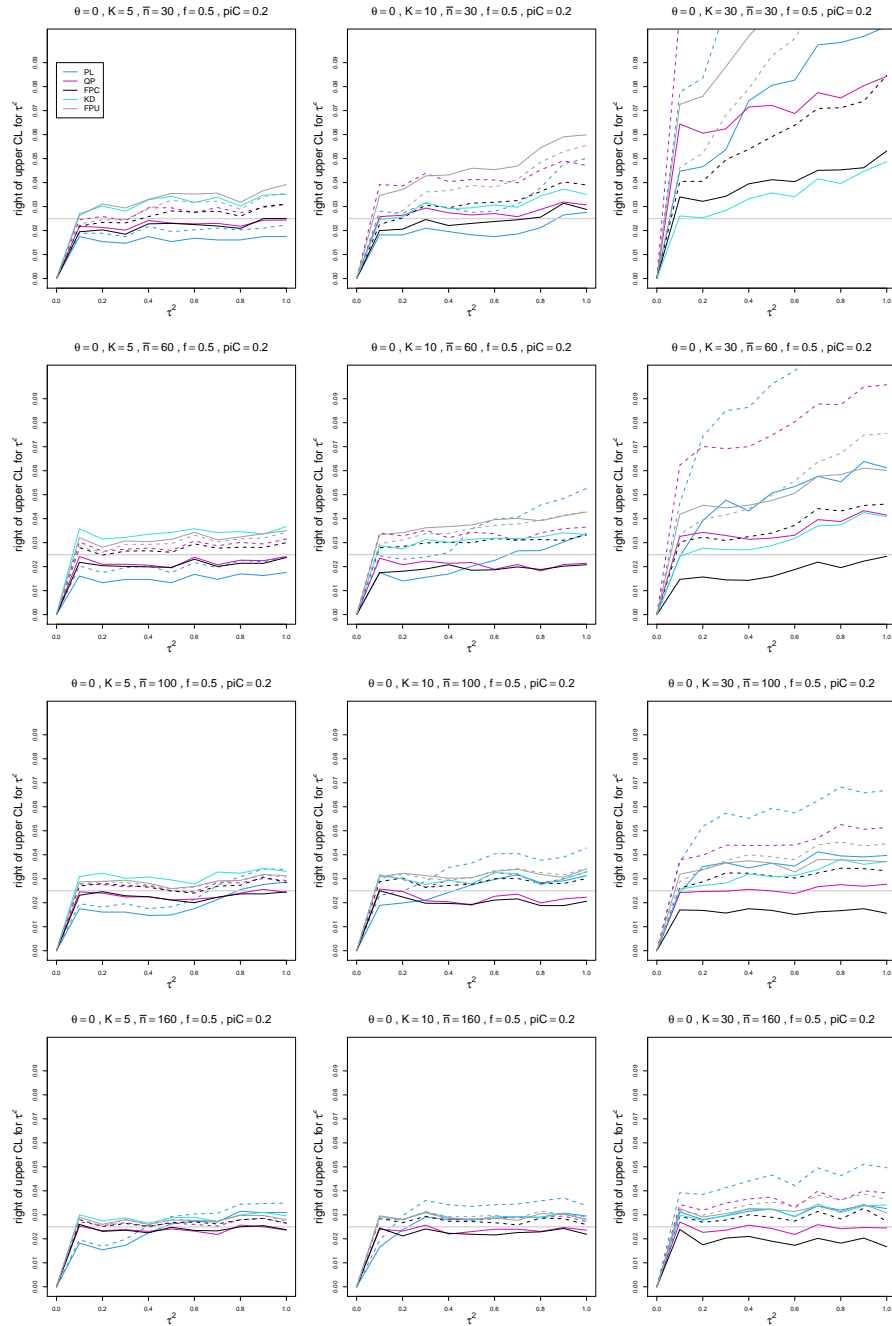


Figure E.14: Miss-right probability of PL, QP, KD, FPC, and FPU 95% confidence intervals for between-study variance of LOR vs τ^2 , for unequal sample sizes $\bar{n} = 30, 60, 100$ and 160 , $p_{iC} = .2$, $\theta = 0$ and $f = 0.5$. Solid lines: PL, QP, and FPC “only”, FPU model-based, and KD. Dashed lines: PL, QP, and FPC “always” and FPU naïve.

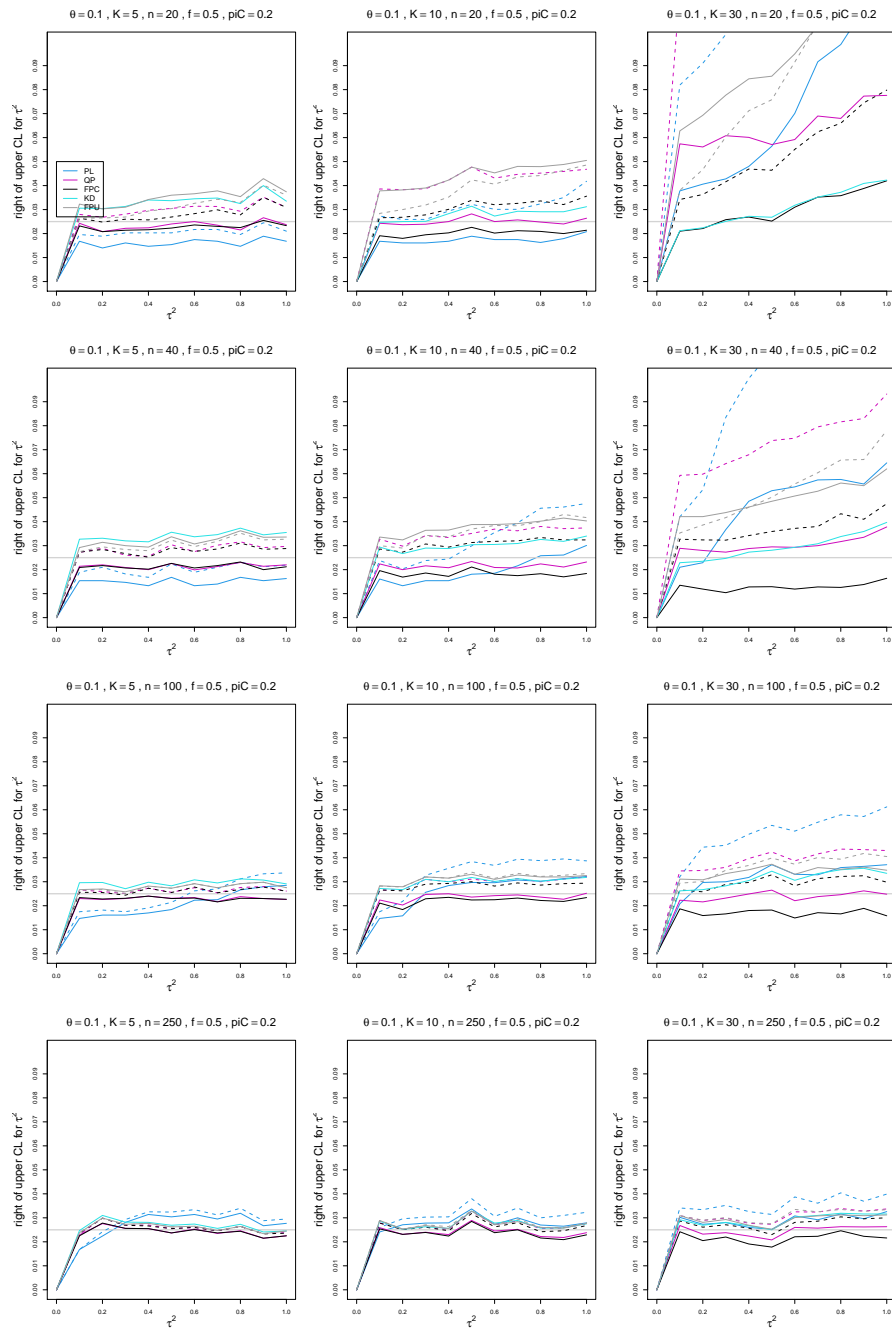


Figure E.15: Miss-right probability of PL, QP, KD, FPC, and FPU 95% confidence intervals for between-study variance of LOR vs τ^2 , for equal sample sizes $n = 20, 40, 100$ and 250 , $piC = .2$, $\theta = 0.1$ and $f = 0.5$. Solid lines: PL, QP, and FPC “only”, FPU model-based, and KD. Dashed lines: PL, QP and FPC “always” and FPU naïve.

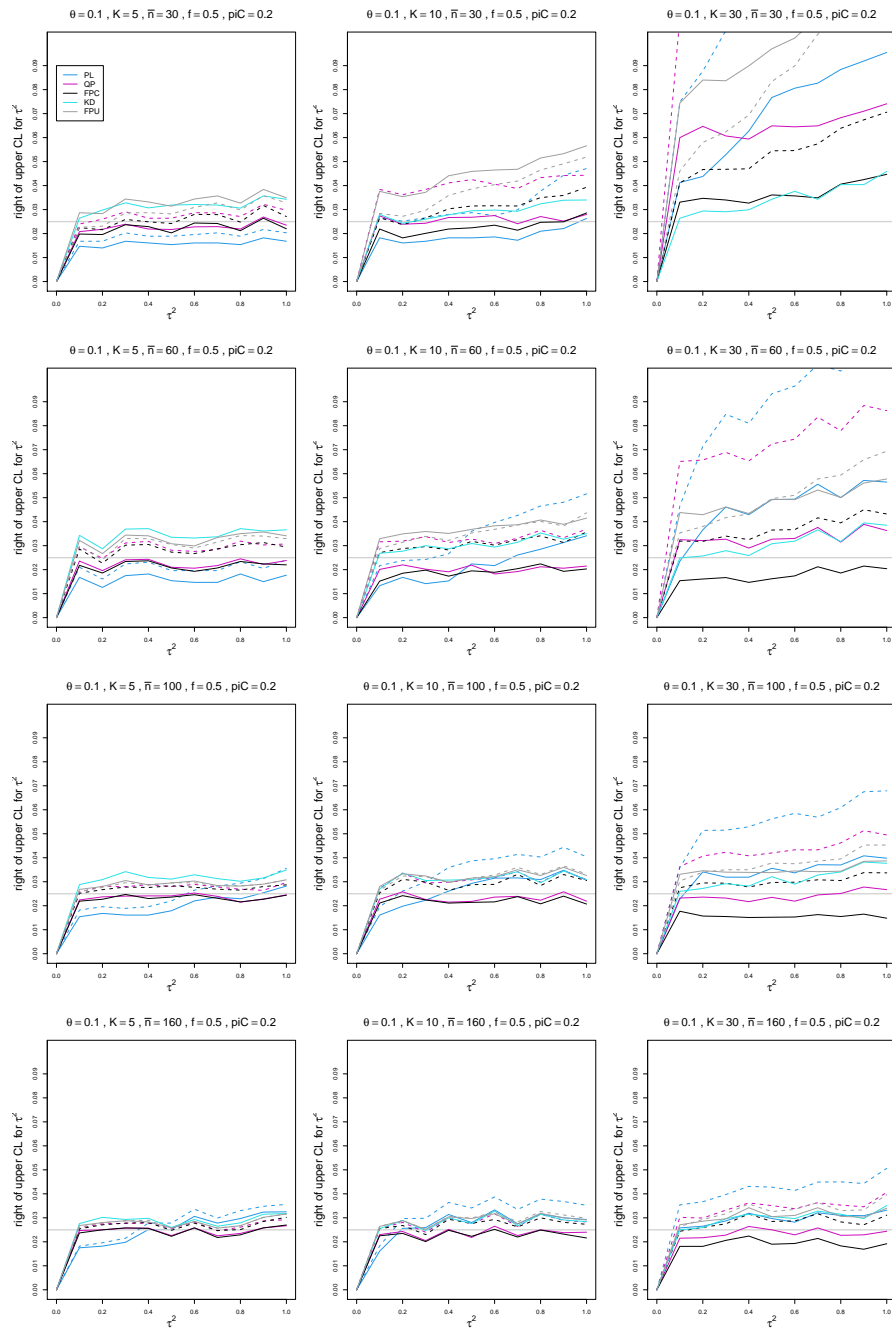


Figure E.16: Miss-right probability of PL, QP, KD, FPC, and FPU 95% confidence intervals for between-study variance of LOR vs τ^2 , for unequal sample sizes $\bar{n} = 30, 60, 100$ and 160 , $piC = .2$, $\theta = 0.1$ and $f = 0.5$. Solid lines: PL, QP, and FPC “only”, FPU model-based, and KD. Dashed lines: PL, QP, and FPC “always” and FPU naive.

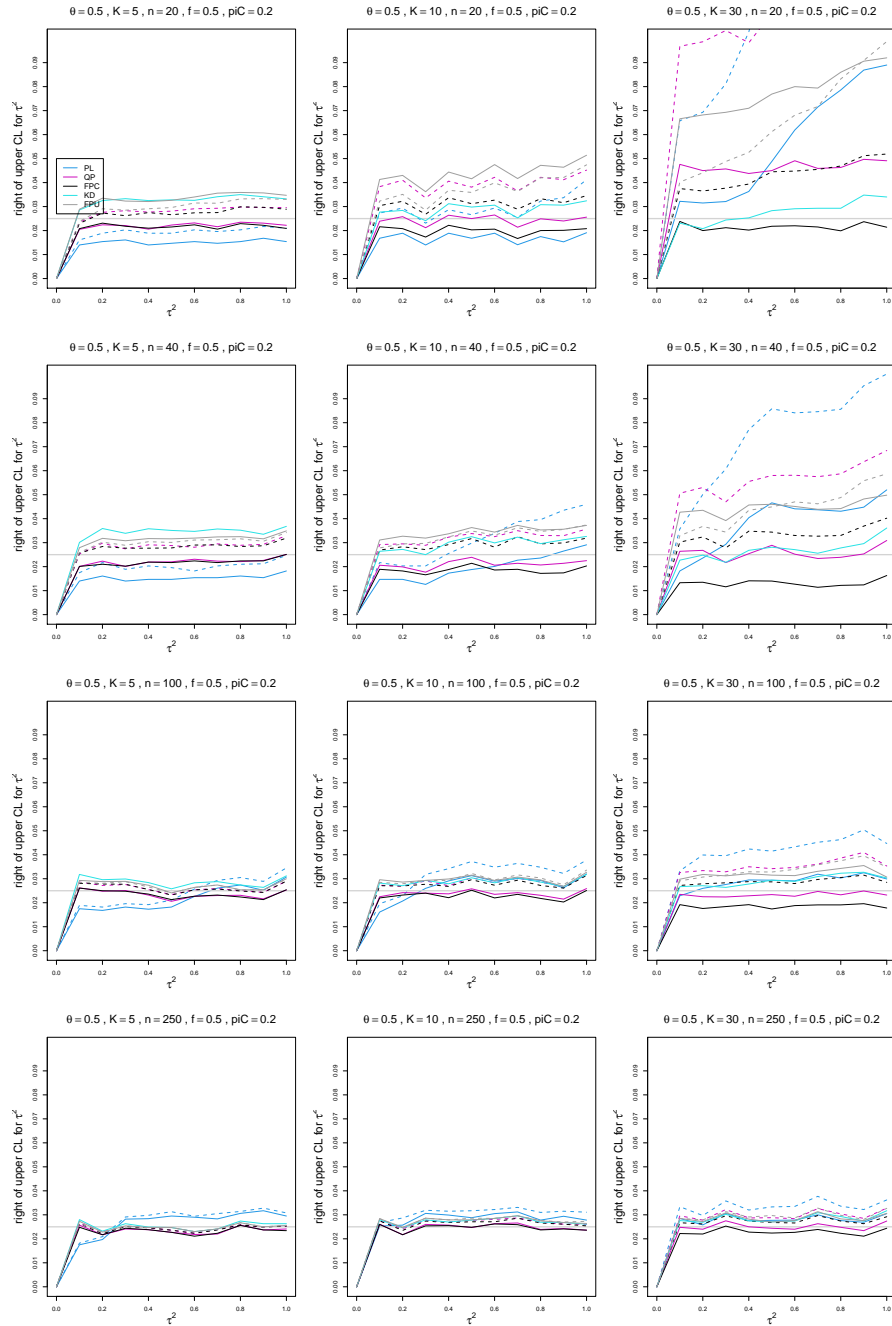


Figure E.17: Miss-right probability of PL, QP, KD, FPC, and FPU 95% confidence intervals for between-study variance of LOR vs τ^2 , for equal sample sizes $n = 20, 40, 100$ and 250 , $p_{iC} = .2$, $\theta = 0.5$ and $f = 0.5$. Solid lines: PL, QP, and FPC “only”, FPU model-based, and KD. Dashed lines: PL, QP and FPC “always” and FPU naïve.

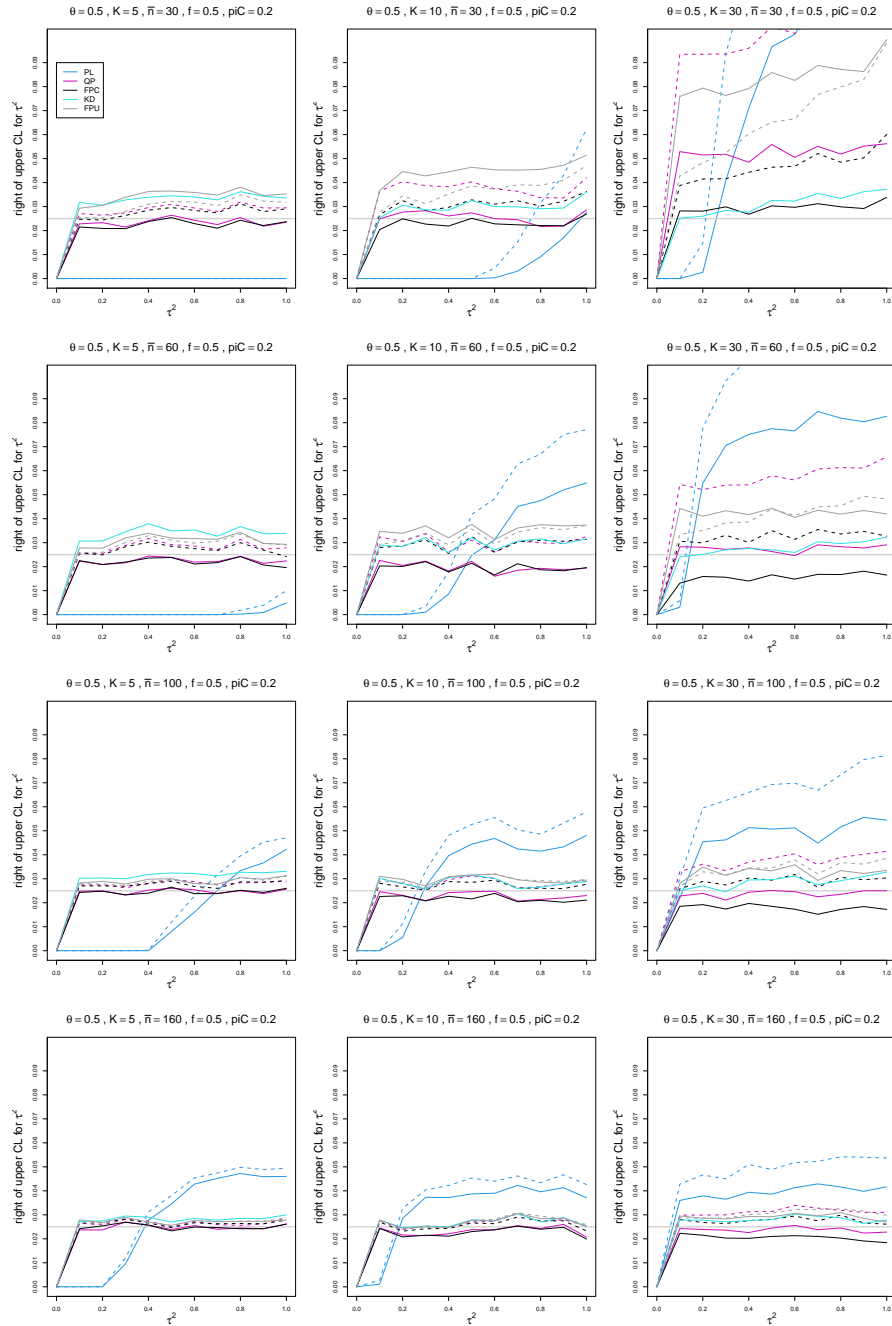


Figure E.18: Miss-right probability of PL, QP, KD, FPC, and FPU 95% confidence intervals for between-study variance of LOR vs τ^2 , for unequal sample sizes $\bar{n} = 30, 60, 100$ and 160 , $p_{iC} = .2$, $\theta = 0.5$ and $f = 0.5$. Solid lines: PL, QP, and FPC “only”, FPU model-based, and KD. Dashed lines: PL, QP, and FPC “always” and FPU naïve.

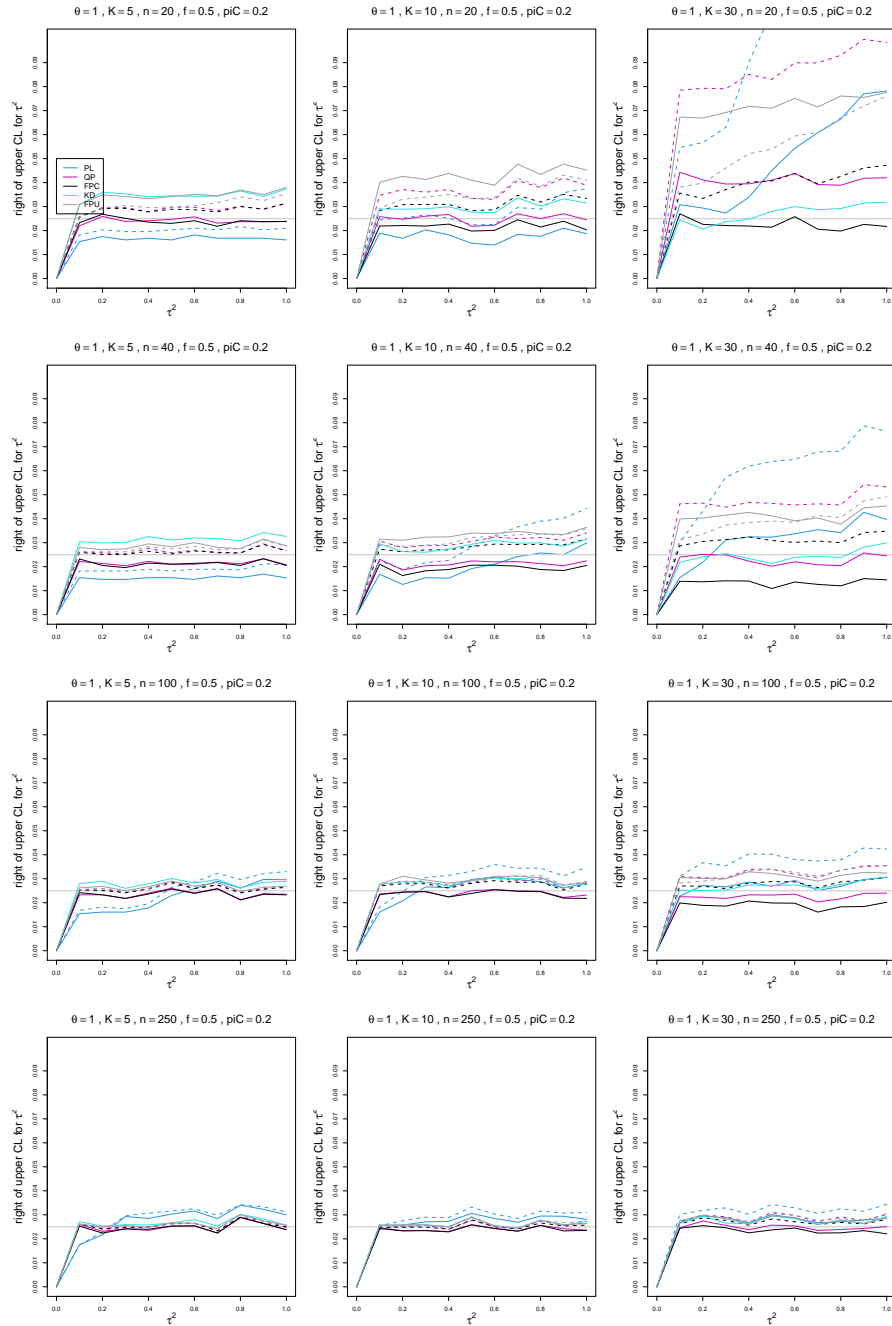


Figure E.19: Miss-right probability of PL, QP, KD, FPC, and FPU 95% confidence intervals for between-study variance of LOR vs τ^2 , for equal sample sizes $n = 20, 40, 100$ and 250 , $p_{iC} = .2$, $\theta = 1$ and $f = 0.5$. Solid lines: PL, QP, and FPC “only”, FPU model-based, and KD. Dashed lines: PL, QP and FPC “always” and FPU naïve.

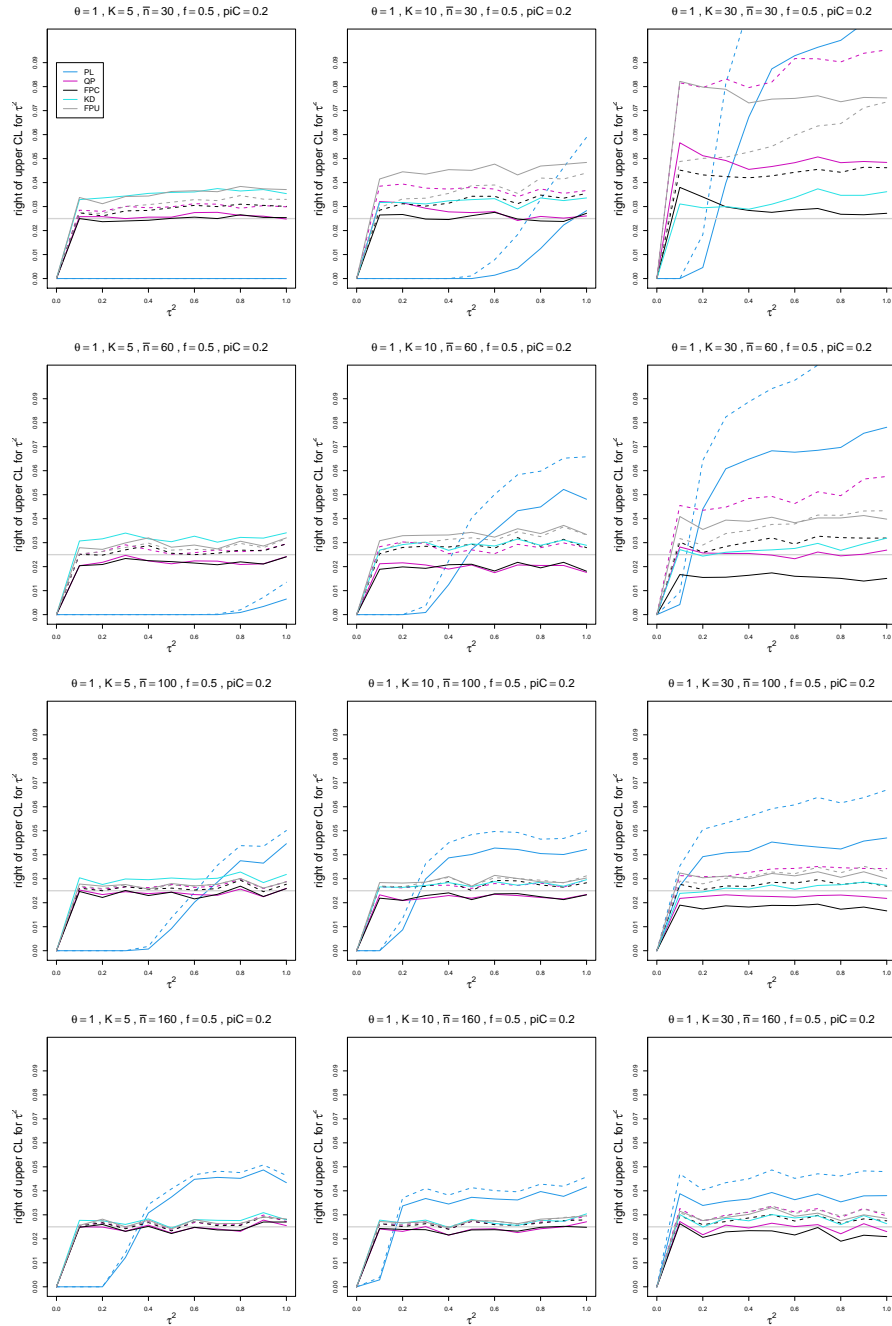


Figure E.20: Miss-right probability of PL, QP, KD, FPC, and FPU 95% confidence intervals for between-study variance of LOR vs τ^2 , for unequal sample sizes $\bar{n} = 30, 60, 100$ and 160 , $p_{iC} = .2$, $\theta = 1$ and $f = 0.5$. Solid lines: PL, QP, and FPC “only”, FPU model-based, and KD. Dashed lines: PL, QP, and FPC “always” and FPU naïve.

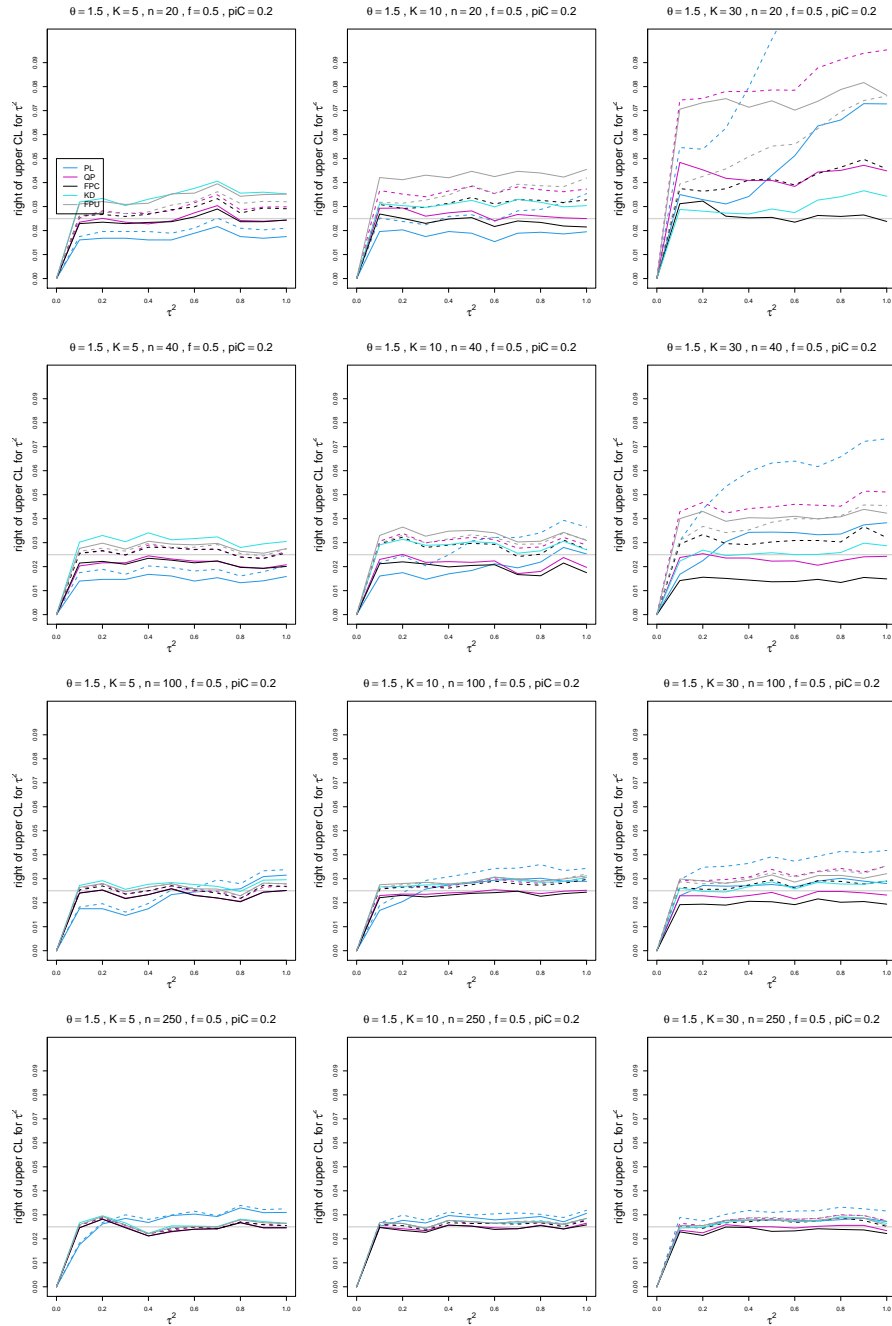


Figure E.21: Miss-right probability of PL, QP, KD, FPC, and FPU 95% confidence intervals for between-study variance of LOR vs τ^2 , for equal sample sizes $n = 20, 40, 100$ and 250 , $piC = .2$, $\theta = 1.5$ and $f = 0.5$. Solid lines: PL, QP, and FPC “only”, FPU model-based, and KD. Dashed lines: PL, QP and FPC “always” and FPU naïve.

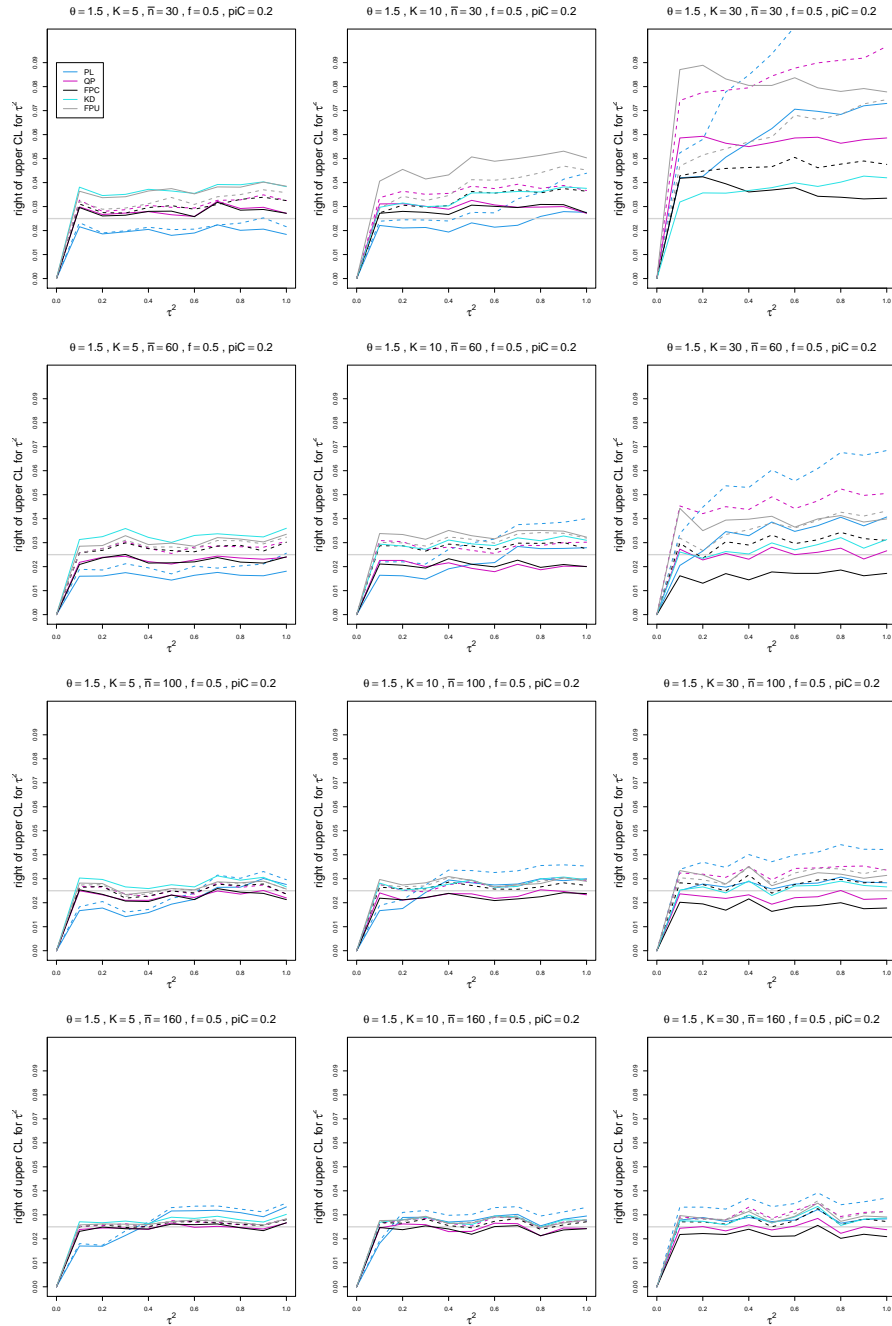


Figure E.22: Miss-right probability of PL, QP, KD, FPC, and FPU 95% confidence intervals for between-study variance of LOR vs τ^2 , for unequal sample sizes $\bar{n} = 30, 60, 100$ and 160 , $piC = .2$, $\theta = 1.5$ and $f = 0.5$. Solid lines: PL, QP, and FPC “only”, FPU model-based, and KD. Dashed lines: PL, QP, and FPC “always” and FPU naïve.

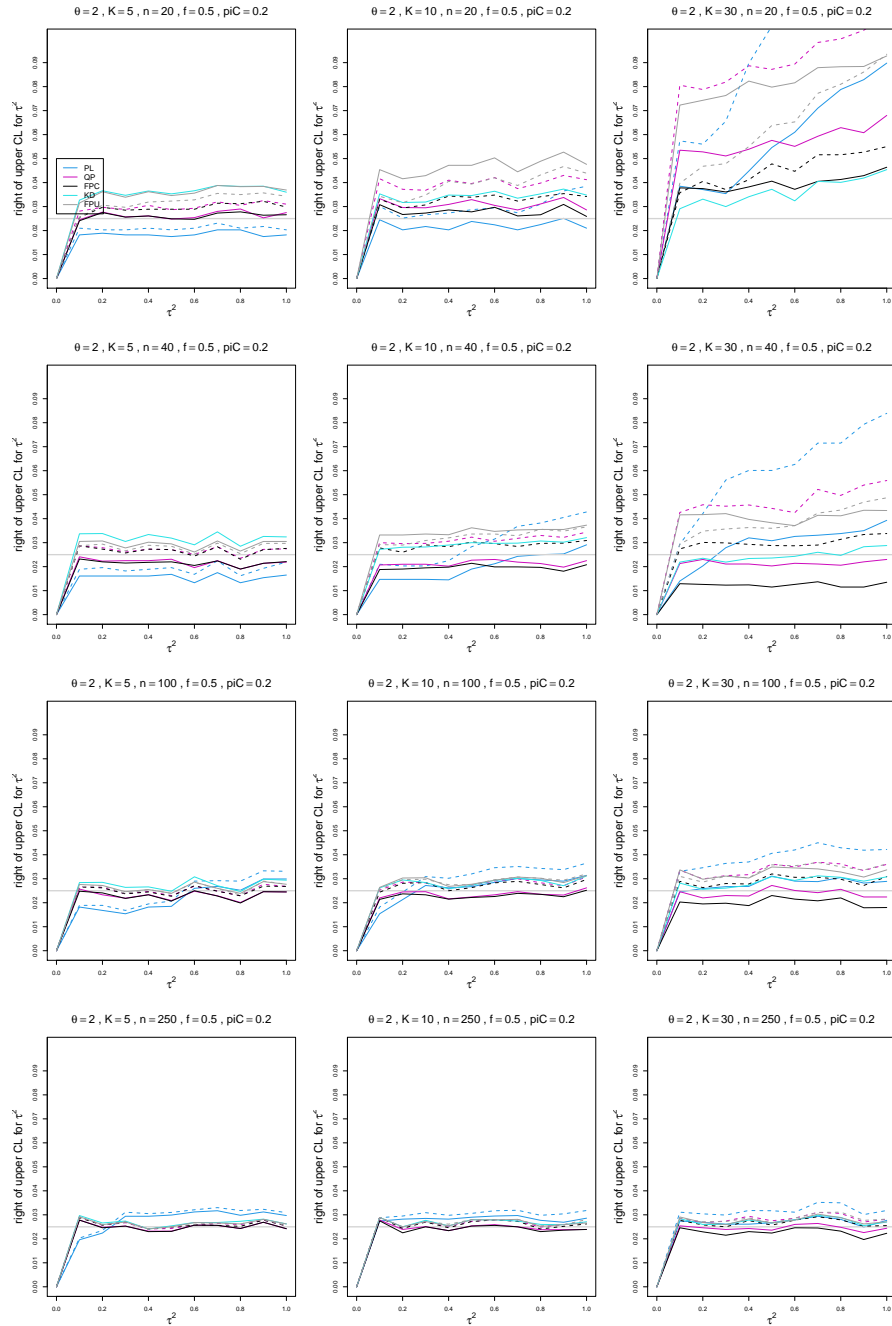


Figure E.23: Miss-right probability of PL, QP, KD, FPC, and FPU 95% confidence intervals for between-study variance of LOR vs τ^2 , for equal sample sizes $n = 20, 40, 100$ and 250 , $p_{iC} = .2$, $\theta = 2$ and $f = 0.5$. Solid lines: PL, QP, and FPC “only”, FPU model-based, and KD. Dashed lines: PL, QP and FPC “always” and FPU naïve.

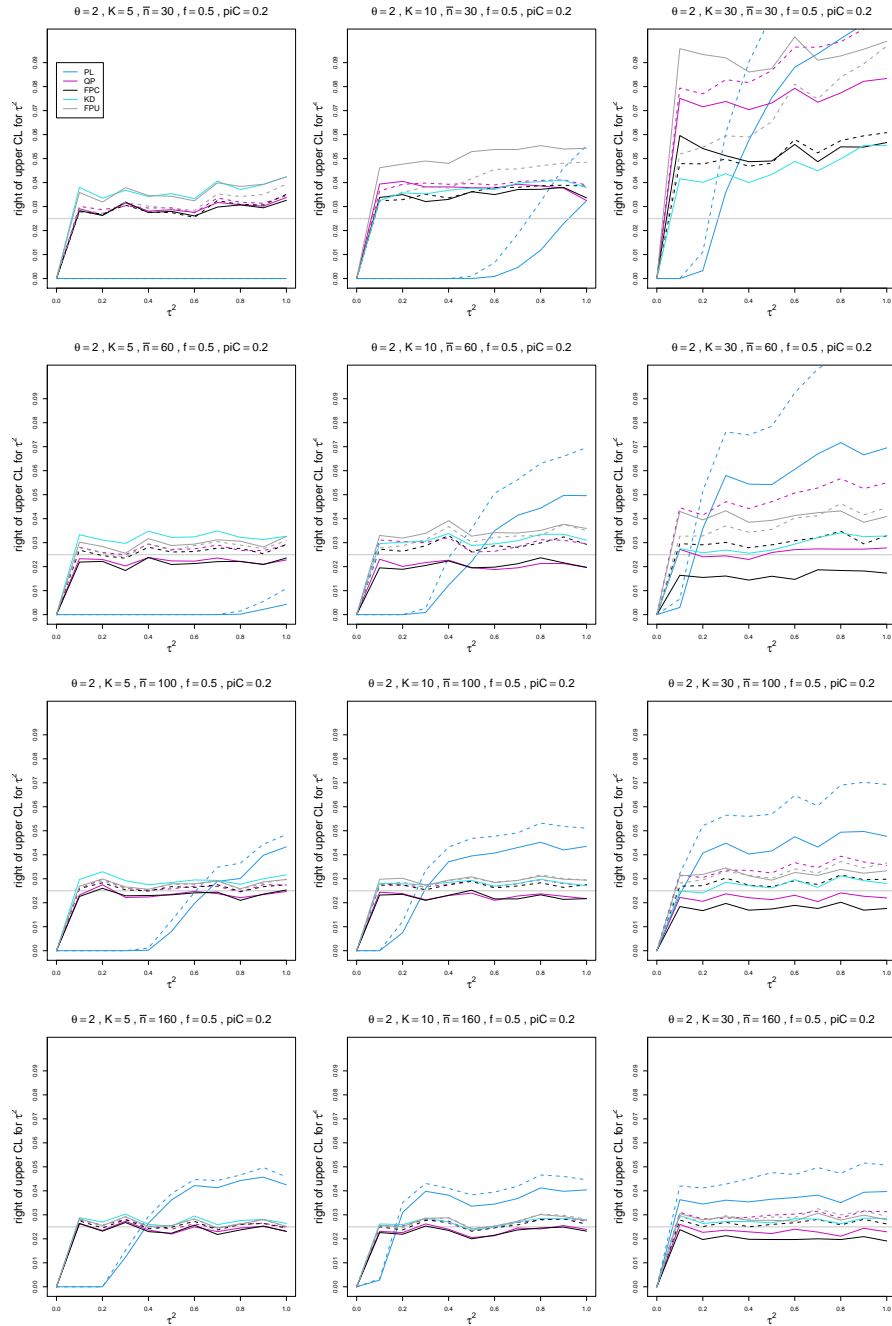


Figure E.24: Miss-right probability of PL, QP, KD, FPC, and FPU 95% confidence intervals for between-study variance of LOR vs τ^2 , for unequal sample sizes $\bar{n} = 30, 60, 100$ and $160, p_{iC} = .2, \theta = 2$ and $f = 0.5$. Solid lines: PL, QP, and FPC “only”, FPU model-based, and KD. Dashed lines: PL, QP, and FPC “always” and FPU naïve.

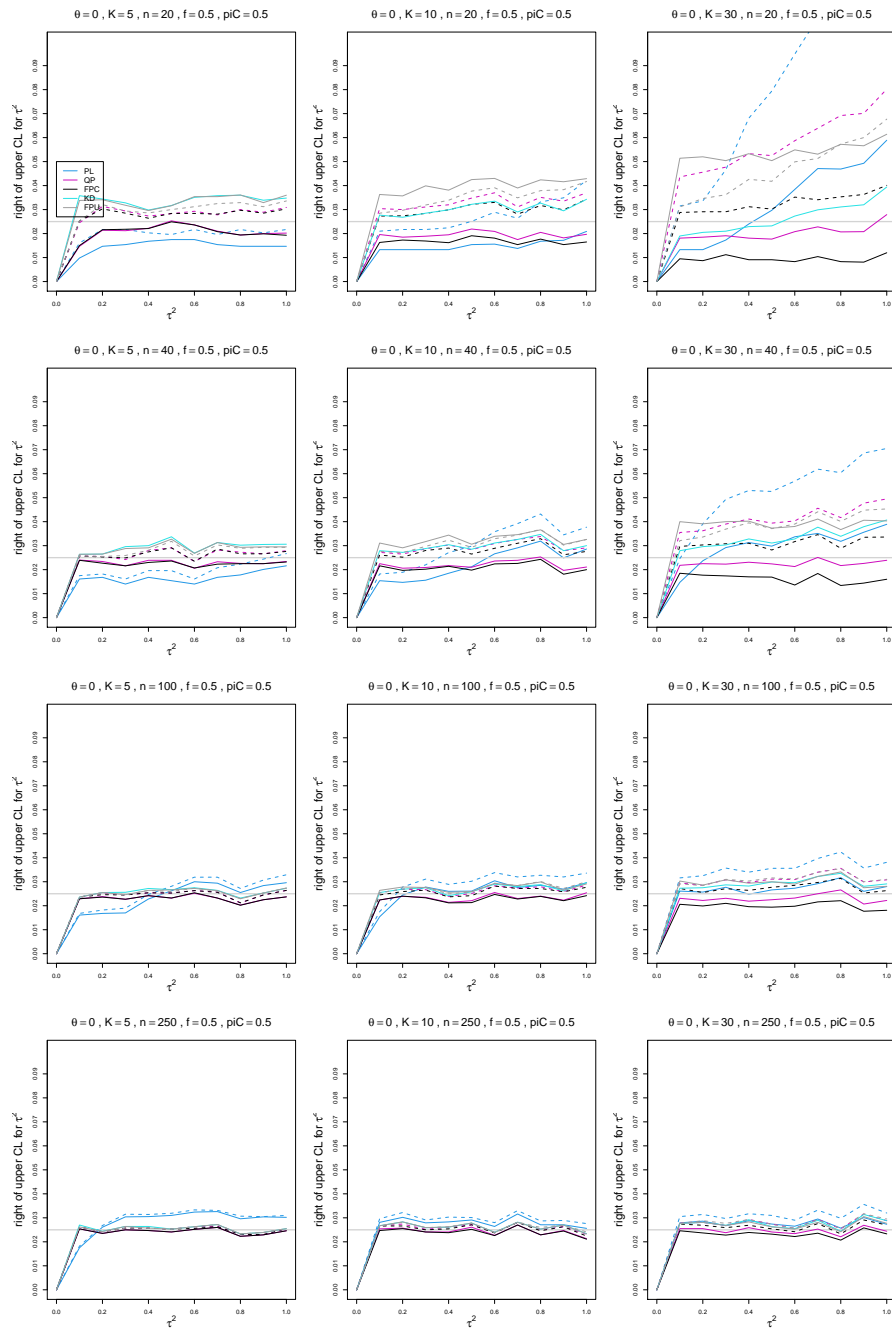


Figure E.25: Miss-right probability of PL, QP, KD, FPC, and FPU 95% confidence intervals for between-study variance of LOR vs τ^2 , for equal sample sizes $n = 20, 40, 100$ and 250 , $piC = .5$, $\theta = 0$ and $f = 0.5$. Solid lines: PL, QP, and FPC “only”, FPU model-based, and KD. Dashed lines: PL, QP and FPC “always” and FPU naïve.

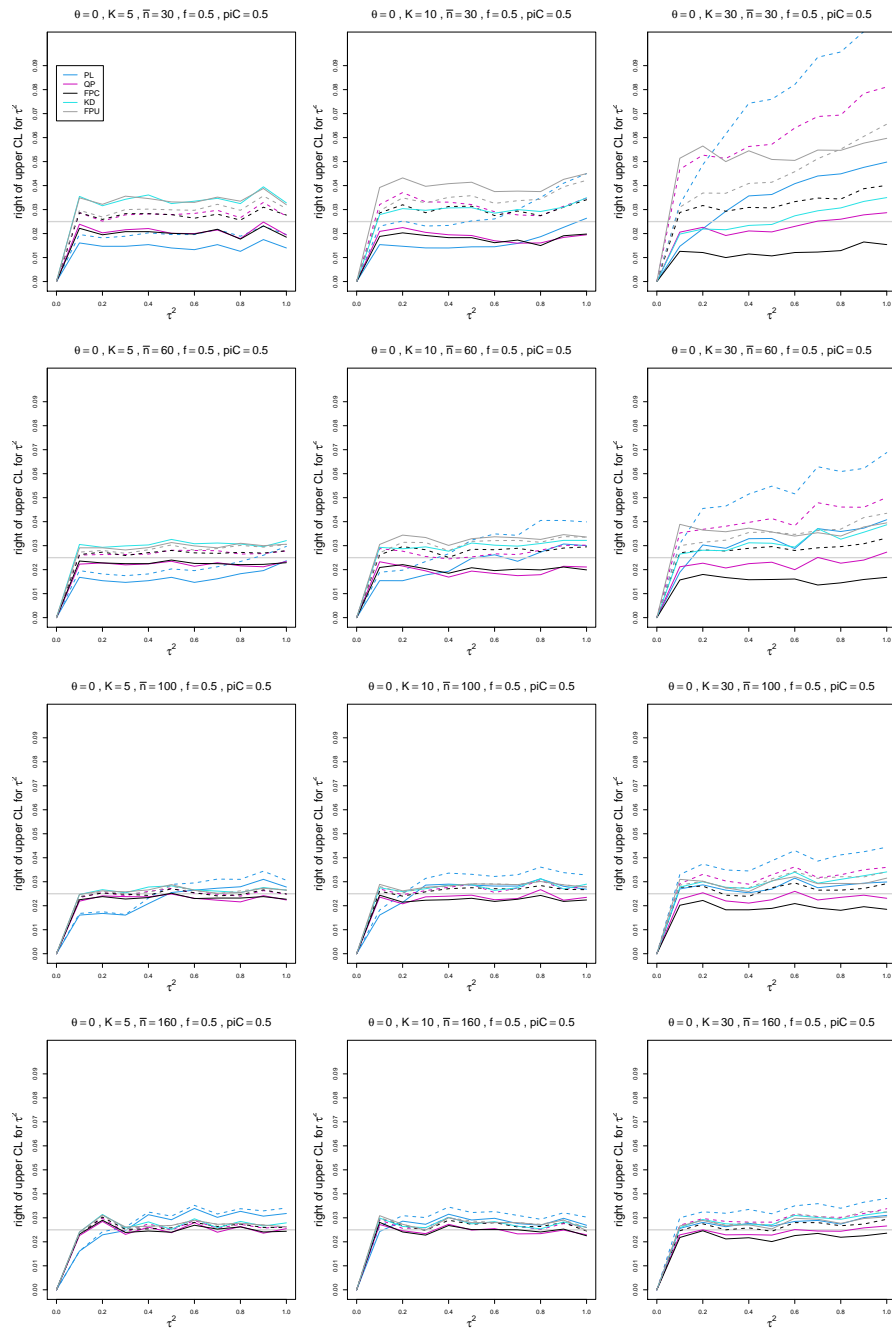


Figure E.26: Miss-right probability of PL, QP, KD, FPC, and FPU 95% confidence intervals for between-study variance of LOR vs τ^2 , for unequal sample sizes $\bar{n} = 30, 60, 100$ and 160 , $p_{iC} = .5$, $\theta = 0$ and $f = 0.5$. Solid lines: PL, QP, and FPC “only”, FPU model-based, and KD. Dashed lines: PL, QP, and FPC “always” and FPU naïve.

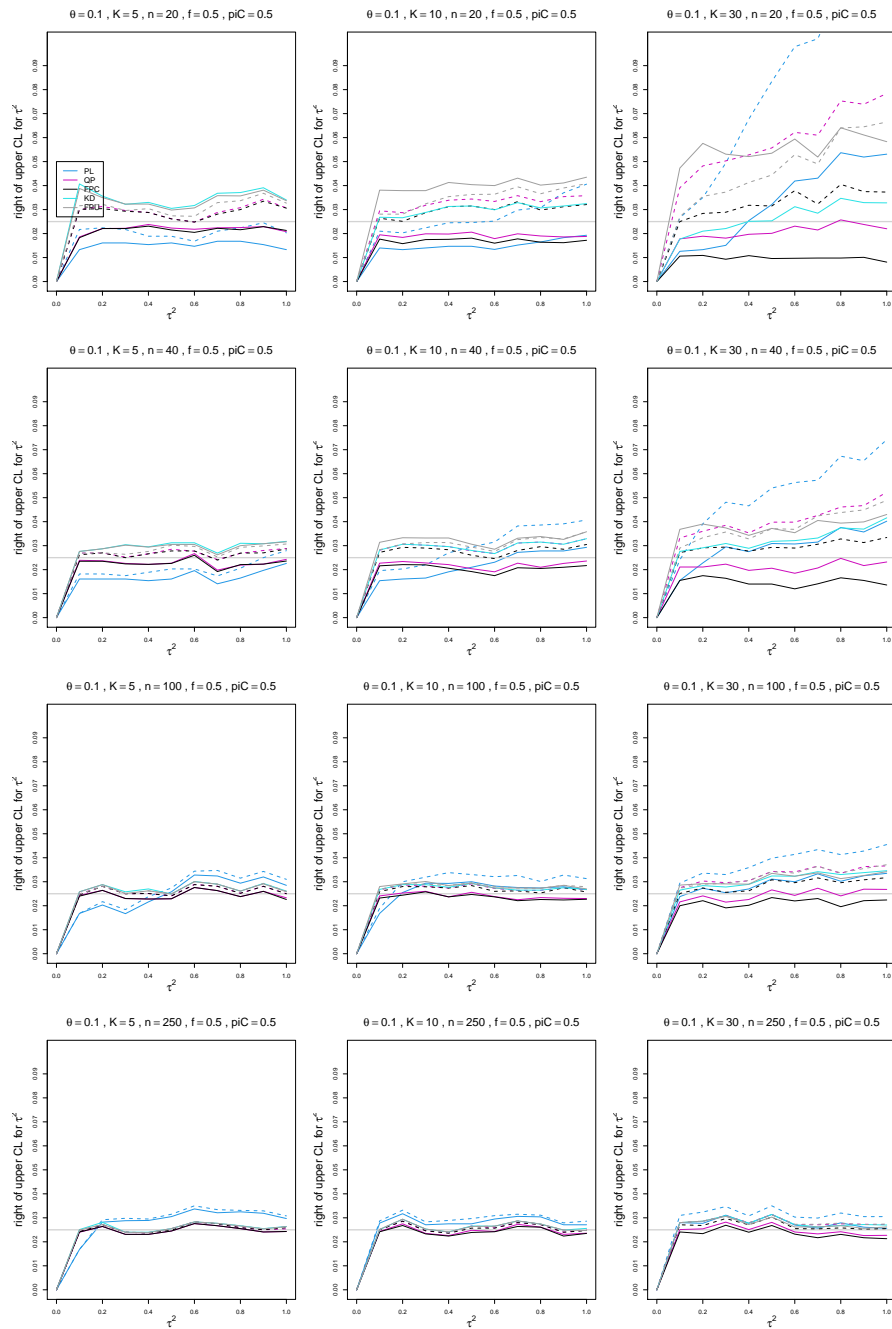


Figure E.27: Miss-right probability of PL, QP, KD, FPC, and FPU 95% confidence intervals for between-study variance of LOR vs τ^2 , for equal sample sizes $n = 20, 40, 100$ and 250 , $piC = .5$, $\theta = 0.1$ and $f = 0.5$. Solid lines: PL, QP, and FPC “only”, FPU model-based, and KD. Dashed lines: PL, QP and FPC “always” and FPU naïve.

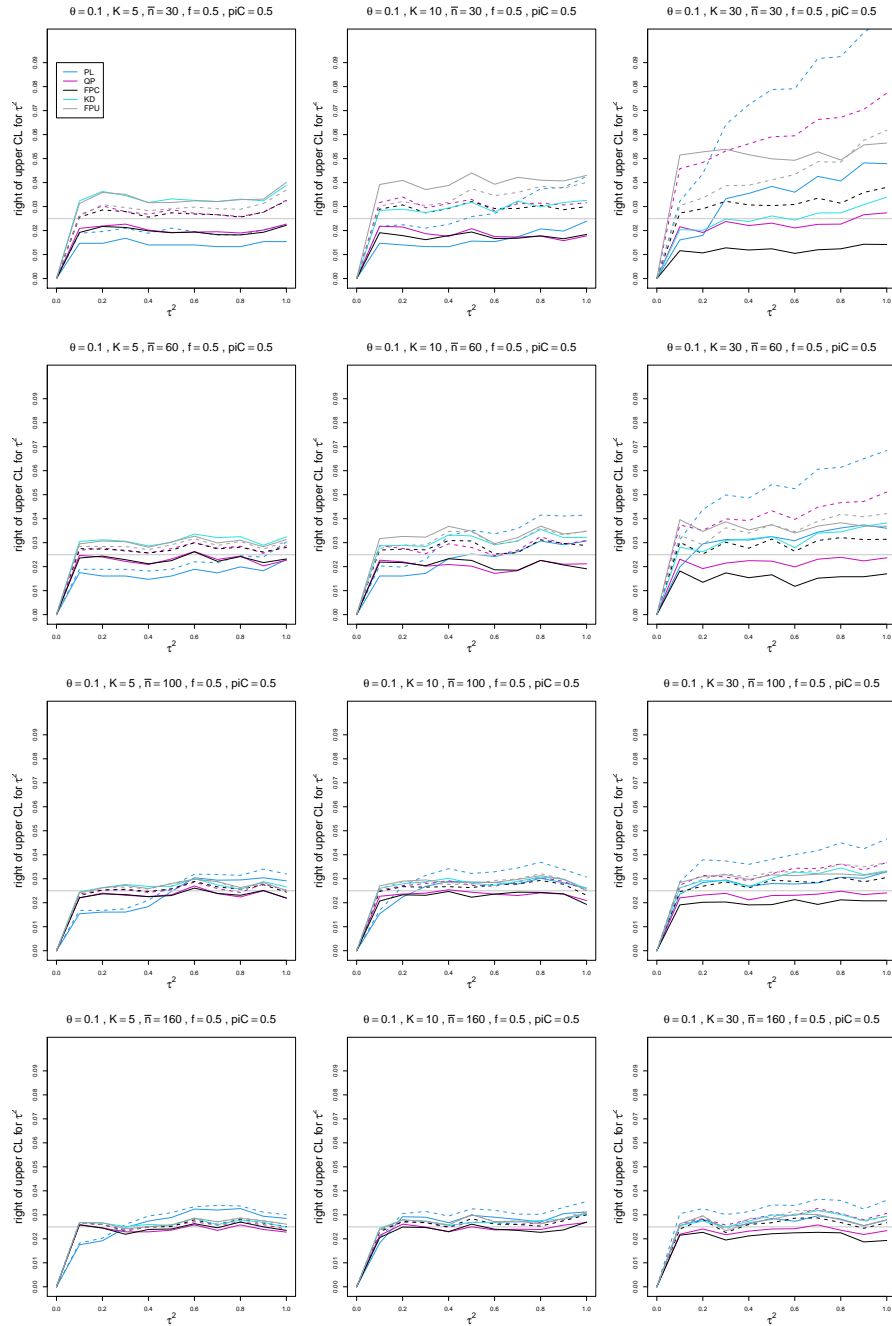


Figure E.28: Miss-right probability of PL, QP, KD, FPC, and FPU 95% confidence intervals for between-study variance of LOR vs τ^2 , for unequal sample sizes $\bar{n} = 30, 60, 100$ and 160 , $p_{iC} = .5$, $\theta = 0.1$ and $f = 0.5$. Solid lines: PL, QP, and FPC “only”, FPU model-based, and KD. Dashed lines: PL, QP, and FPC “always” and FPU naïve.

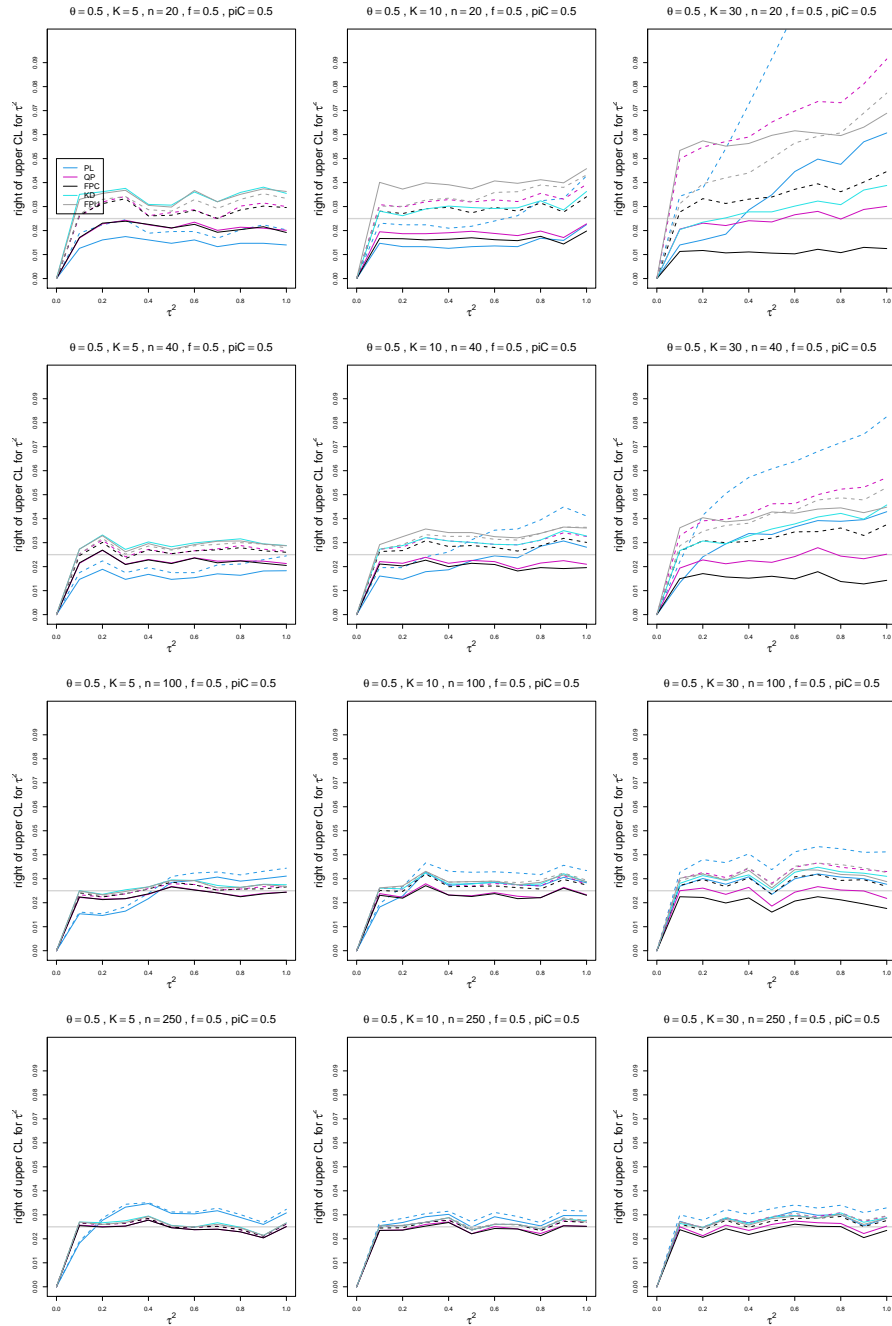


Figure E.29: Miss-right probability of PL, QP, KD, FPC, and FPU 95% confidence intervals for between-study variance of LOR vs τ^2 , for equal sample sizes $n = 20, 40, 100$ and 250 , $piC = .5$, $\theta = 0.5$ and $f = 0.5$. Solid lines: PL, QP, and FPC “only”, FPU model-based, and KD. Dashed lines: PL, QP and FPC “always” and FPU naïve.

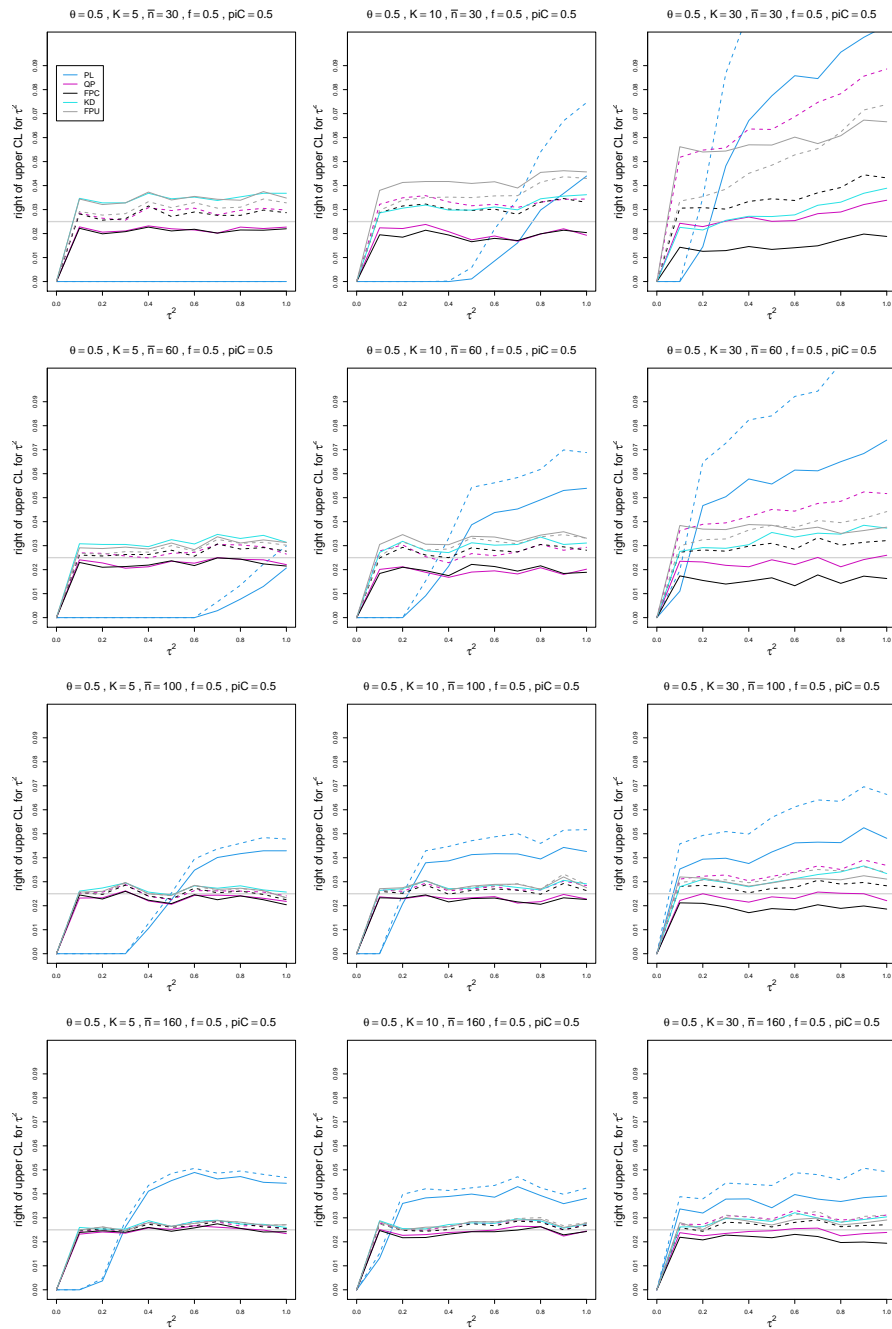


Figure E.30: Miss-right probability of PL, QP, KD, FPC, and FPU 95% confidence intervals for between-study variance of LOR vs τ^2 , for unequal sample sizes $\bar{n} = 30, 60, 100$ and 160 , $\pi_C = .5$, $\theta = 0.5$ and $f = 0.5$. Solid lines: PL, QP, and FPC “only”, FPU model-based, and KD. Dashed lines: PL, QP, and FPC “always” and FPU naïve.

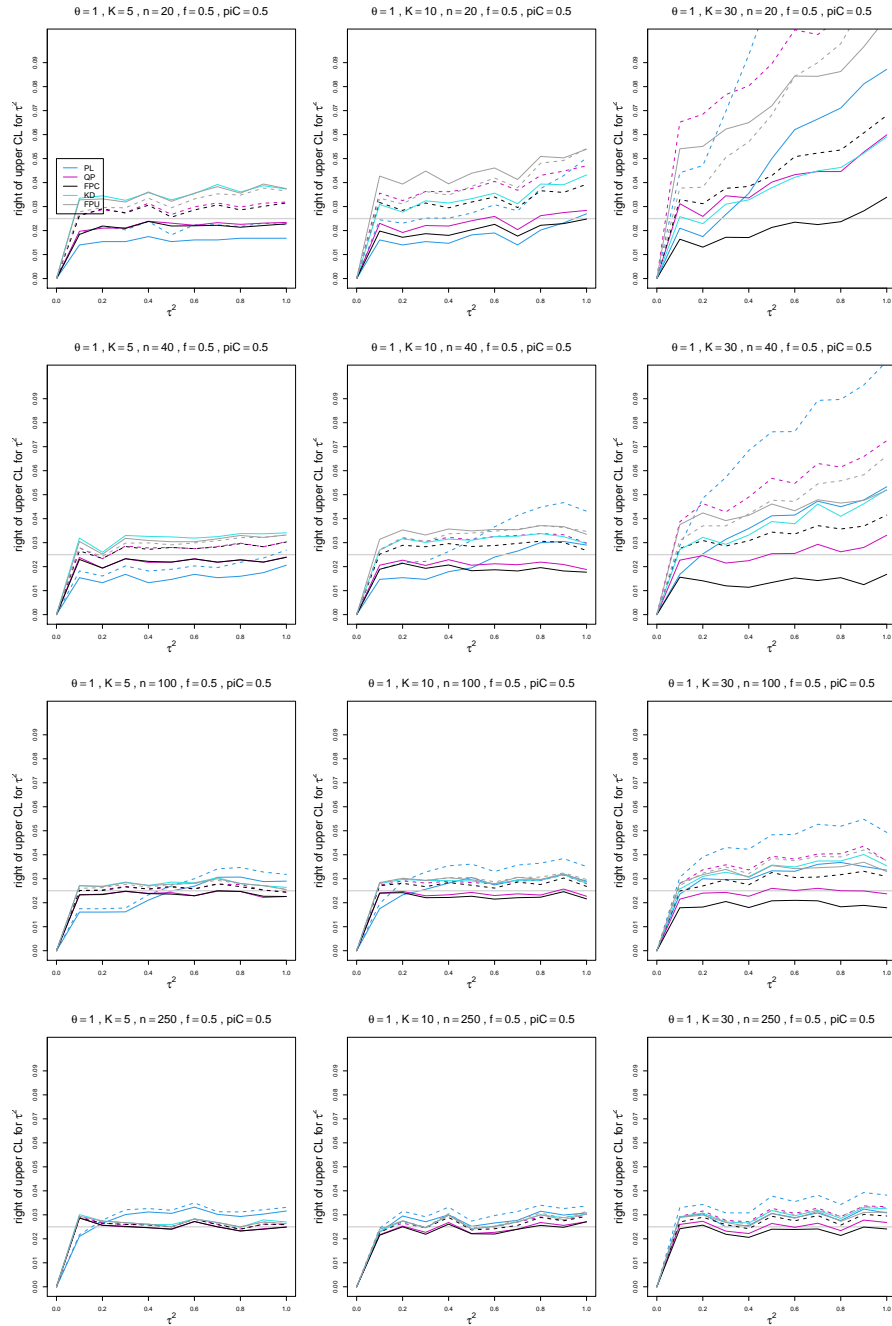


Figure E.31: Miss-right probability of PL, QP, KD, FPC, and FPU 95% confidence intervals for between-study variance of LOR vs τ^2 , for equal sample sizes $n = 20, 40, 100$ and 250 , $p_{iC} = .5$, $\theta = 1$ and $f = 0.5$. Solid lines: PL, QP, and FPC “only”, FPU model-based, and KD. Dashed lines: PL, QP and FPC “always” and FPU naïve.

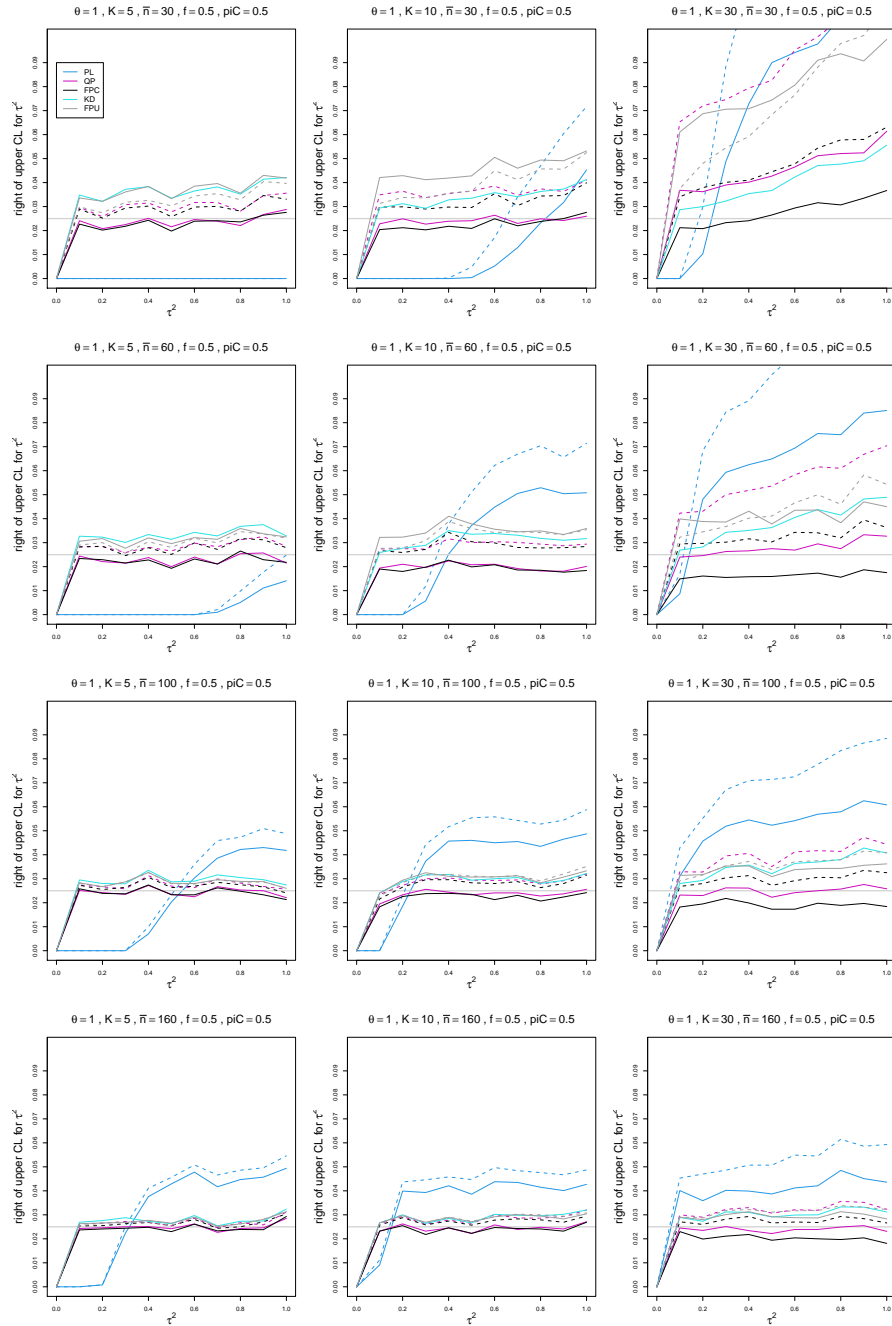


Figure E.32: Miss-right probability of PL, QP, KD, FPC, and FPU 95% confidence intervals for between-study variance of LOR vs τ^2 , for unequal sample sizes $\bar{n} = 30, 60, 100$ and 160 , $p_{iC} = .5$, $\theta = 1$ and $f = 0.5$. Solid lines: PL, QP, and FPC “only”, FPU model-based, and KD. Dashed lines: PL, QP, and FPC “always” and FPU naïve.

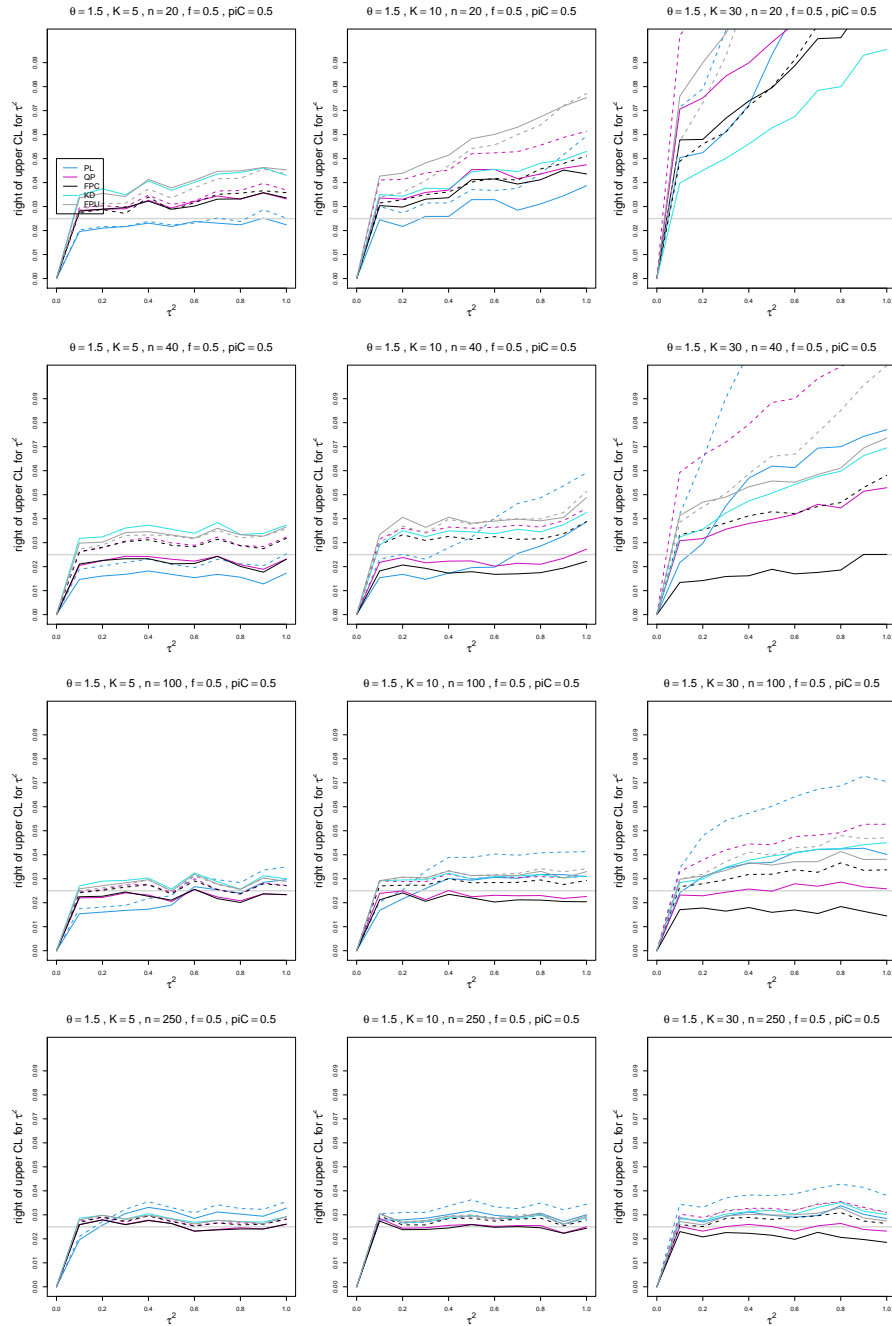


Figure E.33: Miss-right probability of PL, QP, KD, FPC, and FPU 95% confidence intervals for between-study variance of LOR vs τ^2 , for equal sample sizes $n = 20, 40, 100$ and 250 , $piC = .5$, $\theta = 1.5$ and $f = 0.5$. Solid lines: PL, QP, and FPC “only”, FPU model-based, and KD. Dashed lines: PL, QP and FPC “always” and FPU naïve.

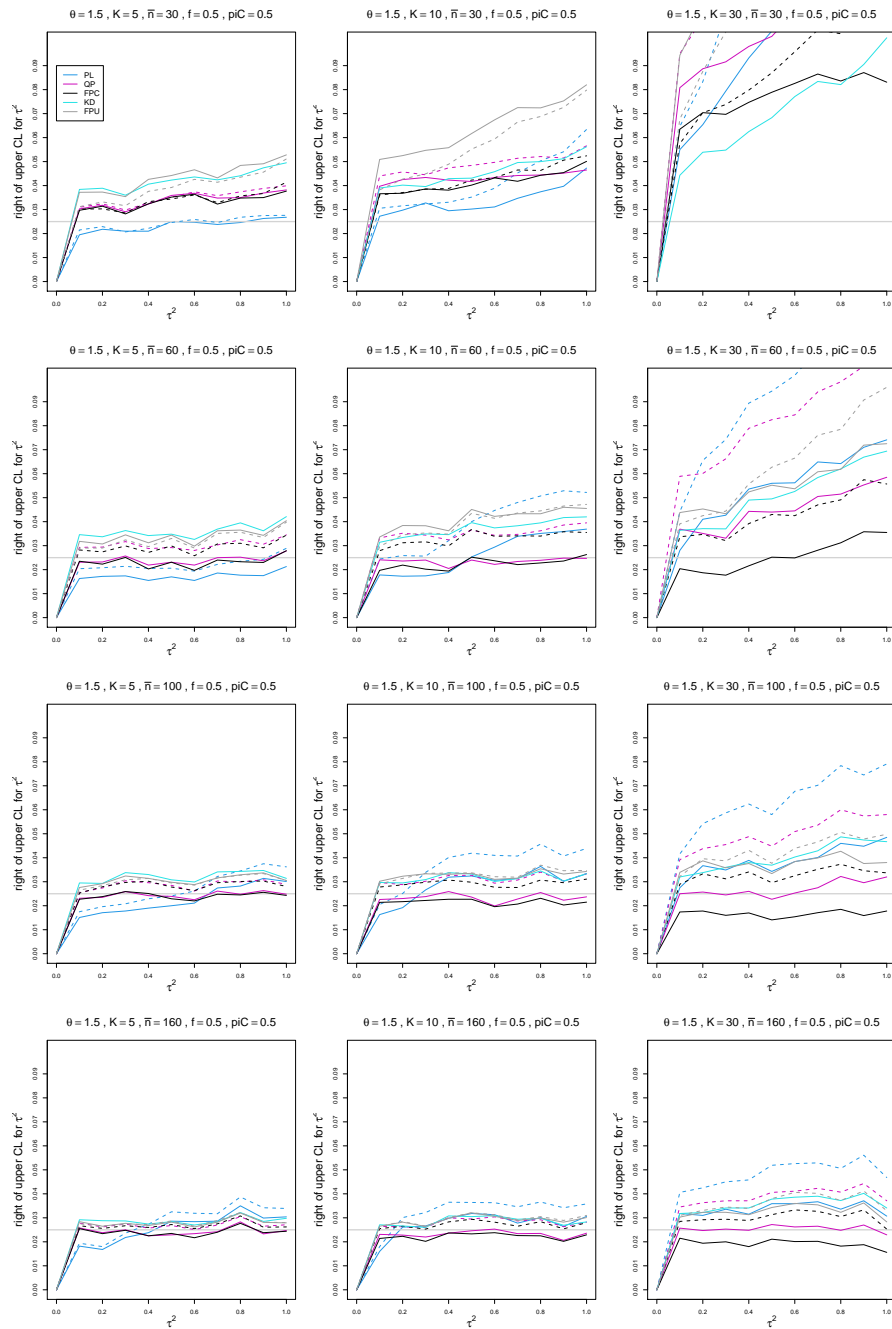


Figure E.34: Miss-right probability of PL, QP, KD, FPC, and FPU 95% confidence intervals for between-study variance of LOR vs τ^2 , for unequal sample sizes $\bar{n} = 30, 60, 100$ and 160 , $p_{iC} = .5$, $\theta = 1.5$ and $f = 0.5$. Solid lines: PL, QP, and FPC “only”, FPU model-based, and KD. Dashed lines: PL, QP, and FPC “always” and FPU naïve.

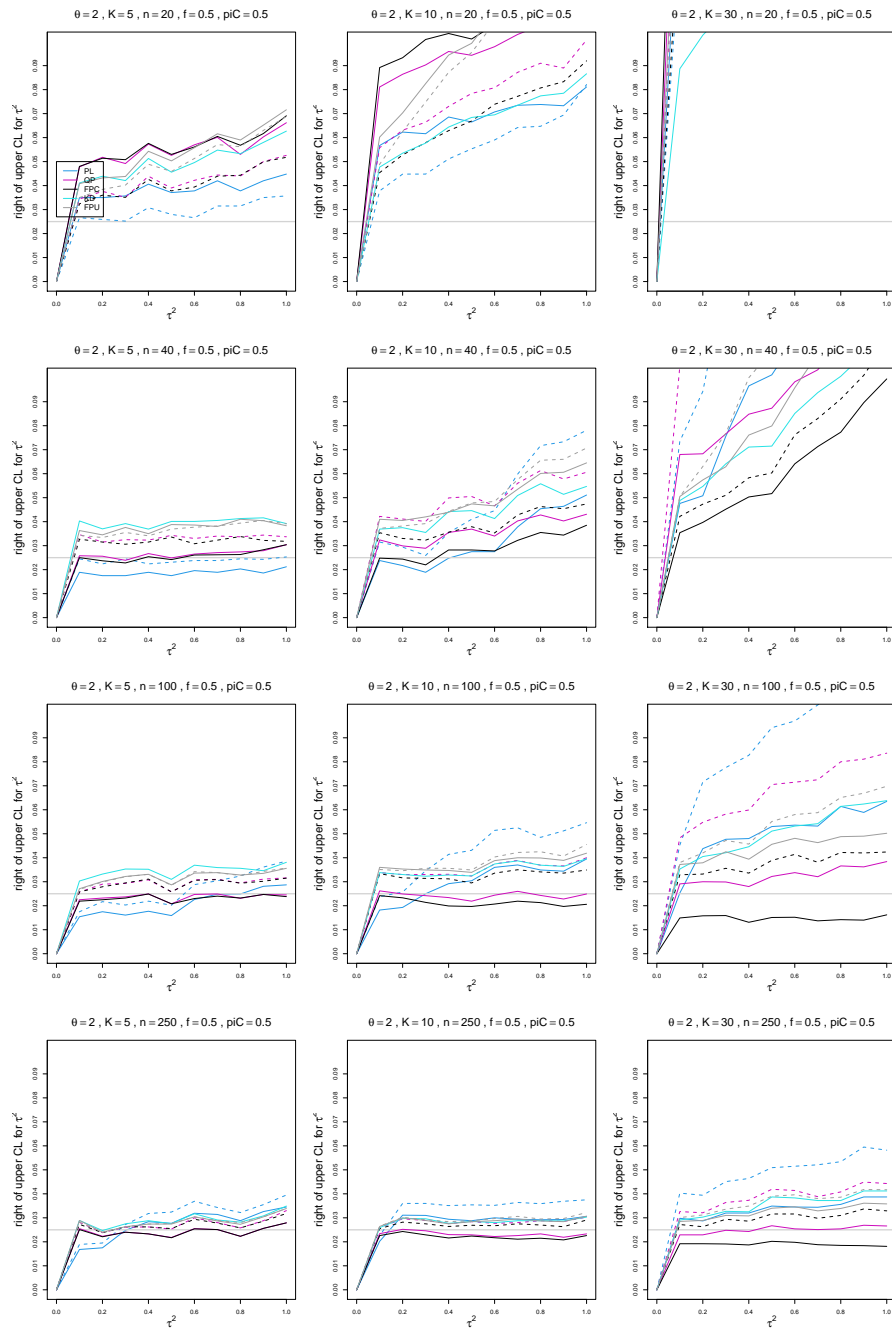


Figure E.35: Miss-right probability of PL, QP, KD, FPC, and FPU 95% confidence intervals for between-study variance of LOR vs τ^2 , for equal sample sizes $n = 20, 40, 100$ and 250 , $p_{iC} = .5$, $\theta = 2$ and $f = 0.5$. Solid lines: PL, QP, and FPC “only”, FPU model-based, and KD. Dashed lines: PL, QP and FPC “always” and FPU naïve.

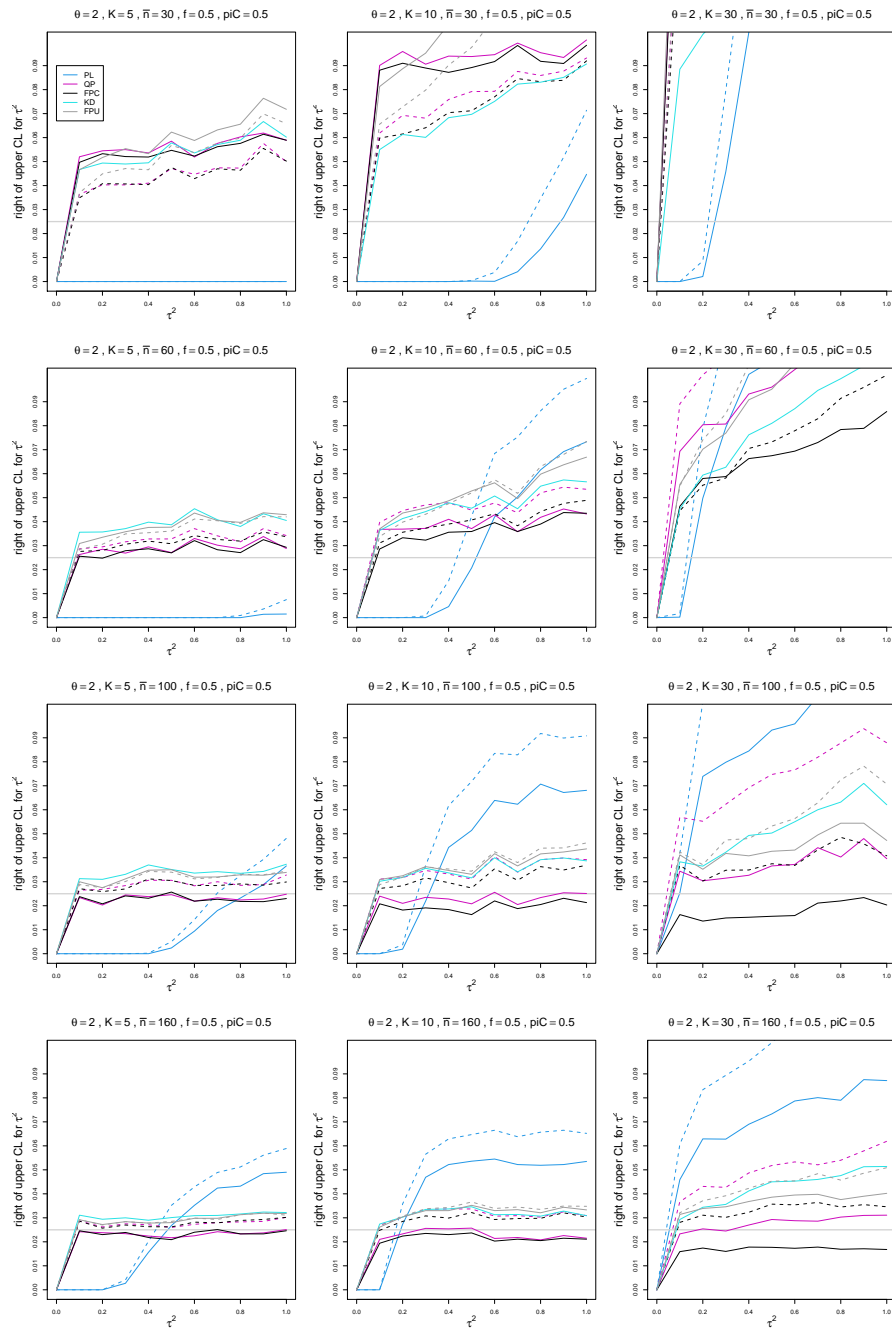


Figure E.36: Miss-right probability of PL, QP, KD, FPC, and FPU 95% confidence intervals for between-study variance of LOR vs τ^2 , for unequal sample sizes $\bar{n} = 30, 60, 100$ and 160 , $p_{iC} = .5$, $\theta = 2$ and $f = 0.5$. Solid lines: PL, QP, and FPC “only”, FPU model-based, and KD. Dashed lines: PL, QP, and FPC “always” and FPU naive.